1-1-2013

Using Model Proteins to Study Tyrosine Oxidation-Reduction: Reversible Voltammograms, Long-Lived Radicals and Detailed Design of the Radical Site

Melissa C. Martínez-Rivera
University of Pennsylvania, melissahrh@gmail.com

Using Model Proteins to Study Tyrosine Oxidation-Reduction: Reversible Voltammograms, Long-Lived Radicals and Detailed Design of the Radical Site

Abstract
Amino acid radicals have been found as key components in a number of biological redox processes. In specific, redox–active tyrosine residues play an essential role in DNA biosynthesis and photosynthesis, among other processes. The thermodynamic and kinetic properties of one–electron redox reactions involving tyrosine have long been obscured by the highly unstable nature of the products of tyrosine oxidation. Remarkable control of these species is achieved within natural proteins. Proteins must, therefore, provide interactions to the amino acid cofactor to generate, control and direct the redox chemistry within the protein milieu. Electrochemical characterization of redox–active tyrosine residues inside natural radical proteins is highly challenging due to potential oxidation of other cofactors and residues. Numerous small–molecule models have been generated in which factors that affect tyrosine/phenol redox chemistry have been elucidated, such as hydrogen–bonding. Although these models have contributed to our knowledge about these systems, these lack the protein environment that certainly renders a stabilizing environment for these species. We have developed a *de novo*–designed model protein family in which to study these reactions. The family of α_3X proteins consists of a well–structured, pH–stable, three–helix bundle with a single redox–active residue within the core of the protein. Construction and characterization of tyrosine–containing (α_3Y, α_3Y–K29H, and α_3Y–K36H) and tyrosine–analogue–containing (2MP– α_3C, 3MP– α_3C, and 4MP– α_3C) proteins are described in this dissertation work. Electrochemical characterization of α_3Y and 2MP– α_3C by Square Wave Voltammetry has allowed us to obtain fully reversible voltammograms and formal reduction potentials for the long–lived neutral radicals formed within these proteins. In the case of α_3Y, we have also found that the protein scaffold is intimately involved in the electron transfer process. We have also achieved the introduction of a tyrosine–histidine interacting pair in two α_3Y variants. This interacting complex is of great interest and will provide insights into how interaction with these basic residues might impact tyrosine redox chemistry within a protein scaffold. In addition, the solution NMR structure of 4MP– α_3C is reported and compared to the previously determined 2MP– α_3C structure. Key structural features are described that are likely to have a major impact on the protein redox properties.

Degree Type
Dissertation

Degree Name
Doctor of Philosophy (PhD)

Graduate Group
Biochemistry & Molecular Biophysics

First Advisor
Cecilia Tommos

Keywords
amino acid radical, protein electrochemistry, protein voltammetry, redox chemistry, square wave voltammetry, tyrosine redox

Subject Categories
Biochemistry | Biophysics

USING MODEL PROTEINS TO STUDY TYROSINE OXIDATION-REDUCTION: REVERSIBLE VOLTAMMOGRAMS, LONG-LIVED RADICALS AND DETAILED DESIGN OF THE RADICAL SITE

Melissa C. Martínez-Rivera

A DISSERTATION

in

Biochemistry and Molecular Biophysics

Presented to the Faculties of the University of Pennsylvania

in

Partial Fulfillment of the Requirements for the

Degree of Doctor of Philosophy

2013

Supervisor of Dissertation

_____
Cecilia Tommos
Research Assistant Professor of Biochemistry and Biophysics

Graduate Group Chairperson

_____
Kathryn M. Ferguson
Associate Professor of Physiology

Dissertation Committee

Fevzi Daldal, Professor of Biology
P. Leslie Dutton, Eldridge Reeves Johnson Professor of Biochemistry and Biophysics
Brian R. Gibney, Associate Professor of Chemistry, CUNY – Brooklyn College
Kristen W. Lynch, Associate Professor of Biochemistry and Biophysics
Sergei Vinogradov, Associate Professor of Biochemistry and Biophysics
A. Joshua Wand, Benjamin Rush Professor of Biochemistry and Biophysics

USING MODEL PROTEINS TO STUDY TYROSINE OXIDATION-REDUCTION: REVERSIBLE VOLTAMMOGRAMS, LONG-LIVED RADICALS AND DETAILED DESIGN OF THE RADICAL SITE.

DEDICATION

A mis padres, Josefina Rivera y Dámaso Martínez

ACKNOWLEDGEMENTS

I would like to acknowledge all the people that have contributed to me being here, people that have been with me in good and bad moments, and that have assisted me and taught me so much, inside and outside the lab.

First of all, I would like to thank my parents, Josefina Rivera and Dámaso Martínez. To whom I owe everything, and even though are not with me anymore, will continue to be my guides, the major influence throughout the rest of my life. Mami, Papi, sé que no tenían sueño más grande que vernos a todos nosotros salir adelante, y estamos en camino para lograr muchas metas. Sin sus enseñanzas y su gran ejemplo, eso no hubiera sido posible.

Secondly, I would like to acknowledge the rest of my family. My siblings: Mahida, Plomo, Darío and Lorna. Muchas que hemos pasado, pero para siempre estaremos unidos y apoyándonos mutuamente. Los quiero. My nieces, Mahia and Joselyn, for making my life happier. My grandma and aunts: Tata, Raquel, Haydeé, Isabel, Evelyn and Anita. En verdad que ustedes, sin duda, han sido como segundas madres para mí. Gracias por todos estos años de cariño y enseñanzas. Nunca podré agradecerles suficiente por todo lo que han hecho por mí y mis hermanos. My cousins, which are like brothers and sisters to me (Jimmy, Tito, Emanuel, Omar, Xavier, Yoly, Jorge, Papo, Angeli, Raúl, Emily and José), and the rest of my family (Abuelo Masio, Abuelo Pilín, Abuela Jacín, Chani, mis tíos Quique y Tito, Milli, Ruty, Bety, Ivonne, Day, Kelo, Daisita, Junito, tío Jimmy, Tita, Aracelis, Nito, Patricia, Meche, Joel, Gabo, Xiomar, Allan).

I would like to thank Dr. C. Tommos for allowing me to join and work in her lab. Also, I would like to thank the members of my Thesis Committee: Kristen Lynch, Josh Wand, Leslie Dutton, and Fevzi Daldal, and additional members, Sergei Vinogradov and Brian Gibney.

I would also like to acknowledge friends, inside and outside the lab, that have seen me through my graduate student life and made my time here so much more enjoyable: Annette Medina, Doriann de Jesús, Edgardo Falcón, Nyamekye Obeng-Adjei, Gabe Krigsfeld, Ellen (Yinan) Fu, Ashima Mitra, Vanessa Matos, Bruce Berry, Vignesh Kasinath, Arnaldo Díaz, Igor Dodevski, Matt Stetz, Mitk'El Santiago, Agustín Díaz, Teshell Ponteen-Greene, Amalia Ávila.

Special thanks to former and current labmates, and people that have assisted and taught me during my time at Penn: Kathy Valentine, Walter Englander, Leland Mayne, Greg Caputo, William DeGrado, Jane Vanderkooi, Bogumil Zelent, Joseph Kielec, Sarah Chung, Nathaniel Nucci, Vonni Moorman, John Gledhill, Nimu Sidhu, Li Liang, Sabrina Bédard, Kyle Harpole, Adam Seitz, Cory Rice, Nataline Meinhardt, Katie Sarachan, Danielle Kamis, Bryan Marques, Christine Jorge, Jakob Dogan.

I would like to gratefully acknowledge the administrative staff at the Biomedical Graduate Studies and at the graduate group of Biochemistry and Molecular Biophysics, especially Ruth Keris, Angie Young, Ilene Kretchman, Namrata Narain, Joanne Kuloszewski, and Lisa Ward.

Finally, I would like to thank the National Institute of Health for funding via RO1 GM079190, a minority supplement to GM079190, and in the form of a NIGMS Individual Predoctoral Kirschstein-NRSA Fellowship (GM096756).

Gracias.

ABSTRACT

USING MODEL PROTEINS TO STUDY TYROSINE OXIDATION-REDUCTION: REVERSIBLE VOLTAMMOGRAMS, LONG-LIVED RADICALS AND DETAILED DESIGN OF THE RADICAL SITE

Melissa C. Martínez Rivera

Cecilia Tommos

Amino acid radicals have been found as key components in a number of biological redox processes. In specific, redox-active tyrosine residues play an essential role in DNA biosynthesis and photosynthesis, among other processes. The thermodynamic and kinetic properties of one-electron redox reactions involving tyrosine have long been obscured by the highly unstable nature of the products of tyrosine oxidation. Remarkable control of these species is achieved within natural proteins. Proteins must, therefore, provide interactions to the amino acid cofactor to generate, control and direct the redox chemistry within the protein milieu. Electrochemical characterization of redox-active tyrosine residues inside natural radical proteins is highly challenging due to potential oxidation of other cofactors and residues. Numerous small-molecule models have been generated in which factors that affect tyrosine/phenol redox chemistry have been elucidated, such as hydrogen-bonding. Although these models have contributed to our knowledge about these systems, these lack the protein environment that certainly renders a stabilizing environment for these species. We have developed a *de novo*-designed model protein family in which

to study these reactions. The family of α_3X proteins consists of a well-structured, pH-stable, three-helix bundle with a single redox-active residue within the core of the protein. Construction and characterization of tyrosine-containing (α_3Y, α_3Y-K29H, and α_3Y-K36H) and tyrosine-analogue-containing (2MP-α_3C, 3MP-α_3C, and 4MP-α_3C) proteins are described in this dissertation work. Electrochemical characterization of α_3Y and 2MP-α_3C by Square Wave Voltammetry has allowed us to obtain fully reversible voltammograms and formal reduction potentials for the long-lived neutral radicals formed within these proteins. In the case of α_3Y, we have also found that the protein scaffold is intimately involved in the electron transfer process. We have also achieved the introduction of a tyrosine-histidine interacting pair in two α_3Y variants. This interacting complex is of great interest and will provide insights into how interaction with these basic residues might impact tyrosine redox chemistry within a protein scaffold. In addition, the solution NMR structure of 4MP-α_3C is reported and compared to the previously determined 2MP-α_3C structure. Key structural features are described that are likely to have a major impact on the protein redox properties.

TABLE OF CONTENTS

LIST OF TABLES

LIST OF ILLUSTRATIONS

LIST OF ABBREVIATIONS

γ	gyromagnetic ratio
ΔE_S	step potential in DPV and SWV
$\Delta G°$	standard Gibbs free energy
ΔG^{H_2O}	global protein stability at zero denaturant concentration
$[\Theta]_{222}$	mean residue ellipticity at 222 nm
2MP	2-mercaptophenol
3MP	3-mercaptophenol
4MP	4-mercaptophenol
APB	sodium acetate/potassium phosphate/sodium borate buffer cocktail
AVS	Assignment Validation Suite
bCys	*N*-acetyl-$_L$-cysteine methyl ester
BMRB	Biological Magnetic Resonance Bank
bpy	2,2′-bipyridine
CD	circular dichroism
CNS	Crystallography and NMR System
CPET	concerted proton-electron transfer
CV	cyclic voltammetry
$D_{aliphatic}$	diffusion coefficient calculated using NMR signal from aliphatic protons
D_{amide}	diffusion coefficient calculated using NMR signal from amide protons
D_{OX}	diffusion coefficient for oxidized state
D_{RED}	diffusion coefficient for reduced state
dNDP	deoxynucleoside diphosphate
DNA	deoxyribonucleic acid
DOSY	Diffusion Ordered Spectroscopy
DP	differential pulse
DPV	Differential Pulse Voltammetry
DSS	2,2-dimethyl-2-silapentane-5-sulfonate sodium salt
E	reduction potential at specified non-standard conditions
$E°$	standard reduction potential
$E°'$	formal potential
$E_{1/2}$	half-wave potential
E_{DP}	pulse amplitude for DPV
E_{anode}	anodic peak potential
$E_{cathode}$	cathodic peak potential
E_{for}	forward peak potential (SWV)
E_{net}	net peak potential (SWV)
E_{rev}	reverse peak potential (SWV)
E_P	peak potential (DPV)
E_{SW}	pulse amplitude for SWV
EC	Electrode-driven/Chemical mechanism

EPR	Electron Paramagnetic Resonance
EPT	electron-proton transfer
ET	electron transfer
ETC	Electron Transfer Chain
f	square wave frequency
F	Faraday constant (96,485 C mol^{-1})
GC	glassy carbon
HMQC	Heteronuclear Multiple Quantum Coherence
HOPG	Highly Oriented Pyrolytic Graphite
HPLC	High Performance Liquid Chromatography
HSQC	Heteronuclear Single Quantum Coherence
i	electric current
I_{for}	forward current (SWV)
I_{net}	net current (SWV)
I_{rev}	reverse current (SWV)
k^0	standard heterogeneous rate constant
k_{chem}	homogeneous rate constant of the coupled chemical reaction
k_{for}	forward heterogeneous rate constant
k_{rev}	reverse heterogeneous rate constants
MP	mercaptophenol
MV	methyl viologen
n	mol of electrons transferred in redox reaction
N/A	not applicable
NHE	Normal Hydrogen Electrode
NDP	nucleoside diphosphate
NMR	Nuclear Magnetic Resonance
NATA	*N*-acetyl-L-tryptophanamide
NAYA	*N*-acetyl-L-tyrosinamide
NOE	Nuclear Overhauser Effect
NOESY	Nuclear Overhauser Effect Spectroscopy
OEC	Oxygen Evolving Complex
PCET	proton-coupled electron transfer
PET	proton-electron transfer
PF_6^-	hexafluorophosphate
PGE	pyrolytic graphite edge
pI	isoelectric point
pK_A	negative log of dissociation constant
pK_{APP}	apparent pK_A
pK_{OX}	pK_A of oxidized state
pK_{RED}	pK_A of reduced state
PSII	photosystem II
PT	proton transfer
Q_A	plastoquinone A
Q_B	plastoquinone B
R	ideal gas constant (8.314 J K^{-1} mol^{-1})
RMSD	root mean square deviation
RNR	ribonucleotide reductase

ROE	Rotating Frame Overhauser Effect
ROESY	Rotating Frame Overhauser Effect Spectroscopy
RRD	radical-radical dimerization
RSD	radical-substrate dimerization
S/N	signal-to-noise ratio
SAM	S-adenosyl methionine
SASA	solvent accessible surface area
SW	square wave
SWV	square wave voltammetry
$t_{1/2}$	halflife
t_p	pulse time (DPV and SWV)
TALOS+	Torsion Angle Likeness Obtained from Shift and Sequence Similarity
TOCSY	Total Correlation Spectroscopy
TTBP	2,4,6-tri-*tert*-butyl phenol
TRIS	tris(hydroxymethyl)aminomethane
UV	ultraviolet
w/v	weight per volume

CHAPTER 1. Introduction to Tyrosine One-Electron Redox Chemistry

1.1. Amino Acids as Radical Redox Cofactors in Natural Systems

Amino acid radicals have been proven to be one-electron redox cofactors in a number of essential biological processes.[1] Several enzymes known to be essential for DNA synthesis,[2,3] DNA repair,[4,5] oxygenic photosynthesis,[6-8] and sugar metabolism,[9,10] among other biological processes, have been classified as amino acid radical enzymes. The amino acid-based radicals in these proteins possess properties different from their characteristics in solution.[11-13] For instance, biocatalytic amino acid radical chemistry is reversible, which is not the case for these reactions in solution.[14,15] Thus, emerges the question of how proteins generate, control, and direct the redox chemistry of these unstable species for catalytic and long-range radical transfer reactions. Proteins must, therefore, provide key environmental characteristics that allow these species to have lifetimes long enough to be able to participate in these enzymatic reactions, and also to be part of multiple turnovers in these proteins.

The amino acid residues that have been identified as redox cofactors, so far, are glycine (GLY), cysteine (CYS), tryptophan (TRP), and tyrosine (TYR), as well as modified tryptophans and tyrosines.[1] Glycyl radicals have been identified in systems, such as pyruvate formate lyase,[16] anaerobic ribonucleotide reductase (class-III RNR),[17] which form part of the Radical-SAM superfamily of proteins.[18] The involvement of a thiyl radical is believed to be a common theme for the catalytic cycle of all ribonucleotide reductase enzymes.[19] Tryptophanyl radicals are found in cytochrome *c* peroxidase,[20,21] in DNA

photolyase,[5] in the MauG/pre-methylamine dehydrogenase complex,[22,23] among other systems. Lastly, tyrosine radicals are redox-active species in the class-I RNRs,[2,3] photosystem II (PSII),[6-8] galactose oxidase (in this case, modified),[10] cytochrome *c* oxidase (also, modified),[24] prostaglandin H synthase,[25-27] bovine liver catalase,[28,29] among others. All the previously mentioned protein systems are responsible for essential reactions in biological systems.

1.2. Tyrosine Redox Chemistry and Proton-Coupled Electron Transfer

Throughout this dissertation work, we will mainly focus on the redox properties of the amino acid tyrosine. Enzymatic tyrosine reduction-oxidation (redox) chemistry has been the focus of numerous research efforts for the last four decades.[2] The discovery of its involvement in essential biological processes, such as DNA biosynthesis and plant photosynthesis, as noted above, has spiked the interest in understanding the intricacies of electron transfer involving this aromatic residue within a protein system. Tyrosine redox chemistry comprises three distinct reactions involving three different redox pairs. The dominant redox pair depends on the pH of the solution and on the dissociation constant of the reduced and of the oxidized state of tyrosine. When the pH of the solution is below the pK_A of the oxidized state of tyrosine (pK_{OX}), fully reduced tyrosine (Y-OH) loses an electron (e^-), and the tyrosine cation radical (Y-OH$^{\bullet+}$) is formed. At pH values above the pK_A of the reduced state (pK_{RED}), an electron is released from the deprotonated state of tyrosine (Y-O$^-$) and a neutral radical (Y-O$^\bullet$) is generated. The values for pK_{OX} and pK_{RED} for free

tyrosine in solution have been reported to be -2 and 10, respectively.[30] For pH values within that pH range, the dominant redox process involves the Y-O$^{\bullet}$/Y-OH redox pair. In this case, fully reduced tyrosine loses an electron as well as a proton (H^+), generating thus a neutral radical. Electron transfer (ET), in this case, is coupled to proton release. Processes such as this are collectively known as proton-coupled electron transfer (PCET). This term was first coined by Meyer and coworkers.[31] These three redox couples are illustrated in Figure 1.1.

$$\mathbf{A}: \quad Y-OH^{\bullet+} + e^- \Leftrightarrow Y-OH$$
$$\mathbf{B}: \quad Y-O^{\bullet} + e^- + H^+ \Leftrightarrow Y-OH \quad \longleftrightarrow \quad \textbf{Proton-Coupled ET}$$
$$\mathbf{C}: \quad Y-O^{\bullet} + e^- \Leftrightarrow Y-O^-$$

Figure 1.1. Reduction-oxidation reactions involving tyrosine (Y). H^+ and e^- represent a proton and electron, respectively. Reaction **A** dominates at pH < pK_{OX}. Reaction **B** occurs at pK_{OX} < pH < pK_{RED}. Reaction **C** governs the thermodynamics of ET at pH > pK_{RED}. Note that redox reactions are, by convention, written as reduction reactions.

1.3. Voltammetry on phenol-based compounds typically follows EC mechanisms

Tyrosine radicals are unstable species with intermolecular recombination rates in the 10^8 M^{-1} s^{-1} range.[32-34] An oxidized tyrosine molecule can react with another oxidized tyrosine molecule, as well as with fully reduced tyrosine; these follow-up (or coupled) reactions are known as radical-radical dimerization (RRD) and radical-substrate dimerization (RSD) reactions, respectively.[35] This depletion of redox-active material due to follow-up chemical reactions renders the system electrochemically irreversible, meaning that the oxidized species is reduced chemically and not via an electrode. A

process in which an electrode-driven reaction is followed by a chemical reaction is said to occur via an EC mechanism (see Figure 1.2).[36-38] "E" stands for electrode-driven reaction which is associated to the electron transfer, as well as proton transfer (PT), in the case of PCET. These reactions are characterized by a forward and reverse heterogeneous rate constants, k_{for} and k_{rev}, respectively. These rate constants are designated as heterogeneous rate constants due to the different phases involved in the reaction: the protein solution and the surface of the electrode.[39] "C" stands for side (or coupled) chemical reactions due to the high reactivity of the generated radical. The chemical reaction, in the case of tyrosine, is usually irreversible and is described by a "chemical" rate constant, or k_{chem}.[11,36] Competition between the reverse electrode reaction and the side chemical reaction is determined by the relative magnitude of k_{rev} and k_{chem}. Consideration of EC mechanisms will be essential for the understanding of these redox systems.

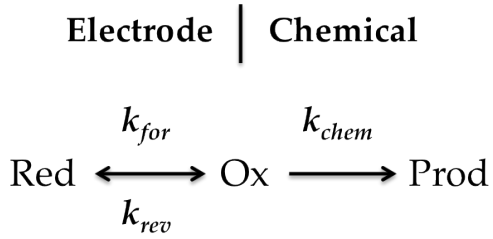

Figure 1.2. Reaction representing an EC mechanism. In this type of mechanism, the "electrode-driven" reaction is followed by a side (or coupled) "chemical" reaction. The variables k_{for} and k_{rev} represent the forward and reverse rate constants for the electrode-driven reaction, and k_{chem} represents the rate constant for the chemical reaction. **Red** and **Ox** represent the reduced and oxidized state, while **Prod** represents the irreversible product of the coupled chemical reaction.

1.4. The Role of Redox-Active Tyrosine in Natural Protein Systems

Tyrosine reduction-oxidation reactions are essential for the enzymatic mechanism of numerous proteins, including *Escherichia coli* (*E. coli*) ribonucleotide reductase (RNR), photosystem II (PSII), and several other enzymes, as mentioned in Section 1.1. The first tyrosine to be identified as a protein tyrosyl radical was tyrosine 122 (Y122) in the R2 (β_2) subunit of *E. coli* RNR.[2,3,40] RNRs catalyze the conversion of nucleoside diphosphates (NDP) into deoxynucleoside diphosphates (dNDP). The *E. coli* protein is composed of two homodimeric subunits, R1 (α_2) and R2 (β_2). NDP reduction takes place in the R1 subunit, and the R2 subunit contains a redox center composed of two non-heme irons and Y122. Each turnover requires radical propagation from the radical Y122$^{\bullet}$ to the active site in R1, where a cysteinyl radical, C439$^{\bullet}$, initiates NDP reduction.[41,42] The generation of the tyrosyl radical requires the presence of molecular oxygen (O_2), a reductant, and the diferrous form of the metallo cofactor in the R2 subunit. If Y122 is removed by site-directed mutagenesis or is not in its oxidized state, the activity of the enzyme is essentially abolished. According to a docking model of the crystal structures of R1 and R2,[43] and to Electron Paramagnetic Resonance (EPR) distance measurements,[44] the distance between Y122 and the active site is approximately 35 Å. Thus, Y122 cannot be directly involved in substrate reduction; electron transfer fails to be effective at distances longer than 14 Å.[45] The current hypothesis for the mechanism of RNR consists on a long-range radical transfer pathway initiated by Y122 and that ultimately generates the C439 thiyl radical in the R1 subunit. Analysis on the conservation of amino acid residues and the docking model of the crystal

structures of both subunits[43,46] reveals several conserved residues that could be involved in this long-range radical transfer pathway. The residues involved in this radical propagation pathway are Y122, W48, Y356 in the β_2 subunit, and Y731, Y730 and C439 in the α_2 subunit.[47] Figure 1.3 shows these residues in the docking model of subunits R1 and R2, along with the diiron metallo cofactor, other residues involved in proton transfer and distances (in Å) between some residues.[47] The involvement of these residues in the pathway has been confirmed by replacing them with unnatural amino acids that differ in reduction potential relative to the original residue with the aim of generating long-lived radical intermediates within the pathway.[48-50] As seen, *E. coli* RNR represents a system in which TYR redox chemistry is key for the enzymatic mechanism.

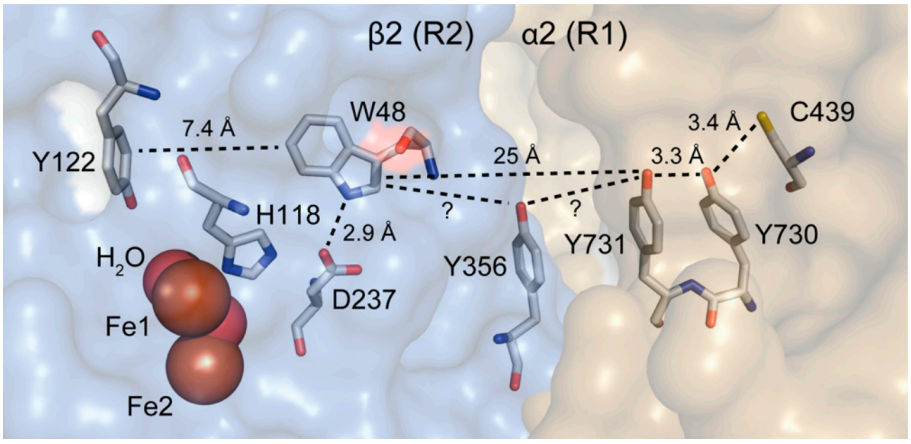

Figure 1.3. Electron-transfer pathway for E. coli ribonucleotide reductase.[47] This figure shows a section of the docking model generated from the crystal structures of both subunits of RNR, R1 (α2) and R2 (β2). Key amino acid residues involved in the pathway are visualized in stick representation. This figure also displays known distances between these residues, in Å.

Tyrosine oxidation is, also, a key component in the enzymatic activity of the water-splitting protein-pigment complex, photosystem II (PSII).[1,19] PSII is found in the thylakoid membranes of chloroplasts and cyanobacteria. This enzyme mediates the light-driven reduction of plastoquinones, Q_A and Q_B, Q_B being the ultimate electron and proton carrier of PSII. Water (H_2O) is the electron source for this system, and O_2 is released as a by-product. The active site is composed of a Mn_4CaO_5 cluster and a redox-active tyrosine (residue 161 on the D1 reaction-center protein) denoted Y_Z.[51] Catalysis is initiated by light absorption by a specialized chlorophyll complex, P680. Photoexcited P680, P680*, serves as the primary electron donor in the system. P680* transfers an electron to a pheophytin *a* molecule ($Pheo_{D1}$), thus generating the cation radical $P680^{\bullet+}$. This electron is then transferred from pheophytin to Q_A and, subsequently, to Q_B. Two proton-coupled reductions of Q_B form the plastoquinol Q_BH_2, which is then released into the thylakoid membrane to continue on the Electron Transfer Chain (ETC).[19] In order for the protein to be able to participate in multiple turnovers, re-reduction of $P680^{\bullet+}$ is required. $P680^{\bullet+}$ is a highly oxidizing species, with an estimated operating potential of around 1.25 V vs. the Normal Hydrogen Electrode (NHE).[19,52,53] Its reduction potential is sufficiently high to oxidize nearby tyrosine residue, Y_Z,[6,7] which operating potential has been estimated to be approximately 1.1 – 1.2 V.[1,19,54] This electron transfer event occurs in nanoseconds, and results in regeneration of reduced P680 and neutral radical Y_Z-$O^{\bullet}$. The phenolic proton of Y_Z-$O^{\bullet}$ is released and a histidine residue, H190, of the D1 subunit serves as the primary proton acceptor. Mutations of H190 abolish photoautotrophic growth.[55]

Moreover, the recently determined 1.9-Å-resolution crystal structure from *Thermosynechococcus vulcanus* (*T. vulcanus*) reveals that both Y_Z and H190 participate in a low-barrier hydrogen bond (2.5 Å in length), which is part of a hydrogen-bonding network that includes water molecules and several other residues (see Figure 1.4).[51] This hydrogen-bonding network creates an exit pathway in which protons released may reach the lumenal bulk solution.

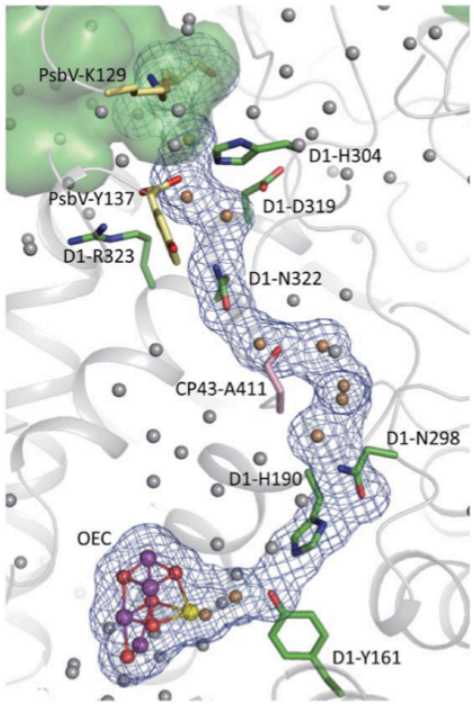

Figure 1.4. Hydrogen-bond network around Y_Z in *Thermosynechococcus vulcanus* photosystem II.[51] Figure shows a section of the PSII crystal structure at a resolution 1.9 Å. Stick representations of the Mn_4CaO_5 cluster (or OEC), redox-active Y_Z, and other residues involved in the hydrogen-bond network that goes from the manganese cluster to the lumenal bulk phase (green area in upper left corner) are shown. Water molecules involved in the network are shown in orange; other water molecules are depicted in gray.

Re-reduction of Y_Z occurs via oxidation of the Mn_4CaO_5 cluster, more commonly referred to as the Oxygen-Evolving Complex (OEC).[19] While P680 and Y_Z are re-reduced in each cycle, the OEC continues to accumulate oxidizing power in each of four cycles (corresponding to each photon absorbed by P680) necessary for the full reduction of two Q_B molecules and the oxidation of two H_2O molecules. Each cycle generates a different oxidation state for the Mn_4CaO_5 cluster; these differ in the oxidation states of the four manganese (Mn) atoms in the cluster. The different oxidation states of the OEC are denoted as S_0, S_1, S_2, S_3, and S_4.[1,19] The S_0 state corresponds to the manganese cluster before absorption of the initial photon by P680. The subsequent states correspond to the number of electrons extracted from the cluster. One electron has been extracted from OEC in the S_1 state, two electrons from S_2, and so forth. After the fourth cycle, in which OEC is in its S_4 oxidation state, oxidation of two water molecules occurs, O_2 is released, and the OEC returns back to oxidation state S_0. The enzymatic mechanism of PSII illustrates the importance of tyrosine redox chemistry in biology. Y_Z is an essential intermediate between the photooxidized P680 and the Mn_4CaO_5 cluster. The interactions and chemistry between the aforementioned components of the electron transfer pathway in PSII (OEC, Y_Z, H190 and P680) have served as inspiration for the generation of numerous small-molecule models with the objective to mimic the charge separation achieved in this system, and to elucidate the role that each of them plays in the overall enzyme reaction. Examples will be discussed in Section 1.5.

The description above represents just a brief description of class-I RNR and PSII, proteins that utilize amino acid-based radicals as part of their catalytic

cycles. Even though these amino acid-based radical species do play key roles in several biological reactions, little is known about the thermodynamic properties of their reduction-oxidation reactions. Studying these radical species in natural proteins has proven to be a very challenging task.[13,19] First of all, the oxidation reactions for these four amino acids occur at very highly positive potentials. At these highly oxidizing potentials, other cofactors and non-catalytically active amino acids may be oxidized, resulting in the potential destruction of the native protein.[15] For example, PSII from *T. vulcanus* contains more than 50 cofactors in each monomer, including 35 chlorophylls, 11 β-carotenes, two hemes, two plastoquinones, and two pheophytins, among others.[51] It is, indeed, almost impossible to study the electrochemical characteristics of a single TYR residue among all other tyrosines, tryptophans, cysteines and glycines, and other cofactors. Another obstacle towards their characterization in natural proteins is the fact that the spectral features of amino acid radicals are very weak and are easily obscured by other cofactors and/or added redox mediators, which complicates characterization by redox titration methods.[15,56] Models in which these tyrosine radicals can be studied within a protein framework are of utmost importance to improve our understanding of amino acid radical chemistry.[1]

1.5. Small-Molecule Models for Tyrosine-Based PCET

Due to the difficulty of studying electron transfer processes in natural systems, research efforts have focused substantially on the development of small-molecule models that mimic the essential components involved in electron transfer events in these proteins. PSII-bio-inspired small-molecule

constructs have contributed greatly to our knowledge of how this enzyme functions. Substantial work has been done on systems in which a tyrosine or tyrosine-like compound is linked either to a photosensitizer to generate the tyrosyl radical or to a hydrogen-bonding partner to study how the redox process is influenced by interactions to the phenol group. Description and examples of these systems are presented below.

1.5.1. Small-Molecule Models that Involve Intramolecular ET and Intermolecular PT: Tyrosine-Photosensitizer Supramolecular Complexes

Work on photosensitizers has focused mainly on attaching tyrosine or tyrosine-like compounds to a metal complex with a high reduction potential in its photoexcited state. Ruthenium (Ru) polypyridyl complexes have been covalently attached to these compounds (e.g. Compound 1 in Figure 1.5) and, once photoexcited by a laser flash, they reduce an external electron acceptor, such as methyl viologen (MV) or $[Co(NH_3)_5Cl]^{2+}$.[57-60] The oxidized state of these complexes is highly oxidizing with reduction potentials close to +1.3 V, thus triggering proton-coupled intramolecular electron transfer from tyrosine to the Ru complex. The metal-complex sensitizers play the role of special chlorophyll complex P680 from PSII by extracting an electron from the tyrosine moiety. Time-resolved emission, transient absorption spectroscopy and EPR spectroscopy have been utilized to monitor the oxidation state of both the photosensitizer, the tyrosyl moiety and the initial electron acceptor (e.g. MV^+), thus providing a tool to obtain rate constants for the electron transfer event of interest. In addition, groups that can form hydrogen-bonding interactions to

these tyrosine moieties, such as dipicolylamine groups, have been attached to these supramolecular complexes and have been found to increase the rate of electron transfer.[58] Rhenium (Re) polypyridyl complexes have also been used for studies of this type.[61]

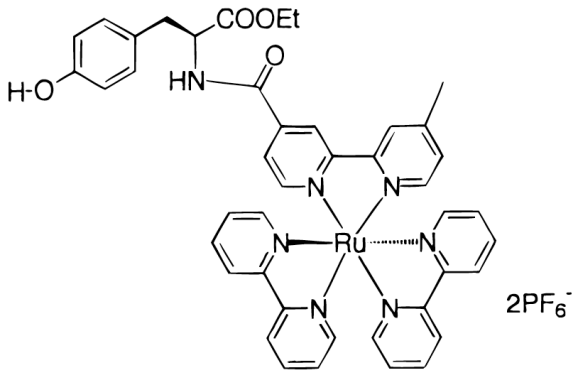

1

Figure 1.5. Schematic structure of model compound 1 ([$Ru^{II}(bpy)_2$(4-Me-4′-(CONH)-L-tyrosine ethyl ester)-2-2′-bpy]$(PF_6)_2$).[60] Model compound 1 consists of a supramolecular complex that attaches a tyrosine moiety to a Ru(II) metal complex that acts as a photosensitizer.

1.5.2. Small-Molecule Models that Involve Intermolecular ET and Intramolecular PT: Phenol/Tyrosine Intramolecularly Bound to Hydrogen-Bonding Partners

Another set of small-molecule models that have been generated consists of tyrosine moieties covalently attached to hydrogen-bonding partners. Alkylamine groups have been utilized, such as primary and tertiary amine, pyridine and imidazole groups.[62-64] These studies aim at elucidating the effects of interactions to the phenol group on the electron transfer process and on the stability of the phenoxyl radical generated. Sterically hindered 2,4,6-

trisubstituted phenols having two *tert*-butyl groups at the 2 (*ortho*) and 4 (*para*) positions and an attached basic group at the 6 (*ortho*) position have been synthesized. The *tert*-butyl groups are utilized to sterically shield the radical and minimize the occurrence of side reactions such as dimerization of the phenoxyl radicals.[65,66] Matsumura and coworkers generated models comprising of 2,4-di-*tert*-butyl-6-alkylamino phenols and were able to obtain quasireversible cyclic voltammograms. This effect may be due to the presence of the hydrogen-bonding group that maintains the proton local, allowing thus for the reverse PCET process to occur.[63] These results contrast to the irreversible redox behavior exhibited by 2,4,6-tri-*tert*-butyl phenol (TTBP).[67] The strength and nature of the hydrogen-bonding interactions also affects the stability of the generated phenoxyl radical and the rates of oxidation.[62,68,69] Numerous groups have designed base-attached phenol compounds of the kind described in this section.[64,70,71] Small-peptide models have also been designed and described in the literature.[72,73]

1.5.3. Tyrosine PCET Occurs Via Concerted Proton-Electron Transfer at Biologically Relevant pH Conditions

From the studies mentioned above, it is clear that the nature of the proton acceptor is essential for determining the thermodynamics of proton-coupled electron transfer involving tyrosine-like compounds. Savéant's group has focused instead on the kinetics of the ET process.[74] Their goal is to distinguish between three possible PCET mechanisms: PET (proton transfer precedes electron transfer, EPT (electron precedes proton transfer), and CPET

(proton and electron transfer are concerted). Two studies from this group have shed light onto mechanisms of electron transfer involving 2,4,6-tri-*tert*-butylphenol and phenol as a function of the solution pH in buffered and unbuffered media.[66,75] Electrochemical measurements in buffered media provided apparent potential versus pH (Pourbaix) diagrams, while data resulting from unbuffered media allowed for discrimination against or in favor of the PET mechanism. Electrochemical measurements on TTBP in 50/50:water/ethanol unbuffered solutions reveal that the PET dominates at high pH, resulting in a single current response due to the oxidation of the phenoxide anion.[66] As the solution pH is lowered, the PET mechanism gives way to another mechanism, which is reflected on the appearance of a new current response that grows at the expense of the PET peak current. At pH 10.5, both peaks are present which illustrates the competition between both mechanisms (PET and the second mechanism). This mechanism emerging at lower pH values was assigned to CPET rather than EPT due to a significant kinetic (hydrogen/deuterium) isotope effect and also because of the disagreement of EPT simulations with the experimental data. Similar measurements were carried out in unbuffered water solutions containing phenol, and comparable results were obtained. The use of unbuffered media in these studies is of great significance. In these solutions, the only available H^+ acceptor is the hydroxyl anion, which means that the PET mechanism can be effectively shut down as the pH decreases, thus allowing CPET and EPT to compete for kinetic control of the PCET process. In the case of phenol and TTBP, CPET was determined to be the dominant mechanism at lower pH

values, where water is the sole proton acceptor. From these studies, we see that at the biological pH range, it is likely that the dominant PCET mechanism is CPET.

1.6. Summary

We have seen that TYR is a key component in biologically important processes such as DNA synthesis and photosynthesis, and that electrochemical studies in these systems is a highly challenging task. For this purpose, small-molecule models have been generated and significant progress has been achieved in understanding what factors alter redox reactions involving TYR residues. In these models, however, the amino acid is entirely exposed to the solvent. Therefore, these models lack the protein environment that certainly affects the redox properties of amino acids residues, in comparison to their properties in bulk solution.[11,12] It is clear that protein-like models are needed in order to make more accurate predictions about amino acid radical behavior.

In order to fulfill this inherent gap between studies in natural and small-molecule systems, our lab has taken the approach of studying amino acid radical chemistry in *de novo*-designed model proteins. These models extend the relative simplicity of small-molecule systems into a protein environment without the complication of the presence of redox cofactors and other potentially redox-active residues. Previous work on this approach is discussed in Chapter 2.

CHAPTER 2: Description of the α_3X Model Protein System

2.1. Development of de novo-Designed Family of Proteins: the α_3X Protein Family

As has been described in Chapter 1, there are numerous small-molecule, as well as peptide models, that aim at elucidating the intricacies of tyrosine reduction-oxidation reactions. These models have contributed significantly to our knowledge of how these reactions occur and what interactions influence their thermodynamic and kinetic properties in solution. However, these constructs all contain fully solvent-exposed tyrosine moieties and lack the microenvironment provided by a protein scaffold. Proteins provide unique interactions that allow the radical species to be generated, and to be stable long enough to participate in several turnovers of the radical enzyme.

There is an imperative need for the development of protein models that start with the simplest features of interest until a more complete picture can be more effectively achieved and studied. *De novo*-designed proteins present a very feasible approach for the engineering of cofactors in minimal models that, at the same time, retain protein properties that tune cofactor reactivity. Initially, *de novo* design was primarily concerned with deciphering the primary sequence code for secondary structure.[76-78] The specifics on how to construct a protein with a specific fold are still very far from perfect but significant achievements have been done.[79] Now that the protein design field has accomplished to engineer unique secondary and tertiary structure, the next step is to engineer in function into these *de novo*-designed protein structures.[13,76,80-83]

To fill the existing gap between the small-molecule models and the natural systems, a series of *de novo*-designed proteins has been developed with the objective of studying electron transfer involving amino acid radicals as a function of protein environment.[13,84] By reducing the complexity of the radical-containing system, studies can be performed to learn more about the protein-environment features that influence the reduction-oxidation properties of aromatic-residue redox cofactors. Electrostatic interactions, hydrogen-bonding interactions, as well as solvent exposure are examples of the different environmental factors that can influence the thermodynamics and kinetics of amino acid radical chemistry.[85]

These *de novo*-designed proteins were initially designed to satisfy a number of criteria in order for them to be a suitable model system for radical enzymes. (1) The objective is to investigate how protein environment modulates tyrosine redox chemistry. The protein scaffold must form specific and stable interactions with the redox-active residue, which will be possible if the protein has a well-defined structure. Therefore, the first criterion for our model system is that it should form stable and well-defined secondary and tertiary structures in solution. (2) Moreover, as mentioned in Chapter 1, tyrosine reduction potentials are pH-dependent due to the proton-coupled nature of the electron transfer in the physiological pH range, making pH a critical parameter to monitor in order to understand these systems. Consequently, the structural properties of the model protein must not be significantly perturbed as a function of pH. (3) In addition, the protein should contain a single redox-active residue, which should be buried within the protein core. The radical should be

formed within the protein interior to avoid influence from the bulk solution. (4) Lastly, the protein scaffold itself should be redox-inert and not contain residues with reduction potentials close to that of the amino acid radical cofactor. This will prevent possible side reactions between the amino acid radical cofactor and the protein matrix, and will also isolate any redox signal to the amino acid radical of interest.

2.2. Generation and Characterization of TRP- and TYR-Containing Model Proteins: α_3W and α_3Y

Two model proteins were initially generated: α_3W and α_3Y.[13] Both proteins consist of a 65-residue three-helix-bundle, with a single aromatic residue; α_3W contains a single TRP residue at position 32, while α_3Y contains a single tyrosine at the corresponding position. This can be seen from their respective amino acid sequences: RVKALEEKVKALEEKVKALGGGGRIEEL-KKK**X**EELKKKIEELGGGGEVKKVEEEVKKLEEEIKKL, where **X** denotes either a TRP or a TYR residue for α_3W and α_3Y, respectively. Both proteins were characterized in detail and it was found that they satisfy the criteria mentioned above. (1) Both these model proteins were shown to form well-defined secondary and tertiary structures in solution, as evidenced by circular dichroism (CD) spectroscopy and nuclear magnetic resonance (NMR) spectroscopy.[13] (2) It was also found that the structure for both proteins remains stable through a broad range of pHs, from pH ~4 to pH 10. This was shown by monitoring the CD signal as a function of pH for both proteins, as well as by

monitoring the fluorescence of W32 and the absorbance of deprotonated Y32 (Y32-O$^-$) as a function of pH. (3) Both the W32 and Y32 residues were shown to reside within the interior of the protein. The optical properties of tryptophan and tyrosine are known to depend on their surrounding environment.[86-89] The fluorescence of W32 shows a blue shift compared to the fluorescence of a tryptophan analogue, *N*-acetyl-L-tryptophanamide (NATA), in solution. This is indicative of an indolyl group going from water-solvated to a lower-dielectric environment.[89] By following the absorbance of Y32 as a function of pH, the pK_{APP} of Y32 was determined and compared to the pK_A of a tyrosine analogue, *N*-acetyl-L-tyrosinamide (NAYA), in solution. Y32 has a pK_{APP} of 11.3, which is 1.2 pH units higher than the pK_A determined for NAYA. Higher pK_A value indicates that creating the charged deprotonated tyrosine is less favorable, thus suggesting that the phenol group resides in a hydrophobic environment, shielded from bulk solution. NMR spectroscopy was also used to obtain information on the environment surrounding the aromatic residues in α_3W and α_3Y. Two-dimensional ^{1}H-^{1}H Nuclear Overhauser Effect (NOESY)[90] spectra were collected and it was seen that the aromatic protons for both W32 and Y32 are surrounded mainly by aliphatic protons, including methyl protons, which are typically found at the hydrophobic cores of proteins.[91] In summary, optical and NMR spectroscopy provided evidence that both W32 and Y32 are sequestered within the interior of α_3W and α_3Y, respectively. (4) Finally, it was also determined that the protein scaffold is not redox active at the potentials required to study the aromatic radicals. The only residue in the α_3W/α_3Y

sequence that might oxidize at potentials within the vicinity of the reduction potential of TRP and TYR are the glycines that compose the helix-connecting loops. However, glycines are expected to have reduction potentials higher than tryptophan and tyrosine.[19] Moreover, electrochemical measurements of free glycine in solution were obtained at the same conditions as the protein experiments and no current response was seen, indicating that glycines are not redox-active within the potential range surveyed.[13] In conclusion, both the protein models, α_3W and α_3Y, are suitable models to investigate amino acid redox chemistry within a protein as a function of protein environment.

2.3. Generation and Characterization of Mercaptophenol-Bound, CYS-containing Model Proteins: 2MP-α_3C, 3MP-α_3C, and 4MP-α_3C

In addition to the α_3W and α_3Y proteins, another protein was added to the α_3X family of model proteins, α_3C.[84] α_3C shares the same sequence as the two previously characterized proteins but differs in the identity of the residue at position 32. While α_3W and α_3Y contain a tryptophan and tyrosine residue in position 32, respectively, α_3C contains a cysteine residue. Via disulfide formation, residue C32 was covalently attached to the three different constitutional isomers of mercaptophenol (MP). Three proteins are, thus, generated from these binding reactions: 2MP-α_3C, 3MP-α_3C, and 4MP-α_3C. The 2MP, 3MP, and 4MP acronyms refer to the ortho-, meta-, and para-substituted mercaptophenol molecules, respectively (see Figure 2.1). The modified residue

for these three proteins is, from here on, referred to as 2MP-C32, 3MP-C32, and 4MP-C32.

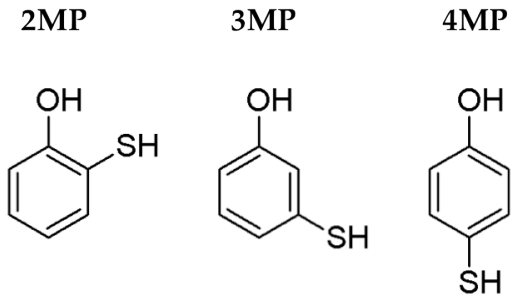

Figure 2.1. Schematic structures of the three constitutional isomers of the mercaptophenol (MP) molecule.[84] Molecules 2MP, 3MP, and 4MP refer to the molecules in which the sulfur atom is in the ortho, meta, and para position, respectively. The carbon atom bound to the OH group is designated as carbon 1.

The binding of these molecules to the cysteine residue in α_3C creates tyrosine analogues in which the hydroxyl group is rotated along the phenol ring, with the aim of creating different degrees of solvent exposure for the hydroxyl group. Reference 84 describes the structural and preliminary electrochemical characterization of α_3C and the three MP-bound proteins. According to α_3W-derived models of the MP-bound α_3C protein molecules (α_3W PDB id: 1LQ7), the OH group of protein-bound 2MP and 3MP was expected to be directed towards the inside of the protein. In contrast, the OH group of protein-bound 4MP was hypothesized to be in a more solvent exposed position. The objective was to investigate how varying degrees of solvent exposure to the phenol hydroxyl group may influence the redox properties of these tyrosine analogues.

The structural properties of α_3C and the three MP-α_3C proteins were explored using CD spectroscopy. These four proteins are highly α-helical, similar to α_3W and α_3Y, as revealed by their spectral characteristics in the far-UV region.[84] Their α-helical content was determined by using their mean residue ellipticity at 222 nm ($[\Theta]_{222}$) and using Equation 2.1.[92,93]

$$[\Theta]_{222} = \left(f_H - \frac{ik}{N}\right)[\Theta]_{222}^{\infty}, \tag{2.1}$$

where the $[\Theta]_{222}$ is the observed mean residue ellipticity at a wavelength of 222 nm in its conventional units (deg cm^2 dmol^{-1}) (see Section 7.6 for equation that describes the relationship between $[\Theta]_{222}$ and the observed CD signal), $[\Theta]_{222}^{\infty}$ is the mean residue ellipticity at 222 nm of a helix of infinite length (-39.5 mdeg cm^2 dmol^{-1}), f_H is the fraction of helix in the molecule, i is the number of helical segments, N is the total number of residues, and k is a wavelength-dependent constant (2.57 for 222 nm). The helical percentage was calculated to be 71%, 78%, 83%, and 81% for α_3C, 2MP-α_3C, 3MP-α_3C, and 4MP-α_3C, respectively. The structurally characterized α_3W was previously determined to be 76% helical,[56] meaning that binding of the mercaptophenol molecules does not significantly disrupt the formation of the secondary structure of the construct. The stability of the proteins was examined by determining the free energy change for conversion of native to unfolded protein in the absence of denaturant, ΔG^{H_2O}. ΔG^{H_2O} values for all proteins were obtained by making use of the method

described by Santoro and Bolen (see Section 7.6),[94] and it was found that the protein stabilities of the MP-α_3C proteins are not significantly reduced by binding of the MP molecules.[84]

As mentioned above, the molecular models for 4MP-α_3C, 3MP-α_3C, and 2MP-α_3C predict a solvent exposed environment for the OH group of protein-bound 4MP, while the protein-bound 3MP and 2MP contain an OH group that is more exposed to the protein milieu. In order to confirm these predictions, preliminary voltammetry data was collected on the three MP-bound α_3C proteins. Differential pulse voltammetry (see Section 3.3 for description of this technique) was used in this earlier report to see if differences were observed in the electrochemical responses of each of the MP-bound proteins when compared to the MP molecules bound to blocked cysteine (bCys) in solution. It is known that reduction potentials are sensitive to changes in the environment surrounding the redox center.[13] The DPV response was obtained as a function of pH, and the results were plotted as peak potential versus pH (see Figure 2.2).[84] The electrochemical data for 2MP-α_3C and 3MP-α_3C show a consistent increase in the peak potentials at corresponding pH values of ~120 and ~110 mV, respectively, when compared to the bCys-bound compounds. On the other hand, the results from 4MP bound to α_3C and bCys show essentially identical electrochemical profiles. Due to the instability of the products generated by TYR one-electron redox chemistry, thorough analysis of the electrochemical data becomes highly challenging (see Section 3.4). So far, no conclusion can be drawn regarding the difference in potentials obtained for 2MP-α_3C, 3MP-α_3C

and their small-molecule counterparts. However, the fact that the resulting voltammetry data for 4MP-α_3C and 4MP-bCys is essentially identical suggests a comparable environment surrounding 4MP in both the protein and the small-molecule compound.

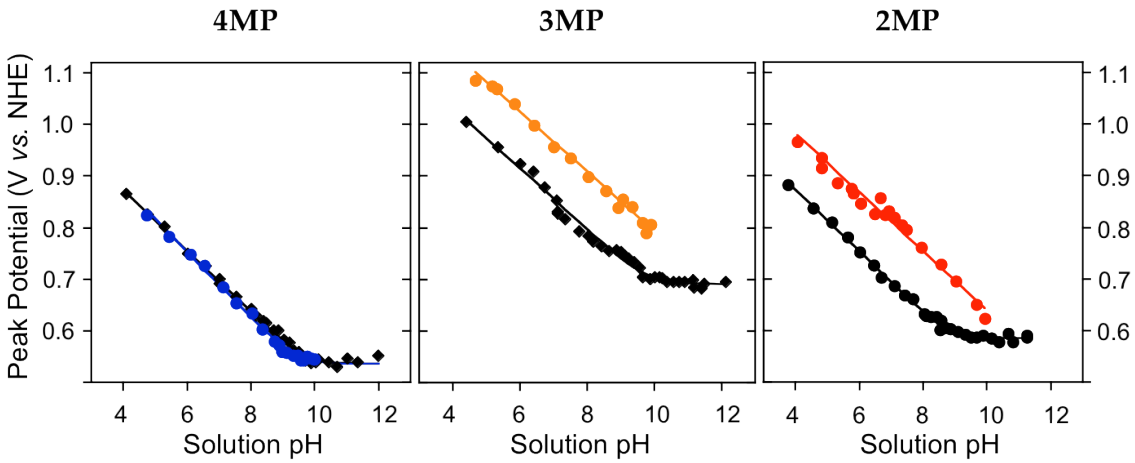

Figure 2.2. Differential pulse voltammetry (DPV) peak potentials (E_P) as a function of solution pH.[84] Blue, orange, and red circles represent E_P values obtained from samples containing α_3C-bound 4MP, 3MP and 2MP, respectively. Data depicted in black was obtained from samples containing bCys-bound 4MP, 3MP and 2MP. Lines represent fitting of the data (see ref 84). Samples were prepared in buffer containing potassium phosphate (KPi) 10 mM and potassium chloride (KCl) 100 mM. Experiments were carried out at room temperature under an argon (Ar) atmosphere, using a silver/silver chloride (Ag/AgCl) reference electrode. All peak potentials are referenced to the normal hydrogen electrode (NHE) by $E_{NHE} = E_{Ag/AgCl} + 0.196$ V.[39]

Additional experiments were done to investigate the solvent-exposed nature of the environment surrounding 4MP in 4MP-α_3C. Far-UV CD spectra were collected for 4MP-α_3C at pH 7.6 and pH 10.[84] The pK_A of the tyrosine analogue was determined to be 9.45. The protonated state of 4MP is expected to dominate at pH 7.6, while the deprotonated state will be the major species at

pH 10. Generation of a charged species, due to deprotonation, and lack of polar/charged residues in the core of our protein system may induce disturbances in the three-helix bundle structure. However, the CD spectra of 4MP-α_3C at both pH values display no significant differences.[84] These results further provide evidence for the hypothesis that 4MP is significantly solvent exposed when bound to α_3C.

The main advantage of the MP-α_3C protein system is that it provides protein-bound tyrosine analogues with differing degrees of exposure to bulk solvent without introducing major changes in the overall structure of the protein. To investigate this issue further, it is essential to obtain structural models for the MP-bound α_3C proteins. Obtaining a high-resolution structure of these proteins will provide insights into what kind of interactions play a role in tuning tyrosine/phenol redox chemistry. The solution NMR structure of 2MP-α_3C has been obtained and it is discussed below.

The high-resolution solution NMR structure of 2MP-α_3C has been determined in our lab.[95] An ensemble of 32 refined structures form the NMR-derived structural model. The root mean square deviation (RMSD) to the mean coordinates is 0.46 Å for backbone atoms and 0.95 Å for all heavy atoms. The structural statistics for the ensemble are reported in Appendix A. The NMR structure shows that the atoms associated with C32 are completely shielded from the bulk solvent, with a solvent accessible surface area (SASA) of 0 ± 0 %. The 2MP-C32 side chain is found in a sequestered position sandwiched between two helices in the structure. The buried position of the cysteine forces

the polar OH group of the attached phenol inside of the protein, as designed. The average SASA across the structural ensemble is 3.5 ± 0.7 % for the 2MP-C32 residue, 2.0 ± 3.1 % for the phenol hydroxyl oxygen, and 4.0 ± 5.4 % for the phenol hydroxyl proton. See Appendix A for SASA analysis of the 2MP-C32 residue. The NMR structure also reveals that the phenol is involved in an inter-helical hydrogen bond to residue GLU 13. The phenol oxygen/GLU 13 carboxyl oxygen distance is 3.2 ± 0.5 Å across the NMR family of structures. GLU 13 has an average SASA of 12.1 ± 2.6 %, which is significantly lower than the other 16 GLU residues in the protein.[95] From the NMR structure of 2MP-α_3C, we also observe that this hydrogen bond interacts with the sidechain amino group of LYS 17 and/or LYS 36. These observations are critical and will aid us in the understanding the electrochemical behavior of the tyrosine analogue 2MP bound to α_3C. The next step in order to obtain insights into the redox behavior of the MP-bound proteins will be to determine the high-resolution NMR structure of the 4MP-α_3C protein. The calculation of this structure has been achieved and will be discussed in Chapter 5.

Certainly, the marked differences in electrochemical behavior between 4MP-α_3C and the other two MP-α_3C proteins in the preliminary voltammetry study presented above was the main motivation for the structural characterization of the MP-bound proteins. However, as we will see throughout this work, the irreversible nature of TYR radical chemistry complicates results obtained from voltammetry data. In Chapter 3 and Chapter 5, this issue is addressed for the proteins α_3Y and 2MP-α_3C, respectively.

2.4. Summary

In order to provide more protein-like models for the TYR redox cofactors, a series of *de novo*-designed model proteins have been developed to fill the gap between the small-molecule and natural systems. The α_3X system has been generated. This family of proteins includes the α_3W, α_3Y, and α_3C variants. We propose the use of these model proteins to establish the thermodynamic principles of amino acid radical chemistry in proteins. Further development of the α_3X protein model system is the main subject of this doctoral work. In specific, work on the α_3Y protein system will be the focus of Chapter 3 and 4, while work on the α_3C protein system will be further discussed in Chapter 5.

CHAPTER 3: Reversible Redox Chemistry of a Protein Tyrosyl Radical

3.1. Electrochemical Approach for Characterization of Redox Properties

The main goal of this work is to investigate how properties of and interactions to the protein scaffold modulate the redox properties of tyrosine radical cofactors. In order to gain more knowledge on this subject, we need to be able to measure the thermodynamics of these reduction-oxidation reactions inside of a stable and well-structured protein background. As discussed in the previous chapter, α_3Y is a well-structured three-helix-bundle protein and shows properties similar to that of natural proteins,[13] which makes it a suitable model system for exploring tyrosine radical chemistry.

A key property of a redox system is the standard reduction potential, $E°$. The standard reduction potential is directly related to the standard Gibbs free energy change of the reduction process (gain of electrons) by

$$\Delta G° = -nF\Delta E°, \tag{3.1}$$

where $\Delta G°$ is the standard Gibbs free energy change, F is the Faraday constant describing the charge per mol of electrons (96,485 C mol^{-1}), and n is the number of equivalents of electrons transferred in the given reaction. From Equation 3.1, we see that a positive reduction potential represents a thermodynamically favorable reduction reaction, whereas a negative value for the reduction potential describes a non-favorable process. In the case of an oxidation reaction,

this relationship is inversed. Thermodynamically favored oxidation reactions possess negative reduction potentials and non-favored oxidation reactions will have positive reduction potentials.

Standard reduction potentials are relative values measured against the reduction potential of a well-defined redox system. The absolute zero in the reduction potential scale is arbitrarily assigned to the conversion of protonated hydrogen to molecular hydrogen:

$$2H^+ + 2e^- \rightleftharpoons H_2(g),$$

where the reaction occurs at standard conditions, that is 298 Kelvin (K), unit activity (a) for species in liquid phase, and partial pressure of 1 atm for species in gaseous phase. An electrode in which this reaction occurs is denoted as the Normal Hydrogen Electrode (NHE), and standard reduction potentials of all other redox systems are expressed relative to it. When the NHE cannot be used as reference, other reference redox systems of known potential may be used to replace it, given that the obtained reduction potential values are corrected accordingly.

In most occasions, it is not possible to obtain measurements at standard conditions. Experimental systems may require non-standard conditions, such as temperature other than 298 K, or activities that do not equal unity. For systems such as these, a relationship exists between the standard reduction potential and the potential of the system at specified experimental conditions. This relationship is described by the Nernst equation (Equation 3.2):

$$E = E° + \frac{RT}{nF} ln \frac{a_{OX}}{a_{RED}},$$

(3.2)

where E is the reduction potential at specified non-standard experimental conditions, R is the gas constant (8.314 J mol^{-1} K^{-1}), and a_{OX} and a_{RED} represent the activities of the oxidized and reduced states, respectively. Activity can also be expressed as γ_A[A], where γ_A and [A] represent the activity coefficient and molar concentration of a given species A. Given that activity coefficients are not readily available, the concept of the formal potential $E°'$ is introduced to avoid the need for obtaining these values. The formal potential $E°'$ is defined in Equation 3.3:

$$E°' = E° + \frac{RT}{nF} ln \frac{\gamma_{OX}}{\gamma_{RED}}.$$

(3.3)

This allows for redefinition of E (Equation 3.4) as

$$E = E°' + \frac{RT}{nF} ln \frac{[OX]}{[RED]},$$

(3.4)

where [OX] and [RED] are the molar concentrations of the oxidized and reduced states, respectively. By replacing the constants in the equation, and taking the temperature to be 25 °C, the Nernst equation can be expressed as in Equation 3.5.

$$E = E^{\circ\prime} + \frac{0.059\,V}{n} \log \frac{[OX]}{[RED]}.$$

(3.5)

By obtaining *E*, and knowing the molar concentrations of the species involved, we can obtain the formal potential. Obtaining values for formal potentials for our protein-bound tyrosine system will be one of the main objectives of this work.

Voltammetry techniques will comprise the experimental approach of choice to obtain reduction potentials for the single tyrosine residue, Y32, in α_3Y. A typical voltammetry experiment consists of the monitoring of current *i* due to an electron transfer, or Faradaic, process as a function of an applied potential used to oxidize or reduce the electrochemically active species of interest. The experimental setup utilized for the voltammetry measurements consists of a three-electrode system (see Figure 3.1), in which a working electrode, a reference electrode, and a counter (or auxiliary) electrode are all immersed in the solution containing the electroactive analyte, and are all connected to a potentiostat. The potential applied on the system is generated at the working electrode and the redox reaction of interest occurs at its surface. The reference electrode contains the reference redox system and sets the electrical potential to which the potential of interest is measured against (see above), and the counter electrode is a non-reactive high-surface-area electrode that helps minimize electrical resistance in the solution. Measurements were carried out in a temperature-controlled, Faraday cage-protected three-electrode cell. The

reference electrode was a silver/silver chloride (Ag/AgCl) electrode, and the counter electrode was a platinum (Pt) wire.

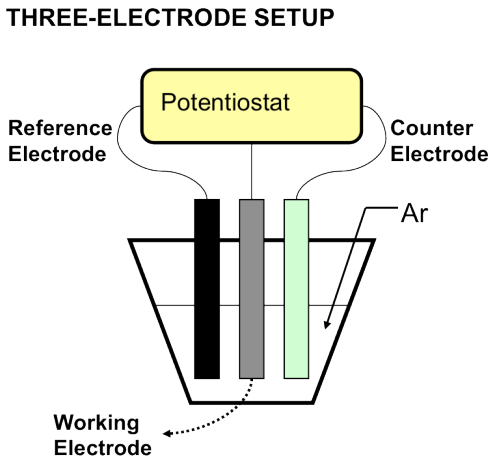

Figure 3.1. Three-electrode electrochemical cell setup. The reference, working and counter electrode are illustrated as black, gray and light green bars, respectively. All three electrodes are immersed in the sample solution, and are connected to a potentiostat. The solution is purged with Ar gas.

3.2. Cyclic Voltammetry of α_3Y and N-acetyl-L-tyrosinamide (NAYA)

One of the most commonly used electrochemical methods is cyclic voltammetry (CV) due to its straightforward and powerful diagnostic properties.[39] The CV experiment consists of an applied potential that increases linearly with time (forward scan), it reaches a maximum potential, and then the direction of the scan switches back (reverse scan) until it reaches the initial potential of the experiment (see Figure 3.2).

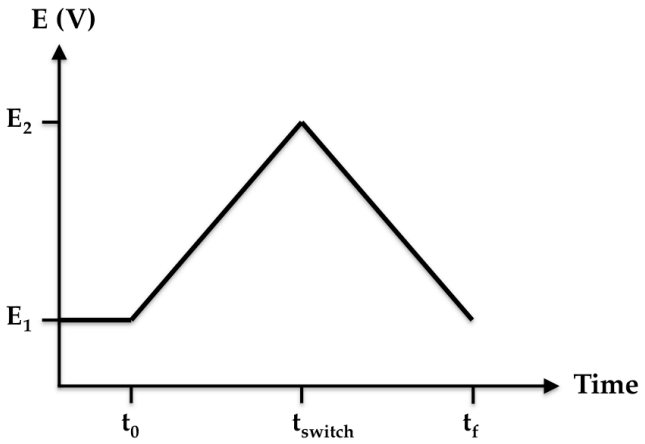

Figure 3.2. Applied potential vs. time plot for the cyclic voltammetry (CV) experiment. The CV experiment starts at an initial applied potential E_1 at time t_0. The applied potential is linearly changed until it reaches a maximum (or switch) potential E_2 at time t_{switch}. This first segment of the experiment is denominated as forward scan. Then the potential scan reverses and decreases linearly until it reaches back to the initial potential at time t_f. This second part of the experiment is denoted as the reverse scan. In the case of tyrosine, oxidation occurs during the forward scan and takes place in the anode, whereas reduction occurs during the reverse scan and takes place in the cathode.

In the case of tyrosine, the initial species is fully reduced tyrosine and it becomes oxidized on the forward scan. The reverse scan would induce re-reduction on the generated oxidized species. The aspect of the resulting voltammogram reveals key information about the redox system under study. Factors that affect the resulting voltammogram include the formal potential of the redox couple ($E^{0\prime}$), the standard heterogeneous rate constant (k^0) for the electrode-driven reaction, and the diffusion coefficients of the oxidized (D_{OR}) and reduced (D_{RED}) states.[39] A CV voltammogram usually displays two current traces as a function of applied potential. Figure 3.3 shows an example of a typical cyclic voltammogram.[96]

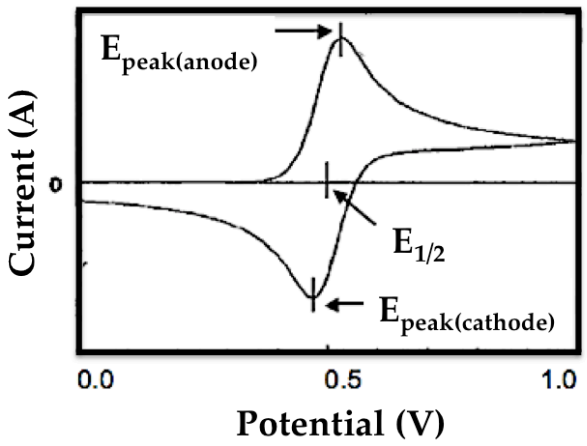

Figure 3.3. Typical CV trace for a reversible system.[96] This figure illustrates the typical wave shape for data resulting from a completely reversible redox system. The half-wave potential ($E_{1/2}$) of the redox couple occurs at the middle point between the peak potentials for the forward (E_{anode}) and reverse ($E_{cathode}$) scans, which will be separated by 59 mV for a reversible one-electron transfer process.

The upper portion of the plot represents the current generated in the forward scan (anodic current), and the lower part displays the current response resulting from the reverse scan (cathodic current). The peak positions, E_{anode} and $E_{cathode}$, are the peak potentials of the cyclic voltammogram, and the middle point between the peak potentials equals the half-wave ($E_{1/2}$) potential. $E_{1/2}$ approximates the formal potential of the redox couple for diffusion-controlled systems (see Equation 3.6).[39]

$$E_{1/2} = E^{\circ\prime} + \frac{RT}{nF}\ln\left(\frac{[D_{RED}]}{[D_{OX}]}\right)^{1/2}. \tag{3.6}$$

The separation between the peak potentials, also, reveals information about the kinetics of the reaction. For a fast diffusion-controlled reversible process, the

separation equals 59 mV. For slower kinetics, this separation increases. For completely irreversible system, no reverse current is generated, and therefore no $E_{cathode}$ is obtained. Diffusion (mass transport to the surface of the electrode) also plays a role in determining the characteristics of the resulting voltammogram.[39] The electroactive species need to be transported from solution to the surface of the electrode, and the rate of this mass transport will have significant effects on the position of the peak potentials. If mass transport is slow enough to thwart effective electron transfer to/from the electrode surface, we will see an increase in the separation between the peak potentials. If mass transport does not hinder ET, then the kinetics will depend solely on the intrinsic ET heterogeneous rate constant. In the extreme case where the redox-active species of interest is adsorbed to the surface of the electrode (diffusion plays no role in the system), both peak potentials will appear exactly at the same applied potential.[39]

Cyclic voltammetry has been used previously to analyze the redox properties of tyrosine and phenol molecules in solution.[11,12,74] Cyclic voltammograms were, therefore, obtained for α_3Y and for a tyrosine analogue, NAYA, free in solution.[97] Figure 3.4 shows the cyclic voltammograms for both molecules. Sample and experimental conditions were similar for both protein and NAYA samples (see legend of Figure 3.4). The only difference between samples was the concentration of supporting electrolyte: 40 mM potassium chloride for α_3Y samples and 200 mM KCl for NAYA samples. At lower KCl concentrations, the NAYA voltammograms displayed characteristics consistent with electrode adsorption.

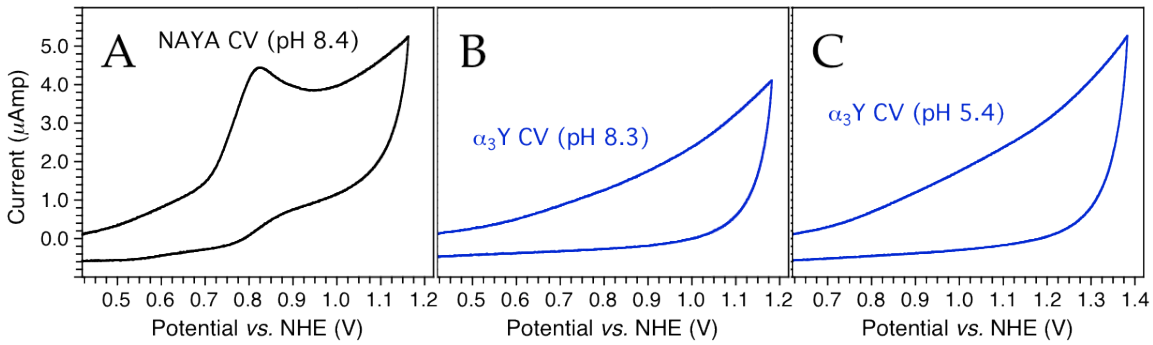

Figure 3.4. Cyclic voltammograms for α_3Y and NAYA. Panel **(A)** shows the CV for 200 μM NAYA in 20 mM potassium phosphate, 20 mM sodium borate and 200 mM KCl at pH 8.43. Panel **(B)** shows the CV for 210 μM α_3Y at 20 mM potassium phosphate, 20 mM sodium borate and 40 mM KCl at pH 8.33. Panel **(C)** shows the CV for 210 μM α_3Y in 20 mM sodium acetate, 20 mM potassium phosphate and 40 mM KCl at pH 5.43. *Experimental settings*: scan rate 0.2 V/s, iR compensation 103 ohm.

From the voltammograms, we see that NAYA gives rise to a electrochemically irreversible Faradaic response at pH 8.4, as expected.[11] On the other hand, α_3Y does not generate a current signal. The response from α_3Y could not be improved by changing the protein concentration, buffer conditions, or acquisition parameters. Thus, we conclude that cyclic voltammetry is not a viable approach for the electrochemical analysis of the α_3Y system, due to insufficient sensitivity for detecting current originating from the protein sample.

3.3. Differential pulse voltammetry of α_3Y and N-acetyl-L-tyrosinamide (NAYA)

We set out then to utilize an electrochemical method with higher sensitivity, differential pulse voltammetry (DPV; see Figure 3.5).[39,98,99] The differential pulse experiment starts at a base applied potential E, and after a

determined time denoted pre-electrolysis time, a potential pulse of amplitude E_{DP} and duration t_p is applied. The time composed of the pre-electrolysis time and the time of the pulse, denoted as interval time, comprises a cycle in the experiment. After the duration of the pulse, the potential goes back to a new resting potential $E + m\Delta E_S$, where ΔE_S is the potential step of a potential staircase, and m represents the number of the cycle and equals 1, 2, 3, …, m. The potential during the pre-electrolysis time sets an equilibrium between the oxidized and reduced states, and the pulse acts upon this equilibrium. Values of t_p range between 2 and 100 milliseconds (ms), while the pre-electrolysis time ranges between 0.1 and 4 seconds. Pulse amplitudes are usually not set to larger than 100 mV in order to avoid significant degradation of the resolution of the voltammogram. The current is sampled just before the beginning (τ') and before the end (τ) of the applied pulse, and the difference between these current measurements is plotted against the resting potential of the corresponding cycle. The resulting voltammogram contains a peak signal which maximum intensity sits on a potential (E_P) equal to the half-wave potential ($E_{1/2}$) plus half of the pulse amplitude ($E_{DP}/2$).[39]

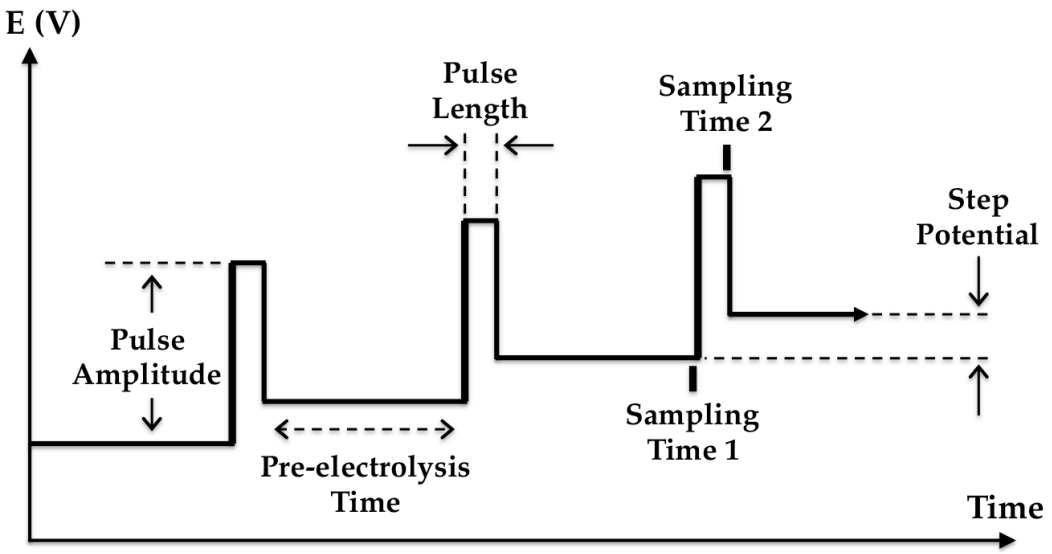

Figure 3.5. Applied potential vs. time plot for the differential pulse voltammetry experiment. See text (Section 3.3) for explanation of experiment and parameters.

The gain in sensitivity for DPV comes from the subtraction of the sampled currents at each cycle of the experiment. Generation of potential at the electrode is achieved by creating an excess or deficiency of electrons at its surface. A charging current flows to produce this accumulation of charge. This, in turn, causes a flow of cations/anions from the bulk solution to the electrode, creating a charge difference and, hence a capacitance, at the electrode-solution interface. The aforementioned charging current can obscure currents from Faradaic processes. Background current arising from this charging current decreases exponentially during the lifetime of the pulse. If this current does not change significantly between the sampling times, then the subtraction of the sampled currents (before the beginning and before the end of the pulse of each

cycle) results in cancellation of current contributions arising from the charging process of the electrode.

Differential pulse measurements were performed on α_3Y and NAYA samples, and the voltammograms are shown in Figure 3.6. We see that α_3Y does generate a Faradaic signal. The protein current signal is one order of magnitude less intense than the signal obtained for NAYA. The current range for the α_3Y Faradaic signal is in the 0.1 μAmp range, while the signal for NAYA is in the 1.0 μAmp range. Differential pulse voltammograms were also obtained for α_3C, the Y32C variant of α_3Y, which contains a cysteine at position 32 instead of a tyrosine residue (see Section 2.3). We see that α_3C generates no Faradaic signal. Moreover, samples containing α_3C generate similar voltammograms as those obtained for buffer solutions, meaning that the protein scaffold itself has no Faradaic response and that it is not redox-active in the potential range of interest. Hence, we conclude that the Faradaic current seen for the α_3Y DP voltammograms arises from oxidation of residue Y32. Therefore, we have achieved the development of the first system in which an electrochemical response can be observed from a redox-active tyrosine in a redox-inert and well-structured protein environment.

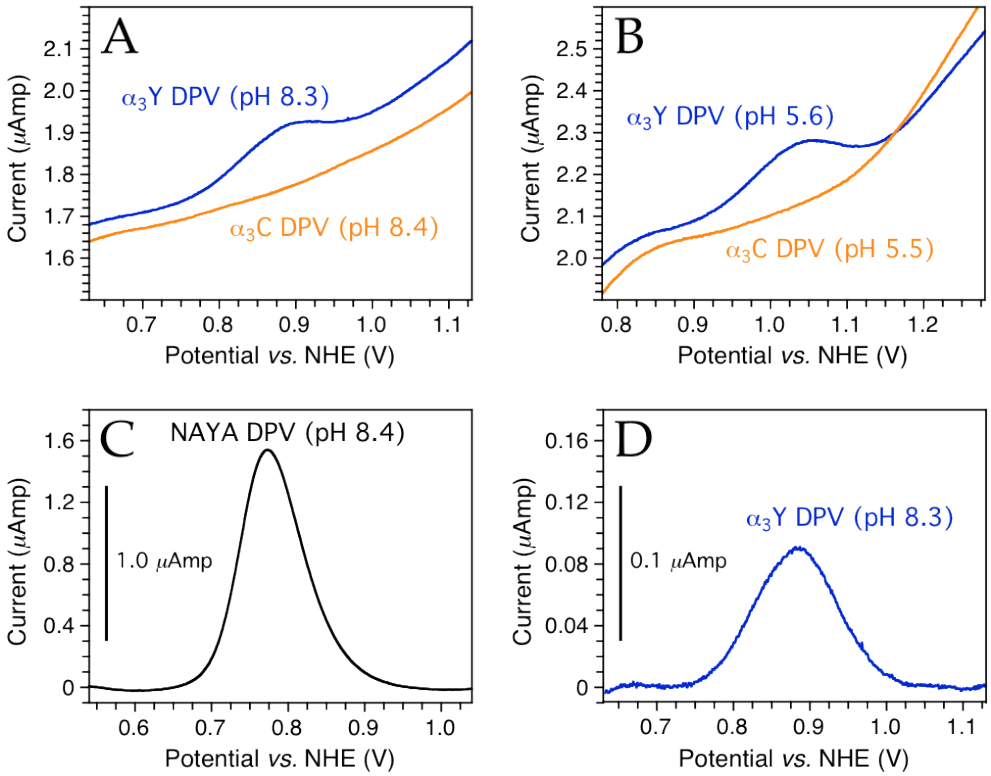

Figure 3.6 Differential pulse voltammograms for α_3Y and NAYA. DPV of α_3Y, α_3C and NAYA are depicted in blue, orange, and black, respectively. Panel **(A)** shows the raw traces for 210 μM α_3Y in 20 mM sodium phosphate, 20 mM sodium borate, 40 mM KCl, pH 8.33 and 200 μM α_3C in 20 mM sodium phosphate, 20 mM sodium borate, 40 mM KCl, at pH 8.45. *Experimental settings*: interval time 0.1 s, step potential 1.05 mV, scan rate 10.5 mV/s, pulse time 8 ms, pulse amplitude 50 mV. Panel **(B)** shows the raw traces for 210 μM α_3Y in 20 mM sodium acetate, 20 mM sodium phosphate, 40 mM KCl, pH 5.56, and 200 μM α_3C in 20 mM sodium acetate, 20 mM sodium phosphate, 40 mM KCl, at pH 5.46; interval time 0.1 s, step potential 1.05 mV, scan rate 10.5 mV/s, pulse time 5 ms, pulse amplitude 50 mV. Panel **(C)** shows the baseline-subtracted trace for 200 μM NAYA in 20 mM sodium phosphate, 20 mM sodium borate, 200 mM KCl, pH 8.37; interval time 0.1 s, step potential 1.05 mV, scan rate 10.5 mV/s, pulse time 8 ms, pulse amplitude 50 mV. Panel **(D)** shows the baseline-subtracted version of the α_3Y differential pulse voltammogram shown in Panel A.

Initial characterization of the redox properties of α_3Y did not give rise to a Faradaic response.[13] In that earlier study, voltammetry experiments on α_3Y only yielded an electrochemical signal at conditions in which the protein was

known to be unfolded. Several factors can be accounted for contributing to those results, such as the type of working electrode utilized, sample conditions, and the acquisition parameters used during the experiment. Voltammetry is highly sensitive to the size of the analyte and its orientation on the surface of the electrode since there must be electronic contact between the redox-active species and the working electrode. The type of working electrode utilized, and how this working electrode is prepared for the experiment are crucial factors that will determine the interaction between the protein and the electrode surface. The working electrode must also provide the potential range necessary for surveying the electrode potentials of tyrosine radicals, which are at the high end of the biological cofactor potential range. In this case, we have chosen to use a glassy carbon working electrode, which provides a potential window that ranges to up to +1.3 V vs. NHE.[39,100] The glassy carbon electrode was activated by polishing its surface in an Al_2O_3/water slurry, which is expected to generate a hydrophilic surface with C-O functionalities such as hydroxyls, carbonyls, ethers, and carboxylates.[101-103] This pretreatment process was refined by iteratively polishing, sonicating and rinsing the surface of the electrode until a reproducible Faradaic response was obtained. It was also of great importance to determine the proper sample conditions to use for the experiments. Protein concentration, buffer composition and concentration, and supporting electrolyte concentration were taken into account. In addition, the acquisition parameters for the DPV experiments were systematically explored in order to determine parameters that would give rise to optimal current signal. The DPV experimental parameters, as discussed above, include the pulse amplitude and

length, the step potential and the pre-electrolysis time. The optimal experimental conditions are expected to differ between different sample conditions. Taking into account all of these factors allowed us to obtain sample and experimental conditions that gave rise to the first Faradaic response arising from a tyrosine in a folded protein structure.

DPV measurements were conducted at varying pH values in order to investigate differences in the measured peak potential as a function of solution pH. A plot of $E_{1/2}$ versus pH, or Pourbaix diagram, is displayed in Figure 3.7. The Pourbaix diagram of α_3Y illustrates the pH dependence of the half-wave potential obtained from the DP voltammograms.

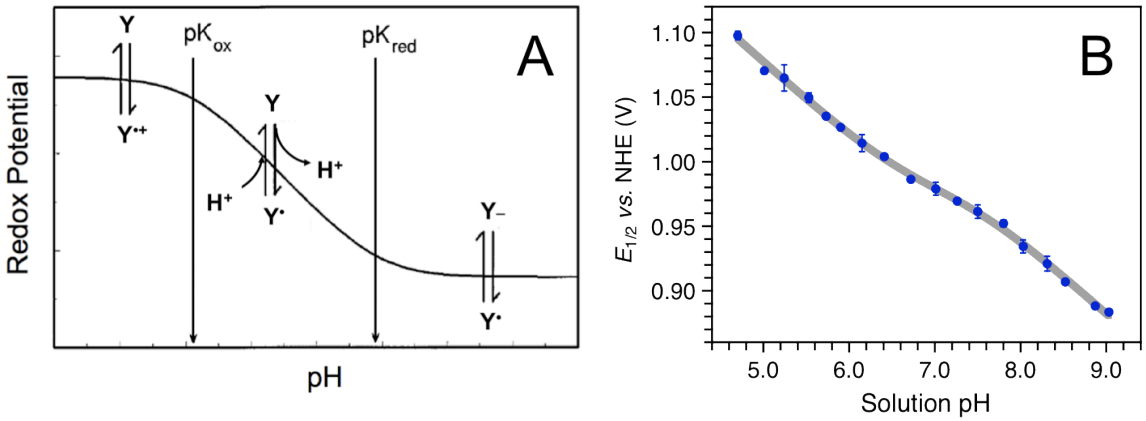

Figure 3.7. Pourbaix (half-wave potential vs pH) diagram. Panel **(A)** depicts the shape of a typical Pourbaix diagram. The vertical lines delineate the areas of the plot were a different redox couple is present, which is determined by the pK_{OX} and pK_{RED} values for this species (see Section 1.2 and Figure 1.1). Panel **(B)** illustrates experimental half-wave potential ($E_{1/2}$) as a function of pH (blue circles) obtained for the protein α_3Y. The gray line represents a nonlinear regression curve fit to Equation 3.8. Sample: 200 μM α_3Y in 10 mM sodium acetate, 10 mM potassium phosphate, 10 mM sodium borate and 100 mM potassium chloride at 23 °C. DPV settings: GC working electrode, interval time 0.1 s, step potential 1.95 mV, scan rate 19.5 mV s^{-1}, pulse time 2 ms, pulse amplitude 25 mV. *Fitting results*: p$K_{RED(Y)}$ values used was 11.3, as determined by pH titration of the Y32 residue (see Section 4.1), $E_{1/2(pH0)}$ = 1.37 ± 0.01 V, RT/nF = 0.059 ± 0.002 V, p$K_{RED(B)}$ = 6.7 ± 0.1, p$K_{OX(B)}$ = 7.4 ± 0.1, χ^2 = 0.00011925, R^2 = 0.9983.

As explained in Section 1.2, we expect a pH dependence due to the coupling of protonic reactions to the tyrosine oxidation reaction. The Nernst equation for a PCET process (Equation 3.7) describes this pH dependence:

$$E = E^{\circ\prime} + \frac{0.059\,V}{n}\log\frac{[OX][H^+]}{[RED]} = E^{\circ\prime} + \frac{0.059\,V}{n}\log\frac{[OX]}{[RED]} - \frac{0.059\,V}{n}pH, \tag{3.7}$$

where [H+] is the molar concentration of proton. From the pH-dependent Nernst equation, we see that the reduction potential decreases by 59 mV per pH unit.[39,100] Thus, the Pourbaix diagram is expected to show a linear relationship and have a slope, $\frac{\delta E_{1/2}}{\delta pH}$, close to - 59 mV/pH unit. A typical Pourbaix diagram is shown in Figure 3.7.[104] As expected for tyrosine, the plot contains two pH-independent regions (at pH > pK_{RED} and pH <pK_{OX}) and a pH-dependent region (pK_{OX} < pH < pK_{RED}). Voltammetric measurements were only performed in the pH-dependent region due to the pH-stability range of α_3Y (see Figure 4.4 and Table 4.1 in Chapter 4). We observe that the Pourbaix plot obtained for α_3Y deviates from linearity. A possible explanation for this nonlinearity in the pH dependence is that the proton released in the PCET reaction does not go directly to bulk solution upon oxidation but remains within the protein scaffold. In order to compensate for charges formed within the interior of the protein, residues adjacent to the oxidation site may exhibit shifts in their pK_A values upon oxidation, thus being able to capture the released proton.[105] Mathematical treatment for systems in which an additional species, other than

the redox-active species, is involved in the PCET event has been described previously by Clark.[106] The peak potentials arising from such systems are described by Equation 3.8.

$$E_{1/2} = E_{1/2(pH0)} + \frac{RT}{nF}\ln\frac{[H^+]^2 + K_{red(B)}[H^+] + K_{red(B)}K_{red(Y)}}{K_{ox(B)} + [H^+]}, \quad (3.8)$$

where $E_{1/2(pH0)}$ represents the peak potential at pH equal to zero, $K_{red(Y)}$ is the dissociation constant for tyrosine in its reduced state, and $K_{red(B)}$ and $K_{ox(B)}$ are the dissociation constants for an additional residue B when tyrosine is in its reduced and oxidized states, respectively. The α_3Y Pourbaix diagram was fitted to Equation 3.8 assuming a pK_{RED} value of 11.3 for residue Y32 (as determined by following the tyrosinate absorbance at 293; see Figure 4.4 and Table 4.1)[97]; fitting stats are shown in the figure legend. From the fitting, we obtain the pK_{RED} and pK_{OX} values of the additional residue involved in PCET to be 6.7 and 7.4, respectively. These results suggest that, upon oxidation of Y32, the protonated state of residue B is favored. This may indicate proton capture by residue B upon tyrosine oxidation. From these results, we see that we have achieved the development of a protein scaffold that interacts with the TYR radical and is involved in the PCET process. This observation will be discussed further in Section 3.6.

3.4. Coupled Chemical Reactions Compromise Electrochemical Analysis of Tyrosine Redox Couple

Due to the experimental challenges of examining tyrosine radical chemistry in natural systems, we have developed a model protein system in which to study these species. As was discussed in Chapter 2, the α_3Y model protein provides a stable, well-structured and redox-inert protein framework that allows for electrochemical characterization of tyrosyl radical species. The main objective of these studies is to be able to obtain reduction potentials for tyrosine within a protein scaffold, and also to investigate how these are tuned by the protein matrix. In order to obtain meaningful reduction potentials, the electrochemical data from the protein-bound tyrosine must represent an electrochemically reversible process. The degree of reversibility can be affected by several parameters, including slow heterogeneous electron transfer between the electrode and the electroactive species[39], and coupled chemical reactions[36-38].

Electron transfer involving tyrosine/phenol compounds usually generates highly reactive species that do not survive during the time scale of a typical voltammetric experiment. This irreversibility compromises the results obtained from various electrochemical methods. In the case of cyclic voltammetry, the reverse (reductive) scan shows no current response due to consumption of the generated oxidized species by coupled chemical reactions, making thorough analysis of the voltammogram difficult.[11] The position of the peak potential of the forward scan in CV is also influenced by coupled chemical reactions, as seen from Equation 3.9.[11,75]

$$E_p = E^0 - 0.9\frac{RT}{nF} + \left(\frac{RT}{3nF}\right)\ln\frac{2k_{chem}CRT}{3nFv},$$

(3.9)

where C is the concentration of electroactive species, and v is the experimental scan rate. From Equation 3.9, we see that to obtain the standard potential, we would need to know the rate constant for the side chemical reaction. Also, we observe that by increasing the scan rate of the experiment, we can decrease the contribution of the third term of Equation 3.9. It might seem like an easy solution to simply run the CV experiment at faster scan rates to, in a way, outcompete following chemical reactions. Unfortunately, with scan rates fast enough to avoid these side reactions, the use of CV presents other complications.[107] Rapid changes in electrode potential induce a large double-layer charging current at the surface of the working electrode that can easily mask the small Faradaic current originating from the electron transfer process of interest.

The other electrochemical method that we have used is differential pulse voltammetry. In the case of DPV, the peak signal generated will be less intense, broader, and also will be shifted toward extreme potentials.[39] In DPV, the reduced and oxidized species are let to coexist during the pre-electrolysis time, which can last from 0.1 to 4 seconds. This long time before the pulse allows for chemical reactions, such as dimerization, to occur. Thus, we anticipate that neither CV nor DPV will allow us to obtain completely reversible voltammograms arising from the electron transfer process involving protein-bound tyrosine.

3.5. Square wave voltammetry can address issues arising from electrochemical irreversibility

In order to address the issue of electrochemical irreversibility, another voltammetric method was explored. Square wave voltammetry (SWV) has the same advantage as DPV in that it is highly sensitive, and also possesses the diagnostic power of CV.[39] Analysis of square wave voltammograms provides mechanistic, thermodynamic, as well as kinetic information about the system under study.[108] Figure 3.8 illustrates a plot of applied potential versus time for SWV. The square wave experiment consists on an applied potential that is increased linearly in small fixed increments (ΔE_S); similar to the potential staircase in DPV (see Section 3.3). At every increment a forward (in this case, oxidative) pulse of amplitude (E_{SW}) is applied followed by a reverse (reductive) pulse of the same amplitude, from which forward (I_{for}) and reverse (I_{rev}) currents are generated, respectively. A net (or difference) current (I_{net}) is derived by subtracting the reverse from the forward current. The potential of maximum current in the net voltammogram is denoted the net peak potential (E_{net}), which equals the difference between the potential of maximum absolute current for the forward and the reverse voltammograms (E_{for} and E_{rev}, respectively). The period (τ) of the square wave equals two times the pulse time (t_p) and is the inverse of the square wave frequency (f).

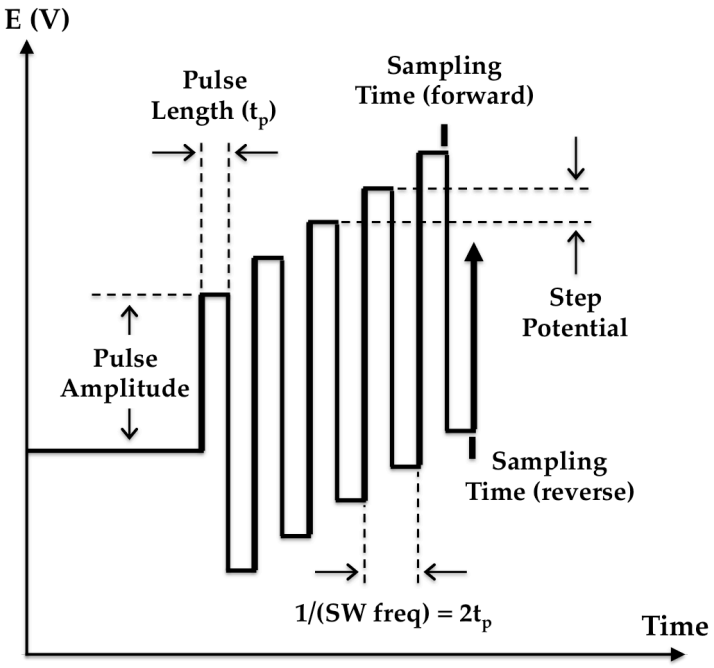

Figure 3.8. Applied potential vs. time plot for the square wave voltammetry (SWV) experiment. See text (Section 3.5) for explanation of experiment and parameters.

The resulting voltammograms display the forward, reverse, and net currents as a function of applied potential. For a reversible electrode process, the net current voltammogram displays a peak with maximum intensity (E_{net}) at a potential equal to $E_{1/2}$.[39] $E_{1/2}$ is known to equal the formal potential ($E^{0\prime}$) of the redox couple for diffusion-controlled systems in which the diffusion coefficient of the molecule does not change with changes in the oxidation state (see Equation 3.6).[39,100] Thus, achievement of a reversible system is of essence for determining formal potentials and to investigate their dependence on protein environment. Once we obtain these values, we can then explore their dependence on protein environment.

The extent of reversibility/irreversibility of a redox system is highly dependent on the time scale of the electrochemical experiment performed, as noted in Section 3.4.[100] Using SWV, we gain access to faster time scales, and, at the same time, we achieve background current suppression. The background suppression arises from two factors.[39,108] During each pulse time, the double layer charging current decreases exponentially with time, while the Faradaic current is inversely proportional to the square-root of time. Thus, at the end of each pulse (when the current is sampled), the charging current may be smaller than the Faradaic current. In addition, the charging current is partly eliminated, just as in DPV, because of the differential nature of the data. The current is sampled just before the end of each pulse, and the reverse current is subtracted from the forward current at each potential step. Given that the pulse amplitude is small, the background charging current does not change significantly between the anodic and the cathodic current sampling time.[108] Hence, the current subtraction results in the cancellation of the background contributions from the total current observed. This allows us to reach faster experimental time scales without the disadvantage of background currents obscuring the Faradaic signal of interest.

Previous electrochemical measurements on the α_3Y protein were performed using CV and DPV.[97] The cyclic voltammetry experiments yielded no current response due to the low sensitivity of this method. DPV, however, did display a signal unique to the tyrosine residue in the protein. DPV measurements were performed on a glassy carbon (GC) electrode and produced voltammograms with good signal-to-noise ratio (*S*/*N*). However,

SWV measurements on a GC electrode yielded responses with significantly lower *S/N*. We set out to explore the use of a different working electrode to be able to obtain good response from SWV. We decided to use electrodes that expose the edge plane of highly oriented pyrolytic graphite (HOPG), more commonly known as pyrolytic edge plane (PGE) electrodes. HOPG is composed of a lamellar arrangement of condensed stacked polyaromatic planes (graphene sheets) that are held together by van der Waals interactions between the layers.[101] The edge plane refers to the surface perpendicular to the layers, and can be activated to contain surface oxygen functional groups, as in the glassy carbon electrode (see Section 3.3). Square wave measurements were, thus, conducted using a PGE electrode. Several control experiments, either on a DPV/GC, DPV/PGE, or a SWV/PGE system, were done to find optimal conditions for electrochemical measurements in this electrode.

3.5.1. Optimization of Sample Conditions and Experimental Parameters

As discussed previously, sample conditions are one of the main factors that can affect the electrochemical response of a redox system. The buffer system of choice is composed of 20 mM sodium acetate, 20 mM potassium phosphate, and 20 mM sodium borate (APB buffer cocktail). The pK_A values for these buffers are 4.76 for acetate, 2.15, 7.20 and 12.3 for phosphate, and 9.24 for borate.[109] The combined buffering capacity of these buffers comprises a wide pH range (~1.2 to ~13.3). This buffer cocktail will allow us to effectively control the pH of our protein solution as we investigate the electrochemical response as a function of pH. In addition to buffer, an essential component of the

electrochemical sample is the supporting electrolyte. The supporting electrolyte is usually composed of a substance capable of conducting electricity without interfering in the redox reaction of interest; in this case, we have chosen to use potassium chloride (KCl) as it is a standard electrolyte that has been extensively used for electrochemical experiments in aqueous solutions.[39] The presence of supporting electrolyte aids in reducing the electrical resistance of the sample solution. However, an excess of this component may weaken the interactions between the analyte and the surface of the electrode. In our experimental setting, the protein under study is mainly positively charged due to the residues on the surface of the protein which include 17 positively charged lysine residues. The theoretical pI for this protein is ~8.79, as calculated by using the Bioinformatics Resource Portal, ExPASy.[110] The surface of the electrode is mainly negatively charged, as noted in Section 3.3. In order to assess the optimal salt concentration for the α_3Y experiments, control experiments were conducted in which $E_{1/2}$ was monitored as a function of the KCl concentration. The measurements were conducted using DPV at a PGE electrode at both acidic and alkaline pH, and the results are shown in Figure 3.9A. Figure 3.9A displays the obtained $E_{1/2}$ as a function of [KCl] for samples at pH 5.5 and 8.4 . At acidic pH, $E_{1/2}$ varies by 20 mV in the [KCl] range of 0 to 60 mM. At [KCl] of 75 to 140 mM, however, the half-wave potential reaches a plateau at 1,057 ± 3 mV. At alkaline pH conditions, $E_{1/2}$ is independent of salt concentration from 0 to 140 mM KCl, with an average $E_{1/2}$ value equal to 909 ± 1 mV. Measurements were done at higher [KCl] (> 140 mM) but the *S*/*N* achieved at these conditions was poor enough to make the analysis of the

response and the determination of $E_{1/2}$ increasingly more challenging. Thus, the optimal KCl concentration range was determined to be within 80 to 140 mM. Subsequent electrochemical experiments were done on samples containing 80 mM KCl.

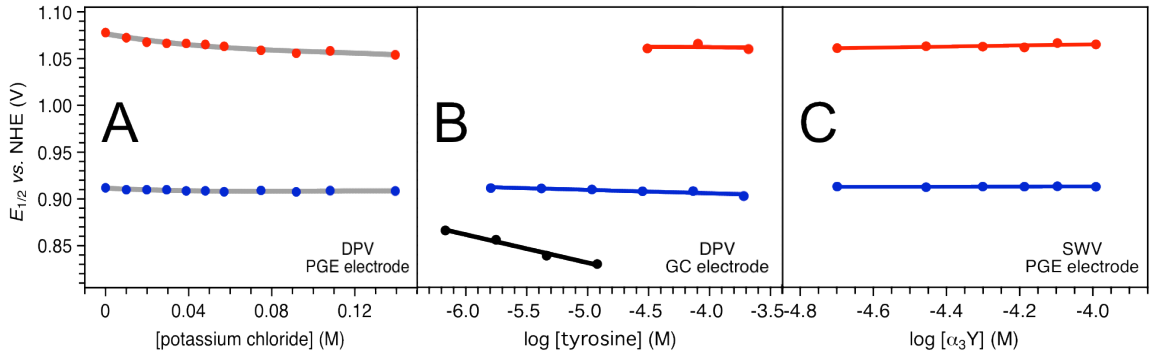

Figure 3.9. Optimization and control voltammetry experiments for the α_3Y system. **(A)** DPV $E_{1/2}$ as a function of concentration at pH 5.51 ± 0.01 (red circles) and pH 8.40 ± 0.01 (blue circles) using a PGE electrode. *Sample*: 60 μM α_3Y in 20 mM sodium acetate and 20 mM potassium phosphate (pH 5.5); 60 μM α_3Y in 20 mM potassium phosphate and 20 mM sodium borate (pH 8.4); temperature 25 °C. *Experimental settings*: interval time 0.1 s, step potential 0.9 mV, scan rate 9.0 mV s^{-1}, pulse time 7-8 ms, pulse amplitude 50 mV. **(B)** DPV $E_{1/2}$ potential of α_3Y as a function of protein concentration at pH 5.44 ± 0.03 (red circles) and pH 8.66 ± 0.02 (blue circles) using a GC electrode. *Sample*: α_3Y in 10 mM APB buffer and 100 mM potassium chloride at a temperature of 23 °C. *Experimental settings*: interval time 0.1 s, step potential 1.05 mV, scan rate 10.5 mV s^{-1}, pulse time 3-8 ms, pulse amplitude 50 mV. DPV $E_{1/2}$ potential of *N*-acetyl tyrosinamide (NAYA) as a function of NAYA concentration (black circles), using a GC electrode, is also shown. *Sample*: NAYA dissolved in 20 mM sodium acetate, 20 mM potassium phosphate and 200 mM potassium chloride at pH 5.46 ± 0.01. **(C)** SWV E_{net} potential of α_3Y as a function of the protein concentration pH 5.52 ± 0.01 (red circles) and pH 8.43 ± 0.01 (blue circles) using a PGE electrode. *Sample*: α_3Y in 20 mM APB buffer and 80 mM potassium chloride at a temperature of 25 °C. *Experimental settings*: step potential 0.15 mV, SW pulse amplitude 25 mV, SW frequency 190 Hz. All experiments were performed under an argon atmosphere. All potential values are referenced to NHE.

Optimal protein concentrations were also explored. SWV measurements were conducted by monitoring the peak potential of the net current

voltammogram (E_{net}) as a function of α_3Y concentration. Both acidic and alkaline conditions were examined. These control measurements were carried out in order to rule out two potential processes that may drastically influence the current response arising from the α_3Y system. The first process involves distorting interactions between the protein and the electrode surface, such as self-inhibition.[75,111] The second process involves dimerization reactions of the oxidized species, such as radical-radical and radical-substrate (in this case, radical-protein) dimerization reactions.[35] Figure 3.9C displays the results of these measurements. E_{net} values for samples at pH 5.5 and pH 8.4 remained independent of protein concentration throughout 20 to 100 μM α_3Y. The average E_{net} values at pH 5.5 and pH 8.4 were 1,063 ± 2 mV and 913 ± 1 mV, respectively. Either below or above this concentration range, voltammogram *S*/*N* degraded significantly. At concentrations lower than 20 μM, the protein concentration may be reaching the limit of the sensitivity of this technique for this system, thus degrading the signal intensity. At concentrations higher than 100 μM, other effects may come into play that distort the interaction between the protein and the electrode surface.[35,75] Measurements as a function of α_3Y concentration were also performed using DPV at a GC working electrode (see Figure 3.9B). Similar results were obtained in this setup, where no significant change in the peak potential was observed. Values of $E_{1/2}$ were 1,062 ± 5 mV and 909 ± 4 mV for pH 5.4 (30 – 200 μM) and pH 8.7 (2 – 200 μM), respectively. Furthermore, equivalent experiments were done on the freely solvated blocked tyrosine, NAYA, (black circles in Figure 3.9B), and a slope of -30.1 ± 2.6 mV per

decade of NAYA concentration. This slope is indicative of fast intermolecular radical-substrate dimerization reactions of the oxidized solvated small-molecule tyrosine analogue.[35] From the protein and small-molecule concentration series, we have shown that α_3Y does not undergo intermolecular radical-radical nor radical-substrate dimerization upon oxidation, under the sample conditions surveyed.[35]

SWV can also aid us in assessing the type of electrode kinetics that dictates the electron transfer reaction.[36,37,108,112] The electrode-driven reaction can occur with the pertinent species diffused in solution; the alternative situation will have the electroactive species adsorbed to the surface of the electrode. By varying the amplitude of the square wave E_{SW}, at low SW frequencies, we can determine if the oxidation is confined to the surface of the electrode or if the reaction follows diffusion-controlled kinetics. Voltammograms of surface-confined electrode reactions measured at low SW frequencies and large overpotentials (large pulse amplitudes) are expected to show a split in the peak response.[108,113] A series of measurements, at both acidic and alkaline conditions, were performed to explore this further. Figure 3.10 shows the voltammograms of 80 μM α_3Y in 20 mM APB buffer and 80 mM KCl measured at a PGE electrode. Square wave traces with E_{SW} values of 25, 50, and 75 mV were obtained for samples with solution pH 8.4 (SW frequency = 60 Hz) and at pH 5.2 (SW frequency = 190 Hz). The resulting data show that the peaks become broader for larger E_{SW} but no split in the current response was observed. On the basis of these results, we conclude that the α_3Y oxidation reaction at a PGE

electrode does not follow surface-confined kinetics but follows diffusion-controlled kinetics.

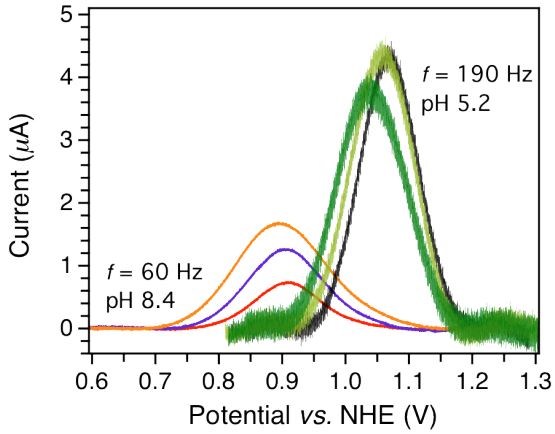

Figure 3.10. Square wave voltammograms collected for α_3Y as a function of pulse amplitude. Figure shows two data sets collected at two different pH values: pH 5.2 and 8.4. At each pH value, data was collected at three different pulse amplitude values: 25 mV (red and black traces), 50 mV (blue and light green traces) and 75 mV (orange and medium green traces). *Sample*: 80 μM α_3Y in 20 mM APB buffer and 80 mM potassium chloride at a temperature of 25 °C under an Ar atmosphere. *Experimental settings*: PGE working electrode, step potential 0.15 mV, SW pulse amplitude 25, 50 and 75 mV, SW frequency 60 Hz (pH 8.4) and 190 Hz (pH 5.2).

Additional experiments were done to examine the reproducibility of DPV and SWV. Representative voltammograms are shown in Figure 3.11 and 3.12 for DPV and SWV traces, respectively. Differential pulse voltammograms were recorded in triplicates of samples containing 200 μM α_3Y, 10 mM APB buffer, and 100 mM KCl at pH 8.6. $E_{1/2}$ values were obtained by either taking the maximum-intensity potential of background-corrected voltammograms or by taking the potential value at the zero-crossing of the first derivative of the background-corrected trace. The values obtained were 899 ± 3 mV and 902 ± 3

mV for the maximum-intensity and the first-derivative methods, respectively. Measurements of independent samples displayed an error of ± 4 mV. Square wave voltammograms were obtained in triplicates for samples containing 80 μM α_3Y, 20 mM APB buffer, and 80 mM KCl at pH 8.6 and at pH 5.4. $E_{1/2}$ values extracted from triplicates of the high-pH samples generated error bars of ± 3 mV for SW frequencies between 30 and 960 Hz. Low-pH samples yielded error bars of ± 2 mV for measurements done at SW frequencies: 190 and 540 Hz. Independent samples generated deviations in the same range as the triplicates. In all, measurements performed using either DPV and SWV displayed deviations of, at most, 4 mV for traces from the same and independent samples. These results show that the electrochemical voltammograms obtained for the α_3Y system are highly reproducible for both DPV and SWV.

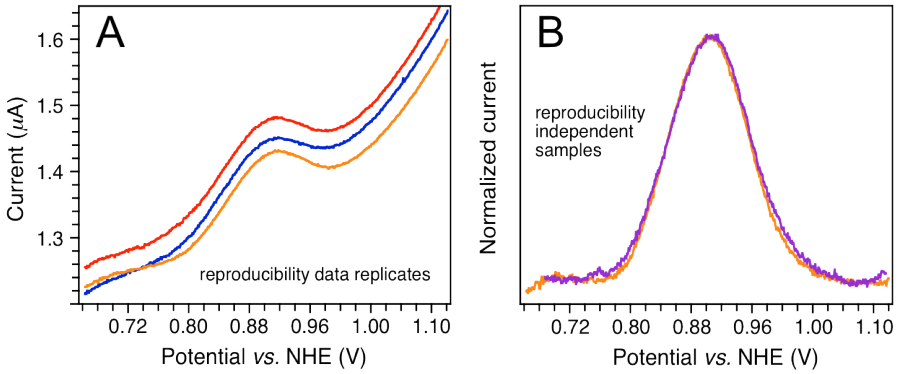

Figure 3.11. Reproducibility of DPV measurements. (A) α_3Y raw DP voltammograms in triplicate (pH 8.59). **(B)** Background-corrected α_3Y DP voltammograms obtained from two independent measurements using identical experimental settings. *Sample*: 200 μM α_3Y in 10 mM APB buffer and 100 mM KCl at a temperature of 23 °C. *Experimental settings*: GC working electrode, interval time 0.1 s, step potential 1.05 mV, scan rate 10.5 mV s^{-1}, pulse time 6 ms, pulse amplitude 50 mV.

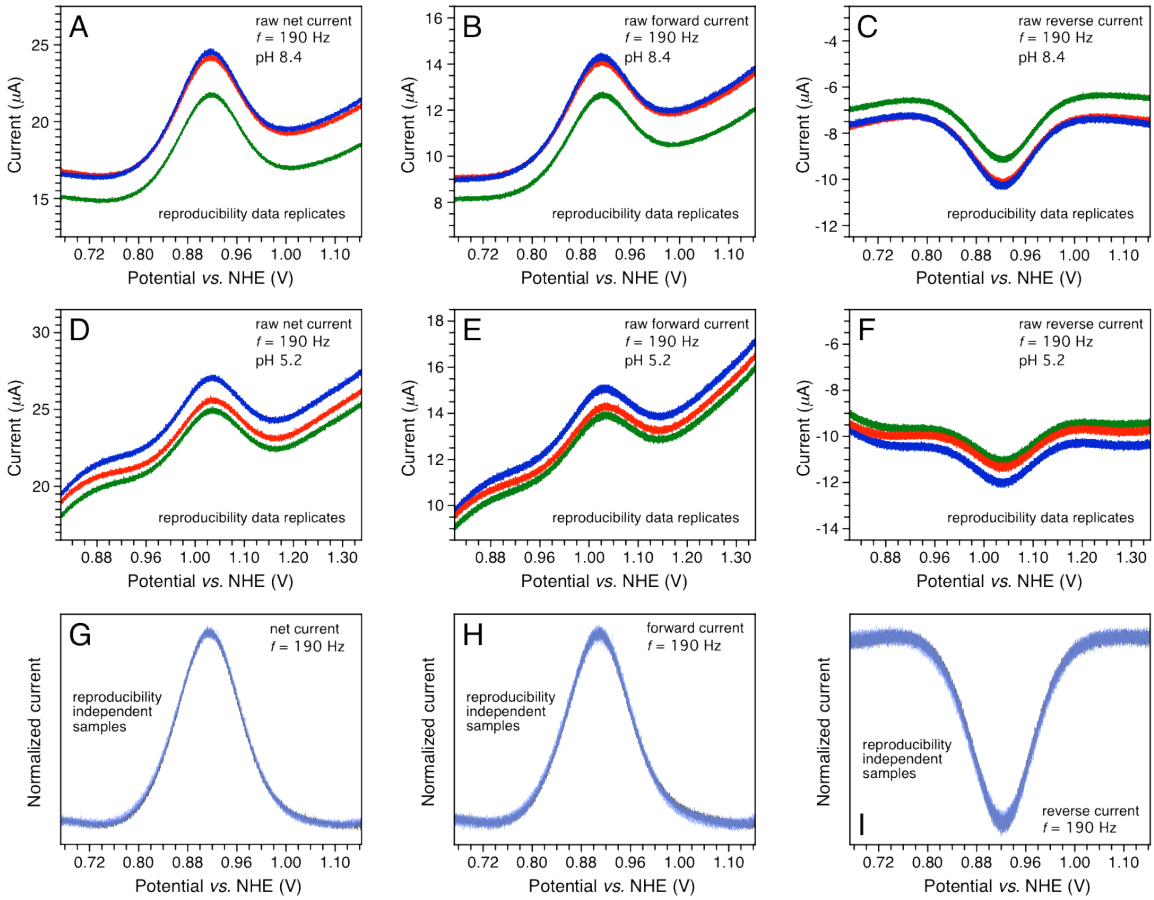

Figure 3.12. Reproducibility of SWV measurements. This figure shows typical α_3Y raw SW voltammograms for net **(A)**, forward **(B)** and reverse **(C)** currents for samples at pH 8.40. Also shown are typical α_3Y raw SW voltammograms for net **(D)**, forward **(E)** and reverse **(F)** currents for samples at pH 5.52. **(A)** – **(F)** show triplicates of the data. Panels **(G)**, **(H)** and **(I)** show net, forward and reverse background-corrected voltammograms, respectively, obtained from two independent measurements at pH 8.41. *Sample*: 80 μM α_3Y in 20 mM APB buffer and 80 mM potassium chloride at a temperature of 25 °C under an Ar atmosphere. *Experimental settings*: PGE working electrode, step potential 0.15 mV, SW pulse amplitude 25 mV, SW frequency 190 Hz.

3.5.2. Experimental Timescale in SWV Can Be Set to Outcompete Coupled Chemical Reactions

Once the optimal conditions for voltammetric measurements were defined and the type of electrode kinetics was determined, a series of

experiments were conducted as a function of the square wave frequency *f*. The frequency is a key parameter in the SW experiment. As discussed above, *f* defines the pulse time t_p, hence dictating the time the generated oxidized species is let to exist before the reductive pulse is applied. By varying *f*, the SW experiment can be set to outcompete side chemical reactions; the practical frequency range for SWV goes from 8 to 2000 Hz, which translates to a t_p practical range of 63 ms – 250 μs.[108] In that situation, the voltammograms obtained result from a purely electrode-driven electron transfer process without the influence from coupled chemical reactions (see EC mechanism in Section 1.3).

SWV experiments were conducted on a 80 μM α_3Y sample containing a 20 mM APB buffer cocktail, 80 mM KCl as supporting electrolyte and a solution pH of 8.4.[114] Measurements were done using frequency values from 30 to 960 Hz (equivalent to pulse times from 16.7 ms to 521 μs). Panels A, B, and C of Figure 3.13 display representative forward and reverse background-corrected voltammograms from this frequency series, for 190, 540, and 750 Hz, respectively.

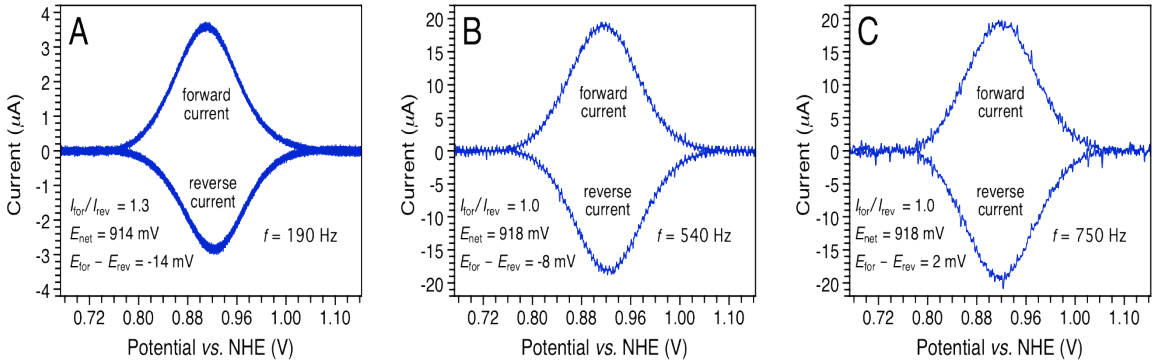

Figure 3.13. Representative square wave voltammograms obtained for α_3Y for frequency series. The full frequency series data includes voltammograms obtained at frequencies: 30 – 960 Hz, which corresponds to a time pulse range of 16.7 ms to 521 μs. Panels in this figure show α_3Y forward (oxidation) and reverse (reduction) square wave voltammograms obtained at SW frequency values of 190 **(A)**, 540 **(B)** and 750 **(C)** Hz. *Sample*: 80 μM α_3Y in 20 mM APB buffer and 80 mM potassium chloride at pH 8.40 ± 0.01 at a temperature of 25 °C under an Ar atmosphere. *Experimental settings*: PGE working electrode, step potential 0.15 mV, SW pulse amplitude 25 mV. All potentials are referenced to NHE.

The following values were extracted from the frequency series data: forward, reverse and net peak potentials (E_{for}, E_{rev} and E_{net}), the ratio of forward-reverse peak intensities (I_{for}/I_{rev}) and the difference between the forward and reverse peak potentials, $E_{for} - E_{rev}$. These values are listed in Table 3.1. Figure 3.14 displays a plot of E_{for}, E_{rev}, and E_{net} as a function of SW frequency. The data shows how the values of E_{for}, E_{rev}, and E_{net} become independent of the SW frequency at f equal to 750 Hz. Independence on SW frequency is characteristic of a fully reversible electrode-driven electron transfer process.[36,108] Furthermore, a decrease in the value of I_{for}/I_{rev} is observed, from its value at 30 Hz (1.71 ± 0.14) until it reaches a limiting value of 1.01 ± 0.02 in the 750 – 960 Hz range. Current response is directly proportional to the amount of electroactive species being oxidized/reduced.[39] Hence, these results suggest that all of the molecules

that get oxidized during the oxidative pulse are subsequently re-reduced by the electrode during the reductive pulse, further providing support for the reversible nature of the electrode process at frequencies larger than 750 Hz.

Table 3.1. α_3Y Electrochemical Data Extracted from the SWV Frequency Series.

Freq. (Hz^{-1})	t_p (ms)	E_{for} (mV)	E_{rev} (mV)	E_{net} (mV)	$\lvert E_{for}-E_{rev} \rvert$ (mV)	I_{for}/I_{rev}
30	16.67	900.8 ± 4.9	910.5 ± 4.5	905.1 ± 0.5	9.7	1.7 ± 0.1
60	8.33	905.7 ± 3.4	917.0 ± 1.9	910.3 ± 2.5	11.3	1.6 ± 0.1
120	4.17	907.5 ± 1.7	920.9 ± 0.9	913.5 ± 1.2	13.4	1.4 ± 0.0
190	2.63	907.6 ± 1.2	922.0 ± 0.8	914.0 ± 1.0	14.4	1.3 ± 0.0
240	2.08	910.3 ± 1.8	923.7 ± 1.3	916.4 ± 1.5	13.4	1.2 ± 0.0
300	1.67	909.3 ± 0.7	922.1 ± 0.4	915.3 ± 0.6	12.8	1.2 ± 0.0
440	1.14	912.8 ± 0.6	921.7 ± 0.4	917.2 ± 0.4	8.9	1.1 ± 0.0
540	0.93	914.1 ± 1.3	921.8 ± 2.0	917.9 ± 1.4	7.7	1.1 ± 0.0
750	0.67	919.1 ± 1.5	917.6 ± 2.3	918.3 ± 1.9	1.5	1.0 ± 0.0
960	0.52	918.6 ± 0.5	916.7 ± 0.6	917.7 ± 0.4	1.9	1.0 ± 0.0

All potential values are referenced to NHE. Error values represent standard deviation of triplicate measurements. Sample and experimental settings are described in the legend of Figure 3.13.

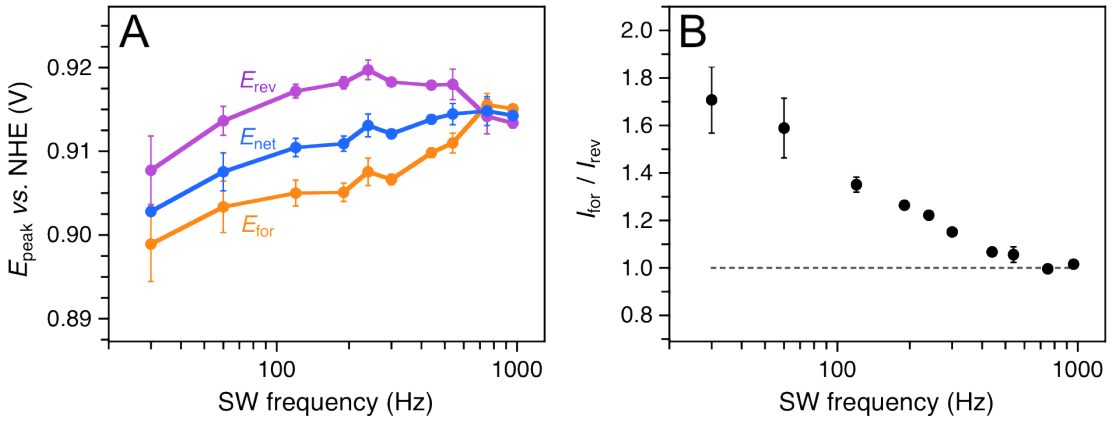

Figure 3.14. Analysis of SW frequency series obtained from electrochemical characterization of α_3Y. Panel **(A)** shows the net (E_{net}), forward (E_{for}) and reverse (E_{rev}) peak potentials of voltammograms obtained for α_3Y as a function of SW frequency. Panel **(B)** shows the ratio of forward and reverse current (I_{for}/I_{rev}) as a function of SW frequency. Sample and experimental settings are described in the legend of Figure 3.13.

The net potential obtained from a fully reversible electrode process equals the half-wave potential of the redox couple which, in turn, equals the formal potential for diffusion-controlled systems if the diffusion coefficient does not depend on the oxidation state of the molecule (see Equation 3.6). The diffusion coefficient for the reduced state of α_3Y (D_{red}) was determined by making use of pulsed field gradient NMR experiments.[115] The absolute intensity of each spectrum was plotted against magnetic field gradient strength and the plot was fitted to Equation 3.10.[115]

$$E = exp\left\{-\frac{4}{\pi^2}\gamma^2 D\delta^2\left[\left(\Delta - 4\delta^2 - \frac{5}{2}\delta\right)g^2 + \delta g g_1 + (3\delta + 8\delta_2)g_1^2\right]\right\}, \quad (3.10)$$

where E, in this case (not to be confused with potential), is the diffusion-based spin-echo attenuation for the double echo PGSTE-WATERGATE NMR pulse sequence with half sine shaped gradients, γ is the gyromagnetic ratio for the hydrogen nucleus in radians Gauss^{-1} s^{-1} (2π*4257.7 Gauss^{-1} s^{-1}), D is the diffusion constant in cm^2 s^{-1}, δ is the duration of the pulsed gradient (0.006 s), Δ is the diffusion time (0.1 s), δ_2 is the second delay time in the pulse sequence (0.002 s), g is the effective pulse gradient which equals the difference between pulse gradient 1 (g_1) and pulse gradient 2 (g_2) in the pulse sequence, which are gradients of different amplitudes. The value of g_2 is fixed at 15.889 Gauss cm^{-1},

while g_1 is varied linearly in each of the experiments. Figure 3.15 shows the degradation of the signal intensity as a function of field gradient strength.

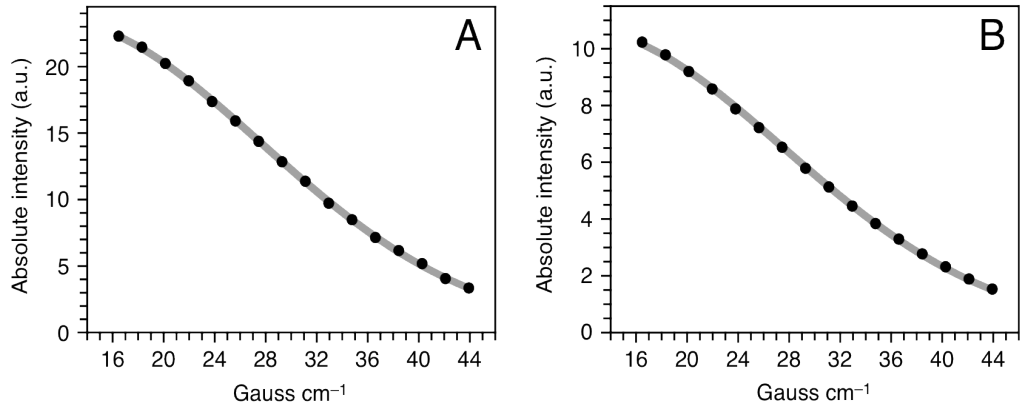

Figure 3.15. Determination of diffusion constant of α_3Y by pulsed field NMR. Panels **(A)** and **(B)** show diffusion attenuation plots for signal intensities for amide (HN) and aliphatic (HC) protons, respectively, as a function of magnetic field gradient strength. Gray lines represent fits to Equation 3.9.[115] Fits for HN data yielded an R^2 value of 0.9999 and a χ^2 value of 9.5678×10^{12}. Fit for HC data yielded an R^2 value of 0.9998 and a χ^2 value of 2.7612×10^{14}. *Sample*: 500 μM α_3Y in 20 mM deuterated sodium acetate, 20 mM potassium phosphate, 20 mM sodium borate and 140 mM potassium chloride in a 5% D_2O/95% H_2O solvent system at pH 6.6 and at a temperature of 25 °C. *Experimental settings*: magnet 11.7 Tesla (500 Hz); complex points for 1st dimension 8192; number of scans 1504; sweep width for 1st and 2nd dimension 16.8 and 10.3, respectively; proton carrier set at 4.698 ppm; pulsed field gradient was varied linearly for each point (16 total points) in the 2nd dimension from 16.5 to 43.9 Gauss cm^{-1}, generating 16 spectra, each with a different pulse field gradient value. Each point in the plots represents the absolute signal intensity (volume) of each of the 16 generated spectra.

The diffusion coefficient was calculated separately for amide (D_{amide}) and aliphatic ($D_{aliphatic}$) proton signals: (1.464 ± 0.006) and $(1.472 \pm 0.008) \times 10^{-6}$ cm^2 s^{-1}, respectively. An average between these two values is reported as D_{red}. The D_{red} value was calculated to be $1.47 \pm 0.01 \times 10^{-6}$ cm^2 s^{-1}. This value falls within the range known for small soluble proteins and it is unlikely to change significantly due to the loss of an electron and a proton upon oxidation.[114] Thus, the E_{net} values obtained from SWV at the frequency range of 750 – 960 Hz can be taken

as formal potential values for the α_3Y redox system. We conclude that the formal potential for the protein Y-OH/Y-O$^{\bullet}$ redox couple in α_3Y equals 918 ± 2 mV at pH 8.4.

Given that the protein Y-OH/Y-O$^{\bullet}$ redox couple starts showing reversible behavior at a frequency value of 750 Hz (pulse time equal to 667 μs), the neutral protein radical survives for, at most, 667 μs before side chemical reactions begin to have an influence over the thermodynamics of the electron transfer process. Moreover, according to theoretical treatments of EC mechanisms for square wave voltammetry, the influence of the coupled chemical reaction on the net peak potential approaches zero when

$$\log\left(2t_p k_{chem}\right) \leq -1.5, \tag{3.11}$$

where k_{chem} describes the homogeneous rate constant of the coupled chemical reaction.[37,112] The value of t_p can be readily obtained from the frequency of the experiment (freq = $1/2t_p$). Hence, by using the relationship described in Equation 3.11, we can obtain an upper limit for the value of k_{chem}. From the measurements as a function of square wave frequency, we observe that coupled chemical reactions cease to influence the net peak potential at a frequency value of 120 Hz, evidenced by a standard deviation of ± 2 mV in the 120 – 960 Hz range. As described, k_{chem} can be readily calculated to be ≤ 4 s^{-1}. It was determined in Section 3.5.1 that α_3Y does not undergo intermolecular radical-radical nor radical-protein dimerization upon oxidation in the concentration

range of 20 – 100 μM. Coupled chemical reactions, in that concentration range, are likely to arise from intramolecular radical-substrate reaction within the protein matrix. Assuming first-order kinetics for the side chemical reactions, a halflife ($t_{1/2}$) value can be obtained from the homogeneous rate constant by using the following relationship (Equation 3.12)[117]:

$$t_{1/2} = \frac{\ln 2}{k_{chem}}. \tag{3.12}$$

According to this kinetic relationship, k_{chem} value of ≤ 4 s^{-1} corresponds to a radical halflife of ≥ 170 ms.

The environment surrounding the tyrosine radical site is mainly composed of aliphatic protons, as was determined previously by ^{1}H-^{1}H 2D NOESY experiments.[13] Likely, side reactions of Y32-O$^{\bullet}$ might involve hydrogen abstraction from the C–H groups residing at the core of the protein. The kinetics of these reactions are typically described by low rate constants,[118] which allows the radical to survive for long enough for it to be re-reduced in our experimental setup.

3.5.3. Quasireversible electrochemical behavior for α_3Y at acidic sample conditions

Square wave voltammograms were also collected at acidic solution pH. SW voltammograms for α_3Y samples (80 μM protein in 20 mM APB buffer and 80 mM KCl) at pH 5.5 are shown in Figure 3.16. The analysis of these voltammograms was complicated by the decrease in signal intensity at lower

pH, and also by the shift of the peak potential to higher potential values, where background currents arising from water oxidation and the electrode itself are more pronounced.[39,101] Voltammograms with satisfactory *S/N* were obtained using SW frequency values of 190 and 540 Hz.

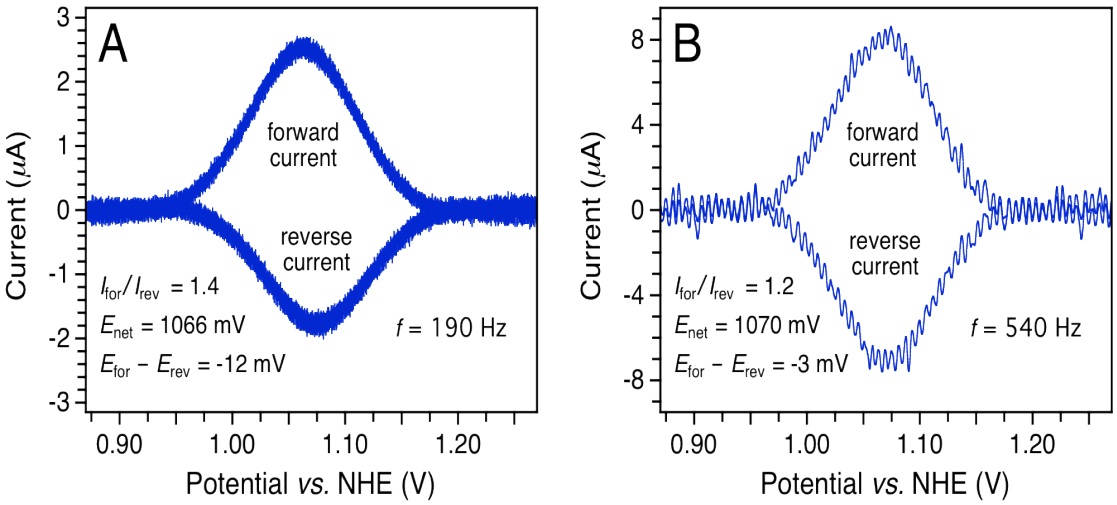

Figure 3.16. Square wave voltammograms obtained for α_3Y sample in acidic conditions. Forward and reverse current as a function of applied potential for α_3Y samples using SW frequency values of **(A)** 190 and **(B)** 540 Hz. *Sample*: 80 μM α_3Y in 20 mM APB buffer and 80 mM potassium chloride at pH 5.52 ± 0.01 at a temperature of 25 °C under an Ar atmosphere. *Experimental settings*: PGE working electrode, step potential 0.15 mV, pulse amplitude 25 mV.

Comparison of the resulting forward, reverse and net voltammograms for both these experimental conditions yields several observations. First, the I_{for}/I_{rev} ratio shows a decrease from 1.44 ± 0.03 at 190 Hz to 1.15 ± 0.01 at 540 Hz. Second, the difference in potential between the forward and reverse peak potentials is reduced at the higher frequency value. Finally, the net peak potential increases from 1,066 ± 2 mV at 190 Hz to 1,070 ± 1 mV at 540 Hz. All these observations

are consistent with the results obtained for α_3Y samples at higher pH. The voltammograms at these frequencies describe electrode-driven ET processes in the upper range of the quasireversible regime, meaning that the E_{net} value obtained deviates from $E°'$ by, at most, ~6 mV.[108] We conclude that the net peak potential obtained at measurements performed at 540 Hz (1,070 ± 1 mV) closely approximates the formal potential of the protein Y-OH/Y-O$^{\bullet}$ redox couple at pH 5.5.

3.6. Connection between results obtained via DPV and SWV

Further information from the α_3Y system can be extracted by comparing the results obtained from SWV and DPV (pH series in Section 3.3). The formal potential at pH 8.4 (≥ 750 Hz) obtained from SWV is 918 ± 2 mV. DPV yields a $E_{1/2}$ value of 916 ± 3 mV at the same pH value. We observe that there is no significant difference between the values obtained at this pH, meaning that the electrochemical response monitored by DPV at pH 8.4 is, also, representative of a fully reversible electron transfer process. On the other hand, comparison of potentials obtained by both techniques at pH 5.5 yields a difference of ~ 22 ± 3 mV, with DPV yielding lower potential values. This difference may result from the influence of coupled protonic reactions within the protein matrix. It is well known that the thermodynamic and kinetic characteristics of tyrosine are strongly influenced by hydrogen-bonding interactions (see Section 1.5), as well as by the chemical nature of the species accepting the released proton upon oxidation.[85] As discussed in Section 3.3, a residue B is hypothesized to capture

the phenolic proton upon tyrosine oxidation. At pH 5.5, residue B is already protonated, thus rendering it unavailable to participate in protonic reactions associated with the redox event. This fact may alter the heterogeneous ET rate constant, driving the reaction towards the quasireversible regime; this effect is reflected in the shift of the obtained $E_{1/2}$.[108] On the contrary, at the higher pH value, residue B is deprotonated and able to capture the proton released by Y32, aiding the reaction and driving it towards the reversible regime.

3.7. Summary

In this chapter, we have utilized the electrochemical approach to obtain thermodynamic and kinetic information for a PCET process involving a tyrosine residue inside a stable, well-structured and redox-inert protein framework. The protein used was the *de novo*-designed three-helix bundle protein α_3Y. The electrochemical experiments and setup are described. Several voltammetry techniques are utilized with the aim of gaining insights into the redox chemistry of residue Y32. Cyclic voltammetry proves not to be sensitive enough to detect Faradaic responses from Y32, whereas a current response is achieved by differential pulse voltammetry. Using DPV, a half-wave potential vs. pH (or Pourbaix) diagram is obtained. Analysis of the Pourbaix diagram suggests the involvement of an additional residue in the PCET process. The pK_A of this residue of unknown identity is increased upon oxidation of Y32, suggesting that the protonated state of this residue is favored upon ET. With these results, we anticipate that the protein scaffold not only participates in the

PCET process induced by the DPV oxidative pulse but also that it modulates the redox behavior of Y32.

Several factors are taken into consideration in order to further investigate the influence of the protein scaffold on the redox chemistry of Y32. The products of tyrosine oxidation are typically highly reactive molecules that become involved in side chemical reactions, thus obscuring the reversible/irreversible nature of the ET process. This issue was addressed by developing the use of square wave voltammetry for these protein systems. SWV allows us to reach faster experimental time scales without the disadvantage of large background currents (such as in CV) that complicate the current signal obtained. Once sample and experimental conditions were achieved for our system, a series of measurements were carried out as a function of SW frequency with the objective of making the reverse electrochemical reaction (re-reduction) fast enough to outcompete coupled chemical reactions. If this objective is achieved, the resulting voltammograms would reflect a purely PCET event without the influence of coupled chemical reactions. This experiment was carried out by obtaining voltammograms at frequency values that ranged from 30 to 960 Hz (pulse times from 16.7 ms to 521 μs). It was found that, in this system, the pulse time can be set short enough for the reductive pulse to effectively outcompete side chemical reactions; thus allowing access to the reversible regime. This occurred at frequency values equal or larger than 750 Hz (pulse times equal or shorter than 667 μs) for protein solutions at pH 8.4. Thus, we have achieved the development of the first model protein system in which oxidation of a TYR residue is completely

reversible. Assuming that the diffusion constant of the protein is independent of its oxidation state, we conclude that the half-wave potential obtained at these frequencies represent the formal potential for the Y32-OH/Y32-O$^{\bullet}$ redox couple at pH 8.4: 918 ± 2 mV. Following theoretical treatments for these systems,[37,112] we have provided evidence that the neutral Y32 radical generated upon electrochemically induced oxidation has a halflife of at least 170 ms.

The electrochemical behavior of Y32 was also explored at acidic sample conditions (pH 5.5) and it was found that due to degradation of the signal intensity and increased contribution from background currents, voltammograms of satisfactory signal-to-noise ratio could only be obtained at two SW frequency values, 190 and 540 Hz (pulse times, 2.6 ms and 926 μs, respectively). These voltammograms represent a PCET process occurring within the upper range of the quasireversible regime at which half-wave potentials obtained only differ from the formal potential by, at most, 6 mV. Thus, we can conclude that the half-wave potential obtained at these conditions ($E_{1/2}$ = 1070 ± 1 mV) closely approximates the formal potential of the Y32-OH/Y32-O$^{\bullet}$ redox couple at pH 5.5.

On the basis of the SWV results, the results obtained by DPV were reassessed. At alkaline sample conditions (pH 8.4), these two voltammetry techniques yield comparable results; $E_{1/2}$ equals 918 ± 2 mV and 916 ±3 mV for SWV and DPV, respectively. Thus, indicating that at pH 8.4, DPV gives rise to half-wave potential values arising from a reversible PCET redox system. However, at acidic conditions (pH 5.5), a decrease is encountered in the DPV-derived results in comparison with the results obtained with SWV. Involvement

of the protein scaffold in the PCET event may be responsible for this difference between the electrochemical behavior at low and high pH. As mentioned earlier, the pK_A of a residue of unknown identity increases upon oxidation of Y32. At pH 8.4, this residue is deprotonated which may allow it to act as a proton acceptor in the process. As with the small-molecule models described in Section 1.5, proton acceptors that keep the proton local to the oxidation site decrease the level of irreversibility of the ET process. On the other hand, the additional residue is already protonated at pH 5.5. In this case, this residue cannot capture the released proton and cannot aid the ET process. Proton release, in this case, might become rate-limiting and drive the electron-transfer reaction into the upper quasireversible regime.

In conclusion, we have achieved the development of a system in which the protein scaffold is intimately involved in the PCET event triggered by electrochemically applied potentials. We have captured two situations, one in which a protein residue acts as a proton acceptor and assists the electrode-driven oxidation-reduction process, and the other in which this residue does not play a role in the process. Both situations give rise to differences in the obtained potentials, which suggests that interactions to the protein milieu can modulate the thermodynamics of the proton-coupled electron transfer involving the tyrosine residue.

CHAPTER 4: Generation of an Interaction Between a Tyrosine and a Histidine Inside a Model Protein

4.1. Generation and characterization of HIS-containing α_3Y variants

We have seen from earlier studies[13] and from Chapter 3, that α_3Y is a viable model for radical proteins. The protein is well-structured, and we have provided evidence that the protein scaffold becomes involved in TYR PCET and that it can provide an stabilizing environment for an oxidized TYR residue. The next step in the development of this protein model system is to engineer specific interactions to the tyrosine radical within the protein milieu and investigate how the redox properties of TYR are influenced by them. Inspired by the natural systems and by the small-molecule model systems previously discussed, we have set out to re-engineer the α_3Y protein to introduce a histidine residue close to the side chain of Y32. The aim is to create an interaction between the phenol headgroup of Y32 and the imidazole ring of the introduced histidine. The initial α_3Y sequence originally contains no histidines (see sequence in Section 2.2). Owing to the similar structural characteristics between α_3Y and α_3W, the NMR structure of α_3W (pdb id: 1LQ7)[56] was used to generate several α_3Y models with different Y32 χ^1 dihedral angles, in order to identify potential sites in the protein in which a histidine residue could have its imidazole side chain in close proximity to the Y32 phenol group. Histidine was modeled into each identified site, which generated a number of Y32/HIS χ^1 rotamer combinations. Models in which the imidazole ring and the Y32

hydroxyl group were within 5 Å were chosen for further examination. This modeling step generated eight α_3Y-HIS variants: α_3Y-V9H, α_3Y-L12H, α_3Y-E13H, α_3Y-K29H, α_3Y-E33H, α_3Y-K36H, α_3Y-L58H and α_3Y-I62H. The positions of the introduced histidines are highlighted in the α_3Y structure model shown in Figure 4.1.

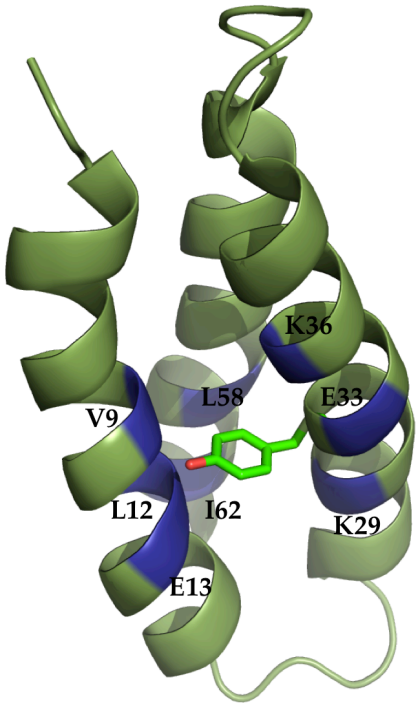

Figure 4.1. Cartoon representation of α_3Y model with HIS mutation sites highlighted. Model of α_3Y structure is depicted in green and was generated by inserting a single W32Y mutation in the α_3W structure (PDB id: 1LQ7)[56] using the program PyMOL[119]. The single TYR residue is shown in stick representation. The sites of mutation (V9, L12, E13, K29, E33, K36, L58 and I62) are highlighted in blue.

The eight α_3Y-HIS variants were characterized in detail to assess their structural stability and the extent to which they contained a detectable

interaction between the redox-active tyrosine residue, Y32, and the introduced histidine residue. Interaction between the Y32 phenol group and the imidazole ring of the incorporated histidine residue was investigated by obtaining absorbance and fluorescence data on the variants. It is known that the optical properties of tyrosine molecules are sensitive to the dielectric and hydrogen-bonding properties of its surrounding medium.[86-88] The absorption spectra of NAYA and Y32 in α_3Y exemplify this behavior. The absorption spectrum of α_3Y is red shifted relative to the corresponding spectrum for NAYA, which is consistent with a tyrosine molecule going from being fully solvent exposed to being shielded from bulk solution. This confirms the previous report that Y32 in α_3Y is sequestered in the core of the protein.[13] Furthermore, from the structure of α_3W, the solvent accessible surface area (SASA) of W32 was calculated to be (2.6 ± 1.4) % across the NMR structural ensemble.[56] Absorbance spectra for Y32 in α_3Y and each of the α_3Y-HIS variants were obtained. Inspection of these absorption spectra reveals no significant differences between the α_3Y-HIS variants. However, fluorescence excitation and emission spectra provided more distinguishing information. Excitation and emission spectra of proteins α_3Y-E13H, α_3Y-E33H and α_3Y-E58H are not distinguishable from those obtained for α_3Y. Emission spectra for these three proteins at both acidic and alkaline pH are shown in Figure 4.2. We anticipate that the introduced imidazole group is not in sufficient proximity to the side chain of Y32, and decided to exclude these three proteins from further characterization.

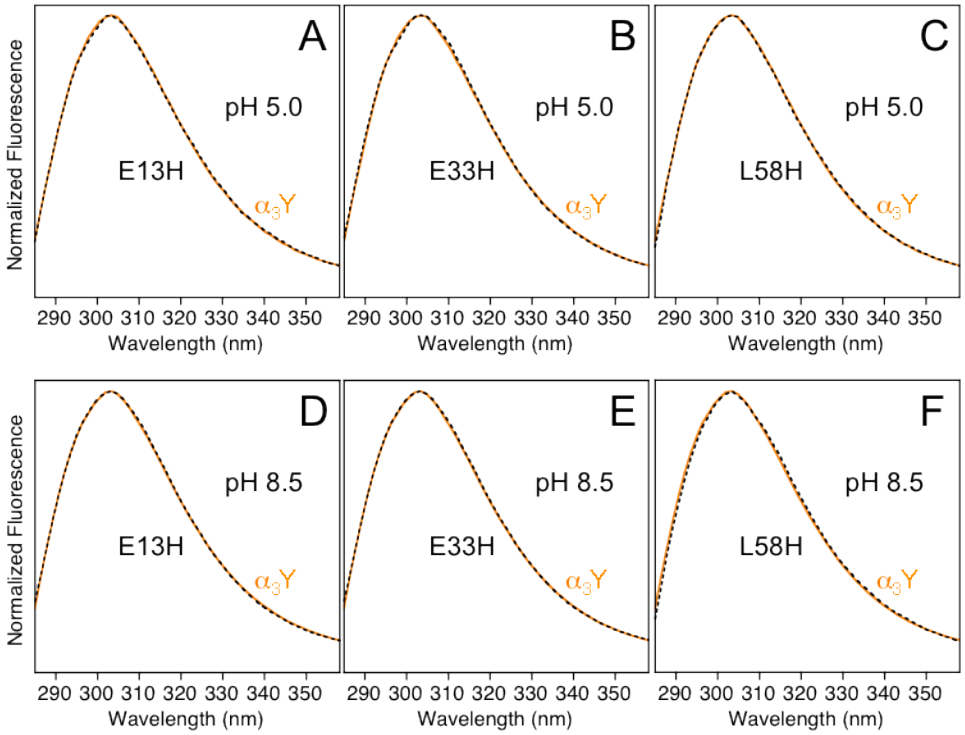

Figure 4.2. Fluorescence emission spectra for α_3Y-E13H, α_3Y-E33H, and α_3Y-L58H at acidic and alkaline conditions. The orange spectra represent α_3Y while the dashed black spectra represent three different α_3Y-HIS variants at pH 5.0 (panels **A**, **B** and **C**) and at pH 8.5 (panels **D**, **E** and **F**). The pH 5.0 samples were prepared in 15 mM sodium acetate and 30 mM KCl. The pH 8.5 samples were prepared in 15 mM TRIS and 30 mM KCl. The spectra were obtained at room temperature.

Excitation and emission spectra for α_3Y-V9H, α_3Y-L12H, α_3Y-K29H, α_3Y-K36H and α_3Y-I62H did, however, show shifts relative to α_3Y spectra. Fluorescence spectra that showed differences between α_3Y and the variant protein are shown in Figure 4.3. These five proteins were chosen for further characterization.

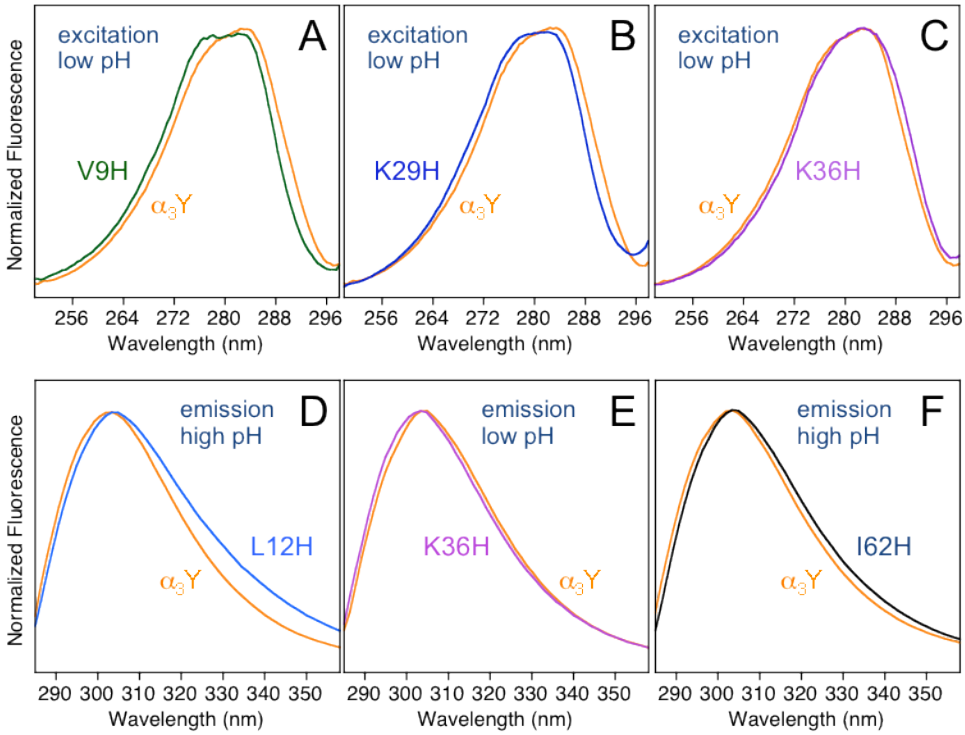

Figure 4.3 Fluorescence emission and excitation spectra for α_3Y-HIS variants. Y32 fluorescence excitation (panels **A**, **B** and **C**) and/or emission (panels **D**, **E** and **F**) spectra. Samples conditions were as follows: (**A**) α_3Y (orange) and α_3Y-V9H (green) in 15 mM sodium acetate, 30 mM KCl, pH 5.0; (**B**) α_3Y (orange) and α_3Y-K29H (blue) in 10 mM sodium acetate, 30 mM KCl, pH 5.5; (**C**) α_3Y (orange) in 15 mM sodium acetate, 30 mM KCl, pH 5.0 and α_3Y-K36H (magenta) in 10 mM sodium acetate, 30 mM KCl, pH 5.5; (**D**) α_3Y (orange) and α_3Y-L12H (cyan) in 10 mM TRIS, 15 mM KCl, pH 8.2; (**E**) α_3Y (orange) in 15 mM sodium acetate, 30 mM KCl, pH 5.0 and α_3Y-K36H (magenta) in 10 mM sodium acetate, 30 mM KCl, pH 5.5; (**F**) α_3Y (orange) and α_3Y-L58H (black) in 15 mM TRIS, 30 mM KCl, pH 8.5. The spectra were obtained at room temperature.

In order to confirm that these spectral shifts are due to changes in local interactions to the Y32 residue, these proteins must not reflect changes in the their global structure. In addition, the proteins should remain stable throughout a pH range that includes both protonation states of the HIS residue. Apparent pK_A (pK_{APP}) values were obtained for Y32 and the corresponding HIS residue in each of the five variants. pK_{APP} values for tyrosine were determined by

monitoring the tyrosinate absorption at 293 nm as a function of pH (see Figure 4.4), while pK_{APP} values for histidine were obtained by following the NMR chemical shift of the histidine ε1 ring proton as a function of pH (see Figure 4.4). The pK_{APP} values are listed in Table 4.1.

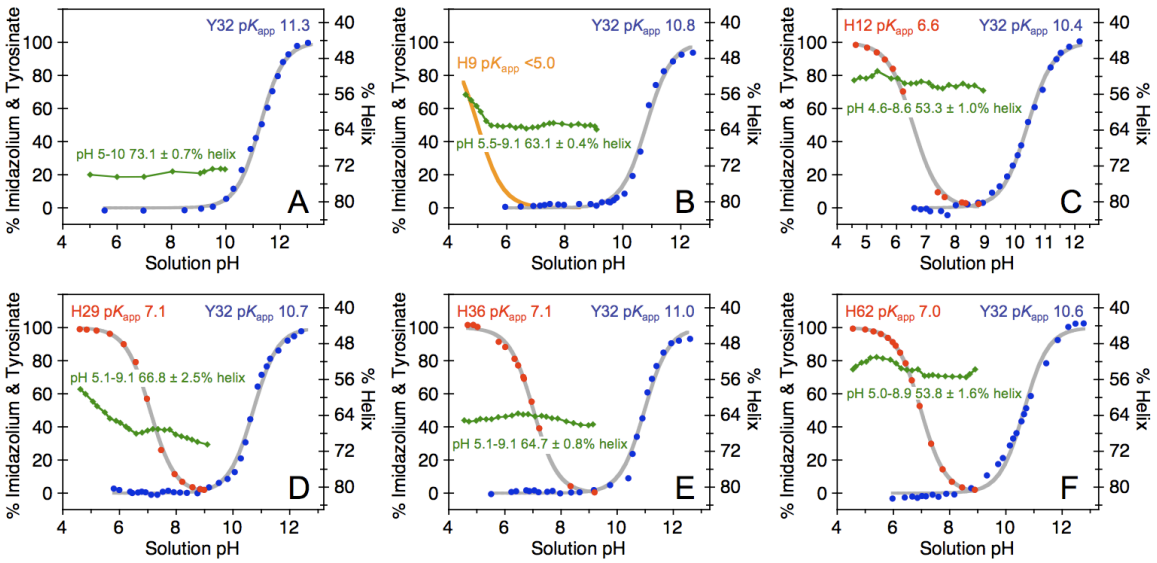

Figure 4.4. Determination of physicochemical properties of α_3Y and the single-site HIS variants. pH titrations of Y32 (blue circles) and HIS residues (red circles) are shown for **(A)** α_3Y, **(B)** α_3Y-V9H, **(C)** α_3Y-L12H, **(D)** α_3Y-K29H, **(E)** α_3Y-K36H, **(F)** α_3Y-I62H. pK_{APP} values were derived by nonlinear curve fitting (gray lines, Table 4.1). See Section 7.4 and 7.5 for more details on the determination of the pK_{APP} values and fitting statistics. α-helical content as a function of pH are also shown for each protein (green diamonds). See Section 7.6 for more details on the determination of helical content.

The structural integrity of each of the five remaining variants was verified by determining their absolute α-helical content and the pH stability of this parameter, as well as the global protein stability. CD spectroscopy was applied by measuring the mean residue ellipticity at 222 nm ($[\Theta]_{222}$) as a function of pH for pH stability experiments (see Section 2.3)[92], and as a function of

concentration of urea for determination of global protein stability[94]. A plot of the pH dependence of the degree of helicity is shown in Figure 4.4, and mean values are listed in Table 4.1. The degree of helicity of α_3Y-V9H, α_3Y-K29H and α_3Y-K36H showed only a minor decrease (~5 – 10 %) compared to α_3Y. These three proteins displayed well-defined unfolding/folding transitions in their chemical denaturation plots, which is indicative of a two-state folding process.[94] Chemical denaturation plots are shown in Figure 4.5. Table 4.1 lists the global protein stabilities derived from these denaturation experiments.

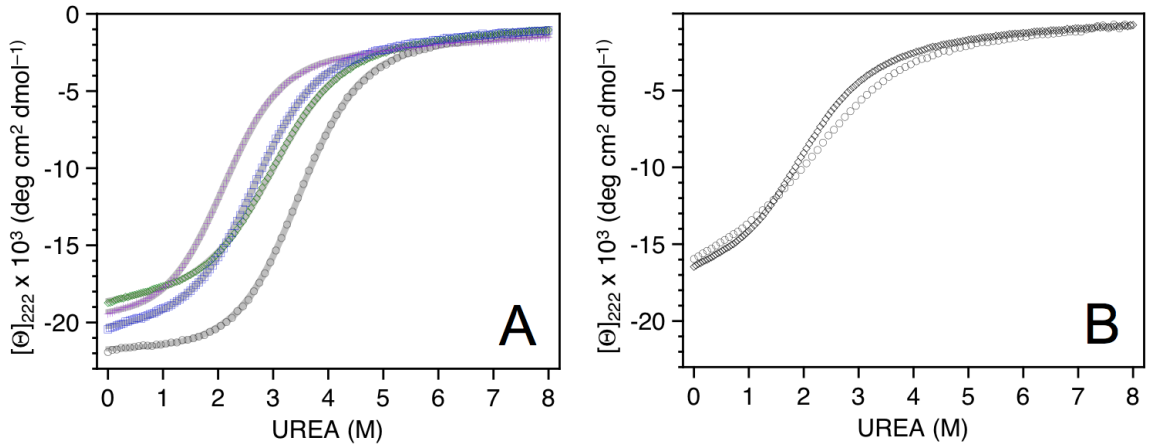

Figure 4.5. Chemical denaturation of α_3Y and HIS variants. Panel **(A)** displays urea-induced unfolding/folding transitions of α_3Y (black circles), α_3Y-V9H (green diamonds), α_3Y-K29H (blue squares), α_3Y-K36H (magenta crosses) while panel **(B)** displays data obtained on the α_3Y-L12H (circles) and α_3Y-I62H (diamonds) proteins. The gray lines represent nonlinear curve fits to determine the stability of the protein in the absence of denaturant (see Table 4.1).[94] See Section 7.6 for more details on the determination of the global stability and fitting statistics. *Sample*: proteins were dissolved in 10 mM APB buffer at pH 8.2 at a temperature of 25 °C.

In contrast, α_3Y-L12H and α_3Y-I62H contained ~20 % less helical content than α_3Y. Both these proteins show poorly defined denaturation curves, indicative of structurally perturbed protein folds. The proteins α_3Y-L12H and α_3Y-I62H were, therefore, not included in further steps of characterization.

Table 4.1. Physical Properties of α_3Y-HIS Variants[a]

Protein	pK_{APP} Y32[b]	pK_{APP} HIS[b]	Y32 Em (pH)[c]	$[\Theta]_{222}$[d]	% α-Helix[e]	ΔG^{H2O} [f]
α_3Y	11.3		8.1	-21.9	73.1 ± 0.7 (pH 5.0 – 10.0)	-3.7
α_3Y-V9H	10.8	< 5.0	n.d.	-18.7	63.1 ± 0.4 (pH 5.5 – 9.1)	-3.0
α_3Y-L12H	10.4	6.6	n.d.	-16.0	53.3 ± 1.0 (pH 4.6 – 8.6)	n.d.
α_3Y-K29H	10.7	7.1	7.4	-20.4	66.8 ± 2.5 (pH 5.1 – 9.1)	-2.8
α_3Y-K36H	11.0	7.0	7.1	-19.5	64.7 ± 0.8 (pH 5.1 – 9.1)	-2.4
α_3Y-I62H	10.6	7.0	n.d.	-16.5	53.8 ± 1.6 (pH 5.0 – 8.9)	n.d.

[a]Em (nm); $[\Theta]_{222}$ x 10^3 (degree cm^2 dmol^{-1}); ΔG (kcal mol^{-1}); n.d., not determined. [b]Apparent tyrosinate/imidazolium pK_A values of Y32 and histidine residues obtained by fitting the pH-titration curves in Figure 4.4 to a single pK_A. Statistical errors ≤ 0.1. See Section 7.4 and 7.5 for more details on the determination of the pK_{APP} values and fitting statistics. [c]Apparent pK_A values obtained by fitting the pH-titration curves in Figure 4.6 to a single pK_A. Statistical errors ≤ 0.1. See Section 7.7 for more details on the determination of the pK_{APP} values and fitting statistics. [d]Mean residue ellipticity measured at pH 8.2 and 25 °C. See Section 7.6 for more details on the determination of the helical content. [e]Scaled relative to α_3W (76 ± 1 % α-helical at pH 4 – 10).[13,56] [f]Global protein stabilities obtained by fitting urea-denaturation curves in Figure 4.5. Data collected at pH 8.2 and 25 °C. Fitting errors < ± 0.03 kcal mol^{-1}. See Section 7.6 for more details on the determination of the global stabilities and fitting statistics.

As mentioned above, the pK_{APP} values for tyrosine and histidine residues were evaluated for α_3Y and its HIS variants (Table 4.1). To determine how the

interaction between Y32 and HIS affects the properties of the tyrosine radical, it is of essence that we can monitor its redox properties across the titratable pH range of the incorporated histidine without introducing pH-induced structural changes. α_3Y-K29H and α_3Y-K36H remain (66.8 ± 2.5) % and (64.7 ± 0.8) % α-helical, respectively, at ± 2 pH units around the pK_{APP} of the histidine residues, H29 and H36 (see Figure 4.4 and Table 4.1). Although α_3Y-V9H shows characteristics of a well-defined and pH stable protein, the pK_{APP} of H9 falls outside of the stable pH range for this protein. As a result, α_3Y-V9H was not considered for further experiments.

4.2. Characterization of Y32/HIS interaction in α_3Y-K29H and α_3Y-K36H

The fluorescence emission of the tyrosine residue in α_3Y and the two selected variants, α_3Y-K29H and α_3Y-K36H, was explored as a function of pH. Apparent pK_A values for Y32 were obtained by inspecting the pH dependence of the emission center of mass (υ_p), which was calculated using Equation 4.1.[120]

$$\langle \upsilon_p \rangle = \frac{\Sigma \upsilon_i F_i}{\Sigma F_i}, \tag{4.1}$$

where F_i is the emission intensity collected at frequency υ_i (cm^{-1}). Using an excitation wavelength of 276 nm for the three proteins, the fluorescence was measured in the pH range of ~5-9, and the data fitted to a single pK_A. Plots of

emission center of mass as a function of pH are displayed in Figure 4.6, and the data is summarized in Table 4.1.

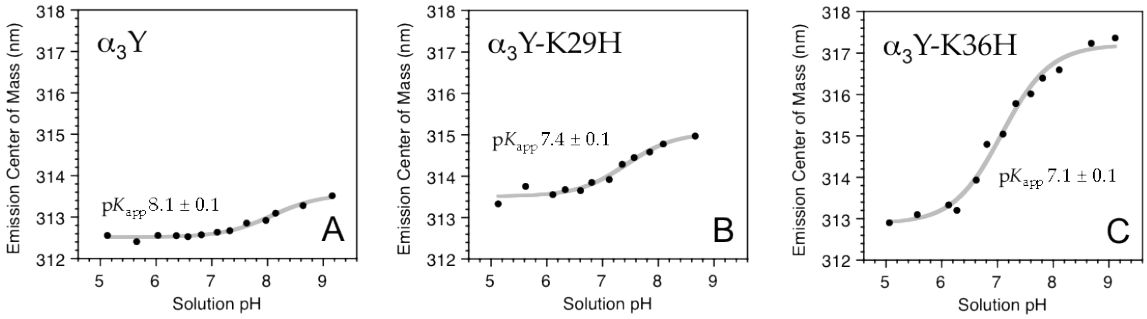

Figure 4.6. Fluorescence emission center of mass as a function of pH. Emission center of mass at different pH values are displayed for **(A)** α_3Y, **(B)** α_3Y-K29H and **(C)** α_3Y-K36H. pK_{APP} values were derived by nonlinear curve fitting (gray lines, Table 4.1). See Section 7.7 for more details on the determination of the pK_{APP} values and fitting statistics.

For α_3Y, measurements showed a 1.0 nm shift in the emission center of mass, and a pK_{APP} for Y32 of 8.1 ± 0.1. This observation may be due to pH-induced change in the electrostatic environment of the tyrosine, the hydrogen-bonding properties of the phenol hydroxyl group, or a combination thereof.[121,122] The protein α_3Y-K36H showed a 4.5 nm shift as a function of pH and a pK_{APP} for Y32 emission of 7.1 ± 0.1, which coincides with the pK_{APP} obtained for H36 via NMR (see Table 4.1). This correlation between the two pK_{APP} values suggests that Y32 fluorescence is sensitive to the protonation state of H36 and that the phenol and imidazole side chains are in close proximity. The emission center of mass of Y32 in α_3Y-K29H is shifted by 1.6 nm and titrates with a pK_{APP} of 7.4 ± 0.1, which is close to the H29 pK_{APP} value of 7.1 ± 0.1 determined by NMR. As in the case for

Y32 and H36 in α_3Y-K36H, Y32 and H29 in α_3Y-K29H seem to be somehow structurally connected. The observed changes in Y32 fluorescence most likely reflect electrostatic interactions between Y32 and the introduced histidine residues. On the other hand, changes in the protonation state of histidine affects the hydrogen-bonding environment of the Y32 hydroxyl group. Either of these explanations suggests that the imidazole ring of the introduced histidine in both proteins, α_3Y-K29H and α_3Y-K36H, resides near or at the Y32 site.

4.3. Structural stability of α_3Y-K29H and α_3Y-K36H as a Function of pH

The solution properties of the α_3Y-K29H and α_3Y-K36H were explored in order to establish the aggregation state and stability of the tertiary structure of these proteins as a function of pH. It has been previously established by sedimentation equilibrium ultracentrifugation and analytical size-exclusion chromatography that α_3Y is a monomeric protein with well-defined secondary and tertiary structures in solution across a concentration range of 4 – 850 μM.[13] Hence, α_3Y was used as a standard to which the solution properties of the variant proteins were compared. Size-exclusion chromatograms for α_3Y, α_3Y-K29H and α_3Y-K36H at neutral pH and at a concentration of ~250 μM are shown in Figure 4.7. The chromatograms display elution profiles consistent with a single major species (95%, 91% and 93% for α_3Y, α_3Y-K29H and α_3Y-K36H, respectively). The retention times are essentially identical between the three proteins (13.1 ± 0.1 mL), indicating that there are no significant differences

in the hydrodynamic properties between them. Therefore, we conclude that both α_3Y-HIS variants are monomer species in solution at neutral pH.

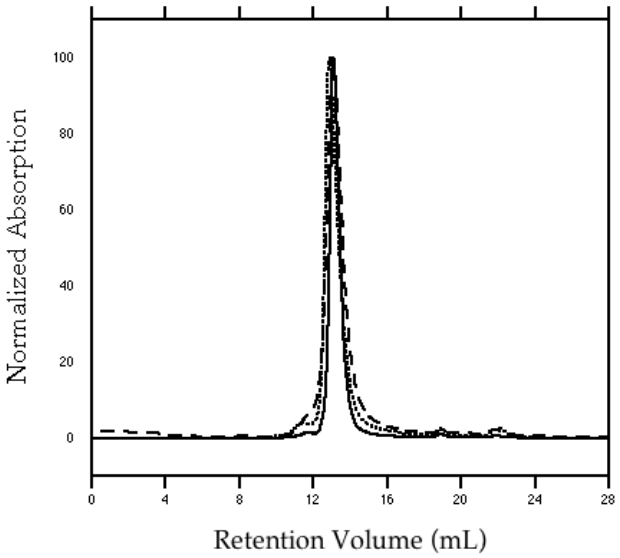

Figure 4.7. Size exclusion chromatograms for α_3Y, α_3Y-K29H and α_3Y-K36H. Elution profiles of α_3Y (solid line), α_3Y-K29H (dotted line) and α_3Y-K36H (dashed line) are displayed. Experimental settings: chromatography was carried out in a Superdex^{TM} 75 gel filtration column equilibrated with 10 mM APB buffer, 100 mM KCl at pH 7.0 and at room temperature. See Section 7.8 for more details on the size-exclusion experiments.

Two-dimensional NMR was used to further investigate the aggregation state of the α_3Y-HIS variants, as well as their tertiary structure, as a function of pH. ^{15}N-Heteronuclear Single Quantum Coherence (HSQC)[123-129] spectra were acquired for α_3Y-K29H and α_3Y-K36H at three different pH values (5.5, 7.0, and 8.5) and at two different temperatures (25 °C and 35 °C). These spectra display peaks resulting from through-bond interactions between amide nitrogen and

hydrogen atoms. The position of every peak in the spectra is characteristic to a specific local protein environment, thus providing us with a reporter of changes in local interactions to residues in the protein.[130,131] The spectra for α_3Y-K29H and α_3Y-K36H are shown in Figure 4.8. The spectra at pH 7.0 and 25 °C for both proteins display narrow spectral line widths, large chemical shift dispersion and no population of minor peaks. These spectral characteristics confirm that both proteins are monomeric and well-structured at these conditions, as seen by size-exclusion chromatography. Furthermore, we see no significant changes in the spectral line widths, overall chemical shift dispersion and population of peaks in the spectra collected at pH 5.5 and 8.5. Changing the acquisition temperature from 25 °C to 35 °C did not create major disturbances in the overall appearance of the ^{15}N-HSQC spectra either. Thus, the two α_3Y-HIS variants are monomeric proteins in solution with well-defined tertiary structures in the pH range from 5.5 to 8.5.

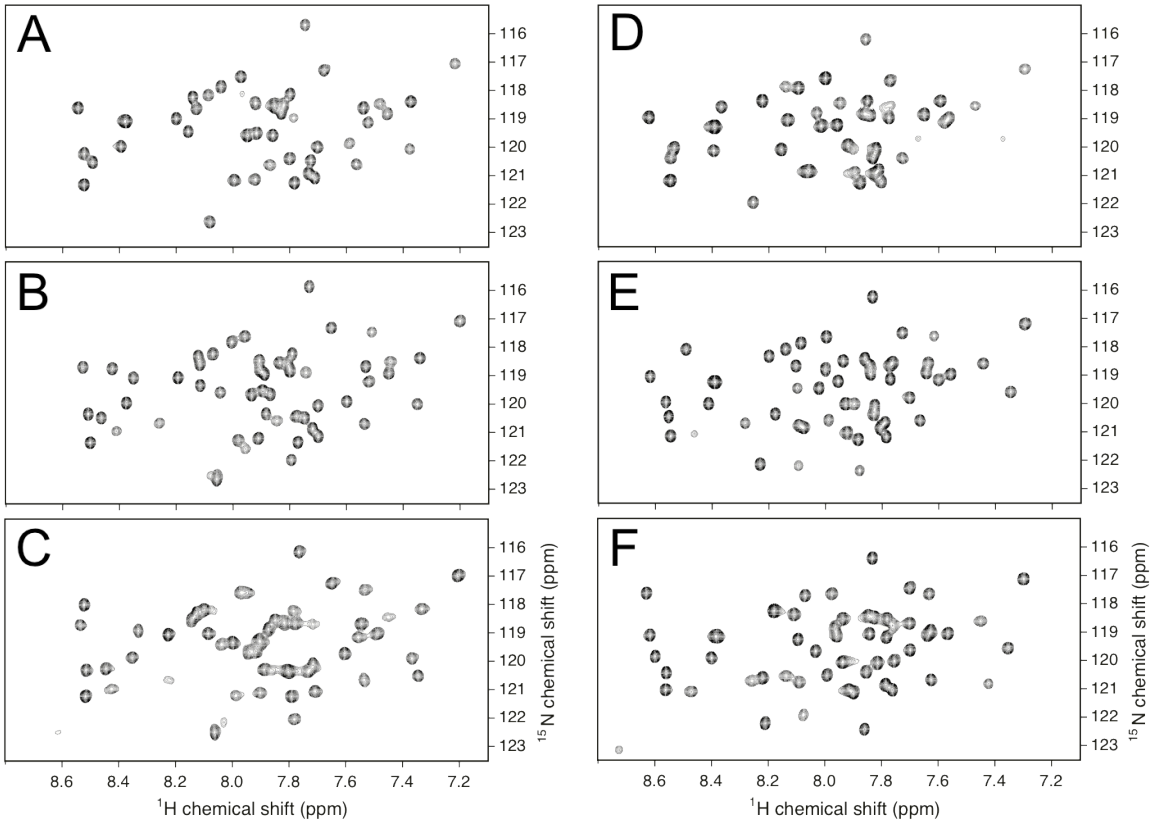

Figure 4.8. Two dimensional ^{15}N-HSQC spectra of α_3Y-K29H and α_3Y-K36H as a function of pH. Spectra show through-bond correlations between amide nitrogen and hydrogen atoms of the same residue. α_3Y-K29H spectra at pH 8.5, 7.0 and 5.5 are shown in Panels **(A)**, **(B)** and **(C)**, respectively. α_3Y-K36H spectra at pH 8.4, 7.0 and 5.5 are shown in Panels **(D)**, **(E)** and **(F)**, respectively. *Samples*: ~200 μM ^{15}N-labeled protein; buffer 25 mM deuterated sodium acetate, 25 mM sodium chloride for samples at acidic pH; buffer 25 mM sodium phosphate, 25 mM sodium chloride for samples at neutral pH; buffer 25 mM deuterated TRIS, 25 mM sodium chloride for samples at alkaline pH. All samples in 8% D_2O/92% H_2O solvent system and at 25 °C. *Experimental settings*: Data acquired in a 17.6 T magnet (750 MHz). Number of scans 64. Direct dimension (^{1}H): complex points 1024, carrier at 4.701 ± 0.001 ppm, spectral width 14 ppm. Indirect dimension (^{15}N): complex points 64, carrier at 117 ppm, spectral width 18 ppm.

4.4. Solvent accessibility of Y32 in the α_3Y-HIS variants

In order to assess the level of solvent accessibility of the tyrosine residues in the α_3Y histidine variants, α_3Y-K29H and α_3Y-K36H, two-dimensional ^{1}H-^{1}H

NOESY spectra were collected on both proteins. ^{1}H-^{1}H NOESY spectra show distance correlations between protons that are within 5 Å of each other.[90] This correlation arises from the NOE interaction, which is a dipole-dipole interaction between two nuclei that depends strongly on distance, with a r^{-6} dependence. Information extracted from this type of data reports on what types of protons are near the Y32 site, thus providing information on the environment surrounding the tyrosine side chain. The spectra were collected at two pH values, 5.6 and ~8.5, in order to gain information on the protein environment of Y32 at both protonation states of histidine (see Figure 4.9).

Assignment of the chemical shift values for the delta (Hδ1, Hδ2) and epsilon (Hε1, Hε2) protons for Y32 was achieved by examining the intraresidue NOE patterns seen in the spectra. The tyrosine Hδ1 and Hδ2 protons are expected to have strong NOE correlations with the alpha (Hα) and beta (Hβ1, Hβ2) protons of the same residue. There will also be correlations between Hε1 and Hε2 protons of Y32 and its own alpha and beta protons but the observed peaks will be of lesser intensity when compared to the peaks arising from the delta protons, due to the longer distance between these atoms in the residue. Following this rationale, the resonances for the Y32 ring protons were assigned in the ^{1}H-^{1}H NOESY spectra; chemical shift values for the protons of residue Y32, at both acidic and alkaline pH, in both proteins are listed in Table 4.2.

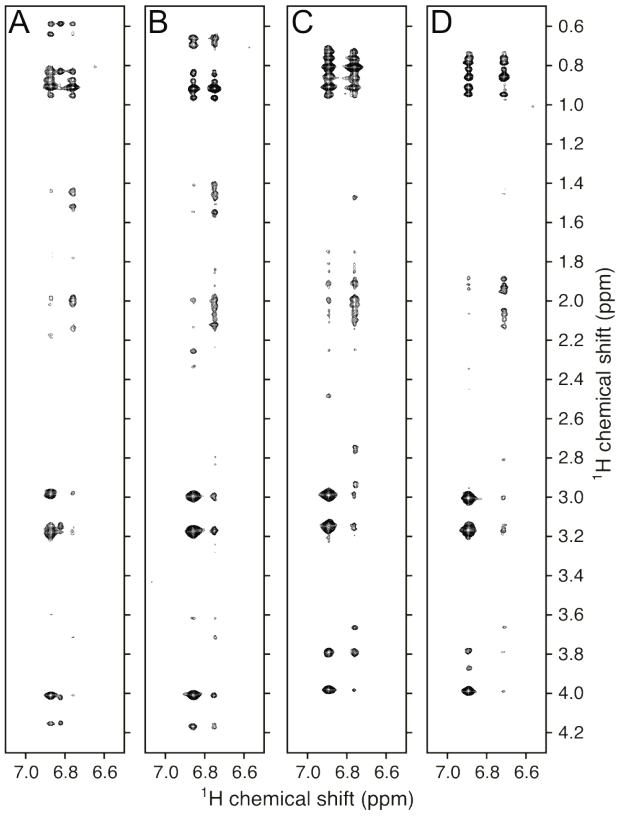

Figure 4.9. Two dimensional ^{1}H-^{1}H NOESY spectra of α_3Y-K29H and α_3Y-K36H. Spectra show through-space correlations between protons within 5 Å. α_3Y-K29H spectra at pH 8.5 and 5.6 are shown in Panels **(A)** and **(B),** respectively. α_3Y-K36H spectra at pH 8.4 and 5.6 are shown in Panels **(C)**, and **(D)**, respectively. *Samples*: ~200 μM protein; buffer 22 mM deuterated sodium acetate, 22 mM sodium chloride for samples at acidic pH; buffer 22 mM deuterated TRIS, 22 mM sodium chloride for samples at alkaline pH. All samples in 100% D_2O solvent and at 25 °C. *Experimental settings*: Data acquired in a 17.6 T magnet (750 MHz). Mixing time 150 ms. Number of scans 72. Direct dimension (^{1}H): complex points 2048, carrier at 4.703 ± 0.003 ppm, spectral width 10 ppm. Indirect dimension (^{1}H): complex points 800, carrier at 4.703 ± 0.003 ppm, spectral width 10 ppm.

Inspection of the ^{1}H-^{1}H NOESY spectra for both proteins reveals that Y32 is mainly surrounded by aliphatic protons. This is evidenced by NOE correlations to protons with chemical shift values between 0.5 and 4.2 ppm, which correspond to aliphatic protons. Distributions of ^{1}H chemical shift values for

residue types in proteins are available from the Biological Magnetic Resonance Bank (BMRB).[132] Moreover, chemical shift values below 1.0 ppm typically belong to resonances for methyl protons of leucine, valine, and isoleucine residues. These types of residues compose the hydrophobic packing layers of the α_3W protein, as seen in its NMR structure.[56] Both proteins show NOE peaks correlating Y32 to, at least, 12 sets of methyl protons. From these observations, we conclude that the Y32 residue resides in the hydrophobic core of the protein in both the α_3Y-HIS variants.

Table 4.2. Chemical Shift Assignments for Y32 Residue

Protein	pH	Hα	$H\beta_1$	$H\beta_2$	Hδ	Hε
α_3Y-K29H	8.4	4.00	2.97	3.17	6.87	6.75
	5.6	4.00	2.99	3.16	6.86	6.75
α_3Y-K36H	8.5	3.98	2.99	3.15	6.89	6.76
	5.6	3.97	2.99	3.15	6.89	6.71

All chemical shift values are expressed as ppm.

4.5. NMR characterization of Y32/HIS interactions in α_3Y-K29H and α_3Y-K36H

Interactions between the tyrosine at position 32 with H29 or H36 in α_3Y-K29H and α_3Y -K36H were further investigated by examining ^{1}H-^{1}H NOESY[90] and ^{1}H-^{1}H ROESY[133,134] NMR spectra for both proteins. These NMR experiments provide distance information between hydrogens atoms in the protein. NOE/ROE interactions between protons that are within 5 Å of each other will generate a crosspeak in the spectra. Figures 4.10 and 4.11 display the aromatic spectral region for the ^{1}H-^{1}H NOESY and ^{1}H-^{1}H ROESY spectra collected for

both proteins, respectively. Panels A and B in Figure 4.10 and 4.11 represent spectra collected for α_3Y-K29H and α_3Y-K36H samples, respectively.

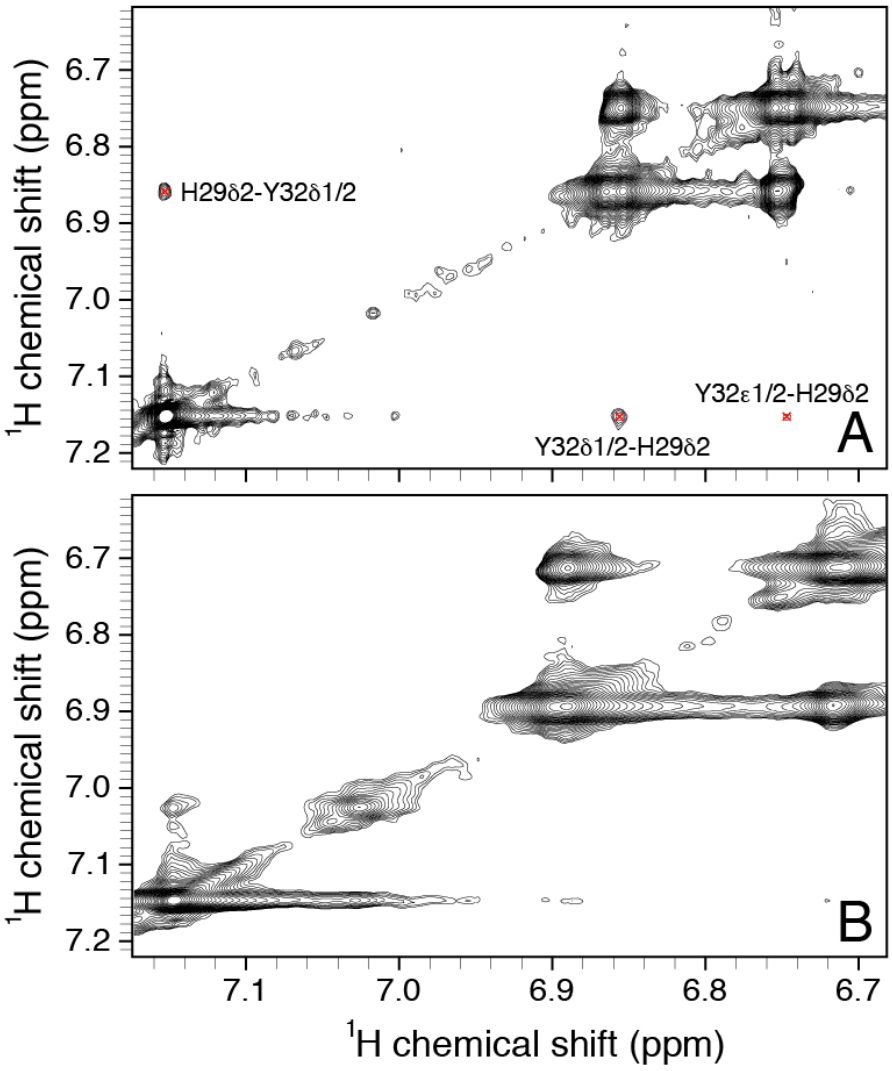

Figure 4.10. Aromatic spectral region of 2D ^{1}H-^{1}H NOESY spectra of α_3Y-K29H and α_3Y-K36H at alkaline pH. Spectra show through-space correlations between aromatic protons within 5 Å. Spectrum of α_3Y-K29H at pH 5.6 is shown in panel **(A)** and spectrum of α_3Y-K36H at pH 5.6 is shown in panel **(B)**. Peaks that represent interactions between the TYR and HIS in the protein are marked with a red "X" symbol, and the interacting protons are written next to the corresponding peak. Sample conditions and experimental settings are described in legend of Figure 4.9.

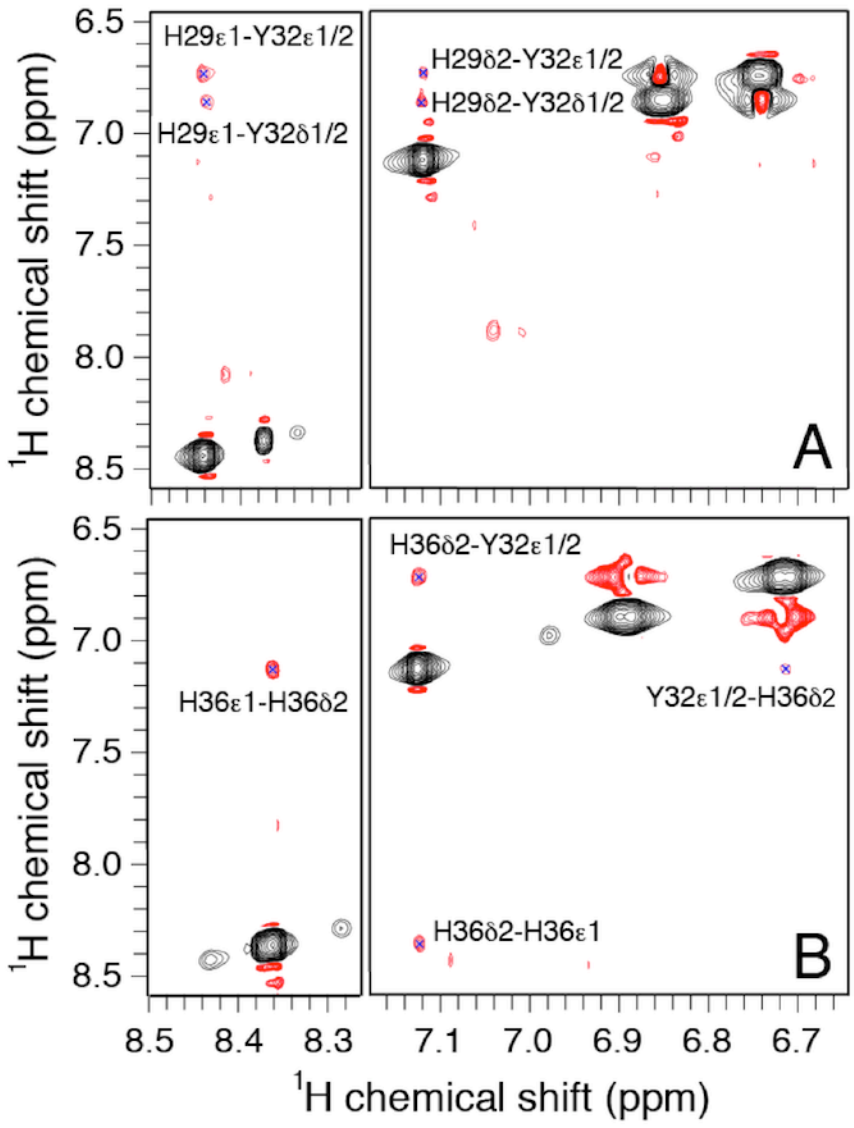

Figure 4.11. Aromatic spectral region of 2D ^{1}H-^{1}H ROESY spectra of α_3Y-K29H and α_3Y-K36H at alkaline pH. Spectra show through-space correlations between aromatic protons within 5 Å. Spectrum of α_3Y-K29H at pH 5.5 is shown in panel **(A)** and spectrum of α_3Y-K36H at pH 5.5 is shown in panel **(B)**. Peaks that represent interactions between the TYR and HIS in the protein are marked with a blue "X" symbol, and the interacting protons are written next to the corresponding peak. *Samples*: ~250 μM protein; buffer 25 mM deuterated TRIS, 25 mM sodium chloride. All samples in 100% D_2O solvent and at 25 °C. *Experimental settings*: Data acquired in a 11.7 T magnet (500 MHz). Mixing time 70 ms. Number of scans 144. Direct dimension (^{1}H): complex points 1024, carrier at 4.703 ± 0.001 ppm, spectral width 10.2 ppm. Indirect dimension (^{1}H): complex points 128, carrier at 4.703 ± 0.001 ppm, spectral width 9.5 ppm.

In order to analyze these spectra, assignment of the chemical shifts of the TYR and HIS ring hydrogens is required. The α_3Y-HIS amino acid sequence only contains two aromatic residues: Y32 and either H29 or H36. Hence, only resonances arising from these two residues will appear in the aromatic region of the spectra. Four resonances are observed in the aromatic spectral region for both proteins, two arising from the TYR Hδ and Hε ring protons and two from the HIS Hδ2 and Hε1 ring protons. The chemical shifts of the ring protons of α_3Y have been assigned, see Section 4.4. The two remaining resonances present in the spectra belong to the HIS ring protons. The resonances for HIS Hε1 protons typically appear at higher chemical shift values than for HIS Hδ2 protons. Following this rationale, the resonances for the ring protons for the HIS residues in both proteins were successfully assigned; the chemical shift values are listed in Table 4.3.

Table 4.3. Chemical Shift Assignments for HIS Residues in α_3Y-HIS Variants at pH 5.6 ± 0.1.

Protein	HIS Hδ2	HIS Hε1
α_3Y-K29H	7.12	8.43
α_3Y-K36H	7.13	8.32

All chemical shift values are expressed in ppm.

Analysis of the ^{1}H-^{1}H NOESY and ^{1}H-^{1}H ROESY spectra reveals two TYR/HIS NOE and four TYR/HIS ROE crosspeaks for α_3Y-K29H, while only one TYR/HIS ROE is detected for α_3Y-K36H. As previously presented experimental

data have suggested, these NMR experiments confirm that indeed the two aromatic residues are in close proximity in both α_3Y HIS variants. Moreover, we observe distinct interactions for the Y32/H29 and the Y32/H36 pairs. The presence of an ROE crosspeak with no corresponding NOE crosspeak suggests motional fluctuations between the interacting protons in the nanosecond timescale. [90,133,134] Given that NOE interactions are only observed for α_3Y-K29H, we predict that the Y32/H29 interaction involves a more motionally restricted ring interaction relative to the Y32/H36 pair, for which only ROE interactions are identified. These observations clearly suggest that insights into structural, as well as dynamic, properties of these proteins are of essence to effectively understand the influence of local environment on the properties of tyrosine.

4.6. Summary

In this chapter, the development of two new members of the α_3X family of proteins is described. Single HIS mutations were done on the α_3Y protein sequence with the aim of creating an interaction between a TYR and a HIS residue within the protein scaffold. Eight HIS variants were originally generated by making the following mutations: V9H, L12H, E13H, K29H, E33H, K36H, L58H, and I62H. Several screening steps were carried out in order to determine what proteins were suitable protein frameworks for examination of a TYR/HIS interaction. The α_3Y-E13H, α_3Y-E33H, and α_3Y-E58H proteins were initially discarded due striking similarity between their fluorescence emission and excitation spectra to the corresponding spectra of α_3Y. These data suggest

that the HIS imidazole group is not in close proximity to the Y32 residue, hence no changes are observed in the fluorescence spectra. The α_3Y-L12H and α_3Y-I62H proteins were not suitable protein frameworks for this study due to significant loss of α-helical content in comparison to the α_3Y protein (more than 20% loss of helical content due to the single-point mutation). Also, their denaturation curves were poorly defined in the "folded" regime of the plot, indicating that the fold of the protein is structurally perturbed. Finally, although the α_3Y-V9H protein is a well structured protein and pH stable throughout a wide pH range, the pK_A value for the HIS residue falls outside of the pH stability range of the protein. The remaining variant proteins, α_3Y-K29H and α_3Y-K36H, did show changes in their fluorescence spectra when compared to α_3Y; thus indicating changes in the environment surrounding the TYR residue. It was also found that the structural integrity of both these proteins is not compromised due to the single-mutation neither due to changes in pH within a pH range of 5.5 to 8.5. Determination of the helical content of both these proteins shows that this parameter is not significantly perturbed due to incorporation of the HIS residue. The helical content is also stable throughout the titratable pH range of the introduced HIS residue. CD denaturation experiments confirmed that these proteins have a stable protein fold in the absence of urea. Size-exclusion chromatography and NMR ^{15}N-HSQC spectra provided evidence that both these are monomeric proteins with stable tertiary structures in solution.

Once the stability of the secondary and tertiary structure, and aggregation state of α_3Y-K29H, α_3Y-K36H were evaluated, other properties of these proteins were explored. The emission center of mass was examined as a function of pH, and it was found that, in contrast to α_3Y, the α_3Y-HIS variants displayed apparent pK_A values with are consistent with the NMR-derived pK_{APP} values of the HIS residues. These results suggest close proximity of the TYR and HIS side chains within the protein scaffold. This conclusion was further confirmed with 2D ^{1}H-^{1}H NOESY and ROESY experiments. These spectra showed crosspeaks that correspond to distance-dependent dipole-dipole interactions between the Y32/H29 and the Y32/H36 residue pairs. From these data, we also observe that the interaction between the Y32/H29 pair is more motionally restricted than the Y32/H36 pair.

CHAPTER 5: Development of Mercaptophenol-Bound α_3C Protein System and Electrochemical Characterization of a Reversible Protein-Bound Phenoxyl Radical

5.1. Short Summary of Previous Work on Mercaptophenol-Bound α_3C Proteins

The α_3C model protein was designed with the purpose of generating protein-bound tyrosine analogues with different degrees of solvent accessible surface area for the phenolic hydroxyl group,[84] as discussed in Chapter 2. α_3C contains a single cysteine residue in the core of the protein at position 32. Binding of the three constitutional isomers of mercaptophenol to C32 created three protein-bound tyrosine analogues: 2MP-C32, 3MP-C32, and 4MP-C32. The three MP-α_3C proteins have been previously characterized. Their secondary structure and global protein stability were examined. The three proteins were found to be highly α-helical (81 ± 3 %),[84] and their unfolding free energy, ΔG^{H_2O}, does not differ significantly from the structurally characterized α_3W.[56]. In addition, preliminary electrochemical characterization was done using DPV, and striking differences were found between 4MP-α_3C and the other two MP-bound proteins (see Section 2.3) that suggest comparable environments surrounding 4MP when bound to α_3C and blocked CYS (bCys) free in solution. This fact would coincide with the initial design of 4MP-α_3C in which the 4MP hydroxyl group is exposed to solvent to a larger extent than the corresponding group in 2MP and 3MP, when bound to the protein. To put this

hypothesis to the test, structural characterization of the MP-α_3C proteins ensued. The solution NMR structure of 2MP-α_3C was obtained and it is described in Section 2.3. This chapter will describe the determination of the solution NMR structure of 4MP-α_3C, as well as further protein characterization of the three MP-bound proteins and the electrochemical characterization of 2MP-α_3C.

5.2. Protein characterization of 2MP-α_3C, 3MP-α_3C, and 4MP-α_3C

As evidenced with the small-molecule studies described in Section 1.5, it is clear that pH is a key parameter to understand systems in which PCET takes place. Furthermore, the electrochemical studies of tyrosine in the α_3Y system (Chapter 3) have confirmed that pH plays an important role on determining the thermodynamics of the PCET process. As with the α_3Y system, the structural integrity of the mercaptophenol-bound proteins must be relatively insensitive to variations of the solution pH, in order to be able to provide reliable pH-dependent electrochemical data. Several experiments were carried out to assess this requirement.

The α-helical content of the MP-α_3C proteins has been previously explored at a pH value of 7.5.[84] In this study, we set out to determine the dependence of this parameter on the solution pH. The helical content percentages were determined as described in Section 2.3. The results of this set of experiments are summarized in Table 5.1, and Figure 5.1 displays a plot of the percentage of α-helical content for 2MP-α_3C, 3MP-α_3C and 4MP-α_3C as a

function of solution pH. We observe that 2MP-α_3C, 3MP-α_3C and 4MP-α_3C are 76.9 ± 1.4 %, 86.2 ± 1.4 % and 76.9 ± 1.0 % α-helical, respectively, in a pH range of ~ 4 – 10. Therefore, we conclude that the secondary structure of the three MP-α_3C proteins remain stable throughout a broad pH range spanning 6 pH units.

Table 5.1. α-Helical Content as a Function of Solution pH.

Protein	pH range	α-Helical (%)	Range (%)
2MP-α_3C	3.8 – 10.0	76.9 ± 1.4[a]	(75.1 – 79.6)[a]
3MP-α_3C	4.1 – 10.5	86.2 ± 1.4[b]	(84.6 – 90.8)[b]
4MP-α_3C	4.1 – 10.5	76.9 ± 1.0[a]	(75.2 – 79.3)[a]

α-Helical content was derived as described in Section 2.3. More details about the determination of this parameter can be found in Section 7.6. *Sample*: ~ 20 μM protein in solution containing 20 mM APB buffer, 40 mM KCl at a temperature of 30 °C. *Experimental settings*: The observed mean residue ellipticity at 222 nm was obtained by measuring the CD signal by automated constant volume titration on a Aviv 202 CD spectrometer in a 10 mm cuvette, using averaging time 1 sec, stir time 0.5 min, pH dead band 0.05, bandwidth 3 nm. See Section 7.6 for relationship between mean residue ellipticity and CD signal. NOTES: [a]The helical content for 2MP-α_3C and 4MP-α_3C were corrected to match the helical content obtained from their respective solution NMR structures at pH 5.5. The NMR structure for 2MP-α_3C is described in Section 2.3, while the NMR structure of 4MP-α_3C will be described in Section 5.3 (below). [b]The helical content for 3MP-α_3C is uncorrected.

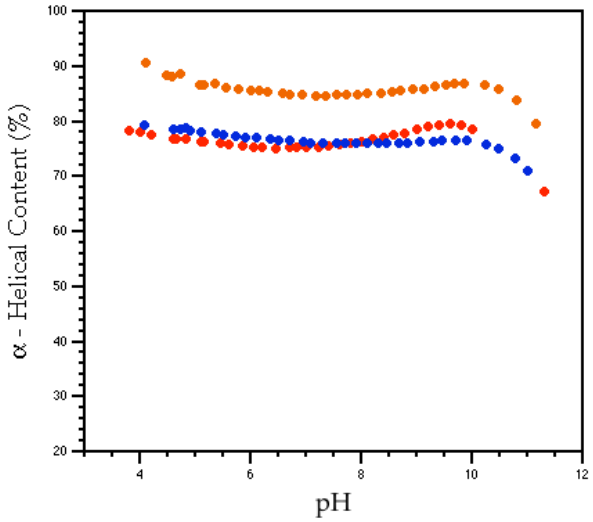

Figure 5.1. α-Helical content of MP-α_3C proteins as a function of pH. Helical content percentage for 2MP-α_3C (red circles), 3MP-α_3C (orange circles) and 4MP-α_3C (blue circles) was calculated as described in Sections 2.3 and 7.6. Sample conditions and experimental settings are described in the legend of Table 5.1.

The aggregation state of the MP-bound proteins was also investigated by performing size exclusion chromatography on samples containing these proteins. Figure 5.2 displays the chromatograms of 2MP- α_3C, 3MP- α_3C and 4MP- α_3C, as well as the chromatograph of the α_3Y protein which was used as a standard representing a well-structured monomeric protein with stable tertiary structure in solution. The MP-α_3C proteins eluted at a retention volume of 13.2 ± 0.2 mL, which corresponds to the retention volume for the α_3Y protein (see Section 4.3 and reference 97). The elution profiles reveal a single major species for all three proteins (94%, 94% and 93% for 2MP-α_3C, 3MP-α_3C and 4MP-α_3C, respectively). This result is also consistent with the size exclusion data obtained

for α_3Y. Thus, we conclude that the three MP-bound proteins form stable monomeric structures in solution.

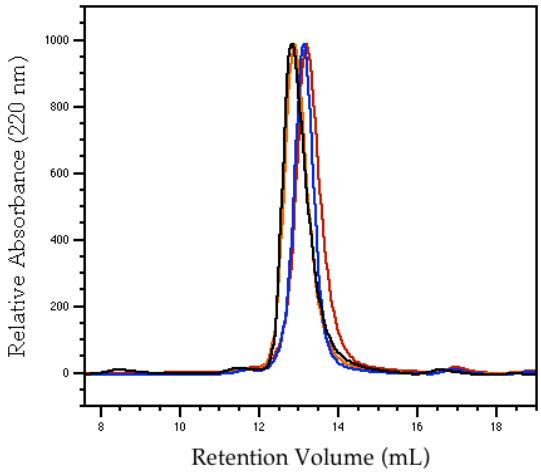

Figure 5.2. Size exclusion chromatograms for mercaptophenol-α_3C proteins. Size exclusion chromatograms for 2MP-α_3C (red), 3MP-α_3C (orange), 4MP-α_3C (blue) and α_3Y (black) were acquired by using an analytical Superdex^{TM} 75 gel filtration column (GE Healthcare) equilibrated with a solution containing 10 mM APB buffer and 100 mM potassium chloride at pH 7 and at room temperature. *Sample*: 250 μM protein dissolved in 20 mM APB buffer and 50 mM potassium chloride at pH 7.7.

Further evidence of the structural stability of the mercaptophenol-bound α_3C proteins was obtained by acquiring the ^{15}N-HSQC and ^{13}C-HSQC NMR spectra. As mentioned in Section 4.3, peaks in HSQC NMR spectra appear at chemical shift values that are highly dependent on local environment. Changes in this local environment are reflected in changes in the position of the peaks in the spectra. The ^{15}N-HSQC spectrum provides information on the backbone amide N and H resonances, while the ^{13}C-HSQC spectrum reports on aliphatic C and H atoms throughout the entire protein.[123-129] The pH dependence of the

appearance of these spectra was examined for 2MP-α_3C and 4MP-α_3C. Figure 5.3 and Figure 5.4 show ^{15}N-HSQC and ^{13}C-HSQC spectra for 2MP-α_3C and 4MP-α_3C, respectively. The ^{15}N-HSQC spectra displayed in Figures 5.3A and 5.4A show that the overall appearance of the spectra does not significantly vary with changes in pH, going from acidic to neutral to alkaline pH. We observe no significant changes in the observed narrow spectral line widths, in the overall chemical shift dispersion and in the population of minor peaks, across the pH range surveyed (pH 5.5, 7.0 and 8.5). pH-induced electrostatic and hydrogen-exchange effects influence peak positions and intensities as expected due to variations in solution pH. These observations confirm a well-defined secondary and tertiary structure, and aggregation state for both proteins, as evidenced by CD spectroscopy and size exclusion chromatography. Examination of the ^{13}C-HSQC spectra (Figures 5.3B and 5.4B) further confirms this conclusion. The positions of the peaks in the ^{13}C-HSQC spectra of 2MP-α_3C are essentially independent of pH. The only resonances that show significant shifts in their chemical shift values are resonances related to the Cα, Cβ, Hα, Hβ1, and Hβ2 atoms of the *N*-terminal serine with residue number -2. The same observations applies for the ^{13}C-HSQC spectrum of 4MP-α_3C.

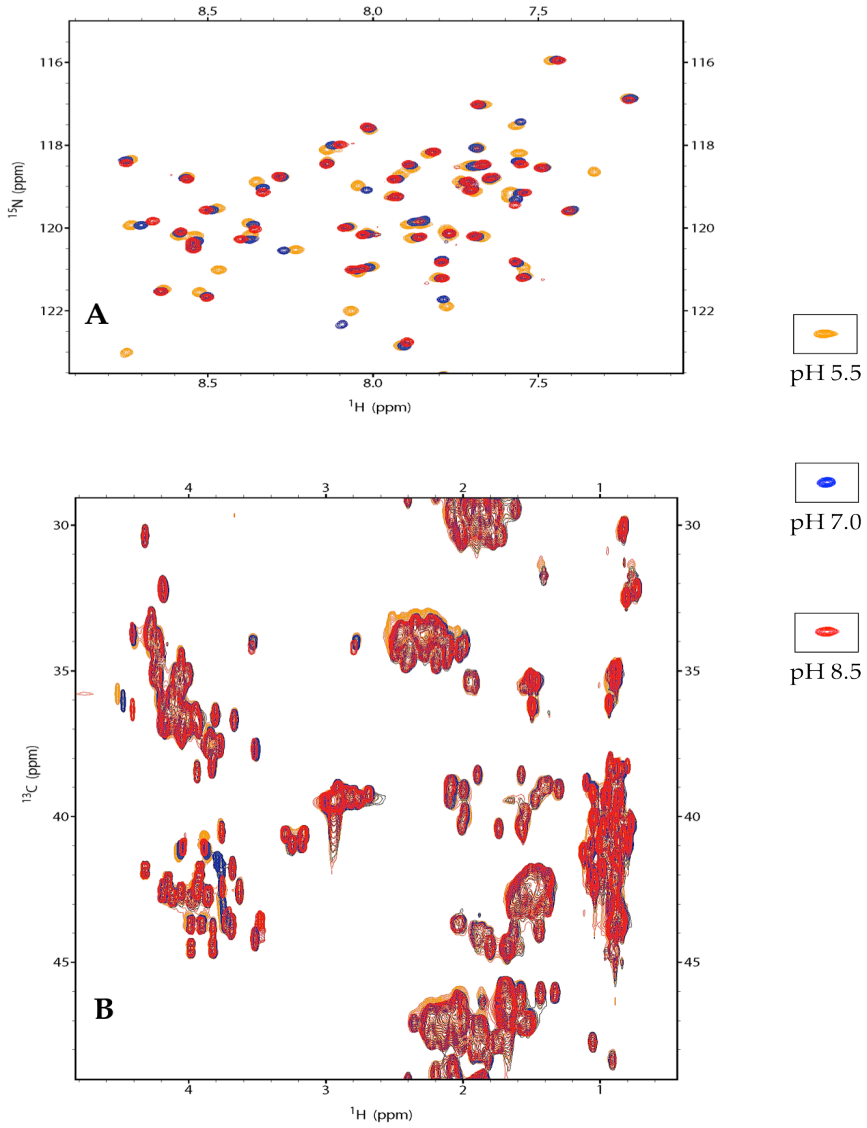

Figure 5.3. Two dimensional HSQC spectra for the 2MP-α_3C protein as a function of pH. Panel **(A)** displays the ^{15}N-HSQC spectrum, while panel **(B)** displays the ^{13}C-HSQC spectrum of 2MP-α_3C. Spectra acquired with samples at pH 5.5, 7.0 and 8.5 are depicted in orange, blue and red, respectively. *Sample*: 700 μM ^{15}N^{13}C -labeled protein; buffer 10 mM deuterated sodium acetate, 10 mM potassium phosphate, 10 mM deuterated TRIS, 20 mM sodium chloride in 8% D_2O/92% H_2O solvent system and at 30 °C. *Experimental settings*: Data acquired in a 17.6 T magnet (750 MHz). For ^{15}N-HSQC: number of scans 8; direct dimension (^{1}H) complex points 1024, carrier at 4.702 ± 0.001 ppm, spectral width 14 ppm; indirect dimension (^{1}H) complex points 200, carrier at 115 ppm, spectral width 17 ppm. For ^{13}C-HSQC: number of scans 16; direct dimension (^{1}H) complex points 1024, carrier at 4.702 ± 0.001 ppm, spectral width 14 ppm; indirect dimension (^{1}H) complex points 100, carrier at 39 ppm, spectral width 20 ppm.

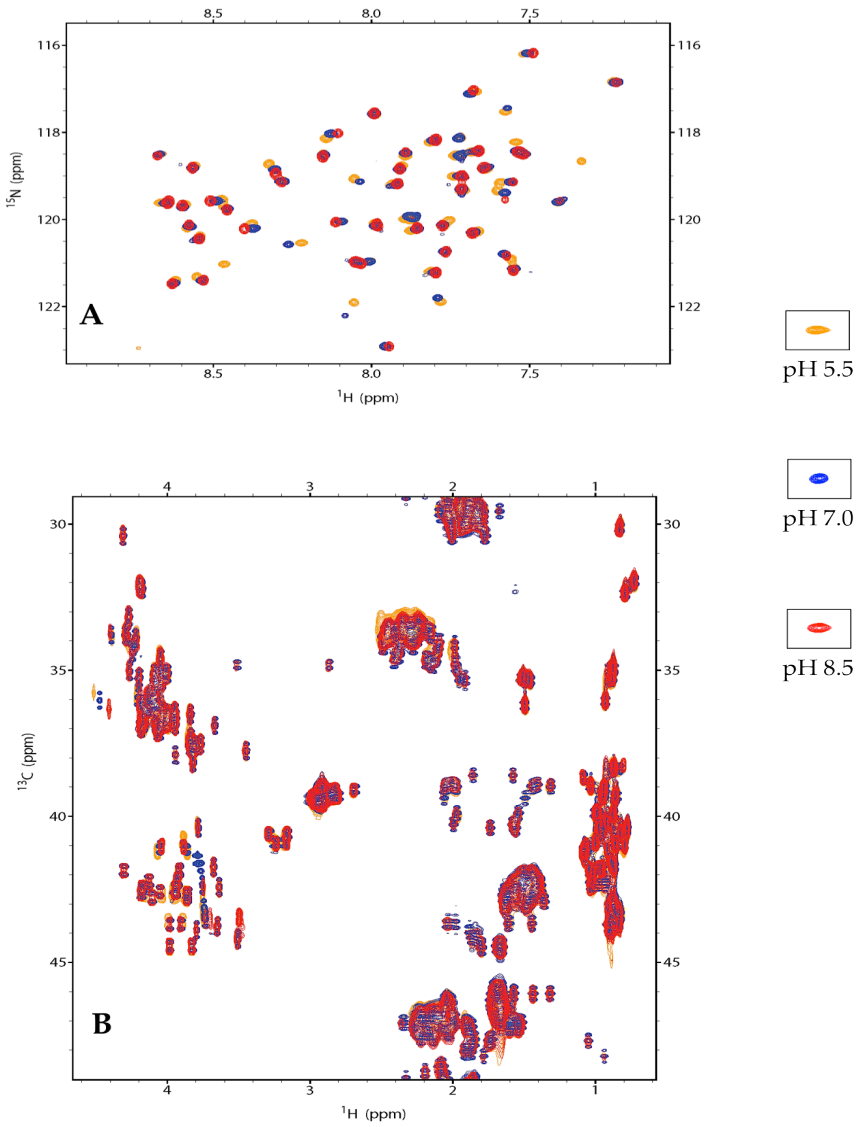

Figure 5.4. Two dimensional HSQC spectra for the 4MP-α_3C protein as a function of pH. Panel **(A)** displays the ^{15}N-HSQC spectrum, while panel **(B)** displays the ^{13}C-HSQC spectrum of 4MP-α_3C. Spectra acquired with samples at pH 5.5, 7.0 and 8.5 are depicted in orange, blue and red, respectively. *Sample*: 630 μM ^{15}N^{13}C-labeled protein; buffer 10 mM deuterated sodium acetate, 10 mM potassium phosphate, 10 mM deuterated TRIS, 20 mM sodium chloride in 8% D_2O/92% H_2O solvent system and at 30 °C. *Experimental settings*: Data acquired in a 17.6 T magnet (750 MHz). For ^{15}N-HSQC: number of scans 8; direct dimension (^{1}H) complex points 1024, carrier at 4.702 ± 0.002 ppm, spectral width 14 ppm; indirect dimension (^{1}H) complex points 200, carrier at 115 ppm, spectral width 17 ppm. For ^{13}C-HSQC: number of scans 16 (except for pH-8.5 spectrum, number of scans 8); direct dimension (^{1}H) complex points 1024, carrier at 4.702 ± 0.001 ppm, spectral width 14 ppm; indirect dimension (^{1}H) complex points 100 (except for pH-7 spectrum, complex points 256), carrier at 39 ppm, spectral width 20 ppm.

5.3. Determination of the solution NMR structure of 4MP-α_3C

The size, solubility and stability in aqueous solutions of the MP-α_3C proteins make them good candidates for determining their solution structure using high-resolution NMR methods. The NMR structural model for 2MP-α_3C has been previously calculated in our lab.[95] See Section 2.3 for details of this structure. The 2MP-C32 residue shows a solvent accessible surface area percentage of 3.5 ± 0.7 %, which confirms the initial hypothesis that the phenol OH group of this molecule mainly participates in interactions with the protein matrix, according to the original design. To test the initial design of 4MP-α_3C, we set out to determine its solution NMR structure, as we have done with the 2MP-α_3C protein. In order to obtain a structural model for a protein using NMR, the first step is to acquire the chemical shift values for the resonances of amide and aliphatic protons, amide nitrogens, and carbons in the protein. The second step is to obtain information about the distance between the assigned atoms. These aforementioned distance restraints are then fed into an structure calculation program along with hydrogen-bond distance and dihedral angle restraints to obtain an ensemble of refined lowest-energy structures that will comprise the final structural model.

5.3.1. NMR Experiments for Chemical Shift Assignment

Several high-resolution NMR experiments provide the data necessary for the assignment of resonances for the hydrogen, nitrogen and carbon nuclei in ^{15}N- and/or ^{13}C-isotopically labeled proteins.[135] These experiments correlate

chemical shift values of the different nuclei given that they are separated by two or three covalent bonds.[130,131] This through-bond interaction, known as scalar coupling (or J-coupling), is mediated by the electrons forming the chemical bonds, and it influences the magnetic field between the two nuclei involved.[130] Chemical shift assignment experiments include the ^{15}N-Heteronuclear Single Quantum Coherence (HSQC) experiment which displays peaks that correlate the resonances of the amide nitrogen and amide hydrogen within the same residue, while the ^{13}C-HSQC correlates aliphatic carbon and hydrogen atoms that are covalently bonded to each other.[123-129] Most backbone resonance assignments are obtained with the following experiments. The HNCO[136-139] and HN(CA)CO[139,140] experiments correlate the chemical shift values for the amide H and N of residue i with the carbonyl carbon of residue i and residue i-1. The CBCA(CO)NH[141] and the HNCACB[142] aid in the assignment of alpha and beta carbons by linking their resonances with the amide H and N of residues i and i+1. Resonance assignment for side chain carbon and hydrogen atoms is achieved, primarily, with Total Correlation Spectroscopy (TOCSY) experiments. These include the H(CC)(CO)NH-TOCSY and the (H)CC(CO)NH-TOCSY that correlate the amide H and N of residue i with the aliphatic hydrogen and carbon atoms of the previous residue, respectively.[143-146] The HCCH-TOCSY links all aliphatic hydrogen and carbon atoms of the same residue.[147,148] See Section 7.10 for information on NMR data collection. Table 5.2 tabulates the information obtained by each of these experiments on a protein residue. In total, 88, 91 and 82 % of the proton, carbon and nitrogen atoms in the protein, respectively, were assigned to a chemical

shift value. The extent of assignment was determined by using the Assignment Validation Suite (AVS)[149] webserver. Furthermore, 96 % amide H and N, 97 % carbonyl C, 99 % Cα, 96 % Hα, and 98 % Cβ atoms were assigned to a chemical shift value.

Table 5.2. Multi-Dimensional NMR Experiments for Resonance Assignments.

NMR Experiment	D1[a]	D2[a]	D3[a]
15N-HSQC[b]	i(HN)	i(N)	N/A
13C-HSQC[b]	i(H)	i(C)	N/A
HNCO[c]	i(HN)	i(N)	i-1(CO)
HN(CA)CO[c]	i(HN)	i(N)	i(CO), i-1(CO)
CBCA(CO)NH[c]	i(HN)	i(N)	i-1(CA), i-1(CB)
HNCACB[c]	i(HN)	i(N)	i(CA), i(CB), i-1(CA), i-1(CB)
H(CC)(CO)NH TOCSY[c]	i(HN)	i(N)	all i-1(H)
CC(CO)NH TOCSY[c]	i(HN)	i(N)	all i-1(C)
HCCH TOCSY[c]	$i(H_J)$[d]	$i(C_J)$[d]	all i(H)

[a]D1, D2 and D3 refer to the 1st, 2nd and 3rd collected dimension in the NMR experiment, respectively. [b]2D experiment: third dimension does not apply (N/A = not applicable). [c]3D experiment. [d]H_J and C_J are covalently bonded. NOTE: See Section 7.10 for information on NMR data collection.

5.3.2. NOE-based NMR experiments and analysis

After chemical shift values are obtained for the amide N and H, the carbonyl C, and the aliphatic C and H atoms in the protein, the next step is to obtain information about the distance between the atoms. Distance restraints for structure determination are obtained primarily by performing experiments that are based on the Nuclear Overhauser Effect (NOE).[130,135] NOE-based, or NOESY, spectra display crosspeaks that correspond to through-space dipole-

dipole interactions between atoms that are within 5 Å of each other, thus providing the most important source of distance constraints that will be utilized for structure calculation. The intensity of the crosspeak is proportional to the strength of the NOE interaction which, in turn, is inversely proportional to the distance between the two nuclei.[130,131] Two four-dimensional NMR experiments were done to identify NOE interactions between assigned protons in the 4MP-α_3C protein. A 4D ^{15}N-HSQC-NOESY-^{13}C-HSQC[150,151] spectrum was acquired, and provided NOE crosspeaks between amide and aliphatic protons, giving also information about which nitrogen and carbon each proton is covalently bonded to, respectively. The 4D ^{13}C-HMQC-NOESY-^{13}C-HMQC[152-154] experiment provides similar information but the NOE interactions occur between aliphatic protons. The NOE crosspeaks displayed in these two 4D NOESY experiments provide information about protons that are either attached to a ^{15}N or a ^{13}C nucleus, which is the case for most hydrogen atoms in the uniformly ^{15}N,^{13}C-labeled 4MP-α_3C protein. However, the ring protons of the covalently bound 4MP molecule are attached to naturally abundant nuclei (98.9/1.1 % for ^{12}C/^{13}C and 99.6/0.4 % for ^{14}N/^{15}N)[131], meaning that NOE interactions between the 4MP hydrogen atoms and the protein matrix cannot be extracted from these spectra. In addition to the two 4D NOESY spectra, a 3D NOESY-^{13}C-HSQC[155,156] spectrum was obtained. This experiment correlates protons attached to ^{13}C to any other proton in its immediate surrounding (5 Å) regardless of the isotopic labeling of its chemical-bond partner. Thus, this 3D experiment allows for attainment of NOE crosspeaks relating protons in the protein and protons in the

unlabeled 4MP ring molecule. See Section 7.10 for information on NMR data collection.

NOE crosspeaks were identified by visualizing the NOESY spectra in the program Sparky.[157] These NOE crosspeaks identified provided NOE distance restraints, which are essential for the structure calculation process. In all, 829 NOE distance restraints were obtained from the acquired NOE spectra (see Table 5.4 for a complete analysis of NOE interactions obtained). Fifty-seven of those restraints involved the 4MP-C32 residue, of which 32 concerned NOE interactions between the 4MP ring protons and surrounding protons.

The NOE crosspeaks in both the 4D NOESY spectra, as well as in the 3D NOESY spectrum, were carefully integrated in Sparky to obtain peak volumes. Special attention was given to peaks that represented classical helical distances. The volume of i(HN) – i(HA) and i(HN) – i-1(HA) NOE crosspeaks were used to calibrate the 4D ^{15}N-HSQC-NOESY-^{13}C-HSQC in order to obtain accurate volumes for the rest of the crosspeaks identified. These NOEs were designated as *na* and *an* NOEs, respectively, and were assigned to a distance of 3 Å and 4 Å, respectively.[158] The i(HA) – i+3(HB) NOEs were used to calibrate the 4D ^{13}C-HMQC-NOESY-^{13}C-HMQC and the 3D NOESY-^{13}C-HSQC spectra, having a calibration distance of 4 Å.[158] Using these calibration NOEs, the volume of all NOE crosspeaks in the NOESY spectra were classified as weak, medium, or strong NOE interactions. The strength of the interaction was related to a range of allowed distance between the interacting protons; these were 1.7 – 5.0 Å, 1.7 – 4.0 Å, and 1.7 – 3.0 Å for weak, medium, and strong interactions, respectively.[159] See Table 5.3 for a summary of binning of peak volume for all

three NOESY spectra. See Appendix D for a list of all NOE restraints. Table D.3 in Appendix D represents lists the NOE-based distance restraints that were used for the structure calculation of 4MP-α_3C (see below).

Table 5.3. Correlation Between NOE Strength and NOE Peak Volume for Multi-Dimensional NOE-Based NMR Experiments.

Experiment	Minimum Peak Volume		
	Weak NOE	Medium NOE	Strong NOE
4D ^{15}N-HSQC-NOESY-^{13}C-HSQC	3×10^7	1.59×10^8	1.56×10^9
4D ^{13}C-HMQC-NOESY-^{13}C-HMQC	1×10^7	4.7×10^8	4.9×10^9
3D NOESY-^{13}C-HSQC	2×10^7	2.52×10^8	1.9×10^9

The minimum peak volume values listed in this table represents the lower limit of the bin containing peak volume values for weak, medium and strong NOE interactions.

5.3.3. Description of structural calculation and solution NMR structure of 4MP-α_3C

In addition to the NOE distance restraints, other information is required by the Crystallographic and NMR System (CNS)[160] to perform a simulated annealing molecular dynamics calculation of the protein structure. Dihedral angle restraints and hydrogen bond distance restraints were also obtained and fed to the CNS suite. The dihedral angle restraints were obtained by using the TALOS+ program[161], which calculates the backbone dihedral ϕ and ψ angles for the protein residues from backbone chemical shift data. From the dihedral angle values obtained, TALOS+ also determines the type of secondary structure element each residue belongs to. Appendix C lists the dihedral angle values and

secondary structure elements for each residue for which backbone chemical shifts are available. According to this data, the 4MP-α_3C is found to be 78 % helical at pH 5.5, with 52 out of 67 residues being part of an α-helix in the protein. This helical content value was used to calibrate the results obtained from the CD pH titration in Section 5.2. Hydrogen bond distance restraints are also used in the structure calculation protocol of CNS. Hydrogen bond restraints have a large impact on the precision of the resulting calculated structures and are usually only enforced in well-defined regions of secondary structure.[130] The hydrogen bond restraint list, Table D.2 in Appendix D, was built by identifying the residues that form part of the three α helices in 4MP-α_3C and by relying on the classical hydrogen bond interactions between residue i(HN) and i+4(CO) in the helical secondary structure.[159] The residues that form part of the three α helices in 4MP-α_3C, as identified by TALOS+ (see Appendix C), are residues V2 – A18 for helix 1, residues R24 – E41 for helix 2, and residues V48 – K64 for helix 3. The rest of the residues in the protein fall in the category of loops. Table D.2 in Appendix D lists hydrogen-bonding interactions between residue i and i+4, and gives them an allowed distance range of 3.0 ± 0.5 in most cases.

The structure calculation of 4MP-α_3C with the CNS suite utilized distance restraints derived from NOESY experiments and from classical α-helical hydrogen-bond interactions, and dihedral angle constraints derived from chemical shift values. The restraint files are composed of lists of the identified interaction/parameter and a range of allowed values for each.

Structure determination protocols aim to find atom coordinates for the protein that will satisfy the provided restraints while minimizing the number of violations to the input data.[130] The calculation process is repeated numerous times, generating trial structures in every calculation, and restraints that generate violations are removed iteratively. This refining process ends when no more violations are obtained from the calculated trial structures, or when the number of violations obtained does not change. In our final calculation, a thousand trial structures were generated and an ensemble of the 32 lowest-energy structures were chosen to be part of the NMR-derived structure. The structural model for 4MP-α_3C is a high-resolution model, as evidenced by the root mean square deviation (RMSD) between the 32 structures in the ensemble, which was calculated by the program MOLMOL[162] to be 1.21 Å for all heavy atoms for all residues in the protein, and 0.48 Å for all backbone atoms. See Table 5.4 for all structural statistics for the 4MP-α_3C ensemble. The quality of the structural ensemble is not only assessed by the RMSD between the coordinates of the 32 structures but also by taking into account how well the three-dimensional structures agree with the experimental restraint data and idealized geometry for protein structures.[130] In both accounts, the 4MP-α_3C structural ensemble yields excellent statistics (Table 5.4), thus confirming the high quality of the structural ensemble obtained. See Figure 5.5 for visualization of the family of protein structures that represent the 4MP-α_3C structural ensemble.

Table 5.4. Experimental Restraints and Structural Statistics for 4MP-α_3C.

	4MP-α_3C
Experimental NOE distance restraints	
Intraresidue	294
Sequential ($\|i-j\| = 1$)	151
Medium range ($1 < \|i-j\| < 5$)	213
Long range ($\|i-j\| > 5$)	171
Total	829
Backbone dihedral angle restraints	108
Hydrogen bond distance restraints	39
Total Restraints	976
Average restricting constraints per restrained residue	15.3
Average long-range constraints per restrained residue	2.7
Ramachandran Plot Summary	
Most favored regions	96.6 %
Additionally allowed regions	1.5 %
Generously allowed regions	0.0 %
Disallowed regions	1.9 %
RMS deviations from experimental restraints	
Distance (Å)	0.0061 ± 0.0005
Dihedral angles (°)	0.16 ± 0.03
RMS deviations from idealized geometry	
Bonds (Å)	0.00114 ± 0.00005
Angles (°)	0.346 ± 0.003
Impropers (°)	0.199 ± 0.008
Average RMS deviations from mean structure	
All residues (backbone atoms)	0.479
All residues (heavy atoms)	1.209
Helical residues (backbone atoms)	0.298
Helical residues (heavy atoms)	1.197

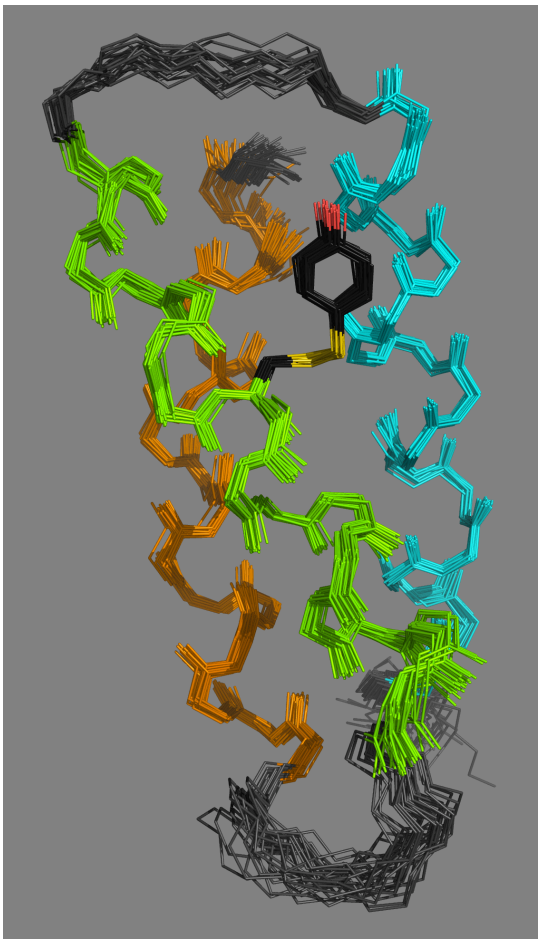

Figure 5.5. Structural ensemble of the 4MP-α_3C protein (RMSD = 1.21 Å). Backbone atoms for all structures are displayed as sticks. Atoms for helix 1 are depicted in cyan, atoms in helix 2 are depicted in light green, and atoms in helix 3 are depicted in orange. Atoms in loops and/or unstructured regions are depicted in gray. Residue 4MP-C32 is shown with black carbon atoms, yellow sulfur atoms and red oxygen atoms; hydrogen atoms are not displayed. This figure was generated with the program PyMol.[119]

5.3.4. Radical site comparison: 2MP-α_3C vs. 4MP-α_3C

Examination of the covalently bound mercaptophenol molecule in both the 2MP-α_3C and 4MP-α_3C proteins reveals key differences. As mentioned in Section 2.3, the protein-bound 2MP molecule has 3.5 ± 0.7 % of its surface area exposed to solvent. The phenol oxygen and hydrogen atoms in the 2MP ligand

are 2.0 ± 3.1 % and 4.0 ± 5.4 % exposed to solvent. A similar SASA analysis was performed on 4MP-α_3C with the program MOLMOL[162], using a solvent probe radius of 1.4 Å and a level 5 precision (see Section 7.12). The 4MP-C32 residue has a SASA percentage of 7.9 ± 2.3, with the hydroxyl oxygen and hydrogen 29.7 ± 20.0 % and 30.6 ± 30.3 % exposed to bulk solution. Figure 5.6 shows the structures of 2MP-α_3C and 4MP-α_3C for comparison, while Figure 5.7 displays the atomic SASA percentages for the 2MP-C32 and 4MP-C32 residues. Atom numbering and SASA analysis for all atoms in the 4MP-C32 residue are described in Appendix E.

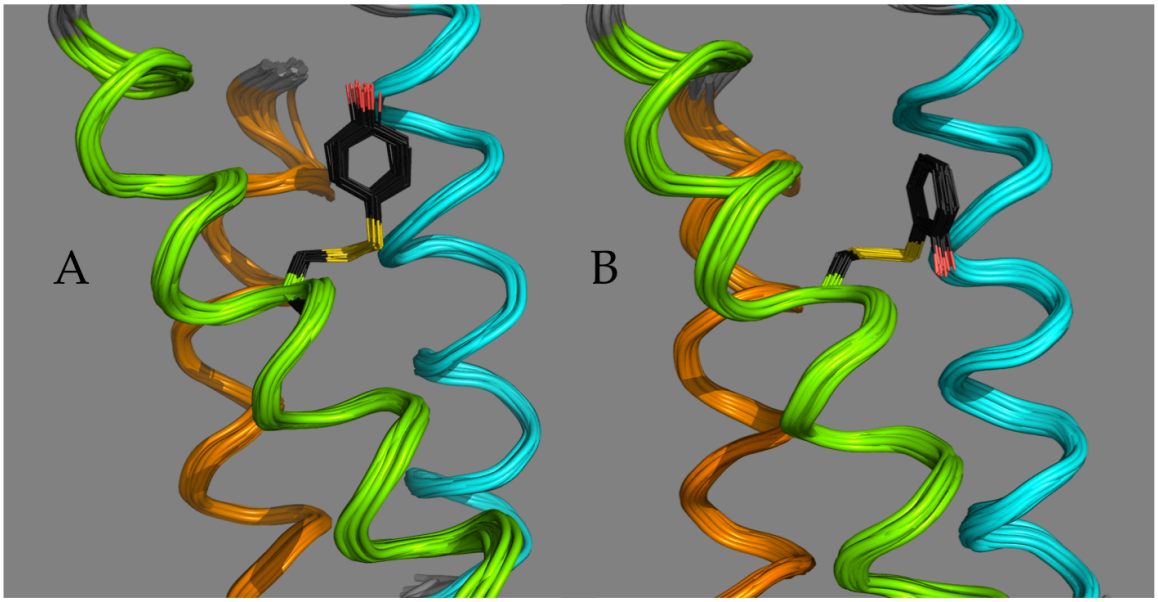

Figure 5.6. Expansions of structures of 2MP-α_3C (RMSD = 0.95 Å) and 4MP-α_3C (RMSD = 1.21 Å). Panel **(A)** shows the 2MP-α_3C protein structure, while panel **(B)** shows the 4MP-α_3C structure. Backbone atoms for all structures are displayed as loops. Atoms for helix 1 are depicted in cyan, atoms in helix 2 are depicted in light green, and atoms in helix 3 are depicted in orange. Atoms in loops and/or unstructured regions are depicted in gray. Residues 2MP-C32 and 4MP-C32 are shown with black carbon atoms, yellow sulfur atoms and red oxygen atoms; hydrogen atoms are not displayed. This figure was generated with the program PyMol.[119]

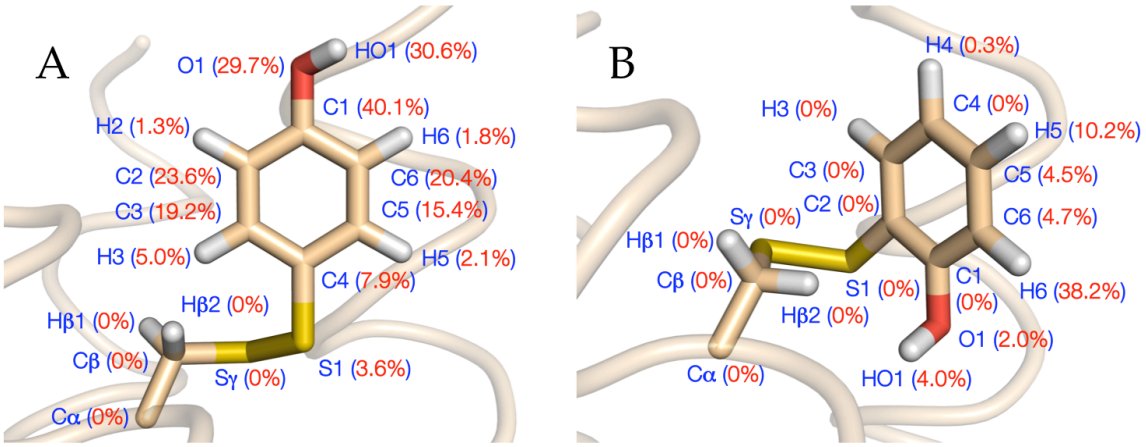

Figure 5.7. SASA analysis for 2MP-C32 and 4MP-C32. Panel **(A)** and **(B)** show stick representations of 2MP-C32 and 4MP-C32, respectively. Carbon atoms are depicted in wheat color, sulfur atoms are depicted in yellow, oxygen atoms are depicted in red, and hydrogen atoms are depicted in white. Names of atoms are shown in blue, while the atomic SASA percentage is shown in red. The SASA analysis was performed using the MOLMOL program.[162] A solvent probe radius of 1.4 Å and a level 5 precision were used for the calculations. See Section 7.12 for more information on this calculations. This figure was generated using the program PyMol.[119]

From the SASA analysis, we see that the initial design of 4MP-α_3C to have the hydroxyl group of the covalently bound molecule being more exposed to solvent than the corresponding group in 2MP-α_3C was successful. We observe that the hydroxyl group of the 4MP ligand is around one order of magnitude more exposed to solvent than the hydroxyl group in 2MP-C32. This difference in the environment of the phenol group is expected to have effects on the redox properties of the protein-bound molecule. Previous studies showed a shift in the DPV-derived peak potentials for 2MP-α_3C when compared to 2MP-bCys in solution, whereas the electrochemical behavior of 4MP-α_3C was essentially identical to its freely solvated counterpart.[84] As has been seen in studies in

small-molecule systems, interactions to the phenol/tyrosine hydroxyl group are essential in determining its redox properties. More detailed electrochemical characterization of these proteins, having these structures available, will provide a more complete picture of what protein environmental factors are essential for radical stabilization within the protein framework.

5.4. Electrochemical characterization of 2MP-α_3C by DPV and SWV

In light of the clear differences in the structures of the 2MP-C32 and 4MP-C32 residues in the 2MP-α_3C and 4MP-α_3C solution NMR structures, a more detailed electrochemical characterization of both proteins is of essence. A preliminary DPV study was carried out in which 4MP-α_3C displayed similar electrochemical behavior as 4MP-bCys while the other two MP-α_3C proteins reflected differences in their electrochemical response. As mentioned in Section 2.3, the instability of the oxidation products and coupled chemical reactions obscure the data, and no definite conclusions can be drawn from that data. In order to address this issue, the redox properties of these proteins will be explored by using square wave voltammetry. SWV has been used to study the electrochemistry of α_3Y and it was found that the experiment can be set to outcompete the coupled chemical reactions (see Chapter 3). Hence, we set out to examine the electrochemical behavior of 2MP-α_3C using this technique.

Similar to the α_3Y SWV studies, several control and optimization experiments were performed in order to find optimal conditions for the examination of the electrochemical behavior of 2MP-α_3C. The effects of salt and

protein concentration on the current response were assessed, as well as the effect of square wave pulse amplitude. Figure 5.8 shows the data resulting from these measurements. The half-wave potential ($E_{1/2}$) derived from DPV was explored as a function of content of KCl at both acidic and alkaline conditions (Figure 5.8A). At low pH, the observed potential is independent of the KCl concentration with an average $E_{1/2}$ (pH 5.61) value of 1003 ± 2 mV across the whole 0 – 140 mM range. At high pH, a very weak influence on $E_{1/2}$ is observed at low KCl concentrations. $E_{1/2}$ (pH 7.70) decreases by 5 ± 1 mV between 0 and 40 mM KCl and then levels out at 884 ± 1 mV for the 40 – 140 mM range. These observations confirm that in the KCl concentration range of 40 – 140 mM, there are no unfavorable interactions between the positively charged protein (pI ~ 8.79; see Section 3.5.1) and the negatively charged surface of the pyrolytic graphite edge (PGE) working electrode. The net peak potential (E_{net}) derived from SWV was also examined as a function of protein concentration (Figure 5.8B). The data obtained shows no dependence on the concentration of 2MP-α_3C in both acidic and alkaline solutions. Average values for E_{net} of 1006 ± 1 mV (pH 5.54; 190 Hz) and 834 ± 1 mV (pH 8.55; 190 Hz) were observed across the 20 – 100 μM protein range. E_{net} is not perturbed by any distorting interactions between the protein and the electrode surface nor influenced by intermolecular radical-radical or radical-substrate reactions.[35] Such events depend on the protein concentration and would result in an slope different than zero. This is not observed. Thus the protein does not unfold on the electrode surface and the oxidized protein is not involved in dimerization reactions. Therefore, we report

optimal sample conditions for electrochemical measurements to be 20 – 100 μM 2MP-α_3C, 20 mM APB buffer, and 40 – 140 mM KCl.

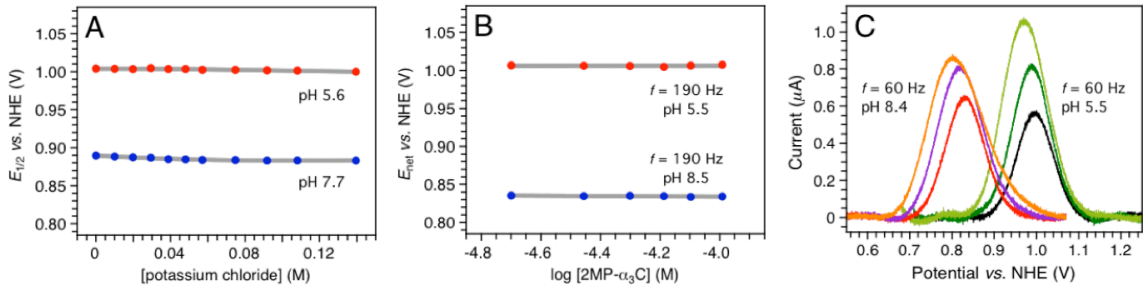

Figure 5.8. Control and optimization voltammetry experiments for 2MP-α_3C sample. **(A)** DPV $E_{1/2}$ potential of 2MP-α_3C as a function of the sample KCl concentration at pH 5.61 ± 0.01 (red circles) and pH 7.70 ± 0.01 (blue circles). *Sample*: 30 μM 2MP-α_3C in 20 mM sodium acetate and 20 mM potassium phosphate (pH 5.61 ± 0.01); 20 μM 2MP-α_3C in 20 mM potassium phosphate and 20 mM sodium borate (7.70 ± 0.01); temperature 25 °C. *Experimental Settings*: DPV, PGE working electrode, interval time 0.1 s, step potential 0.9 mV, scan rate 9.0 mV s^{-1}, modulation time 7-8 ms, modulation amplitude 50 mV. **(B)** SWV E_{net} potential of 2MP-α_3C as a function of the sample protein concentration at pH 5.54 ± 0.02 (red circles) and pH 8.55 ± 0.02 (blue circles). *Sample*: 2MP-α_3C in 20 mM APB, 80 mM KCl; temperature 25° C. *Experimental settings*: PGE working electrode, step potential 0.15 mV, SW pulse amplitude 25 mV, SW frequency 190 Hz. **(C)** 2MP-α_3C SW voltammograms recorded using a SW frequency of 60 Hz and a SW pulse amplitude between 25 and 75 mV. The figure displays two data sets collected at pH 5.55 ± 0.02 and 8.43 ± 0.02. The SW pulse amplitude was 25 mV (red and black), 50 mV (blue and medium green) and 75 mV (orange and light green). *Sample*: 75 μM 2MP-α_3C in 20 mM APB, 80 mM KCl; temperature 25° C. *Experimental settings*: PGE working electrode, step potential 0.15 mV, and SW frequency 60 Hz.

Once optimal sample conditions had been established for the 2MP-α_3C/PGE system, data were collected to investigate whether adsorption or diffusion-controlled electrode kinetics occur at these conditions. Square-wave voltammograms representing a surface-confined redox species are influenced by the SW frequency and the pulse amplitude relative to the heterogeneous ET rate constant of the system.[108,113] A combination of low frequencies and large

pulse amplitudes may result in a splitting of the peak maximum in the net voltammogram. The splitting of the net peak provides a criterion for distinguishing a surface-confined from a diffusion-controlled electrode process. Square-wave voltammograms were collected at 60 Hz (t_p 8.3 ms) and using a pulse amplitude of 25, 50 and 75 mV. Data were collected at both pH 5.5 and 8.4 (Figure 5.8C). The 2MP-α_3C net voltammogram shifts and becomes broader when applying an overpotential of 50 or 75 mV but there is no indication of a splitting of the peak maximum. The lineshape of the 2MP-α_3C net voltammogram as a function of E_{SW} is consistent with diffusion-controlled electrode kinetics at both acidic and alkaline pH, as was seen in Chapter 3 for α_3Y.

In addition to the control experiments previously mentioned, the extent of the reproducibility of the SWV current response was verified and found, and as in the case for the α_3Y protein, that SW voltammogram triplicates and independent measurements are highly reproducible, with peak potentials within 5 mV of each other.

A series of experiments were then conducted as a function of SW frequency in order to assess the level of reversibility of the 2MP-α_3C redox system. In Chapter 3, the α_3Y protein was found to give rise to a reversible redox transition[114] and to outcompete the formation of irreversible products that may arise due to side chemical reactions. Varying the SW frequency results in change of the pulse time of the experiment; higher frequencies are equivalent to shorter pulse times. Figure 5.9 shows representative SW voltammograms from

this frequency series at both acidic and alkaline sample conditions, and Figure 5.10 shows peak potential and I_{for}/I_{rev} ratio as a function of the square wave frequency for the alkaline sample.

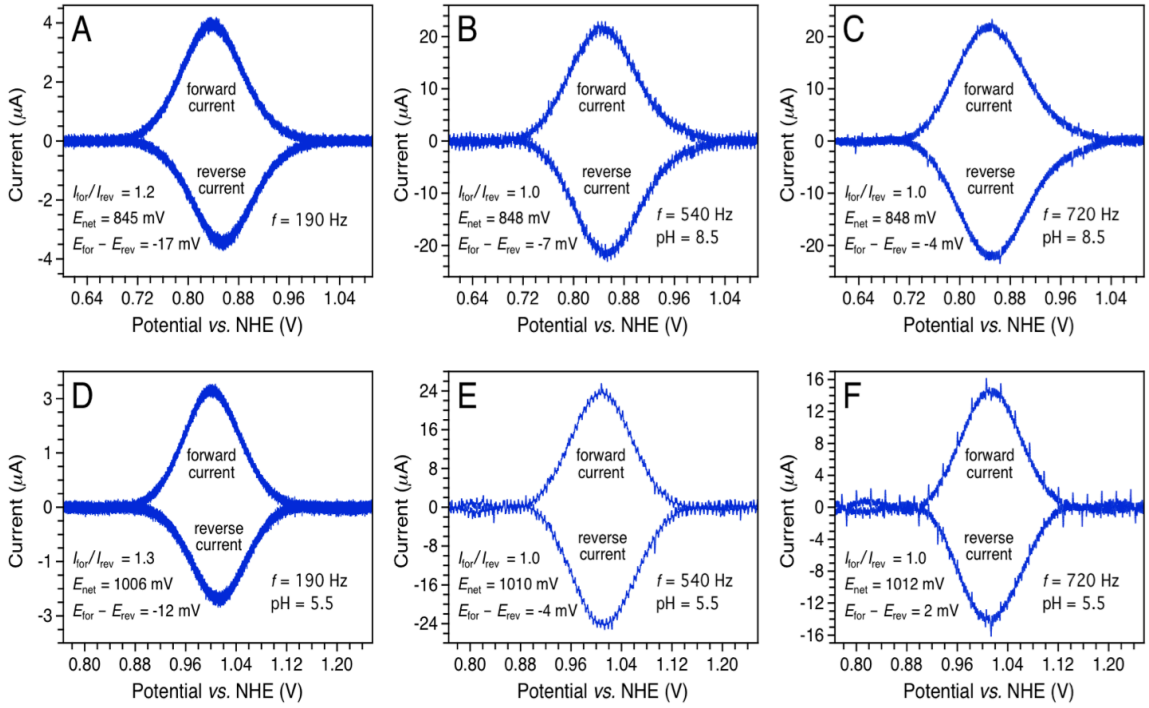

Figure 5.9. Background-corrected forward (oxidation) and reverse (reduction) square-wave voltammograms of 2MP-α_3C. Voltammograms obtained using a SW frequency of (panels **A** and **D**) 190 Hz (t_p 2.6 ms), (panels **B** and **E**) 540 Hz (t_p 926 ms), and (panels **C** and **F**) 720 Hz (t_p 694 ms). The voltammograms displayed in panels (**A**) to (**C**) were obtained at pH 8.51 ± 0.02 and those displayed in panels (**D**) to (**F**) at pH 5.52 ± 0.01. *Sample*: 75 μM α_3Y in 20 mM APB, 80 mM KCl; temperature 25° C. *Experimental settings*: PGE working electrode, step potential 0.15 mV, SW pulse amplitude 25 mV.

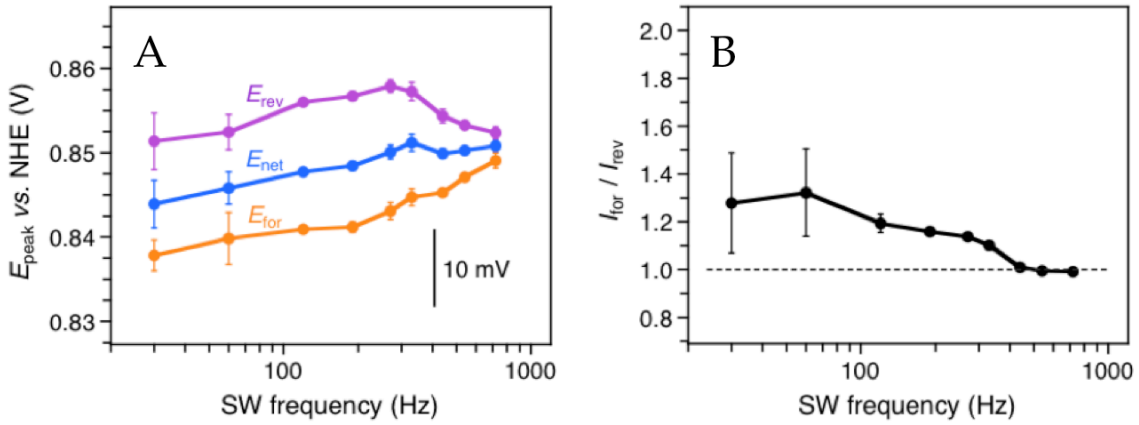

Figure 5.10. Analysis of SW frequency series obtained from electrochemical characterization of 2MP-α_3C. Panel **(A)** shows the net (E_{net}), forward (E_{for}) and reverse (E_{rev}) peak potentials of voltammograms obtained for 2MP-α_3C as a function of SW frequency. Panel **(B)** shows the ratio of forward and reverse current (I_{for}/I_{rev}) as a function of SW frequency. *Sample*: 75 μM 2MP-α_3C in 20 mM APB, 80 mM KCl, pH 8.51 ± 0.02, temperature 25 °C. *Experimental settings*: PGE working electrode, step potential 0.15 mV, SW pulse amplitude 25 mV.

The forward and reverse voltammograms represent the oxidative and reductive currents, respectively. The two pH data sets display the same trend of changing from quasi-reversible to reversible as the frequency increases. E_{net} is highly insensitive to the frequency and increases by only 3 ± 2 mV (pH 8.51) and 6 ± 2 mV (pH 5.52) as the frequency is changed from 190 to 720 Hz. The I_{for}/I_{rev} ratio decreases from 1.2 (pH 8.51) and 1.3 (pH 5.52) to a limiting value of 1.0 at ≥ 540 Hz. $\Delta E = E_{for} - E_{rev}$ decreases from – 17 ± 2 mV to – 4 ± 2 mV (pH 8.51) and from -12 ± 2 mV to 2 ± 2 mV (pH 5.52). Figure 5.10A shows that E_{net} is 847 ± 2 mV (over a 120 – 720 Hz range), E_{for} is 844 ± 2 mV (440 – 720 Hz), and E_{rev} is 851 ± 2 mV (440 – 720 Hz) at pH 8.51 ± 0.01. This is consistent with a fully reversible diffusion-controlled electrode process, which is characterized by peak potentials that are independent of the SW frequency and are separated by only

a few mV.[36,108] From the data shown in Figure 5.10, we conclude that the 2MP-α_3C electrode process is reversible at SW frequencies above ~ 500 Hz at both pH 8.5 and 5.5. Making use of the relationships described in Chapter 3 and assuming that the diffusion coefficient of 2MP-α_3C does not change upon oxidation ($1.4 \pm 0.2 \times 10^{-6}$ cm^2 s^{-1}, as determined by NMR; see Section 7.10.5), we can determine that the voltammograms obtained at frequencies larger than 500 Hz are the result of fully reversible electron transfer. No significant changes in the E_{net} value were found after a SW frequency value of 120 Hz, just as in the case of the protein α_3Y (see Chapter 3.3) Thus, the tyrosyl radical formed from oxidation of 2MP-α_3C has a k_{chem} value of ≤ 4 s^{-1}, which corresponds to a halflife of ≥ 170 ms.

5.5. Summary

Further development of the MP-bound α_3C protein system is discussed in this chapter. Additional experiments were carried out in order to characterize the structural integrity of these proteins as a function of solution pH. Determination of α-helical content, size-exclusion chromatography, and ^{15}N- and ^{13}C-HSQC spectra were analyzed in order to draw the conclusion that these proteins are well-structured monomeric proteins in solution. Furthermore, the solution NMR structure of 4MP-α_3C was determined at a high resolution (RMSD = 1.21 Å) and the phenol radical site was compared to the corresponding site in the 2MP-α_3C NMR structure (Section 2.3 and Appendix A). It was found that, according to initial design, the protein-bound 2MP and

4MP do have differences in the extent of solvent exposure of their phenolic OH group, with the OH of 4MP one order of magnitude more exposed to bulk solvent than the corresponding group in 2MP.

Once the initial design of 2MP-α_3C and 4MP-α_3C has been confirmed successful by the NMR structures, thorough electrochemical characterization ensued. In this work, the electrochemical characterization of 2MP-α_3C was achieved. Using square wave voltammetry, as described in Chapter 3 for α_3Y, optimal electrolyte and protein concentrations were found and the electrode kinetics of the electrode-driven ET was determined to be driven by diffusion-controlled kinetics. A series of measurements were carried out by varying the SW frequency with the aim of finding a frequency value at which the reductive pulse can be set to outcompete coupled chemical reactions. The peak potentials of the voltammogram (net, forward, and reverse) were found to become independent of SW frequency at around 500 Hz, and the tyrosyl radical was found to be a long-lived species, with a halflife of at least 170 ms.

CHAPTER 6: Conclusions

This dissertation work was driven by the remarkable one-electron organic redox chemistry in natural systems. Natural proteins, such as *E. coli* ribonucleotide reductase and photosystem II, employ amino-acid radical cofactors as part of their enzymatic reactions as part of catalysis or as part of long-range electron transfer. In specific, the radical chemistry of tyrosine is of great interest. In the case of In solution, tyrosine oxidation results in highly unstable species that are rapidly consumed by radical chemical reactions, which may include radical-radical and radical-substrate dimerization reactions. Electrochemical characterization of these species is challenging due to these side reactions that mask the thermodynamic and kinetic properties of the initial electron transfer process. In natural proteins, however, the products of tyrosine oxidation are not only stable but the redox chemistry is reversible. Tyrosine residues, as redox cofactors, participate in several protein turnovers. This striking difference in redox behavior must mean that proteins provide interactions to the cofactor that generate, control, and direct the redox chemistry within the protein milieu. The thermodynamics of redox reactions are described by reduction potentials. These values have proven to be almost impossible to obtain in natural systems due to the need to expose the entire protein to highly oxidizing electrode potentials, which can potentially trigger current flow arising from other cofactors and other amino acid residues in these proteins. Due to the challenge of obtaining reduction potentials of amino acid redox cofactors in natural proteins, small-molecule models have been generated

and characterized. These models aim to mimic the key components that drive and control electron transfer in natural proteins. These models have contributed immensely to our knowledge of what factors contribute to the special properties of these species inside of proteins, such as the presence and nature of hydrogen-bonding partners, among others. However, these small-molecule models have the disadvantage that the tyrosine moiety is significantly exposed to bulk solvent, thus lacking the protein environment that allows the redox chemistry to be fully reversible. With the objective of filling the void between the natural systems and the small-molecule models, we have developed a series of *de novo*-designed model proteins that confine the redox-active amino acid to a low-complexity protein environment, when compared to natural systems. Initially, these model proteins were designed to fulfill a set of requirements in order to be viable models for radical proteins. The protein scaffold must be structurally stable in order to be able to form specific and stable interactions with the redox-active residue. Moreover, the structural integrity of the protein must not be affected by changes in pH. pH is a key parameter for the studies of these species and data arising from these systems must not reflect pH-dependent structural perturbations. Finally, the protein background should be redox-inert in the potential range in which the redox-active residue of interest becomes oxidized. Several proteins form part of this family of model proteins: α_3W, α_3Y, and α_3C. These proteins are composed of a 65-residue three-helix bundle, connected by loops comprised of glycine residues, which contain a single TRP, TYR, or CYS residue in the core of the protein, respectively. All three proteins have been found to be structurally stable and monomeric in

solution, and the degree of pH-dependent structural perturbations has been found to be minimal. Also, the protein scaffold has been found to be redox-inert up to a potential of +1.3 volts vs. NHE. Development of the α_3Y and α_3C proteins is described in this dissertation.

The α_3Y system has been characterized electrochemically by use of square wave voltammetry (Chapter 3). SWV is a highly sensitive voltammetry technique which allows access to faster time scales than those reached by the more commonly used cyclic voltammetry and differential pulse voltammetry. Using this technique, fully reversible electrochemistry was achieved as evidenced by the independence of voltammogram peak potentials on the frequency of the square wave experiment. Formal potentials were obtained for α_3Y at pH 8.4: 918 ± 2 mV vs NHE. Moreover, kinetic information was also made available by this technique, with the radical generated in α_3Y found to have a radical half life of at least 170 milliseconds. From these results, we conclude that we have successfully generated the first model in which a tyrosine neutral radical resides inside a protein, and moreover thermodynamic and kinetic information for the process was successfully extracted using protein voltammetry. In addition, comparison of DPV- and SWV-derived electrochemical data suggests the presence of an additional residue that serves as the proton acceptor for the released phenolic proton in the vicinity of the radical site. This observation provides evidence that the protein scaffold is involved in the PCET event involving residue Y32, which makes studies in the α_3Y a relevant mimic of the natural systems. In the RNR and PSII protein

systems, the redox-active tyrosine residue interacts with residues capable of proton capture upon oxidation (see Figures 1.3 and Figure 1.4). Future work on the α_3Y protein will be driven towards the achievement of a more detailed electrochemical characterization of the system at acidic conditions, and towards the identification of the residue of unknown identity that serves as proton acceptor within the protein. Further development of this system will also aim to increase the complexity of this system to study how different interactions to the protein milieu tune the redox chemistry of the tyrosine residue.

In this work, the α_3Y system was also used to create a TYR-HIS interaction within the protein (Chapter 4). Several α_3Y-HIS model proteins were generated by single-point mutations that introduced a histidine residue at sites that were hypothesized to form an interaction between the two aromatic side chains. Two of the eight generated HIS variants were found to be structurally stable through a wide pH range, and were also found to contain a interaction between the tyrosine and histidine side chains. The proteins α_3Y-K29H and α_3Y-K36H were thoroughly characterized by several techniques to assess the degree of the TYR-HIS interaction, and NOE-based NMR experiments provided the ultimate confirmation that, according to the initial design, these proteins do contain interacting TYR-HIS pairs, with α_3Y-K29H containing a more motionally restricted interaction than α_3Y-K36H. A TYR-HIS interacting pair is of great interest due to the known Y_Z-H190 interacting pair in photosystem II. In PSII, H190 is the primary proton acceptor of the phenolic proton released by Y_Z upon oxidation by the P680 radical cation. The presence of this histidine is

essential for the activity of the protein. The next step on studies involving the α_3Y-HIS variants will include thorough electrochemical characterization of these proteins, and also investigation of pH-dependent changes in the redox properties of the tyrosine residues in these proteins.

Another of the proteins in the *de novo*-designed family of proteins that was developed in this work is the α_3C protein (Chapter 5). The α_3C protein was bound to the three different constitutional isomers via disulfide linkage through residue C32 to create three proteins that contain protein-bound tyrosine analogues with differing degrees of solvent exposure: 2MP-α_3C, 3MP-α_3C, and 4MP-α_3C. As in the case of α_3Y, these proteins were found to be structurally stable throughout a wide pH range. The design consisted on 4MP-α_3C containing a more solvent-exposed phenolic hydroxyl group than 2MP-α_3C and 3MP-α_3C. The solution NMR structures of 2MP-α_3C and 4MP-α_3C have been determined to a high level of resolution, 0.95 and 1.21 Å, respectively. Comparison of their radical sites yield solvent accessible surface area (SASA) for the 4MP phenolic OH to be one order of magnitude larger than that for the corresponding group in protein-bound 2MP, confirming the success of the initial design of this small molecule-protein system. Electrochemical characterization of the 2MP-α_3C protein by voltammetry methods was achieved by SWV, at both acidic and alkaline sample conditions. The formal potential for the protein-bound MP molecule was determined to be 847 ± 2 mV vs. NHE, at pH 8.5. This value is more than 50 mV less oxidizing than the values obtained for the α_3Y protein, suggesting that oxidation is more thermodynamic favorable

for 2MP-α_3C. These results suggest that the 2MP neutral radical in 2MP-α_3C finds a more stabilizing environment than the Y32 neutral radical in α_3Y. A closer look at the radical site reveals a hydrogen-bonding interaction between 2MP phenolic OH and a carboxylic oxygen of residue E13 in the protein. This interaction will be of great significance in determining future development of this system. Already a variant of 2MP-α_3C has been generated in which residue E13 is mutated to an alanine residue. The redox characteristics of this variant will be explored to determine the importance of the hydrogen-bonding interaction to the redox properties of this neutral phenolic radical. Future work on the MP-α_3C system includes the structural characterization of 3MP-α_3C, and the thorough electrochemical characterization of 4MP-α_3C and 3MP-α_3C.

In conclusion, we have generated a family of proteins that serve as viable models for radical proteins. We have proved that they are structurally stable throughout a wide range of pH values. Electrochemical characterization of thermodynamic and kinetic properties of the electron transfer process has been successfully achieved for tyrosine-containing α_3Y and for tyrosine-analogue-containing 2MP-α_3C. Square wave voltammetry provided timescales fast enough to outcompete any side chemical reactions that might occur upon oxidation of the tyrosine/phenol. Hence, the electrochemistry was found to be fully reversible for both proteins at alkaline pH. The formal reduction potentials for the neutral radicals generated in α_3Y and 2MP-α_3C were found to be 918 ± 2 mV (pH 8.4) and 847 ± 2 mV (pH 8.5), respectively. Reduction potentials for redox-active tyrosines in natural proteins have been estimated for Y_Z and Y_D in

photosystem II and Y122 in *E. coli* ribonucleotide reductase.[84] Estimated reduction potential values for the tyrosines in photosystem II are 970 ± 20 mV (pH 6.0) for Y_Z and 740 ± 20 mV (pH 6.0) for Y_D. The reduction potential for Y122 in E. coli RNR has been estimated to be 1000 ± 100 mV (pH 7.6). We observe that the radicals formed within the α_3X scaffold have formal reduction potentials that fall within the range of reduction potential values of radicals formed in natural proteins. Thus, we have been able to create a protein environment in which the radical can reach reduction potential values as high as the values reached in natural proteins, without destroying the protein scaffold. Additionally, studies at low pH revealed that proton transfer might become rate-limiting and drive the electron-transfer reaction away from the reversible and into the quasireversible regime, thus being able to modulate the redox properties of tyrosine. This fact, together with the structural characteristics of our family of model proteins, makes the α_3X scaffold a suitable model for natural redox proteins. Further structural and electrochemical characterization will surely provide more insights into the one-electron redox chemistry of tyrosine within protein scaffolds, and will certainly contribute to our knowledge of how natural radical proteins function.

CHAPTER 7: Materials and methods

7.1. Protein expression and purification

All proteins were made by QuikChange (Stratagene) using a modified α_3W/pET32b (Novagen) vector as template. The α_3X sequence has the following amino acid sequence: GS-RVKALEEKVKALEEKVKALGGGGRIE-ELKKK**X**EELKKKIEELGGGGEVKKVEEEVKKLEEEIKKL, where **X** denotes either a TRP, TYR, or CYS residue for α_3W, α_3Y and α_3C, respectively. In the sequence, the *N*-terminal GS residues form part of a thrombin cleavage site. These two residues are labeled as -2 and -1 to keep the amino acid numbering consistent with the chemically synthesized 65-residue α_3X protein.[13] All proteins were expressed in LB or minimal media and purified following standard protocols for HIS-tagged proteins (Novagen). Transformed BL21-(DE3)pLys or BL21-CodonPlus(DE3)-RIL cells were harvested either after a 3-4 hour IPTG induction period at 37 °C for LB cultures or after an overnight induction at 30 °C for minimal media cultures, and stored at -20 °C. Cells were subsequently resuspended in 20 mM TRIS-HCl, 500 mM sodium chloride, 5 mM imidazole, pH 7.9 and lysed by sonication. The lysate was clarified by centrifugation, passed over a HISbind (Novagen) nickel column, and the thioredoxin-α_3X fusion protein eluted by an imidazole gradient. Thrombin (T6634; Sigma) was added to the thioredoxin-α_3X protein fraction and the resulting mixture dialyzed against 50 mM TRIS-HCl, 500 mM NaCl, 2.5 mM calcium chloride ($CaCl_2$), pH 8.0 at room temperature overnight. The digestion mixture was

passed over a second nickel column to remove HIS-tagged thioredoxin and any remaining undigested fusion protein. Target proteins were isolated by reverse-phase high performance liquid chromatography (HPLC) (semipreparative TP2181010 column; Grace/Vydac) using an acetonitrile/water gradient containing 0.1 % (w/v) trifluoroacetic acid and stored as lyophilized powder.

7.2 Preparation of mercaptophenol-bound proteins

Lyophilized α_3C was dissolved in 50 mM potassium phosphate, 3.0 M guanidinium hydrochloride, pH 8.0. Dithiothreitol was added at an estimated 5-10 fold excess and the mixture incubated for 15 minutes at room temperature. The buffer was exchanged using PD-10 columns (GE Healthcare) equilibrated in 50 mM potassium phosphate, pH 8.0, and the protein concentration determined immediately by Ellman's assay (5,5'-dithiobis-(2-nitrobenzoic acid); Sigma-Aldrich)[163] under denaturing conditions and using an ε_{412} of 37000 M^{-1} cm^{-1}. The binding reaction was prepared as follows: 1 part α_3C dissolved in 50 mM potassium phosphate, 10 parts 2-, 3-, or 4-mercaptohenol (Sigma-Aldrich) and 3 M guanidinium hydrochloride. The pH was adjusted to 8.0 and the sample placed on a rotisserie at 4 °C overnight. The binding mixture was dialyzed against 50 mM acetate, 30 mM KCl, pH 6.0 at 4 °C for 24 hours, purified by reverse-phase HPLC, and the MP-α_3C protein stored as lyophilized powder.

7.3. Determination of protein concentration

Absorption spectra were collected on a Varian Cary 50 Bio or Hitachi U-3000 UV/Vis spectrometer at room temperature. The absorption at the wavelength of maximum absorption (λ_{max} = 276 nm for α_3Y and α_3Y-HIS variants, and 290 nm for all MP-bound α_3C proteins) was recorded, and used to calculate the concentration of protein by using the Beer-Lambert relationship, $A = \varepsilon bc$, where A represents the absorption obtained from the spectrum, ε is the extinction coefficient of the molecule, b is the cuvette path length, and c is the concentration.[109] The extinction coefficient (ε_{276}) used for α_3Y and all α_3Y-HIS proteins is = 1490 M^{-1} cm^{-1}. The extinction coefficient (ε_{290}) used for 2MP-α_3C, 3MP-α_3C, and 4MP-α_3C is 3700, 3100, and 2300 M^{-1} cm^{-1} respectively.[84]

7.4. Determination of pK_A of TYR residue in α_3Y and α_3Y-HIS proteins.

The absorbance spectra for α_3Y, α_3Y-V9H, α_3Y-L12H, α_3Y-K29H, α_3Y-K36H, α_3Y-I62H were obtained on a Varian Cary 50 Bio or a Hitachi U-3000 UV/Vis spectrometer at room temperature, as a function of pH. The absorption spectrum of the Y32 residue is expected to change at pH values higher than its pK_A due to deprotonation. Figure 7.1 shows the spectra for α_3Y at pH values 7.0 and 12.3. pH-titration samples were prepared by dissolving lyophilized protein in a 10 mM potassium phosphate, 10 mM HEPES (4-(2-hydroxyethyl)-1-piperazineethanesulfonic acid), 10 mM sodium borate, 10 mM CAPS (*N*-cyclohexyl-3-aminopropanesulfonic acid), pH 7.0 buffer to an absorbance at 276

nm of 0.2 (10 mm path length). The solution was split in two equal fractions and the pH carefully adjusted with 12 M hydrochloric acid (HCl) or 10 M sodium hydroxide (NaOH). pH titrations were performed by constant volume titration. The apparent tyrosinate/tyrosine pK_A of Y32 was estimated by measuring at 293 nm and 400 nm (baseline) as a function of pH and fitting the resulting pH-titration curve to a single-pK_A Henderson-Hasselbalch equation[109], by using the nonlinear curve fitting routines in KaleidaGraph (www.synergy.com). The fitting statistics are listed in Table 7.1.

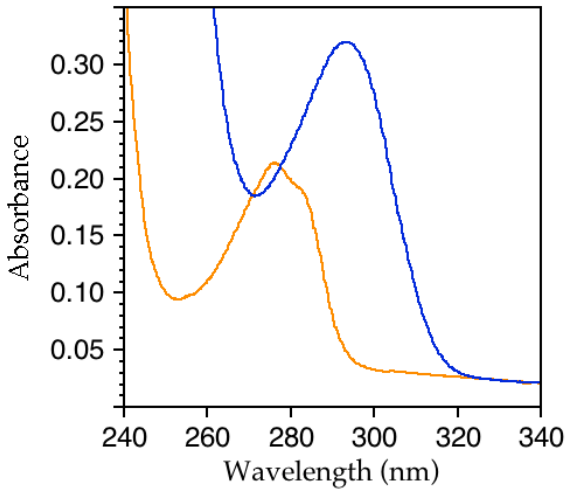

Figure 7.1 Absorption spectrum of α_3Y at neutral and alkaline pH. Orange and blue plots represent spectra collected for samples at pH 7.0 (λ_{max} = 276 nm) and 12.3 (λ_{max} = 293 nm), respectively. *Sample*: α_3Y in a solution containing 10 mM potassium phosphate, 10 mM HEPES, 10 mM sodium borate, 10 mM CAPS at room temperature.

Table 7.1. Determination of pK_{APP} of residue Y32 in α_3Y-HIS proteins

Protein	pK_{APP}	χ^2	R^2
α_3Y	11.26 ± 0.03	0.000847	0.9952
α_3Y-V9H	10.82 ± 0.04	0.003291	0.9913
α_3Y-L12H	10.41 ± 0.02	0.000845	0.9970
α_3Y-K29H	10.72 ± 0.03	0.000681	0.9952
α_3Y-K36H	10.97 ± 0.04	0.000645	0.9915
α_3Y-I62H	10.65 ± 0.04	0.001792	0.9951

See text in this section for sample conditions.

7.5. Determination of pK_A of HIS residue in α_3Y-HIS proteins.

The chemical shift of the Hε1 proton in the HIS imidazole ring was monitored as a function of pH, and used to determine the apparent imidazole/imidazolium pK_A values of the single histidine in the α_3Y-HIS proteins. The position of the Hε1 resonance is highly sensitive to pH (see Figure 7.2). One-dimensional (1D) ^{1}H NMR spectra were collected in a Varian Inova 750 MHz spectrometer equipped with a conventional room temperature probe. pH-titration samples were prepared by dissolving lyophilized protein in a 10 mM deuterated sodium acetate, 10 mM sodium phosphate, 30 mM KCl, pH 4.0 buffer and in a 10 mM sodium phosphate, 10 mM sodium borate, 30 mM KCl, pH 10.0 buffer. Buffers were prepared in D_2O, all samples were ~600 μM in protein and contained 500 μM 2,2-dimethyl-2-silapentane-5-sulfonate sodium salt (DSS) as a chemical-shift standard. pH titrations were conducted by equal volume titration and collecting 1D spectra of the α_3Y-His proteins at 25^o C. Isotope effects were corrected using the following relationship: p$K(H_2O)$ = 0.929 × p$K(D_2O)$ + 0.42.[164] The apparent imidazole/imidazolium pK_A of Y32 was

estimated by obtaining the chemical shift value as a function of pH and fitting the resulting pH-titration curve to a single-pK_A Henderson-Hasselbalch equation[109] and by using the nonlinear curve fitting routines in KaleidaGraph (www.synergy.com). The fitting statistics are listed in Table 7.2.

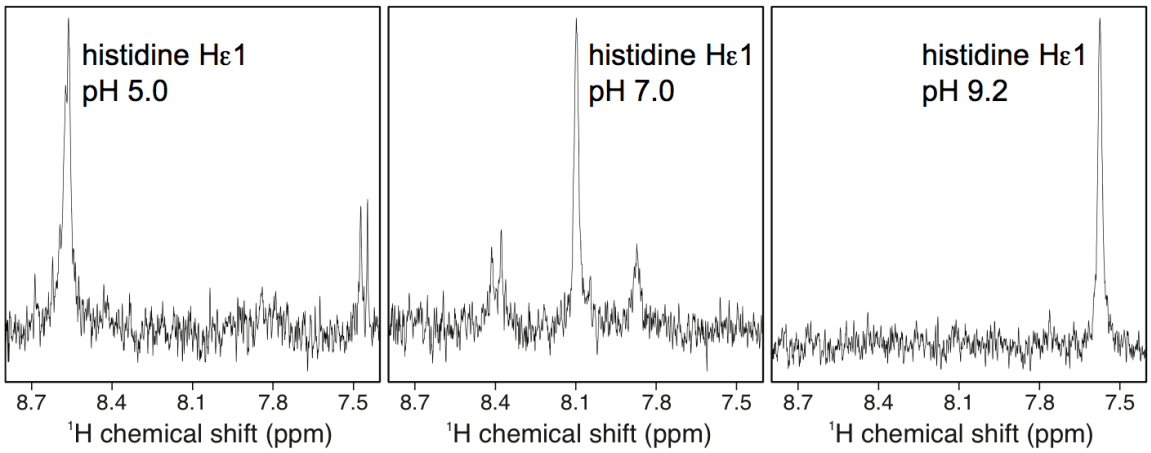

Figure 7.2 One-dimensional NMR spectra of α_3Y-K36H as a function of pH. NMR spectra recorded on α_3Y-K36H at pH 5.0 (left panel), 7.0 (middle) and 9.2 (right). The pH-sensitive resonance of the histidine ε1 ring proton shifts more than 1 ppm across the titrated pH range. α_3Y-K36H was dissolved in D_2O containing a buffer cocktail of deuterated sodium acetate, sodium phosphate, sodium borate and 30 mM KCl. The spectra were collected at 25° C.

Table 7.2. Determination of pK_{APP} of Residue HIS in α_3Y-HIS Proteins

Protein	pK_{APP}	χ^2	R^2
α_3Y-L12H	6.56 ± 0.04	0.002639	0.9987
α_3Y-K29H	7.08 ± 0.02	0.001805	0.9991
α_3Y-K36H	7.02 ± 0.02	0.003854	0.9975
α_3Y-I62H	6.98 ± 0.01	0.000185	0.9999

See text in this section for sample conditions.

7.6. Circular dichroism spectroscopy

CD studies were conducted on an Aviv 202 CD spectrometer.

7.6.1. α_3Y and HIS proteins: **(1)** For the α-helical measurements, lyophilized protein was dissolved in 10 mM APB pH 8.2 buffer to a concentration of ~50 μM. The cuvette path length was 2 mm. The absolute degree of secondary structure was determined by using α_3W as a reference (76 ± 1% α-helical between pH 4 and 10).[56] pH titrations were conducted by constant volume titration and the samples prepared by dissolving protein powder in 10 mM APB pH 7.0 buffer, splitting the solution into two equal fractions, and adjusting the pH with either 12 M HCl or 10 M NaOH. The degree of α-helical content and changes in this parameter were monitored by measuring the mean residue ellipticity at 222 nm ($[\Theta]_{222}$). $[\Theta]_{222}$ was calculated by using Equation 7.1.

$$[\Theta]_{222} = \frac{md/1000}{C * N * l * 10} \tag{7.1}$$

where *md* is the CD signal in millidegrees, *C* is the protein molar concentration in mol L^{-1}, *N* is the number of amino acid residues in the protein, *l* is the cuvette path length. The "1000" and "10" factors in the equation are used to convert the *md* unit to degrees and the *C* unit to dmol L^{-1}, respectively; the conventional units for $[\Theta]_{222}$ are deg cm^2 $dmol^{-1}$. The α-helical percentage is then calculated by using Equation 2.1. **(2)** Chemical denaturation experiments were conducted by

automated constant volume titration of a 10 M urea protein sample into a 0 M urea protein sample. Samples were prepared by diluting protein stock in 10 mM APB pH 8.2 buffer containing either 0 or 10 M urea. The free energy of unfolding in the absence of denaturant (ΔG^{H_2O}) was determined by fitting the urea melt plots to Equation 7.2.[94]

$$[\Theta]_{[Urea\}} = \frac{([\Theta]_U + c_U[Urea]) + ([\Theta]_F + c_F[Urea])exp\left(\frac{\Delta G^{H2O} - m[Urea]}{kT}\right)}{1 + exp\left(\frac{\Delta G^{H2O} - m[Urea]}{kT}\right)}, \tag{7.2}$$

where $[\Theta]_{[Urea]}$ is the CD signal in millidegrees at a given concentration of urea, c_U and c_F are the slopes of the pre- and post-unfolding regimes in the plot, respectively, *[Urea]* is the concentration of urea, *m* is the cooperativity of the unfolding transition, and $[\Theta]_U$ and $[\Theta]_F$ are the contributions to the observed signal arising from unfolded and folded protein, respectively. The fitting statistics are listed in Table 7.3.

Table 7.3. Determination of Global Stability of α_3Y and α_3Y-HIS proteins

Protein	ΔG^{H_2O}	χ^2	R^2
α_3Y	-3.74 ± 0.02	5.1309	0.99996
α_3Y-V9H	-3.00 ± 0.02	7.4578	0.99996
α_3Y-K29H	-2.84 ± 0.03	7.4754	0.99994
α_3Y-K36H	-2.39 ± 0.03	4.0212	0.99992

See text in this section for sample conditions.

The final protein concentrations were 15–40 μM for the pH and urea measurements. All experiments were performed at 25 °C.

7.6.2. For 2MP-α_3C, 3MP-α_3C, and 4MP-α_3C proteins: pH titrations were carried out in a similar fashion as with the α_3Y protein described above. ~20 μM protein was dissolved in solution containing 20 mM APB buffer and 40 mM KCl. The observed mean residue ellipticity at 222 nm ($[\Theta]_{222}$) was measured by automated constant volume titration in a 10 mm cuvette, using an averaging time of 1 sec, stir time of 0.5 min, a bandwidth of 3 nm, and a pH step size of 0.2. All measurements were done at a temperature of 30 °C.

7.7. Assessment of interaction between Y32 and H29/H36 in α_3Y-K29H and α_3Y-K36H

The center of mass of the fluorescence spectra of α_3Y, α_3Y-K29H, and α_3Y-K36H was monitored as a function of pH. Fluorescence spectra were collected on a Horiba Jobin Yvon Spex Fluorolog spectrofluorometer at 23° C. pH-titration samples were prepared by dissolving lyophilized protein in a 10 APB buffer at pH 7.0 to an absorbance at 276 nm of 0.2 (10 mm path length), dividing the sample in two equal fractions, and adjusting the pH with either concentrated phosphoric acid or 10 M NaOH. The experiments were performed by constant volume titration and using an λ_{ex} = 276 nm and λ_{em} = 285-445 nm. The slit width for the excitation and emission light was 0.7 and 2.0 nm, respectively, and the averaging time for each 0.05 nm step was 0.2 seconds.

Tyrosine emission center of mass was calculated as described in Section 4.2 and using Equation 4.1, and the resulting pH-titration curves fitted to a single-pK_A Henderson-Hasselbalch equation[109] The fitting statistics are listed in Table 7.4.

Table 7.4. Determination of pK_{APP} of center of mass of Y32 fluorescence for α_3Y, α_3Y-K29H, and α_3Y-K36H.

Protein	pK_{APP}	χ^2	R^2
α_3Y	8.08 ± 0.09	0.029171	0.9783
α_3Y-K29H	7.1 ± 0.1	0.110830	0.9640
α_3Y-K36H	7.08 ± 0.07	0.425530	0.9866

See text in this section for sample conditions.

7.8. Size exclusion chromatography

Gel filtration was performed using an analytical Superdex™ 75 column (GE Healthcare) equilibrated with 10 mM APB pH 7.0 buffer containing 100 mM KCl. The protein loading concentration for α_3Y, α_3Y-K29H, α_3Y-K36H, 2MP-α_3C, 3MP-α_3C, and 4MP-α_3C was 250 μM. Protein samples were prepared in buffer containing 20 mM APB, 50 mM KCl at pH 7. The protein backbone absorbance at 220 nm was monitored to determine the elution time of all proteins.

7.9. Electrochemistry: experimental and data analysis

7.9.1. Experimental considerations. Cyclic voltammetry (CV) differential pulse voltammetry (DPV) and square wave voltammetry (SWV) were performed using an Autolab PGSTAT12 potentiostat equipped with a temperature-

controlled, Faraday-cage protected three-electrode micro-cell (Princeton Applied Research). The Ag/AgCl reference electrode and the platinum wire counter electrode (Advanced Measurements Inc.) were stored dry and prepared by filling the former with a 3M KCl/saturated AgCl solution and the latter with sample buffer. DPV measurements were carried out using a 3 mm diameter glassy carbon working electrode (Advanced Measurements Inc.). The surface of the glassy carbon electrode was carefully polished between each measurement using a 0.05 μm alumina/water slurry on a glass-plate mounted microcloth pad (Bioanalytical Systems Inc.). The electrode was manually polished for 60 sec., rinsed with water, sonicated in ethanol for 60 sec., and in milli-Q water for another 60 sec., and finally rinsed with an excess of milli-Q water directed against the surface of the electrode. Some DPV and all SWV measurements were carried out using a 3 mm diameter pyrolytic graphite edge electrode (Bio-Logic, USA). The electrode surface was activated between measurement by manually polishing its surface for 60 sec. in a 1.0 μm diamond/water slurry on a diamond polishing pad (Bio-Logic, USA) followed by 60 sec. in a 0.05 μm alumina/water slurry on a microcloth pad (Bioanalytical systems Inc.). The electrode was rinsed with an excess of methanol followed by milli-Q water directed against the surface of the electrode. Measurements were performed immediately following the polishing procedures. The electrochemical cell was also fitted with a pH electrode (Microelectrodes Inc.) connected to a SevenMulti pH meter (Mettler Toledo). The pH was routinely monitored between voltammetry runs. The pH electrode was disconnected from the pH meter

during the active voltammetry measurements to avoid the risk of introducing electric noise. The response and reproducibility of the fully assembled electrochemical cell were checked at the beginning of each experimental day by using standard samples and settings. *i*R compensation was performed by using the Autolab positive feed-back function. Potentials are given as values *vs.* the NHE. All samples were prepared were from ultra-pure chemicals and the measurements performed under an argon atmosphere. Protein concentration, KCl concentration and pH series were obtained by constant volume titrations.

Data series were obtained by typically collecting three to four voltammograms per data point. Correction of background currents was performed by fitting a cubic baseline to the raw voltammograms. DPV half-wave potentials ($E_{1/2}$) were obtained by first-derivative analysis or by fitting a calculated line to the raw voltammogram. The average error in $E_{1/2}$ representing data replicates is ± 3 mV. There was no significant difference in $E_{1/2}$ when using the two different methods of analysis. The average error in the DPV $E_{1/2}$ value from independent measurements is ± 4 mV. There is no significant difference in $E_{1/2}$ from α_3Y DP voltammograms obtained by using a GC or a PGE electrode ($\Delta E_{1/2}$ 5 ± 5 mV). First-derivative analysis was not practical for SWV data due to the increase of noise at higher frequencies. Peak potentials of the net current (E_{net}), forward current (E_{for}) and reverse current (E_{rev}) were obtained by fitting a calculated line to the experimental traces. The average error in E_{net}, E_{for} and E_{rev} is ± 3 mV for data replicates and independent measurements.

Sample conditions and specific experimental settings for voltammetry measurements are noted in the main text for all experiments.

7.9.2. Data processing and analysis. Data processing and analyses were performed using the Autolab GPES software, KaleidaGraph (Synergy Software) and PeakFit (Systat Software Inc.). DPV half-wave potentials ($E_{1/2}$) were derived from the observed DPV peak potentials (E_{peak}) using the Parry-Osteryoung relationship $E_{1/2} = E_{peak} + \Delta E/2$, where ΔE is the pulse amplitude.[98] The α_3Y Pourbaix diagram was fitted to Equation 3.8 by nonlinear regression (fitting stats in legend of Figure 3.7). The $E_{1/2}$ *vs.* pH profile was first simulated using Excel in order to find starting values. Data fitting and evaluations of the data fits were conducted using the GraphPad Prism program (GraphPad Software).

7.10. NMR data collection

All data was collected at 750 MHz (^{1}H) with a Bruker Avance III spectrometer fitted with a cryogenic probe or with a Varian Inova spectrometer equipped with a conventional room temperature probe, except for the ^{1}H-^{1}H ROESY and DOSY experiments which were collected at 500 MHz (^{1}H) with Bruker Avance III spectrometer fitted with a cryogenic probe. Data was processed using Bruker TOPSPIN 2.2.a and/or the Felix 95[165] program. Data was analyzed using Bruker TOPSPIN 2.2.a and/or the SPARKY[157] program.

7.10.1. HSQC spectra for α_3Y-K29H, α_3Y-K36H, 2MP-α_3C, and 4MP-α_3C

Sample conditions and specific experimental settings are described in Figure 4.8 in Section 4.3 for the α_3Y-HIS proteins, and in Figures 5.3 and 5.4 in Section 5.2 for the MP-α_3C proteins.

7.10.2. Two-dimensional NOESY/ROESY spectra for α_3Y-K29H, α_3Y-K36H

Sample conditions and specific experimental settings are described in Figure 4.9 in Section 4.4 for NOESY experiments, and in Figure 4.5 in Section 4.5 for ROESY experiments.

7.10.3. Three-dimensional experiments for resonance assignment: 4MP-α_3C

The sample utilized for these experiments contained ~800 μM ^{15}N,^{13}C-labeled 4MPα_3C in 25 mM deuterated sodium acetate, 25 mM NaCl in a 8%D_2O/92%H_2O or 100% D_2O solvent system at pH 5.5. For 100% D_2O samples, the pH was corrected for isotope effects by using the following relationship: p*K*(H_2O) = 0.929 × p*K*(D_2O) + 0.42.[164] The experiments were done at 30 °C. All the experiments are described in Section 5.2.1, and experimental settings are listed in Table 7.5. The extent of assignment was determined by using the Assignment Validation Suite (AVS)[149] webserver.

Table 7.5. Experimental Settings for Resonance Assignment NMR Experiments.[a]

Experiment	Complex Points (CP)			# Scans	Sweep Width (SW)		
	D1	D2	D3		D1	D2	D3
HNCO	1024	30	56	8	14	17	10
HN(CA)CO	1024	30	56	16	14	18	10
CBCA(CO)NH	1024	30	60	8	14	18	52
HNCACB	1024	30	60	16	14	18	52
H(CC)(CO)NH TOCSY	1024	30	64	16	14	18	9.4
(H)CC(CO)NH TOCSY	1024	30	48	32	14	18	60
HCCH TOCSY	1024	56	100	8	14	20	7

[a]D1, D2 and D3 refer to the 1st, 2nd and 3rd collected dimension in the NMR experiment, respectively. The proton carrier was set at 4.700 ppm for all experiments, except for the HCCH TOCSY which had the carrier position at 4.706 ppm. The nitrogen carrier was set 114.75 ppm, except for the HNCO which had the carrier at 115 ppm. The aliphatic carbon carrier was set at 39.55 ppm for the CBCA(CO)NH and HNCACB experiments, and 39.00 ppm for the TOCSY experiments. The carbonyl carbon carrier was set at 175.7 and 174.8 ppm for the HNCO and HN(CA)CO experiments, respectively.

7.10.4. NOE-based three- and four-dimensional experiments: 4MP-α_3C

Sample conditions are the same as in Section 7.10.3. All the experiments are described in Section 5.3.2, and experimental settings are listed in Table 7.6.

Table 7.6. Experimental Settings for NOE-Based NMR Experiments.[a]

Experiment					
		D1	**D2**	**D3**	**D4**
4D ^{15}N-HSQC-NOESY-^{13}C-HSQC	**Nucleus**	^{1}H	^{15}N	^{1}H	^{13}C
	CP	1024	12	40	14
	SW	14	8.8	8.4	20
	Carrier	4.703	119.6	4.703	41.5
		D1	**D2**	**D3**	**D4**
4D ^{13}C-HMQC-NOESY-^{13}C-HMQC	**Nucleus**	^{1}H	^{13}C	^{1}H	^{13}C
	CP	512	20	40	20
	SW	5	20	5	20
	Carrier	2.6	41.5	2.6	41.5
		D1	**D2**	**D3**	**D4**
3D NOESY-^{13}C-HSQC	**Nucleus**	^{1}H	^{13}C	^{1}H	N/A
	CP	1024	52	128	N/A
	SW	14	20	14	N/A
	Carrier	4.706	39.00	4.706	N/A

[a]D1, D2, D3, and D4 refer to the 1st, 2nd, 3rd, and 4th collected dimension in the NMR experiment, respectively. The 4th dimension does not apply for the 3D NOESY-^{13}C-HSQC experiment. **NOTE:** The mixing time for these NOE-based NMR experiments, collected in the 4MP-α_3C sample, was 140 ms.

7.10.5. Determination of diffusion coefficient for α_3Y and 2MP-α_3C using the DOSY experiment

The samples utilized for these experiments contained 500 μM α_3Y in 20 mM deuterated sodium acetate, 20 mM potassium phosphate, 20 mM sodium borate, and 140 mM NaCl in a 5%D_2O/95%H_2O solvent system at pH 6.6, or 440

μM 2MP-α_3C in 20 mM sodium acetate, 20 mM potassium phosphate, 20 mM sodium borate, and 80 mM NaCl in a 5%D_2O/95%H_2O solvent system at pH 6.6. The experiments were done at 25 °C. Experimental settings for the α_3Y experiment are described in Figure 3.15 in Section 3.5.2. The experiment for 2MP-α_3C was carried out in a similar fashion; the experimental settings are the same except for the number of scans 3000; sweep width for the 1st and 2nd dimension 14.0 and 10.3, respectively; position of proton carrier at 4.812. Fitting statistics for the determination of the diffusion coefficient for both proteins are listed in Table 7.7.

Table 7.7. Determination of Diffusion Coefficient of α_3Y, and 2MP-α_3Y.

Protein	D_{red} x 10^{-6} cm^2 s^{-1}	χ^2	R^2
α_3Y – HN	1.464 ± 0.006	9.5678 x 10^{12}	0.9999
α_3Y – HC	1.472 ± 0.008	2.7612 x 10^{14}	0.9998
2MP-α_3C – HN	1.31 ± 0.02	4.6984 x 10^{12}	0.9982
2MP-α_3C – HC	1.571 ± 0.008	9.5678 x 10^{12}	0.9998

See text in this section for sample conditions.

7.11. Structure determination (CNS)

The structure calculation process and the type of data utilized are described in Section 5.2.3.

In order to calculate trial structures for 4MP-α_3C, the covalently bonded MP molecule had to be taken into account as a modified residue composed of a CYS residue modified with a TYR-like compound. A parameter set for this new modified residue had to be included into the parameter file "protein-

allhdg.top" which is titled "Geometric energy function parameters for distance geometry and simulated annealing (including all hydrogens) with NMR data". This parameter file is included in the "toppar" library of the CNS suite. This parameter set defines atom types and connectivities, dihedral angles, and chiral centers, and also provides partial charges for atoms in the residue. See Table 7.8 for the parameter set built for the residue 4MP-C32. Additionally, a second parameter file, named "protein-allhdg.param", was modified to include new atom connectivities, angles, and dihedral angles which are necessary for the generation of the 4MP-CYS residue. See Table 7.9 for the additional lines added to this parameter file.

Table 7.8. Parameter Set for Residue 4MP-C32. Atom nomenclature treats the 4MP molecule as an extension of the CYS residue. This was defined as CYY for the purpose of the structure calculation.

```
residue CYY             !This residue was added by MMR NOV 2010
 group
  atom N   type=NH1 charge=-0.36 end
  atom HN  type=H   charge= 0.26 end
  atom CA  type=CH1E  charge= 0.00 end
  atom HA  type=HA  charge= 0.10 end
  atom CB  type=CH2E  charge=-0.20 end
  atom HB1 type=HA  charge= 0.10 end
  atom HB2 type=HA  charge= 0.10 end
  atom SG  type=S   charge=0 end
  atom SD  type=S   charge=0 end
  atom CE  type=CY  charge= 0.00 exclude=(CI) end
  atom CZ1 type=CR1E  charge=-0.14 exclude=(CH2) end
  atom HZ1 type=HA  charge= 0.14 end
  atom CZ2 type=CR1E  charge=-0.14 exclude=(CH1) end
  atom HZ2 type=HA  charge= 0.14 end
  atom CH1 type=CR1E  charge=-0.14 exclude=(CZ2) end
  atom HH1 type=HA  charge= 0.14 end
  atom CH2 type=CR1E  charge=-0.14 exclude=(CZ1) end
  atom HH2 type=HA  charge= 0.14 end
  atom CI  type=CY2   charge= 0.20 exclude=(CH1) end
  atom OI  type=OH1  charge=-0.60 end
  atom HI  type=H   charge= 0.40 end
  atom C   type=C   charge= 0.48 end
  atom O   type=O   charge=-0.48 end

 bond N   HN
 bond N   CA    bond CA  HA
 bond CA  CB    bond CB  HB1    bond CB  HB2
 bond CB  SG


 bond SG  SD
 bond SD  CE
 bond CE  CZ1   bond CZ1 HZ1
```

```
  bond CE  CZ2    bond CZ2 HZ2
  bond CZ1 CH1    bond CH1 HH1
  bond CZ2 CH2    bond CH2 HH2
  bond CH1 CI
  bond CH2 CI
  bond CI  OI     bond OI  HI
  bond CA  C
  bond C   O

! chirality
  improper HA  N   C   CB  !chirality CA
  improper HB1 HB2 CA  SG  !stereo CB

! Hs, OH, and CB around the ring
  improper HZ2 CZ2 CH2 CI
  improper HH2 CH2 CI  CH1
  improper OI  CI  CH1 CZ1
  improper HH1 CH1 CZ1 CE
  improper HZ1 CZ1 CE  CZ2
  improper SD  CE  CZ2 CH2

! around the ring
  improper CE  CZ1 CH1 CI
  improper CZ1 CH1 CI  CH2
  improper CH1 CI  CH2 CZ2
  improper CI  CH2 CZ2 CE
  improper CH2 CZ2 CE  CZ1
  improper CZ2 CE  CZ1 CH1


  dihedral SG  CB  CA  N          !modified MMR Oct 2010
  dihedral SD  SG  CB  CA         !modified MMR Oct 2010
  dihedral CE  SD  SG  CB         !modified MMR Oct 2010
  dihedral CZ1 CE  SD  SG         !modified MMR Oct 2010
  dihedral CH2 CI  OI  HI      !UCL Added 12-MAR-00   !modified MMR Oct 2010

end
```

Table 7.9. New bond, angle and dihedral angle definitions added to CNS parameter file.

```
BOND  S    CY      1000.000 {sd=     0.001}      1.740
ANGLe S    S    CY       500.00 {sd=     0.031}    103.7998
ANGLe S    CY   CR1E     500.00 {sd=     0.031}    125.1100
ANGLe  CR1E CR1E CY       500.00 {sd=     0.031}    120.6700
ANGLe  CR1E CR1E CY2      500.00 {sd=     0.031}    119.7000
IMPRoper  HA   CR1E CY   CY2       500.00 {sd=     0.031}    0   -180.0000
IMPRoper  S    CY   CY2  CR1E      500.00 {sd=     0.031}    0    180.0000
IMPRoper  CY   CR1E CR1E CR1E      500.00 {sd=     0.031}    0      0.0000
IMPRoper  CR1E CR1E CR1E CR1E      500.00 {sd=     0.031}    0      0.0000
IMPRoper  CR1E CR1E CR1E CY2       500.00 {sd=     0.031}    0      0.0000
IMPRoper  CR1E CY2  CY   CR1E      500.00 {sd=     0.031}    0      0.0000
IMPRoper  CY2  CY   CR1E CR1E      500.00 {sd=     0.031}    0      0.0000
IMPRoper  CR1E CR1E CY2  CY        500.00 {sd=     0.031}    0      0.0000
IMPRoper  S    CY   CR1E CR1E      500.00 {sd=     0.031}    0    180
DIHEdral  CR1E CY2  OH1  H      0.00 {sd=     0.031}    3  0.0000
DIHEdral  CH1E CH2E S    S      0.00 {sd=     0.031}    3  0.0000
DIHEdral  CH2E S    S    CY     0.00 {sd=     0.031}    3  0.0000
DIHEdral  S    S    CY   CR1E   0.00 {sd=     0.031}    3  0.0000
```

7.12. SASA analysis (MOLMOL)

The SASA analysis was performed using the MOLMOL program.[162] A solvent probe radius of 1.4 Å and a level 5 precision were used for the calculations. The solvent accessible surface area (%) is defined as the percentage ratio of the water-accessible surface area of the listed residue X to the accessible surface area of the same residue placed in a Gly–X–Gly peptide.

APPENDIX A: NMR Solution Structure of 2MP-α_3C

Table A.1. Experimental restraints and structural statistics for 2MP-α_3C

	2MP-α_3C
Experimental NOE distance restraints	
Intraresidue	216
Sequential ($\|i-j\| = 1$)	222
Medium range ($1 < \|i-j\| < 5$)	181
Long range ($\|i-j\| > 5$)	190
Total	809
Backbone dihedral angle restraints	107
Hydrogen bond distance restraints	44
Total Restraints	960
Average restricting constraints per restrained residue	14.8
Average long-range constraints per restrained residue	2.9
Ramachandran Plot Summary	
Most favored regions	96.4 %
Additionally allowed regions	3.2 %
Generously allowed regions	0.3 %
Disallowed regions	0.0 %
RMS deviations from experimental restraints	
Distance (Å)	0.0061 ± 0.0003
Dihedral angles (°)	0.22 ± 0.02
RMS deviations from idealized geometry	
Bonds (Å)	0.0011 ± 0.0001
Angles (°)	0.331 ± 0.004
Impropers (°)	0.202 ± 0.009
Average RMS deviations from mean structure	
All residues (backbone atoms)	0.464
All residues (heavy atoms)	0.949
Helical residues (backbone atoms)	0.273
Helical residues (heavy atoms)	0.901

Table A.2. Solvent accessible surface area (SASA) of atoms associated with the 2MP-C32 residue in 2MP-α_3C

Residue	Atoms	Average SASA (%)	SASA limits (%)
2MP-C32	backbone N	0 ± 0	0
2MP-C32	backbone H	0 ± 0	0
2MP-C32	backbone C	0 ± 0	0
2MP-C32	backbone O	0 ± 0	0
2MP-C32	backbone CA	0 ± 0	0
2MP-C32	backbone HA	0 ± 0	0.0 – 1.6
2MP-C32	sidechain CB	0 ± 0	0
2MP-C32	sidechain HB1	0 ± 0	0
2MP-C32	sidechain HB2	0 ± 0	0
2MP-C32	sidechain SG	0 ± 0	0
2MP-C32	sidechain phenol S	0 ± 0	0
2MP-C32	sidechain phenol C2	0 ± 0	0
2MP-C32	sidechain phenol C3	0 ± 0	0
2MP-C32	sidechain phenol H3	0 ± 0	0
2MP-C32	sidechain phenol C4	0 ± 0	0
2MP-C32	sidechain phenol H4	0.3 ± 0.8	0.0 – 4.2
2MP-C32	sidechain phenol C5	4.5 ± 3.1	0.0 – 11.0
2MP-C32	sidechain phenol H5	10.2 ± 8.1	0.0 – 31.3
2MP-C32	sidechain phenol C6	4.7 ± 1.8	0.5 – 8.2
2MP-C32	sidechain phenol H6	38.2 ± 5.7	22.7 – 47.5
2MP-C32	sidechain phenol C1	0 ± 0	0
2MP-C32	sidechain phenol O	2.0 ± 3.1	0 – 12.3
2MP-C32	sidechain phenol H	4.0 ± 5.4	0 – 20.3
2MP-C32	all atoms	3.5 ± 0.7	2.0 – 5.4

APPENDIX B: Resonance List for 4MP-α_3C protein

Note 1. All chemical shift values are referenced to the standard DSS (4,4-dimethyl-4-silapentane-1-sulfonic acid), as described by Cavanagh, et. al.[130]

Note 2. Residue numbering in this list treats the *N*-terminal GS residues as residues 1 and 2, respectively, for NMR experiments and structure calculation purposes. Note that the numbering throughout the main text of this dissertation treats these two residues are residues -1 and -2, respectively.

Note 3. Chemical shifts belonging to the 4MP molecule are designated under residue number 34* and residue name 4MP-CYS.

Residue #	Residue Name	Atom Name	Chemical Shift (ppm)	Error (ppm)
2	SER	CA	58.277	0.078
2	SER	CB	63.708	0.072
2	SER	HA	4.526	0.008
2	SER	HB2	4.063	0.009
2	SER	HB3	3.868	0.004
3	ARG	CA	58.368	0.06
3	ARG	CB	30.667	0.041
3	ARG	CD	43.418	0.068
3	ARG	CG	27.107	0.068
3	ARG	C	178.507	0.013
3	ARG	HA	4.231	0.002
3	ARG	HB2	1.941	0.001
3	ARG	HB3	1.876	0.01
3	ARG	HD2	3.254	0.002
3	ARG	HD3	3.196	0.008
3	ARG	HG2	1.803	0.002
3	ARG	HG3	1.675	0.001
4	VAL	CA	65.501	0.096
4	VAL	CB	31.714	0.061
4	VAL	CG1	21.704	0.037
4	VAL	CG2	22.791	0.037
4	VAL	C	177.044	0.009
4	VAL	HA	3.788	0.014
4	VAL	HB	2.050	0.003
4	VAL	HG1	0.948	0.003
4	VAL	HG2	0.983	0.006
4	VAL	H	8.070	0.004
4	VAL	N	119.082	0.032
5	LYS	CA	58.682	0.1
5	LYS	CB	31.755	0.069
5	LYS	CD	28.620	0.049
5	LYS	CE	41.948	0.188
5	LYS	CG	24.677	0.129
5	LYS	C	178.641	0.009
5	LYS	HA	4.130	0.006
5	LYS	HB2	1.867	0.013

Residue #	Residue Name	Atom Name	Chemical Shift (ppm)	Error (ppm)
5	LYS	HB3	1.867	0.013
5	LYS	HD2	1.699	0.011
5	LYS	HD3	1.699	0.011
5	LYS	HE2	2.957	0.015
5	LYS	HE3	2.957	0.015
5	LYS	HG2	1.486	0.002
5	LYS	HG3	1.486	0.002
5	LYS	H	7.794	0.001
5	LYS	N	122.031	0.066
6	ALA	CA	54.813	0.074
6	ALA	CB	17.959	0.091
6	ALA	C	181.031	0.01
6	ALA	HA	4.189	0.005
6	ALA	HB	1.470	0.011
6	ALA	H	7.914	0.005
6	ALA	N	119.966	0.032
7	LEU	CA	57.706	0.059
7	LEU	CB	41.948	0.113
7	LEU	CD1	25.591	0.066
7	LEU	CD2	24.283	0.038
7	LEU	CG	26.617	0.067
7	LEU	C	178.440	0.012
7	LEU	HA	4.110	0.008
7	LEU	HB2	2.065	0.007
7	LEU	HB3	1.507	0.012
7	LEU	HD1	0.893	0.005
7	LEU	HD2	0.883	0.003
7	LEU	HG	1.890	0.004
7	LEU	H	7.602	0.007
7	LEU	N	119.348	0.036
8	GLU	CA	59.854	0.022
8	GLU	CB	29.451	0.052
8	GLU	CG	36.334	0.104
8	GLU	C	179.618	0.015
8	GLU	HA	3.853	0.011
8	GLU	HB2	2.209	0.023
8	GLU	HB3	2.209	0.023
8	GLU	HG2	2.404	0.001
8	GLU	HG3	2.149	0.01
8	GLU	H	8.383	0.007
8	GLU	N	120.165	0.022
9	GLU	CA	59.238	0.034
9	GLU	CB	29.363	0.056
9	GLU	CG	36.302	0.047
9	GLU	C	179.724	0
9	GLU	HA	4.011	0.003
9	GLU	HB2	2.130	0.027
9	GLU	HB3	2.130	0.027
9	GLU	HG2	2.450	0.01
9	GLU	HG3	2.296	0.01
9	GLU	H	8.159	0.005
9	GLU	N	118.173	0.018
10	LYS	CA	59.159	0.064

Residue #	Residue Name	Atom Name	Chemical Shift (ppm)	Error (ppm)
10	LYS	CB	32.193	0.071
10	LYS	CD	28.862	0
10	LYS	CE	41.740	0.045
10	LYS	CG	25.186	0.003
10	LYS	C	179.499	0.011
10	LYS	HA	4.175	0
10	LYS	HB2	2.045	0.001
10	LYS	HB3	1.900	0
10	LYS	HD2	1.657	0
10	LYS	HD3	1.657	0
10	LYS	HE2	2.931	0.023
10	LYS	HE3	2.931	0.023
10	LYS	HG2	1.555	0.006
10	LYS	HG3	1.555	0.006
10	LYS	H	8.009	0.007
10	LYS	N	121.005	0.031
11	VAL	CA	66.455	0.058
11	VAL	CB	31.270	0.061
11	VAL	CG1	21.588	0.041
11	VAL	CG2	24.566	0.049
11	VAL	C	177.296	0.007
11	VAL	HA	3.808	0.012
11	VAL	HB	2.093	0.008
11	VAL	HG1	1.045	0.005
11	VAL	HG2	1.027	0.005
11	VAL	H	8.488	0.002
11	VAL	N	119.608	0.015
12	LYS	CA	59.582	0.077
12	LYS	CB	32.049	0.023
12	LYS	CD	29.209	0.1
12	LYS	CE	41.990	0.074
12	LYS	CG	25.149	0.049
12	LYS	C	178.865	0.009
12	LYS	HA	4.175	0.003
12	LYS	HB2	1.916	0.002
12	LYS	HB3	1.916	0.002
12	LYS	HD2	1.653	0
12	LYS	HD3	1.653	0
12	LYS	HE2	2.914	0.007
12	LYS	HE3	2.914	0.007
12	LYS	HG2	1.595	0.002
12	LYS	HG3	1.446	0
12	LYS	H	7.973	0.002
12	LYS	N	123.029	0.021
13	ALA	CA	54.754	0.083
13	ALA	CB	17.857	0.077
13	ALA	C	181.160	0.013
13	ALA	HA	4.203	0.007
13	ALA	HB	1.514	0.008
13	ALA	H	7.556	0.002
13	ALA	N	121.144	0.018
14	LEU	CA	57.951	0.079
14	LEU	CB	41.561	0.05

Residue #	Residue Name	Atom Name	Chemical Shift (ppm)	Error (ppm)
14	LEU	CD1	25.685	0.03
14	LEU	CD2	23.594	0.045
14	LEU	CG	26.344	0.045
14	LEU	C	178.000	0.012
14	LEU	HA	4.058	0.007
14	LEU	HB2	2.068	0.016
14	LEU	HB3	1.469	0.012
14	LEU	HD1	0.886	0.005
14	LEU	HD2	0.872	0.003
14	LEU	HG	1.990	0.004
14	LEU	H	8.102	0.003
14	LEU	N	120.092	0.019
15	GLU	CA	59.441	0.055
15	GLU	CB	28.905	0.058
15	GLU	CG	34.790	0.082
15	GLU	C	178.007	0.013
15	GLU	HA	3.678	0.011
15	GLU	HB2	2.028	0.009
15	GLU	HB3	2.028	0.009
15	GLU	HG2	1.584	0.011
15	GLU	HG3	1.041	0.005
15	GLU	H	8.561	0.002
15	GLU	N	121.384	0.025
16	GLU	CA	59.078	0.07
16	GLU	CB	29.217	0.058
16	GLU	CG	36.055	0.057
16	GLU	C	179.407	0.014
16	GLU	HA	3.855	0.007
16	GLU	HB2	2.078	0.018
16	GLU	HB3	2.078	0.018
16	GLU	HG2	2.379	0.001
16	GLU	HG3	2.258	0.001
16	GLU	H	7.535	0.002
16	GLU	N	116.233	0.021
17	LYS	CA	58.981	0.043
17	LYS	CB	32.513	0.027
17	LYS	CD	28.995	0
17	LYS	CE	42.078	0
17	LYS	CG	25.171	0
17	LYS	C	179.067	0.017
17	LYS	HA	4.116	0.014
17	LYS	HB2	1.969	0.005
17	LYS	HB3	1.969	0.005
17	LYS	H	7.721	0.002
17	LYS	N	119.369	0.022
18	VAL	CA	66.316	0.056
18	VAL	CB	31.685	0.087
18	VAL	CG1	22.532	0.038
18	VAL	CG2	23.819	0.027
18	VAL	C	178.889	0.011
18	VAL	HA	3.667	0.01
18	VAL	HB	2.347	0.008
18	VAL	HG1	1.006	0.006

Residue #	Residue Name	Atom Name	Chemical Shift (ppm)	Error (ppm)
18	VAL	HG2	1.098	0.006
18	VAL	H	8.676	0.002
18	VAL	N	118.533	0.019
19	LYS	CA	59.604	0.078
19	LYS	CB	32.507	0.095
19	LYS	CD	29.611	0.102
19	LYS	CE	41.684	0.159
19	LYS	CG	26.236	0.045
19	LYS	C	178.138	0.012
19	LYS	HA	4.081	0.007
19	LYS	HB2	1.840	0.01
19	LYS	HB3	1.840	0.01
19	LYS	HD2	1.564	0
19	LYS	HD3	1.564	0
19	LYS	HE2	2.835	0.001
19	LYS	HE3	2.697	0.009
19	LYS	HG2	1.618	0.001
19	LYS	HG3	1.460	0.007
19	LYS	H	8.290	0.002
19	LYS	N	119.141	0.028
20	ALA	CA	52.982	0.058
20	ALA	CB	18.794	0.083
20	ALA	C	178.632	0.008
20	ALA	HA	4.325	0.004
20	ALA	HB	1.504	0.006
20	ALA	H	7.420	0.002
20	ALA	N	119.635	0.037
21	LEU	CA	55.732	0.073
21	LEU	CB	42.888	0.056
21	LEU	CD1	26.418	0.041
21	LEU	CD2	22.542	0.043
21	LEU	CG	26.333	0.021
21	LEU	C	177.939	0.01
21	LEU	HA	4.285	0.003
21	LEU	HB2	2.009	0.003
21	LEU	HB3	1.598	0.009
21	LEU	HD1	0.922	0.004
21	LEU	HD2	0.889	0.003
21	LEU	HG	2.043	0.005
21	LEU	H	7.534	0.002
21	LEU	N	118.530	0.026
22	GLY	CA	45.392	0.113
22	GLY	C	173.777	0.006
22	GLY	HA2	4.119	0.005
22	GLY	HA3	3.872	0.004
22	GLY	H	7.822	0.002
22	GLY	N	106.669	0.035
23	GLY	CA	44.880	0.087
23	GLY	C	174.141	0.013
23	GLY	HA2	4.146	0.001
23	GLY	HA3	3.938	0
23	GLY	H	8.139	0.002
23	GLY	N	108.079	0.024

Residue #	Residue Name	Atom Name	Chemical Shift (ppm)	Error (ppm)
24	GLY	CA	44.474	0.11
24	GLY	C	175.115	0.01
24	GLY	HA2	4.316	0.006
24	GLY	HA3	3.930	0.006
24	GLY	H	8.498	0.001
24	GLY	N	107.827	0.017
25	GLY	CA	47.033	0.087
25	GLY	C	176.351	0.008
25	GLY	HA2	3.990	0
25	GLY	HA3	3.838	0.005
25	GLY	H	8.610	0.001
25	GLY	N	108.770	0.022
26	ARG	CA	57.677	0.075
26	ARG	CB	29.808	0.04
26	ARG	CD	43.185	0.054
26	ARG	CG	27.048	0.017
26	ARG	C	177.926	0.009
26	ARG	HA	4.278	0.007
26	ARG	HB2	1.897	0.012
26	ARG	HB3	1.897	0.012
26	ARG	HD2	3.297	0.004
26	ARG	HD3	3.168	0.006
26	ARG	HG2	1.684	0.007
26	ARG	HG3	1.684	0.007
26	ARG	H	8.753	0.001
26	ARG	N	123.017	0.037
27	ILE	CA	62.936	0.032
27	ILE	CB	36.766	0.028
27	ILE	CD1	12.711	0.047
27	ILE	CG1	28.691	0.028
27	ILE	CG2	18.667	0.054
27	ILE	C	177.469	0.004
27	ILE	HA	3.800	0.01
27	ILE	HB	2.004	0.002
27	ILE	HD1	0.840	0.005
27	ILE	HG12	1.452	0.001
27	ILE	HG13	1.335	0.003
27	ILE	HG2	0.945	0.005
27	ILE	H	7.729	0.002
27	ILE	N	118.189	0.039
28	GLU	CA	59.534	0
28	GLU	CB	29.005	0.101
28	GLU	CG	35.996	0
28	GLU	C	179.244	0
28	GLU	HA	3.979	0
28	GLU	HB2	2.065	0
28	GLU	HB3	2.065	0
28	GLU	HG2	2.318	0
28	GLU	HG3	2.318	0
28	GLU	H	7.882	0.002
28	GLU	N	120.047	0.026
29	GLU	CA	59.140	0.056
29	GLU	CB	29.335	0.08

Residue #	Residue Name	Atom Name	Chemical Shift (ppm)	Error (ppm)
29	GLU	CG	36.022	0.017
29	GLU	C	179.239	0.011
29	GLU	HA	4.044	0.021
29	GLU	HB2	2.109	0
29	GLU	HB3	2.109	0
29	GLU	HG2	2.307	0
29	GLU	HG3	2.307	0
29	GLU	H	7.745	0.002
29	GLU	N	118.630	0.079
30	LEU	CA	57.710	0.062
30	LEU	CB	41.592	0.045
30	LEU	CD1	26.204	0.066
30	LEU	CD2	23.121	0.019
30	LEU	CG	26.732	0.049
30	LEU	C	178.823	0.013
30	LEU	HA	4.013	0.003
30	LEU	HB2	1.990	0.007
30	LEU	HB3	1.331	0.004
30	LEU	HD1	0.856	0.005
30	LEU	HD2	0.793	0.006
30	LEU	HG	1.854	0.004
30	LEU	H	7.677	0.002
30	LEU	N	120.335	0.022
31	LYS	CA	60.342	0.042
31	LYS	CB	32.138	0.043
31	LYS	CD	29.672	0.083
31	LYS	CE	41.817	0.204
31	LYS	CG	24.917	0.042
31	LYS	C	177.737	0.015
31	LYS	HA	3.465	0.021
31	LYS	HB2	1.805	0.006
31	LYS	HB3	1.690	0.005
31	LYS	HD2	1.611	0.006
31	LYS	HD3	1.550	0.003
31	LYS	HE2	2.845	0.001
31	LYS	HE3	2.827	0
31	LYS	HG2	1.017	0.003
31	LYS	HG3	0.953	0.005
31	LYS	H	8.558	0.001
31	LYS	N	120.451	0.024
32	LYS	CB	32.131	0.017
32	LYS	CD	29.223	0
32	LYS	CE	42.039	0
32	LYS	CG	25.010	0.051
32	LYS	C	179.543	0.008
32	LYS	HB2	1.872	0.005
32	LYS	HB3	1.872	0.005
32	LYS	HD2	1.659	0
32	LYS	HD3	1.659	0
32	LYS	HE2	2.944	0
32	LYS	HE3	2.944	0
32	LYS	HG2	1.581	0
32	LYS	HG3	1.445	0

Residue #	Residue Name	Atom Name	Chemical Shift (ppm)	Error (ppm)
32	LYS	H	7.694	0.001
32	LYS	N	118.492	0.038
33	LYS	CB	31.932	0.066
33	LYS	CD	28.963	0.076
33	LYS	CE	41.853	0.068
33	LYS	CG	25.152	0.04
33	LYS	C	178.565	0.008
33	LYS	HB2	1.897	0.003
33	LYS	HB3	1.897	0.003
33	LYS	HD2	1.676	0.006
33	LYS	HD3	1.676	0.006
33	LYS	HE2	2.934	0.004
33	LYS	HE3	2.934	0.004
33	LYS	HG2	1.564	0.003
33	LYS	HG3	1.564	0.003
33	LYS	H	7.747	0.002
33	LYS	N	119.048	0.041
34	CYS	CA	60.488	0.049
34	CYS	CB	37.363	0.067
34	CYS	C	175.675	0.009
34	CYS	HA	3.958	0.008
34	CYS	HB2	3.525	0.006
34	CYS	HB3	2.880	0.004
34	CYS	H	6.719	0.003
34	CYS	N	6.735	0.039
34*	4MP-CYS	H2	8.478	0.002
34*	4MP-CYS	H6	7.159	0.002
34*	4MP-CYS	H3	7.141	0.001
34*	4MP-CYS	H5	119.760	0.001
35	GLU	CA	60.020	0.097
35	GLU	CB	29.574	0.016
35	GLU	CG	37.159	0.087
35	GLU	C	179.722	0.012
35	GLU	HA	3.858	0.008
35	GLU	HB2	2.122	0.007
35	GLU	HB3	1.924	0.003
35	GLU	HG2	2.152	0
35	GLU	HG3	1.993	0
35	GLU	H	8.605	0.002
35	GLU	N	119.717	0.044
36	GLU	CA	59.275	0.061
36	GLU	CB	29.565	0.048
36	GLU	CG	36.233	0.024
36	GLU	C	179.424	0.013
36	GLU	HA	4.053	0.002
36	GLU	HB2	2.167	0.005
36	GLU	HB3	2.167	0.005
36	GLU	HG2	2.452	0.001
36	GLU	HG3	2.195	0.007
36	GLU	H	7.999	0.001
36	GLU	N	120.166	0.024
37	LEU	CA	57.814	0.087
37	LEU	CB	41.545	0.041

Residue #	Residue Name	Atom Name	Chemical Shift (ppm)	Error (ppm)
37	LEU	CD1	25.715	0.059
37	LEU	CD2	24.198	0.05
37	LEU	CG	26.838	0.059
37	LEU	C	178.311	0.008
37	LEU	HA	4.067	0.009
37	LEU	HB2	2.018	0.008
37	LEU	HB3	1.435	0.007
37	LEU	HD1	0.879	0.008
37	LEU	HD2	0.897	0.004
37	LEU	HG	1.882	0.005
37	LEU	H	8.053	0.002
37	LEU	N	121.044	0.015
38	LYS	CA	60.693	0.073
38	LYS	CB	32.748	0.062
38	LYS	CD	30.133	0.096
38	LYS	CE	41.875	0.158
38	LYS	CG	25.506	0.048
38	LYS	C	178.941	0.009
38	LYS	HA	3.832	0.009
38	LYS	HB2	2.027	0.003
38	LYS	HB3	1.945	0.002
38	LYS	HD2	1.863	0.008
38	LYS	HD3	1.740	0.004
38	LYS	HE2	2.981	0
38	LYS	HE3	2.965	0
38	LYS	HG2	1.628	0.006
38	LYS	HG3	1.373	0.005
38	LYS	H	8.681	0.002
38	LYS	N	119.667	0.021
39	LYS	CA	58.948	0.038
39	LYS	CB	32.133	0.06
39	LYS	CD	29.070	0.08
39	LYS	CE	42.019	0
39	LYS	CG	24.667	0
39	LYS	C	178.673	0.014
39	LYS	HA	4.114	0.012
39	LYS	HB2	1.929	0.012
39	LYS	HB3	1.929	0.012
39	LYS	HD2	1.679	0.002
39	LYS	HD3	1.679	0.002
39	LYS	HE2	2.968	0
39	LYS	HE3	2.968	0
39	LYS	H	7.553	0.002
39	LYS	N	118.297	0.023
40	LYS	CA	59.262	0.094
40	LYS	CB	32.462	0.068
40	LYS	CD	29.281	0.096
40	LYS	CE	41.892	0
40	LYS	CG	25.562	0.013
40	LYS	C	179.863	0.008
40	LYS	HA	4.068	0.01
40	LYS	HB2	2.043	0.003
40	LYS	HB3	1.843	0.01

Residue #	Residue Name	Atom Name	Chemical Shift (ppm)	Error (ppm)
40	LYS	HD2	1.661	0.003
40	LYS	HD3	1.661	0.003
40	LYS	HE2	2.901	0
40	LYS	HE3	2.901	0
40	LYS	HG2	1.617	0.01
40	LYS	HG3	1.617	0.01
40	LYS	H	7.913	0.002
40	LYS	N	118.797	0.029
41	ILE	CA	64.991	0.05
41	ILE	CB	37.893	0.051
41	ILE	CD1	14.627	0.081
41	ILE	CG1	30.812	0.031
41	ILE	CG2	17.879	0.055
41	ILE	C	178.170	0.015
41	ILE	HA	3.650	0.01
41	ILE	HB	1.972	0.007
41	ILE	HD1	0.741	0.004
41	ILE	HG12	1.798	0.003
41	ILE	HG13	0.957	0.003
41	ILE	HG2	0.894	0.005
41	ILE	H	8.337	0.002
41	ILE	N	118.790	0.021
42	GLU	CA	58.859	0.082
42	GLU	CB	29.350	0.012
42	GLU	CG	36.018	0.035
42	GLU	C	178.731	0.012
42	GLU	HA	4.079	0.004
42	GLU	HB2	2.262	0
42	GLU	HB3	2.262	0
42	GLU	HG2	2.513	0.001
42	GLU	H	7.768	0.001
42	GLU	N	120.181	0.031
43	GLU	CA	56.810	0.072
43	GLU	CB	29.813	0.096
43	GLU	CG	36.293	0.075
43	GLU	C	177.614	0.01
43	GLU	HA	4.265	0.006
43	GLU	HB2	2.180	0.001
43	GLU	HB3	2.050	0.002
43	GLU	HG2	2.477	0.01
43	GLU	HG3	2.272	0.005
43	GLU	H	7.690	0.003
43	GLU	N	117.147	0.031
44	LEU	CA	56.448	0.073
44	LEU	CB	42.524	0.049
44	LEU	CD1	26.127	0.04
44	LEU	CD2	23.645	0.031
44	LEU	CG	26.306	0.027
44	LEU	C	178.664	0.013
44	LEU	HA	4.236	0.003
44	LEU	HB2	1.980	0.004
44	LEU	HB3	1.556	0.003
44	LEU	HD1	0.907	0.003

Residue #	Residue Name	Atom Name	Chemical Shift (ppm)	Error (ppm)
44	LEU	HD2	0.813	0.004
44	LEU	HG	2.046	0.006
44	LEU	H	7.575	0.004
44	LEU	N	120.954	0.031
45	GLY	CA	46.204	0.054
45	GLY	C	174.921	0.013
45	GLY	HA2	3.987	0.002
45	GLY	HA3	3.915	0.001
45	GLY	H	8.231	0.001
45	GLY	N	108.687	0.02
46	GLY	CA	45.258	0.051
46	GLY	C	174.749	0.014
46	GLY	HA2	4.190	0
46	GLY	HA3	3.889	0
46	GLY	H	8.166	0.002
46	GLY	N	108.069	0.016
47	GLY	CA	45.147	0.05
47	GLY	C	174.476	0.007
47	GLY	HA2	4.177	0
47	GLY	HA3	3.982	0
47	GLY	H	8.029	0
47	GLY	N	108.591	0.015
48	GLY	CA	45.272	0.021
48	GLY	C	174.445	0.011
48	GLY	HA2	4.005	0
48	GLY	HA3	4.005	0
48	GLY	H	8.296	0.001
48	GLY	N	108.216	0.019
49	GLU	CA	56.417	0.072
49	GLU	CB	29.618	0.102
49	GLU	CG	36.417	0.047
49	GLU	C	177.168	0.013
49	GLU	HA	4.401	0.004
49	GLU	HB2	2.110	0.018
49	GLU	HB3	2.000	0.001
49	GLU	HG2	2.325	0.006
49	GLU	HG3	2.291	0.006
49	GLU	H	8.481	0.001
49	GLU	N	121.075	0.017
50	VAL	CA	64.916	0.07
50	VAL	CB	32.197	0.069
50	VAL	CG1	20.969	0.038
50	VAL	CG2	21.893	0.1
50	VAL	C	176.847	0.012
50	VAL	HA	3.774	0.004
50	VAL	HB	2.117	0.003
50	VAL	HG1	0.897	0.004
50	VAL	HG2	0.963	0.004
50	VAL	H	8.077	0.003
50	VAL	N	122.039	0.028
51	LYS	CA	59.349	0.046
51	LYS	CB	32.212	0.024
51	LYS	CD	29.140	0.002

Residue #	Residue Name	Atom Name	Chemical Shift (ppm)	Error (ppm)
51	LYS	CE	42.123	0
51	LYS	CG	24.750	0.014
51	LYS	C	178.625	0.007
51	LYS	HA	4.181	0.004
51	LYS	HB2	1.876	0
51	LYS	HB3	1.876	0
51	LYS	HD2	1.692	0
51	LYS	HD3	1.692	0
51	LYS	HE2	2.987	0
51	LYS	HE3	2.987	0
51	LYS	HG2	1.468	0
51	LYS	HG3	1.468	0
51	LYS	H	8.245	0.008
51	LYS	N	120.639	0.032
52	LYS	CA	58.900	0.085
52	LYS	CB	32.065	0.048
52	LYS	CD	28.960	0.04
52	LYS	CE	42.014	0
52	LYS	CG	24.969	0.027
52	LYS	C	179.235	0.012
52	LYS	HA	4.149	0.001
52	LYS	HB2	1.907	0.005
52	LYS	HB3	1.907	0.005
52	LYS	HD2	1.697	0.017
52	LYS	HD3	1.697	0.017
52	LYS	HE2	2.969	0
52	LYS	HE3	2.969	0
52	LYS	HG2	1.497	0.017
52	LYS	HG3	1.497	0.017
52	LYS	H	7.593	0.003
52	LYS	N	117.570	0.029
53	VAL	CA	66.090	0.064
53	VAL	CB	31.299	0.069
53	VAL	CG1	22.773	0.054
53	VAL	CG2	23.446	0.05
53	VAL	C	178.009	0.013
53	VAL	HA	3.756	0.008
53	VAL	HB	2.096	0.005
53	VAL	HG1	0.932	0.005
53	VAL	HG2	1.010	0.004
53	VAL	H	7.599	0.002
53	VAL	N	119.196	0.036
54	GLU	CA	60.184	0.069
54	GLU	CB	29.627	0.026
54	GLU	CG	37.231	0.051
54	GLU	C	179.663	0.009
54	GLU	HA	3.819	0.011
54	GLU	HB2	2.352	0.011
54	GLU	HB3	2.059	0.005
54	GLU	HG2	2.409	0.011
54	GLU	HG3	2.192	0.009
54	GLU	H	8.594	0.001
54	GLU	N	120.185	0.054

Residue #	Residue Name	Atom Name	Chemical Shift (ppm)	Error (ppm)
55	GLU	CA	59.273	0.018
55	GLU	CB	29.369	0
55	GLU	CG	36.239	0
55	GLU	C	179.181	0.018
55	GLU	HA	4.062	0
55	GLU	H	7.903	0.001
55	GLU	N	118.622	0.058
56	GLU	CA	59.638	0.071
56	GLU	CB	30.170	0.115
56	GLU	CG	36.673	0.05
56	GLU	C	179.830	0.013
56	GLU	HA	4.069	0.003
56	GLU	HB2	2.250	0.002
56	GLU	HB3	2.150	0
56	GLU	HG2	2.501	0.005
56	GLU	HG3	2.297	0.003
56	GLU	H	7.885	0.001
56	GLU	N	120.315	0.066
57	VAL	CA	66.772	0.043
57	VAL	CB	31.403	0.027
57	VAL	CG1	21.946	0.045
57	VAL	CG2	24.732	0.037
57	VAL	C	177.044	0
57	VAL	HA	3.520	0.01
57	VAL	HB	2.214	0.003
57	VAL	HG1	0.871	0.003
57	VAL	HG2	1.038	0.003
57	VAL	H	8.635	0.002
57	VAL	N	121.480	0.02
58	LYS	CA	59.435	0.059
58	LYS	CB	32.146	0.066
58	LYS	CD	29.346	0.069
58	LYS	CE	42.062	0.059
58	LYS	CG	24.986	0.035
58	LYS	C	179.083	0
58	LYS	HA	4.178	0.009
58	LYS	HB2	2.040	0.004
58	LYS	HB3	1.860	0.004
58	LYS	HD2	1.682	0
58	LYS	HD3	1.682	0
58	LYS	HE2	2.943	0.005
58	LYS	HE3	2.943	0.005
58	LYS	HG2	1.565	0
58	LYS	HG3	1.565	0
58	LYS	H	7.781	0.004
58	LYS	N	120.214	0.019
59	LYS	CA	59.404	0.021
59	LYS	CB	32.282	0.047
59	LYS	CD	29.182	0.028
59	LYS	CE	42.111	0
59	LYS	CG	25.313	0.106
59	LYS	C	179.266	0.016
59	LYS	HA	4.067	0.008

Residue #	Residue Name	Atom Name	Chemical Shift (ppm)	Error (ppm)
59	LYS	HB2	1.930	0.002
59	LYS	HB3	1.930	0.002
59	LYS	HD2	1.698	0.01
59	LYS	HD3	1.698	0.01
59	LYS	HE2	2.957	0
59	LYS	HE3	2.957	0
59	LYS	HG2	1.610	0
59	LYS	H	7.823	0.002
59	LYS	N	118.249	0.021
60	LEU	CA	57.814	0.085
60	LEU	CB	41.213	0.052
60	LEU	CD1	24.462	0.038
60	LEU	CD2	25.997	0.062
60	LEU	CG	27.222	0.043
60	LEU	C	178.518	0.012
60	LEU	HA	4.210	0.005
60	LEU	HB2	1.869	0.01
60	LEU	HB3	1.599	0.009
60	LEU	HD1	0.966	0.005
60	LEU	HD2	0.843	0.007
60	LEU	HG	1.682	0.005
60	LEU	H	7.821	0.003
60	LEU	N	121.243	0.023
61	GLU	CA	60.088	0.023
61	GLU	CB	29.916	0.096
61	GLU	CG	37.088	0.051
61	GLU	C	179.177	0.017
61	GLU	HA	3.781	0.007
61	GLU	HB2	2.275	0.007
61	GLU	HB3	2.131	0.003
61	GLU	HG2	2.391	0.006
61	GLU	HG3	2.126	0.008
61	GLU	H	8.572	0.001
61	GLU	N	118.814	0.015
62	GLU	CA	59.050	0.035
62	GLU	CB	29.410	0.046
62	GLU	CG	36.233	0.01
62	GLU	C	178.937	0.008
62	GLU	HA	3.981	0.009
62	GLU	HB2	2.157	0.001
62	GLU	HB3	2.157	0.001
62	GLU	HG2	2.376	0.001
62	GLU	HG3	2.376	0.001
62	GLU	H	7.999	0.001
62	GLU	N	117.641	0.011
63	GLU	CA	59.286	0
63	GLU	CB	29.603	0.051
63	GLU	CG	36.138	0.04
63	GLU	C	179.884	0.01
63	GLU	HA	4.002	0.015
63	GLU	HB2	2.230	0.024
63	GLU	HB3	2.080	0.016
63	GLU	HG2	2.341	0.002

Residue #	Residue Name	Atom Name	Chemical Shift (ppm)	Error (ppm)
63	GLU	HG3	2.341	0.002
63	GLU	H	7.943	0.002
63	GLU	N	119.251	0.035
64	ILE	CA	64.299	0.035
64	ILE	CB	37.971	0.041
64	ILE	CD1	15.017	0.05
64	ILE	CG1	30.326	0.041
64	ILE	CG2	17.611	0.08
64	ILE	C	177.754	0.011
64	ILE	HA	3.695	0.008
64	ILE	HB	1.929	0.008
64	ILE	HD1	0.807	0.004
64	ILE	HG12	1.763	0.004
64	ILE	HG13	1.064	0.003
64	ILE	HG2	0.892	0.007
64	ILE	H	8.166	0.001
64	ILE	N	118.543	0.038
65	LYS	CA	58.456	0.018
65	LYS	CB	32.683	0.033
65	LYS	CD	29.510	0.054
65	LYS	CE	42.039	0
65	LYS	CG	25.509	0
65	LYS	C	177.164	0.011
65	LYS	HA	4.097	0
65	LYS	HB2	1.925	0.005
65	LYS	HB3	1.925	0.005
65	LYS	HD2	1.663	0
65	LYS	HD3	1.663	0
65	LYS	HE2	2.928	0
65	LYS	HE3	2.928	0
65	LYS	H	7.648	0.002
65	LYS	N	118.922	0.038
66	LYS	CA	56.319	0.068
66	LYS	CB	32.957	0.03
66	LYS	CD	29.276	0.061
66	LYS	CE	42.049	0.129
66	LYS	CG	25.119	0.033
66	LYS	C	176.001	0.01
66	LYS	HA	4.303	0.004
66	LYS	HB2	2.015	0.006
66	LYS	HB3	1.790	0.007
66	LYS	HD2	1.666	0.003
66	LYS	HD3	1.666	0.003
66	LYS	HE2	2.946	0.009
66	LYS	HE3	2.946	0.009
66	LYS	HG2	1.606	0.005
66	LYS	HG3	1.451	0
66	LYS	H	7.238	0.002
66	LYS	N	116.873	0.022
67	LEU	CA	57.123	0.034
67	LEU	CB	42.992	0.029
67	LEU	CD1	26.380	0.076
67	LEU	CD2	23.181	0.052

Residue #	Residue Name	Atom Name	Chemical Shift (ppm)	Error (ppm)
67	LEU	CG	27.002	0.07
67	LEU	C	182.146	0
67	LEU	HA	4.065	0.003
67	LEU	HB2	1.747	0.003
67	LEU	HB3	1.577	0.003
67	LEU	HD1	0.892	0.009
67	LEU	HD2	0.832	0.007
67	LEU	HG	1.817	0.006
67	LEU	H	7.208	0.001
67	LEU	N	126.384	0.026

APPENDIX C: TALOS+ Analysis of Dihedral Angles and Secondary Structure

Residue	Phi (ϕ)[a]	Psi (ψ)[a]	Prediction	2º structure	Probability
G1					
S2					
R3					
V4	-67 ± 7	-40 ± 6	good	helix	0.98
K5	-63 ± 5	-40 ± 10	good	helix	0.99
A6	-63 ± 6	-42 ± 6	good	helix	0.99
L7	-66 ± 5	-38 ± 6	good	helix	0.99
E8	-66 ± 5	-39 ± 5	good	helix	1
E9	-61 ± 7	-44 ± 6	good	helix	1
K10	-65 ± 7	-40 ± 6	good	helix	1
V11	-64 ± 8	-42 ± 6	good	helix	1
K12	-64 ± 4	-44 ± 6	good	helix	0.99
A13	-66 ± 6	-41 ± 6	good	helix	1
L14	-64 ± 5	-41 ± 4	good	helix	0.99
E15	-65 ± 5	-43 ± 6	good	helix	0.99
E16	-60 ± 6	-43 ± 7	good	helix	0.99
K17	-64 ± 5	-42 ± 6	good	helix	1
V18	-67 ± 4	-38 ± 8	good	helix	1
K19	-62 ± 9	-37 ± 15	good	helix	0.98
A20	-76 ± 19	-34 ± 19	good	helix	0.84
L21	-91 ± 15	-25 ± 25	good	loop	0.7
G22	92 ± 24	11 ± 21	ambiguous	loop	0.91
G23	167 ± 99	175 ± 18	ambiguous	loop	0.9
G24	-94 ± 24	134 ± 30	good	loop	0.92
G25	-53 ± 64	139 ± 50	ambiguous	loop	0.72
R26	-63 ± 7	-41 ± 13	good	helix	0.86
I27	-66 ± 11	-40 ± 6	good	helix	0.97
E28	-64 ± 6	-40 ± 6	good	helix	0.99
E29	-62 ± 5	-43 ± 7	good	helix	1
L30	-65 ± 6	-38 ± 5	good	helix	1
K31	-60 ± 3	-44 ± 6	good	helix	1
K32	-63 ± 5	-42 ± 5	good	helix	0.99
K33	-65 ± 5	-41 ± 7	good	helix	0.95
C34	-63 ± 5	-44 ± 6	good	helix	0.96
E35	-62 ± 4	-41 ± 7	good	helix	0.99

Residue	Phi (ϕ)[a]	Psi (ψ)[a]	Prediction	2º structure	Probability
E36	-64 ± 5	-45 ± 6	good	helix	1
L37	-64 ± 5	-40 ± 3	good	helix	1
K38	-61 ± 5	-44 ± 5	good	helix	0.99
K39	-64 ± 5	-45 ± 3	good	helix	0.99
K40	-66 ± 5	-40 ± 6	good	helix	0.99
I41	-66 ± 7	-41 ± 6	good	helix	0.99
E42	-63 ± 9	-37 ± 8	good	helix	0.97
E43	-74 ± 16	-27 ± 22	good	helix	0.88
L44	-71 ± 19	-33 ± 15	good	helix/loop	0.53/0.47
G45	-90 ± 31	-15 ± 20	ambiguous	loop	0.86
G46	97 ± 15	9 ± 3	dynamic	loop	0.94
G47	-108 ± 45	169 ± 25	dynamic	loop	0.91
G48	-149 ± 83	144 ± 52	ambiguous	loop	0.94
E49	88 ± 30	149 ± 19	good	loop	0.78
V50	-66 ± 19	-35 ± 11	good	helix	0.91
K51	-64 ± 6	-39 ± 11	good	helix	0.99
K52	-64 ± 4	-40 ± 6	good	helix	0.99
V53	-65 ± 7	-45 ± 6	good	helix	1
E54	-62 ± 6	-39 ± 6	good	helix	1
E55	-64 ± 7	-44 ± 6	good	helix	1
E56	-64 ± 4	-42 ± 4	good	helix	1
V57	-66 ± 7	-44 ± 8	good	helix	1
K58	-60 ± 5	-42 ± 7	good	helix	0.99
K59	-64 ± 5	-45 ± 7	good	helix	0.99
L60	-65 ± 5	-40 ± 4	good	helix	1
E61	-65 ± 4	-40 ± 6	good	helix	0.99
E62	-62 ± 7	-47 ± 6	good	helix	1
E63	-67 ± 6	-40 ± 6	good	helix	0.99
I64	-63 ± 5	-42 ± 8	good	helix	0.97
K65	-72± 19	-32 ± 16	good	helix	0.87
K66	-102 ± 18	0 ± 25	good	helix	0.79
L67					

[a]All phi and psi angles are expressed in degrees (°).

APPENDIX D: Restraint Lists Used for Calculation of 4MP-α_3C Structural Model

All restraint lists are written in CNS restraint list format.[166] Each line starts with the word "assign" followed by a description of the atoms to which the restraint (dihedral angle, hydrogen bond or NOE) is going to be applied. After this description, the dihedral angle restraint line is followed by three real numbers and one integer number. The first real number specifies the energy constant in kcal mol^{-1} rad^{-2}, the second real number specifies the angle in degrees to which the dihedral angle is restrained, and the third real number specifies the range around the restrained angle. The integer number specifies the exponent of the restraint function. For the energy constant and the exponent of the restraint function, we have used default values. In the case of the distance restraint lists (hydrogen bond and NOE lists), the description of the atoms involved is followed by a description of the range of values allowed for that specific interaction, which is expressed with three values: the distance and both values for the error bars to each side of the specified distance value.

NOTE: Residue numbering in this list treats the *N*-terminal GS residues as residues 1 and 2, respectively, for NMR experiments and structure calculation purposes. Note that the numbering throughout the main text of this dissertation treats these two residues are residues -1 and -2, respectively.

Table D.1. Dihedral Angle Restraint List

assign (resid 3 and name C) (resid 4 and name N) (resid 4 and name CA) (resid 4 and name C) 1.0 -67.0 17.0 2
assign (resid 4 and name C) (resid 5 and name N) (resid 5 and name CA) (resid 5 and name C) 1.0 -63.0 15.0 2
assign (resid 5 and name C) (resid 6 and name N) (resid 6 and name CA) (resid 6 and name C) 1.0 -63.0 16.0 2
assign (resid 6 and name C) (resid 7 and name N) (resid 7 and name CA) (resid 7 and name C) 1.0 -66.0 15.0 2
assign (resid 7 and name C) (resid 8 and name N) (resid 8 and name CA) (resid 8 and name C) 1.0 -66.0 15.0 2
assign (resid 8 and name C) (resid 9 and name N) (resid 9 and name CA) (resid 9 and name C) 1.0 -61.0 17.0 2
assign (resid 9 and name C) (resid 10 and name N) (resid 10 and name CA) (resid 10 and name C) 1.0 -65.0 17.0 2
assign (resid 10 and name C) (resid 11 and name N) (resid 11 and name CA) (resid 11 and name C) 1.0 -64.0 18.0 2
assign (resid 11 and name C) (resid 12 and name N) (resid 12 and name CA) (resid 12 and name C) 1.0 -64.0 14.0 2
assign (resid 12 and name C) (resid 13 and name N) (resid 13 and name CA) (resid 13 and name C) 1.0 -66.0 16.0 2
assign (resid 13 and name C) (resid 14 and name N) (resid 14 and name CA) (resid 14 and name C) 1.0 -64.0 15.0 2
assign (resid 14 and name C) (resid 15 and name N) (resid 15 and name CA) (resid 15 and name C) 1.0 -65.0 15.0 2
assign (resid 15 and name C) (resid 16 and name N) (resid 16 and name CA) (resid 16 and name C) 1.0 -60.0 16.0 2
assign (resid 16 and name C) (resid 17 and name N) (resid 17 and name CA) (resid 17 and name C) 1.0 -64.0 15.0 2
assign (resid 17 and name C) (resid 18 and name N) (resid 18 and name CA) (resid 18 and name C) 1.0 -67.0 14.0 2
assign (resid 18 and name C) (resid 19 and name N) (resid 19 and name CA) (resid 19 and name C) 1.0 -62.0 19.0 2
assign (resid 19 and name C) (resid 20 and name N) resid 20 and name CA) (resid 20 and name C) 1.0 -76.0 20.0 2
assign (resid 20 and name C) (resid 21 and name N) (resid 21 and name CA) (resid 21 and name C) 1.0 -91.0 20.0 2
assign (resid 25 and name C) (resid 26 and name N) resid 26 and name CA) (resid 26 and name C) 1.0 -63.0 17.0 2
assign (resid 26 and name C) (resid 27 and name N) (resid 27 and name CA) (resid 27 and name C) 1.0 -66.0 20.0 2
assign (resid 27 and name C) (resid 28 and name N) (resid 28 and name CA) (resid 28 and name C) 1.0 -64.0 16.0 2
assign (resid 28 and name C) (resid 29 and name N) (resid 29 and name CA) (resid 29 and name C) 1.0 -62.0 15.0 2
assign (resid 29 and name C) (resid 30 and name N) (resid 30 and name CA) (resid 30 and name C) 1.0 -65.0 16.0 2
assign (resid 30 and name C) (resid 31 and name N) (resid 31 and name CA) (resid 31 and name C) 1.0 -60.0 13.0 2
assign (resid 31 and name C) (resid 32 and name N) (resid 32 and name CA) (resid 32 and name C) 1.0 -63.0 15.0 2
assign (resid 32 and name C) (resid 33 and name N) (resid 33 and name CA) (resid 33 and name C) 1.0 -65.0 15.0 2
assign (resid 33 and name C) (resid 34 and name N) resid 34 and name CA) (resid 34 and name C) 1.0 -63.0 15.0 2
assign (resid 34 and name C) (resid 35 and name N) (resid 35 and name CA) (resid 35 and name C) 1.0 -62.0 14.0 2
assign (resid 35 and name C) (resid 36 and name N) (resid 36 and name CA) (resid 36 and name C) 1.0 -64.0 15.0 2
assign (resid 36 and name C) (resid 37 and name N) resid 37 and name CA) (resid 37 and name C) 1.0 -64.0 15.0 2
assign (resid 37 and name C) (resid 38 and name N) resid 38 and name CA) (resid 38 and name C) 1.0 -61.0 15.0 2
assign (resid 38 and name C) (resid 39 and name N) (resid 39 and name CA) (resid 39 and name C) 1.0 -64.0 15.0 2
assign (resid 39 and name C) (resid 40 and name N) (resid 40 and name CA) (resid 40 and name C) 1.0 -66.0 15.0 2
assign (resid 40 and name C) (resid 41 and name N) (resid 41 and name CA) (resid 41 and name C) 1.0 -66.0 17.0 2
assign (resid 41 and name C) (resid 42 and name N) (resid 42 and name CA) (resid 42 and name C) 1.0 -63.0 19.0 2
assign (resid 42 and name C) (resid 43 and name N) (resid 43 and name CA) (resid 43 and name C) 1.0 -74.0 20.0 2
assign (resid 43 and name C) (resid 44 and name N) (resid 44 and name CA) (resid 44 and name C) 1.0 -71.0 20.0 2
assign (resid 48 and name C) (resid 49 and name N) (resid 49 and name CA) (resid 49 and name C) 1.0 88.0 30.0 2
assign (resid 49 and name C) (resid 50 and name N) (resid 50 and name CA) (resid 50 and name C) 1.0 -66.0 20.0 2
assign (resid 50 and name C) (resid 51 and name N) resid 51 and name CA) (resid 51 and name C) 1.0 -64.0 16.0 2
assign (resid 51 and name C) (resid 52 and name N) (resid 52 and name CA) (resid 52 and name C) 1.0 -64.0 14.0 2
assign (resid 52 and name C) (resid 53 and name N) (resid 53 and name CA) (resid 53 and name C) 1.0 -65.0 17.0 2
assign (resid 53 and name C) (resid 54 and name N) (resid 54 and name CA) (resid 54 and name C) 1.0 -62.0 16.0 2
assign (resid 54 and name C) (resid 55 and name N) (resid 55 and name CA) (resid 55 and name C) 1.0 -64.0 17.0 2
assign (resid 55 and name C) (resid 56 and name N) (resid 56 and name CA) (resid 56 and name C) 1.0 -64.0 14.0 2
assign (resid 56 and name C) (resid 57 and name N) (resid 57 and name CA) (resid 57 and name C) 1.0 -66.0 17.0 2
assign (resid 57 and name C) (resid 58 and name N) (resid 58 and name CA) (resid 58 and name C) 1.0 -60.0 15.0 2
assign (resid 58 and name C) (resid 59 and name N) (resid 59 and name CA) (resid 59 and name C) 1.0 -64.0 15.0 2
assign (resid 59 and name C) (resid 60 and name N) (resid 60 and name CA) (resid 60 and name C) 1.0 -65.0 15.0 2
assign (resid 60 and name C) (resid 61 and name N) (resid 61 and name CA) (resid 61 and name C) 1.0 -65.0 14.0 2
assign (resid 61 and name C) (resid 62 and name N) (resid 62 and name CA) (resid 62 and name C) 1.0 -62.0 17.0 2
assign (resid 62 and name C) (resid 63 and name N) (resid 63 and name CA) (resid 63 and name C) 1.0 -67.0 16.0 2
assign (resid 63 and name C) (resid 64 and name N) (resid 64 and name CA) (resid 64 and name C) 1.0 -63.0 15.0 2
assign (resid 64 and name C) (resid 65 and name N) (resid 65 and name CA) (resid 65 and name C) 1.0 -72.0 20.0 2
assign (resid 65 and name C) (resid 66 and name N) (resid 66 and name CA) (resid 66 and name C) 1.0 -102.0 20.0 2
assign (resid 4 and name N) (resid 4 and name CA) (resid 4 and name C) (resid 5 and name N) 1.0 -40.0 16.0 2
assign (resid 5 and name N) (resid 5 and name CA) (resid 5 and name C) (resid 6 and name N) 1.0 -40.0 20.0 2
assign (resid 6 and name N) (resid 6 and name CA) (resid 6 and name C) (resid 7 and name N) 1.0 -42.0 16.0 2
assign (resid 7 and name N) (resid 7 and name CA) (resid 7 and name C) (resid 8 and name N) 1.0 -38.0 16.0 2
assign (resid 8 and name N) (resid 8 and name CA) resid 8 and name C) (resid 9 and name N) 1.0 -39.0 15.0 2
assign (resid 9 and name N) (resid 9 and name CA) (resid 9 and name C) (resid 10 and name N) 1.0 -44.0 16.0 2
assign (resid 10 and name N) (resid 10 and name CA) (resid 10 and name C) (resid 11 and name N) 1.0 -40.0 16.0 2
assign (resid 11 and name N) (resid 11 and name CA) (resid 11 and name C) (resid 12 and name N) 1.0 -42.0 16.0 2
assign (resid 12 and name N) (resid 12 and name CA) (resid 12 and name C) (resid 13 and name N) 1.0 -44.0 16.0 2
assign (resid 13 and name N) (resid 13 and name CA) (resid 13 and name C) (resid 14 and name N) 1.0 -41.0 16.0 2
assign (resid 14 and name N) (resid 14 and name CA) (resid 14 and name C) (resid 15 and name N) 1.0 -41.0 14.0 2
assign (resid 15 and name N) (resid 15 and name CA) (resid 15 and name C) (resid 16 and name N) 1.0 -43.0 16.0 2
assign (resid 16 and name N) (resid 16 and name CA) (resid 16 and name C) (resid 17 and name N) 1.0 -43.0 17.0 2
assign (resid 17 and name N) (resid 17 and name CA) (resid 17 and name C) (resid 18 and name N) 1.0 -42.0 16.0 2
assign (resid 18 and name N) (resid 18 and name CA) (resid 18 and name C) (resid 19 and name N) 1.0 -38.0 18.0 2
assign (resid 19 and name N) (resid 19 and name CA) (resid 19 and name C) (resid 20 and name N) 1.0 -37.0 20.0 2
assign (resid 20 and name N) (resid 20 and name CA) (resid 20 and name C) (resid 21 and name N) 1.0 -34.0 20.0 2

```
assign (resid  26  and name N ) (resid  26  and name CA ) (resid  26  and name C ) (resid  27  and name N )   1.0  -41.0 20.0 2
assign (resid  27  and name N ) (resid  27  and name CA ) (resid  27  and name C ) (resid  28  and name N )   1.0  -40.0 16.0 2
assign (resid  28  and name N ) (resid  28  and name CA ) (resid  28  and name C ) (resid  29  and name N )   1.0  -40.0 16.0 2
assign (resid  29  and name N ) (resid  29  and name CA ) (resid  29  and name C ) (resid  30  and name N )   1.0  -43.0 17.0 2
assign (resid  30  and name N ) (resid  30  and name CA ) (resid  30  and name C ) (resid  31  and name N )   1.0  -38.0 15.0 2
assign (resid  31  and name N ) (resid  31  and name CA ) (resid  31  and name C ) (resid  32  and name N )   1.0  -44.0 16.0 2
assign (resid  32  and name N ) (resid  32  and name CA ) (resid  32  and name C ) (resid  33  and name N )   1.0  -42.0 15.0 2
assign (resid  33  and name N ) (resid  33  and name CA ) (resid  33  and name C ) (resid  34  and name N )   1.0  -41.0 17.0 2
assign (resid  34  and name N ) (resid  34  and name CA ) (resid  34  and name C ) (resid  35  and name N )   1.0  -44.0 16.0 2
assign (resid  35  and name N ) (resid  35  and name CA ) (resid  35  and name C ) (resid  36  and name N )   1.0  -41.0 17.0 2
assign (resid  36  and name N ) (resid  36  and name CA ) (resid  36  and name C ) (resid  37  and name N )   1.0  -45.0 16.0 2
assign (resid  37  and name N ) (resid  37  and name CA ) (resid  37  and name C ) (resid  38  and name N )   1.0  -40.0 13.0 2
assign (resid  38  and name N ) (resid  38  and name CA ) (resid  38  and name C ) (resid  39  and name N )   1.0  -44.0 15.0 2
assign (resid  39  and name N ) (resid  39  and name CA ) (resid  39  and name C ) (resid  40  and name N )   1.0  -45.0 13.0 2
assign (resid  40  and name N ) (resid  40  and name CA ) (resid  40  and name C ) (resid  41  and name N )   1.0  -40.0 16.0 2
assign (resid  41  and name N ) (resid  41  and name CA ) (resid  41  and name C ) (resid  42  and name N )   1.0  -41.0 16.0 2
assign (resid  42  and name N ) (resid  42  and name CA ) (resid  42  and name C ) (resid  43  and name N )   1.0  -37.0 18.0 2
assign (resid  43  and name N ) (resid  43  and name CA ) (resid  43  and name C ) (resid  44  and name N )   1.0  -27.0 22.0 2
assign (resid  44  and name N ) (resid  45  and name CA ) (resid  45  and name C ) (resid  45  and name N )   1.0  -33.0 20.0 2
assign (resid  49  and name N ) (resid  49  and name CA ) (resid  49  and name C ) (resid  50  and name N )   1.0  149.0 20.0 2
assign (resid  50  and name N ) (resid  50  and name CA ) (resid  50  and name C ) (resid  51  and name N )   1.0  -35.0 20.0 2
assign (resid  51  and name N ) (resid  51  and name CA ) (resid  51  and name C ) (resid  52  and name N )   1.0  -39.0 20.0 2
assign (resid  52  and name N ) (resid  52  and name CA ) (resid  52  and name C ) (resid  53  and name N )   1.0  -40.0 16.0 2
assign (resid  53  and name N ) (resid  53  and name CA ) (resid  53  and name C ) (resid  54  and name N )   1.0  -45.0 16.0 2
assign (resid  54  and name N ) (resid  54  and name CA ) (resid  54  and name C ) (resid  55  and name N )   1.0  -39.0 16.0 2
assign (resid  55  and name N ) (resid  55  and name CA ) (resid  55  and name C ) (resid  56  and name N )   1.0  -44.0 16.0 2
assign (resid  56  and name N ) (resid  56  and name CA ) (resid  56  and name C ) (resid  57  and name N )   1.0  -42.0 14.0 2
assign (resid  57  and name N ) (resid  57  and name CA ) (resid  57  and name C ) (resid  58  and name N )   1.0  -44.0 18.0 2
assign (resid  58  and name N ) (resid  58  and name CA ) (resid  58  and name C ) (resid  59  and name N )   1.0  -42.0 17.0 2
assign (resid  59  and name N ) (resid  59  and name CA ) (resid  59  and name C ) (resid  60  and name N )   1.0  -45.0 17.0 2
assign (resid  60  and name N ) (resid  60  and name CA ) (resid  60  and name C ) (resid  61  and name N )   1.0  -40.0 14.0 2
assign (resid  61  and name N ) (resid  61  and name CA ) (resid  61  and name C ) (resid  62  and name N )   1.0  -40.0 16.0 2
assign (resid  62  and name N ) (resid  62  and name CA ) (resid  62  and name C ) (resid  63  and name N )   1.0  -47.0 16.0 2
assign (resid  63  and name N ) (resid  63  and name CA ) (resid  63  and name C ) (resid  64  and name N )   1.0  -40.0 16.0 2
assign (resid  64  and name N ) (resid  64  and name CA ) (resid  64  and name C ) (resid  65  and name N )   1.0  -42.0 18.0 2
assign (resid  65  and name N ) (resid  65  and name CA ) (resid  65  and name C ) (resid  66  and name N )   1.0  -32.0 20.0 2
assign (resid  34  and name CB ) (resid  34  and name SG ) (resid  34  and name SD ) (resid  34  and name  CE)   1.0  0.0 180.0 2
assign (resid  34  and name HZ1 ) (resid  34  and name CZ1 ) (resid  34  and name CH1 ) (resid  34  and name HH1)   1.0  0.0 0.5 2
assign (resid  34  and name HH1 ) (resid  34  and name CH1 ) (resid  34  and name CI ) (resid  34  and name OH)    1.0  0.0 0.5 2
assign (resid  34  and name OH ) (resid  34  and name CI ) (resid  34  and name CH2 ) (resid  34  and name HH2)   1.0  0.0 0.5 2
assign (resid  34  and name HH2 ) (resid  34  and name CH2 ) (resid  34  and name CZ2 ) (resid  34  and name HZ2)   1.0  0.0 0.5 2
```

Table D.2. Hydrogen Bond Distance Restraint List

assign (residue 3 and name O) (residue 7 and name HN) 3.0 0.5 0.5
assign (residue 4 and name O) (residue 8 and name HN) 2.7 1.2 1.3
assign (residue 5 and name O) (residue 9 and name HN) 3.0 0.5 0.5
assign (residue 6 and name O) (residue 10 and name HN) 3.0 0.5 0.5
assign (residue 7 and name O) (residue 11 and name HN) 3.0 0.5 0.5
assign (residue 8 and name O) (residue 12 and name HN) 3.0 0.5 0.5
assign (residue 9 and name O) (residue 13 and name HN) 3.0 0.5 0.5
assign (residue 10 and name O) (residue 14 and name HN) 2.7 1.2 1.3
assign (residue 11 and name O) (residue 15 and name HN) 3.0 0.5 0.5
assign (residue 12 and name O) (residue 16 and name HN) 3.0 0.5 0.5
assign (residue 13 and name O) (residue 17 and name HN) 3.0 0.5 0.5
assign (residue 14 and name O) (residue 18 and name HN) 3.0 0.5 0.5
assign (residue 16 and name O) (residue 20 and name HN) 3.0 0.5 0.5
assign (residue 26 and name O) (residue 30 and name HN) 3.0 0.5 0.5
assign (residue 27 and name O) (residue 31 and name HN) 2.7 1.2 1.3
assign (residue 28 and name O) (residue 32 and name HN) 2.7 1.2 1.3
assign (residue 29 and name O) (residue 33 and name HN) 3.0 0.5 0.5
assign (residue 30 and name O) (residue 34 and name HN) 3.0 0.5 0.5
assign (residue 31 and name O) (residue 35 and name HN) 2.7 1.2 1.3
assign (residue 32 and name O) (residue 36 and name HN) 3.0 0.5 0.5
assign (residue 33 and name O) (residue 37 and name HN) 3.0 0.5 0.5
assign (residue 34 and name O) (residue 38 and name HN) 2.7 1.2 1.3
assign (residue 35 and name O) (residue 39 and name HN) 3.0 0.5 0.5
assign (residue 36 and name O) (residue 40 and name HN) 3.0 0.5 0.5
assign (residue 37 and name O) (residue 41 and name HN) 3.0 0.5 0.5
assign (residue 38 and name O) (residue 42 and name HN) 3.0 0.5 0.5
assign (residue 39 and name O) (residue 43 and name HN) 3.0 0.5 0.5
assign (residue 50 and name O) (residue 54 and name HN) 3.0 0.5 0.5
assign (residue 51 and name O) (residue 55 and name HN) 3.0 0.5 0.5
assign (residue 52 and name O) (residue 56 and name HN) 3.0 0.5 0.5
assign (residue 54 and name O) (residue 58 and name HN) 3.0 0.5 0.5
assign (residue 55 and name O) (residue 59 and name HN) 3.0 0.5 0.5
assign (residue 56 and name O) (residue 60 and name HN) 3.0 0.5 0.5
assign (residue 57 and name O) (residue 61 and name HN) 2.7 1.2 1.3
assign (residue 58 and name O) (residue 62 and name HN) 3.0 0.5 0.5
assign (residue 59 and name O) (residue 63 and name HN) 3.0 0.5 0.5
assign (residue 60 and name O) (residue 64 and name HN) 3.0 0.5 0.5
assign (residue 61 and name O) (residue 65 and name HN) 3.0 0.5 0.5
assign (residue 62 and name O) (residue 66 and name HN) 3.0 0.5 0.5
assign (residue 63 and name O) (residue 67 and name HN) 3.0 0.5 0.5

Table D.3. NOE Distance Restraint List

NOE interactions between i(HN) and i(HA)

assign (residue 4 and name HN) (residue 4 and name HA)	2.35 0.65 0.65
assign (residue 5 and name HN) (residue 5 and name HA)	2.35 0.65 0.65
assign (residue 6 and name HN) (residue 6 and name HA)	2.35 0.65 0.65
assign (residue 7 and name HN) (residue 7 and name HA)	2.35 0.65 0.65
assign (residue 8 and name HN) (residue 8 and name HA)	2.35 0.65 0.65
assign (residue 9 and name HN) (residue 9 and name HA)	2.35 0.65 0.65
assign (residue 10 and name HN) (residue 10 and name HA)	2.35 0.65 0.65
assign (residue 11 and name HN) (residue 11 and name HA)	2.35 0.65 0.65
assign (residue 12 and name HN) (residue 12 and name HA)	2.35 0.65 0.65
assign (residue 13 and name HN) (residue 13 and name HA)	2.35 0.65 0.65
assign (residue 14 and name HN) (residue 14 and name HA)	2.35 0.65 0.65
assign (residue 15 and name HN) (residue 15 and name HA)	2.35 0.65 0.65
assign (residue 16 and name HN) (residue 16 and name HA)	2.35 0.65 0.65
assign (residue 17 and name HN) (residue 17 and name HA)	2.35 0.65 0.65
assign (residue 18 and name HN) (residue 18 and name HA)	2.35 0.65 0.65
assign (residue 19 and name HN) (residue 19 and name HA)	2.35 0.65 0.65
assign (residue 20 and name HN) (residue 20 and name HA)	2.35 0.65 0.65
assign (residue 21 and name HN) (residue 21 and name HA)	2.35 0.65 0.65
assign (residue 26 and name HN) (residue 26 and name HA)	2.35 0.65 0.65
assign (residue 27 and name HN) (residue 27 and name HA)	2.35 0.65 0.65
assign (residue 28 and name HN) (residue 28 and name HA)	2.35 0.65 0.65
assign (residue 29 and name HN) (residue 29 and name HA)	2.35 0.65 0.65
assign (residue 30 and name HN) (residue 30 and name HA)	2.35 0.65 0.65
assign (residue 31 and name HN) (residue 31 and name HA)	2.35 0.65 0.65
assign (residue 34 and name HN) (residue 34 and name HA)	2.35 0.65 0.65
assign (residue 35 and name HN) (residue 35 and name HA)	2.35 0.65 0.65
assign (residue 36 and name HN) (residue 36 and name HA)	2.35 0.65 0.65
assign (residue 37 and name HN) (residue 37 and name HA)	2.35 0.65 0.65
assign (residue 38 and name HN) (residue 38 and name HA)	2.35 0.65 0.65
assign (residue 39 and name HN) (residue 39 and name HA)	2.35 0.65 0.65
assign (residue 40 and name HN) (residue 40 and name HA)	2.35 0.65 0.65
assign (residue 41 and name HN) (residue 41 and name HA)	2.35 0.65 0.65
assign (residue 42 and name HN) (residue 42 and name HA)	2.35 0.65 0.65
assign (residue 43 and name HN) (residue 43 and name HA)	2.35 0.65 0.65
assign (residue 44 and name HN) (residue 44 and name HA)	2.35 0.65 0.65
assign (residue 49 and name HN) (residue 49 and name HA)	2.35 0.65 0.65
assign (residue 50 and name HN) (residue 50 and name HA)	2.35 0.65 0.65
assign (residue 51 and name HN) (residue 51 and name HA)	2.35 0.65 0.65
assign (residue 52 and name HN) (residue 52 and name HA)	2.35 0.65 0.65
assign (residue 53 and name HN) (residue 53 and name HA)	2.35 0.65 0.65
assign (residue 54 and name HN) (residue 54 and name HA)	2.35 0.65 0.65
assign (residue 55 and name HN) (residue 55 and name HA)	2.35 0.65 0.65
assign (residue 56 and name HN) (residue 56 and name HA)	2.35 0.65 0.65
assign (residue 57 and name HN) (residue 57 and name HA)	2.35 0.65 0.65
assign (residue 58 and name HN) (residue 58 and name HA)	2.35 0.65 0.65
assign (residue 59 and name HN) (residue 59 and name HA)	2.35 0.65 0.65
assign (residue 60 and name HN) (residue 60 and name HA)	2.35 0.65 0.65
assign (residue 61 and name HN) (residue 61 and name HA)	2.35 0.65 0.65
assign (residue 62 and name HN) (residue 62 and name HA)	2.35 0.65 0.65
assign (residue 64 and name HN) (residue 64 and name HA)	2.35 0.65 0.65
assign (residue 65 and name HN) (residue 65 and name HA)	2.35 0.65 0.65
assign (residue 66 and name HN) (residue 66 and name HA)	2.35 0.65 0.65
assign (residue 67 and name HN) (residue 67 and name HA)	2.35 0.65 0.65

NOE interactions between i(HN) and i-1(HA)

assign (residue 4 and name HN) (residue 3 and name HA)	2.85 1.15 1.15
assign (residue 5 and name HN) (residue 4 and name HA)	2.85 1.15 1.15
assign (residue 6 and name HN) (residue 5 and name HA)	2.85 1.15 1.15
assign (residue 7 and name HN) (residue 6 and name HA)	2.85 1.15 1.15
assign (residue 8 and name HN) (residue 7 and name HA)	2.85 1.15 1.15
assign (residue 9 and name HN) (residue 8 and name HA)	2.85 1.15 1.15
assign (residue 10 and name HN) (residue 9 and name HA)	2.85 1.15 1.15
assign (residue 11 and name HN) (residue 10 and name HA)	2.85 1.15 1.15
assign (residue 12 and name HN) (residue 11 and name HA)	2.85 1.15 1.15
assign (residue 13 and name HN) (residue 12 and name HA)	2.85 1.15 1.15
assign (residue 14 and name HN) (residue 13 and name HA)	2.85 1.15 1.15
assign (residue 15 and name HN) (residue 14 and name HA)	2.85 1.15 1.15
assign (residue 16 and name HN) (residue 15 and name HA)	2.85 1.15 1.15
assign (residue 17 and name HN) (residue 16 and name HA)	2.85 1.15 1.15
assign (residue 18 and name HN) (residue 17 and name HA)	2.85 1.15 1.15
assign (residue 19 and name HN) (residue 18 and name HA)	2.85 1.15 1.15

assign (residue 20 and name HN) (residue 19 and name HA) 2.85 1.15 1.15
assign (residue 21 and name HN) (residue 20 and name HA) 2.85 1.15 1.15
assign (residue 27 and name HN) (residue 26 and name HA) 2.85 1.15 1.15
assign (residue 28 and name HN) (residue 27 and name HA) 2.85 1.15 1.15
assign (residue 29 and name HN) (residue 28 and name HA) 2.85 1.15 1.15
assign (residue 30 and name HN) (residue 29 and name HA) 2.85 1.15 1.15
assign (residue 31 and name HN) (residue 30 and name HA) 2.85 1.15 1.15
assign (residue 32 and name HN) (residue 31 and name HA) 2.85 1.15 1.15
assign (residue 35 and name HN) (residue 34 and name HA) 2.85 1.15 1.15
assign (residue 36 and name HN) (residue 35 and name HA) 2.85 1.15 1.15
assign (residue 37 and name HN) (residue 36 and name HA) 2.85 1.15 1.15
assign (residue 38 and name HN) (residue 37 and name HA) 2.85 1.15 1.15
assign (residue 39 and name HN) (residue 38 and name HA) 2.85 1.15 1.15
assign (residue 40 and name HN) (residue 39 and name HA) 2.85 1.15 1.15
assign (residue 41 and name HN) (residue 40 and name HA) 2.85 1.15 1.15
assign (residue 42 and name HN) (residue 41 and name HA) 2.85 1.15 1.15
assign (residue 43 and name HN) (residue 42 and name HA) 2.85 1.15 1.15
assign (residue 44 and name HN) (residue 43 and name HA) 2.85 1.15 1.15
assign (residue 50 and name HN) (residue 49 and name HA) 2.85 1.15 1.15
assign (residue 51 and name HN) (residue 50 and name HA) 2.85 1.15 1.15
assign (residue 52 and name HN) (residue 51 and name HA) 2.85 1.15 1.15
assign (residue 53 and name HN) (residue 52 and name HA) 2.85 1.15 1.15
assign (residue 54 and name HN) (residue 53 and name HA) 2.85 1.15 1.15
assign (residue 55 and name HN) (residue 54 and name HA) 2.85 1.15 1.15
assign (residue 56 and name HN) (residue 55 and name HA) 2.85 1.15 1.15
assign (residue 57 and name HN) (residue 56 and name HA) 2.85 1.15 1.15
assign (residue 58 and name HN) (residue 57 and name HA) 2.85 1.15 1.15
assign (residue 59 and name HN) (residue 58 and name HA) 2.85 1.15 1.15
assign (residue 60 and name HN) (residue 59 and name HA) 2.85 1.15 1.15
assign (residue 61 and name HN) (residue 60 and name HA) 2.85 1.15 1.15
assign (residue 62 and name HN) (residue 61 and name HA) 2.85 1.15 1.15
assign (residue 63 and name HN) (residue 62 and name HA) 2.85 1.15 1.15
assign (residue 65 and name HN) (residue 64 and name HA) 2.85 1.15 1.15
assign (residue 66 and name HN) (residue 65 and name HA) 2.85 1.15 1.15
assign (residue 67 and name HN) (residue 66 and name HA) 2.85 1.15 1.15

NOE interactions to residue S2
assign (residue 2 and name HA) (residue 2 and name HB1) 2.850 1.150 1.150
assign (residue 2 and name HA) (residue 2 and name HB2) 2.850 1.150 1.150
assign (residue 2 and name HA) (residue 5 and name HB#) 2.850 1.150 1.150
assign (residue 2 and name HB1) (residue 2 and name HA) 2.850 1.150 1.150
assign (residue 2 and name HB1) (residue 2 and name HB1) 2.350 0.650 0.650
assign (residue 2 and name HB1) (residue 2 and name HB2) 2.350 0.650 0.650
assign (residue 2 and name HB1) (residue 5 and name HB#) 3.350 1.650 1.650

NOE interactions to residue R3
assign (residue 3 and name HA) (residue 3 and name HB#) 2.850 1.150 1.150
assign (residue 3 and name HA) (residue 3 and name HD#) 2.850 1.150 1.150
assign (residue 3 and name HA) (residue 6 and name HB#) 3.100 1.400 1.400
assign (residue 3 and name HB1) (residue 3 and name HA) 2.850 1.150 1.150
assign (residue 3 and name HB1) (residue 3 and name HD#) 2.850 1.150 1.150
assign (residue 3 and name HB1) (residue 50 and name HG1#) 3.600 1.900 1.900
assign (residue 3 and name HB2) (residue 3 and name HA) 2.850 1.150 1.150
assign (residue 3 and name HB2) (residue 3 and name HD#) 2.850 1.150 1.150
assign (residue 3 and name HD1) (residue 3 and name HB#) 2.850 1.150 1.150
assign (residue 3 and name HG1) (residue 3 and name HA) 2.850 1.150 1.150
assign (residue 3 and name HG1) (residue 3 and name HB#) 2.850 1.150 1.150
assign (residue 3 and name HG1) (residue 3 and name HD#) 2.850 1.150 1.150

NOE interactions to residue V4
assign (residue 4 and name HN) (residue 2 and name HA) 2.850 1.150 1.150
assign (residue 4 and name HN) (residue 2 and name HB1) 3.350 1.650 1.650
assign (residue 4 and name HN) (residue 2 and name HB2) 3.350 1.650 1.650
assign (residue 4 and name HN) (residue 3 and name HB#) 2.850 1.150 1.150
assign (residue 4 and name HN) (residue 3 and name HG#) 3.350 1.650 1.650
assign (residue 4 and name HN) (residue 4 and name HB) 2.350 0.650 0.650
assign (residue 4 and name HN) (residue 4 and name HG2#) 3.100 1.400 1.400
assign (residue 4 and name HN) (residue 7 and name HD1#) 3.350 1.650 1.650
assign (residue 4 and name HA) (residue 4 and name HG2#) 3.100 1.400 1.400
assign (residue 4 and name HA) (residue 7 and name HB1) 2.850 1.150 1.150
assign (residue 4 and name HA) (residue 7 and name HB2) 2.850 1.150 1.150
assign (residue 4 and name HA) (residue 7 and name HD1#) 2.600 0.900 0.900
assign (residue 4 and name HA) (residue 41 and name HG2#) 3.600 1.900 1.900
assign (residue 4 and name HB) (residue 4 and name HA) 2.850 1.150 1.150
assign (residue 4 and name HB) (residue 4 and name HG1#) 3.100 1.400 1.400
assign (residue 4 and name HB) (residue 4 and name HG2#) 3.100 1.400 1.400

assign (residue 4 and name HG1#) (residue 4 and name HA) 3.100 1.400 1.400
assign (residue 4 and name HG1#) (residue 4 and name HB) 3.100 1.400 1.400
assign (residue 4 and name HG2#) (residue 4 and name HA) 3.100 1.400 1.400
assign (residue 4 and name HG2#) (residue 4 and name HB) 3.100 1.400 1.400

NOE interactions to residue K5
assign (residue 5 and name HN) (residue 2 and name HA) 2.850 1.150 1.150
assign (residue 5 and name HN) (residue 2 and name HB1) 3.350 1.650 1.650
assign (residue 5 and name HN) (residue 2 and name HB2) 2.850 1.150 1.150
assign (residue 5 and name HN) (residue 4 and name HG1#) 3.100 1.400 1.400
assign (residue 5 and name HN) (residue 4 and name HG2) 3.350 1.650 1.650
assign (residue 5 and name HN) (residue 5 and name HB#) 2.350 0.650 0.650
assign (residue 5 and name HN) (residue 5 and name HD#) 2.850 1.150 1.150
assign (residue 5 and name HN) (residue 5 and name HG#) 2.850 1.150 1.150
assign (residue 5 and name HN) (residue 6 and name HB#) 3.600 1.900 1.900
assign (residue 5 and name HA) (residue 5 and name HB#) 3.350 1.650 1.650
assign (residue 5 and name HA) (residue 5 and name HD#) 3.350 1.650 1.650
assign (residue 5 and name HA) (residue 5 and name HE#) 3.350 1.650 1.650
assign (residue 5 and name HA) (residue 5 and name HG#) 3.350 1.650 1.650
assign (residue 5 and name HA) (residue 8 and name HB#) 2.350 0.650 0.650
assign (residue 5 and name HA) (residue 8 and name HG2) 3.350 1.650 1.650
assign (residue 5 and name HA) (residue 9 and name HG1) 3.350 1.650 1.650
assign (residue 5 and name HA) (residue 9 and name HG2) 3.350 1.650 1.650
assign (residue 5 and name HB#) (residue 2 and name HA) 2.850 1.150 1.150
assign (residue 5 and name HB#) (residue 2 and name HB1) 3.350 1.650 1.650
assign (residue 5 and name HB#) (residue 2 and name HB2) 2.850 1.150 1.150

NOE interactions to residue A6
assign (residue 6 and name HN) (residue 2 and name HA) 3.350 1.650 1.650
assign (residue 6 and name HN) (residue 5 and name HB#) 2.350 0.650 0.650
assign (residue 6 and name HN) (residue 6 and name HB#) 2.600 0.900 0.900
assign (residue 6 and name HA) (residue 5 and name HB#) 3.350 1.650 1.650
assign (residue 6 and name HA) (residue 6 and name HA) 2.350 0.650 0.650
assign (residue 6 and name HA) (residue 6 and name HB#) 2.600 0.900 0.900
assign (residue 6 and name HA) (residue 9 and name HB#) 2.850 1.150 1.150
assign (residue 6 and name HB#) (residue 3 and name HA) 3.100 1.400 1.400
assign (residue 6 and name HB#) (residue 3 and name HB#) 3.350 1.650 1.650
assign (residue 6 and name HB#) (residue 5 and name HB#) 3.350 1.650 1.650
assign (residue 6 and name HB#) (residue 6 and name HA) 3.100 1.400 1.400
assign (residue 6 and name HB#) (residue 9 and name HB#) 3.350 1.650 1.650

NOE interactions to residue L7
assign (residue 7 and name HN) (residue 4 and name HG1#) 3.100 1.400 1.400
assign (residue 7 and name HN) (residue 6 and name HB#) 3.100 1.400 1.400
assign (residue 7 and name HN) (residue 7 and name HB2) 2.350 0.650 0.650
assign (residue 7 and name HN) (residue 7 and name HD1#) 3.100 1.400 1.400
assign (residue 7 and name HN) (residue 7 and name HG) 2.350 0.650 0.650
assign (residue 7 and name HN) (residue 8 and name HG#) 3.350 1.650 1.650
assign (residue 7 and name HN) (residue 41 and name HD1#) 3.600 1.900 1.900
assign (residue 7 and name HA) (residue 6 and name HB#) 3.100 1.400 1.400
assign (residue 7 and name HA) (residue 7 and name HB1) 2.850 1.150 1.150
assign (residue 7 and name HA) (residue 7 and name HB2) 2.850 1.150 1.150
assign (residue 7 and name HA) (residue 7 and name HD1#) 3.100 1.400 1.400
assign (residue 7 and name HA) (residue 7 and name HD2#) 3.100 1.400 1.400
assign (residue 7 and name HA) (residue 7 and name HG) 2.850 1.150 1.150
assign (residue 7 and name HA) (residue 10 and name HB1) 2.850 1.150 1.150
assign (residue 7 and name HB1) (residue 7 and name HB2) 2.350 0.650 0.650
assign (residue 7 and name HB2) (residue 7 and name HA) 2.850 1.150 1.150
assign (residue 7 and name HB2) (residue 7 and name HB1) 2.350 0.650 0.650
assign (residue 7 and name HB2) (residue 7 and name HD2) 3.350 1.650 1.650
assign (residue 7 and name HD2#) (residue 7 and name HB1) 3.350 1.650 1.650
assign (residue 7 and name HD2#) (residue 7 and name HB2) 3.350 1.650 1.650
assign (residue 7 and name HD2#) (residue 7 and name HG) 3.350 1.650 1.650
assign (residue 7 and name HG) (residue 7 and name HB1) 3.350 1.650 1.650
assign (residue 7 and name HG) (residue 7 and name HB2) 3.350 1.650 1.650

NOE interactions to residue E8
assign (residue 8 and name HN) (residue 4 and name HA) 2.850 1.150 1.150
assign (residue 8 and name HN) (residue 6 and name HA) 3.350 1.650 1.650
assign (residue 8 and name HN) (residue 6 and name HB#) 3.350 1.650 1.650
assign (residue 8 and name HN) (residue 7 and name HB1) 2.850 1.150 1.150
assign (residue 8 and name HN) (residue 7 and name HB2) 2.850 1.150 1.150
assign (residue 8 and name HN) (residue 7 and name HG) 2.850 1.150 1.150
assign (residue 8 and name HN) (residue 8 and name HB#) 2.850 1.150 1.150
assign (residue 8 and name HN) (residue 8 and name HG1) 2.350 0.650 0.650
assign (residue 8 and name HN) (residue 8 and name HG2) 2.850 1.150 1.150

assign (residue 8 and name HN) (residue 41 and name HD1#) 3.350 1.650 1.650
assign (residue 8 and name HN) (residue 41 and name HG2#) 3.100 1.400 1.400
assign (residue 8 and name HN) (residue 50 and name HG2#) 3.600 1.900 1.900
assign (residue 8 and name HA) (residue 11 and name HB) 2.850 1.150 1.150
assign (residue 8 and name HA) (residue 41 and name HG2#) 3.350 1.650 1.650
assign (residue 8 and name HG1) (residue 8 and name HB#) 3.350 1.650 1.650
assign (residue 8 and name HG2) (residue 8 and name HB#) 3.350 1.650 1.650

NOE interactions to residue E9
assign (residue 9 and name HN) (residue 6 and name HA) 2.850 1.150 1.150
assign (residue 9 and name HN) (residue 6 and name HB#) 3.600 1.900 1.900
assign (residue 9 and name HN) (residue 9 and name HB#) 2.350 0.650 0.650
assign (residue 9 and name HG1) (residue 9 and name HB#) 3.350 1.650 1.650

NOE interactions to residue K10
assign (residue 10 and name HN) (residue 10 and name HB2) 3.350 1.650 1.650
assign (residue 10 and name HN) (residue 10 and name HD#) 3.350 1.650 1.650
assign (residue 10 and name HN) (residue 10 and name HE#) 2.850 1.150 1.150
assign (residue 10 and name HN) (residue 10 and name HG#) 2.850 1.150 1.150
assign (residue 10 and name HN) (residue 13 and name HB#) 3.600 1.900 1.900
assign (residue 10 and name HA) (residue 10 and name HB1) 3.350 1.650 1.650
assign (residue 10 and name HA) (residue 10 and name HB2) 2.350 0.650 0.650
assign (residue 10 and name HA) (residue 13 and name HB#) 3.100 1.400 1.400
assign (residue 10 and name HB1) (residue 10 and name HD#) 3.350 1.650 1.650
assign (residue 10 and name HB1) (residue 10 and name HE#) 3.350 1.650 1.650
assign (residue 10 and name HB1) (residue 10 and name HG#) 3.350 1.650 1.650
assign (residue 10 and name HB2) (residue 10 and name HE#) 3.350 1.650 1.650
assign (residue 10 and name HB2) (residue 10 and name HG#) 3.350 1.650 1.650

NOE interactions to residue V11
assign (residue 11 and name HN) (residue 11 and name HB) 2.350 0.650 0.650
assign (residue 11 and name HN) (residue 11 and name HG1#) 3.100 1.400 1.400
assign (residue 11 and name HN) (residue 11 and name HG2#) 3.100 1.400 1.400
assign (residue 11 and name HN) (residue 41 and name HD1#) 3.600 1.900 1.900
assign (residue 11 and name HA) (residue 11 and name HB) 2.850 1.150 1.150
assign (residue 11 and name HA) (residue 11 and name HG1#) 3.100 1.400 1.400
assign (residue 11 and name HA) (residue 11 and name HG2#) 3.100 1.400 1.400
assign (residue 11 and name HA) (residue 14 and name HB1) 2.850 1.150 1.150
assign (residue 11 and name HA) (residue 14 and name HB2) 2.850 1.150 1.150
assign (residue 11 and name HA) (residue 14 and name HD2#) 3.600 1.900 1.900
assign (residue 11 and name HA) (residue 14 and name HG) 2.850 1.150 1.150
assign (residue 11 and name HB) (residue 8 and name HA) 2.850 1.150 1.150
assign (residue 11 and name HG1#) (residue 11 and name HA) 3.100 1.400 1.400
assign (residue 11 and name HG1#) (residue 11 and name HB) 3.100 1.400 1.400
assign (residue 11 and name HG1#) (residue 12 and name HA) 3.600 1.900 1.900
assign (residue 11 and name HG1#) (residue 37 and name HD1#) 3.600 1.900 1.900
assign (residue 11 and name HG1#) (residue 38 and name HA) 3.600 1.900 1.900
assign (residue 11 and name HG1#) (residue 38 and name HB#) 3.600 1.900 1.900
assign (residue 11 and name HG1#) (residue 38 and name HG1) 3.600 1.900 1.900
assign (residue 11 and name HG1#) (residue 38 and name HG2) 3.600 1.900 1.900
assign (residue 11 and name HG1#) (residue 41 and name HB) 3.600 1.900 1.900
assign (residue 11 and name HG1#) (residue 41 and name HD1#) 3.850 2.150 2.150
assign (residue 11 and name HG2#) (residue 7 and name HA) 3.100 1.400 1.400
assign (residue 11 and name HG2#) (residue 11 and name HA) 3.100 1.400 1.400
assign (residue 11 and name HG2#) (residue 11 and name HB) 3.350 1.650 1.650
assign (residue 11 and name HG2#) (residue 41 and name HD1#) 3.350 1.650 1.650
assign (residue 11 and name HG2#) (residue 57 and name HB) 3.600 1.900 1.900

NOE interactions to residue K12
assign (residue 12 and name HN) (residue 11 and name HB) 3.350 1.650 1.650
assign (residue 12 and name HN) (residue 11 and name HG1#) 3.100 1.400 1.400
assign (residue 12 and name HN) (residue 11 and name HG2#) 3.600 1.900 1.900
assign (residue 12 and name HN) (residue 12 and name HB#) 2.350 0.650 0.650
assign (residue 12 and name HN) (residue 12 and name HD#) 3.350 1.650 1.650
assign (residue 12 and name HN) (residue 12 and name HE#) 3.350 1.650 1.650
assign (residue 12 and name HN) (residue 12 and name HG#) 2.850 1.150 1.150
assign (residue 12 and name HN) (residue 13 and name HB#) 3.600 1.900 1.900
assign (residue 12 and name HA) (residue 12 and name HB#) 3.350 1.650 1.650
assign (residue 12 and name HA) (residue 12 and name HD#) 3.350 1.650 1.650
assign (residue 12 and name HA) (residue 12 and name HE#) 3.350 1.650 1.650
assign (residue 12 and name HA) (residue 12 and name HG#) 3.350 1.650 1.650
assign (residue 12 and name HA) (residue 13 and name HB#) 3.350 1.650 1.650
assign (residue 12 and name HD#) (residue 12 and name HB#) 3.350 1.650 1.650
assign (residue 12 and name HD#) (residue 12 and name HE#) 3.350 1.650 1.650
assign (residue 12 and name HD#) (residue 12 and name HG#) 3.350 1.650 1.650
assign (residue 12 and name HE#) (residue 12 and name HB#) 3.350 1.650 1.650

assign (residue 12 and name HE#) (residue 12 and name HG#) 3.350 1.650 1.650
assign (residue 12 and name HE#) (residue 64 and name HG2#) 3.350 1.650 1.650
assign (residue 12 and name HG#) (residue 12 and name HB#) 3.350 1.650 1.650

NOE interactions to residue A13
assign (residue 13 and name HN) (residue 13 and name HB#) 2.600 0.900 0.900
assign (residue 13 and name HA) (residue 13 and name HB#) 3.350 1.650 1.650
assign (residue 13 and name HB#) (residue 10 and name HA) 3.100 1.400 1.400
assign (residue 13 and name HB#) (residue 10 and name HE#) 3.350 1.650 1.650
assign (residue 13 and name HB#) (residue 13 and name HA) 2.600 0.900 0.900
assign (residue 13 and name HB#) (residue 14 and name HD2#) 3.850 2.150 2.150
assign (residue 13 and name HB#) (residue 16 and name HB#) 3.350 1.650 1.650

NOE interactions to residue L14
assign (residue 14 and name HN) (residue 11 and name HA) 2.850 1.150 1.150
assign (residue 14 and name HN) (residue 13 and name HB#) 3.100 1.400 1.400
assign (residue 14 and name HN) (residue 14 and name HB2) 2.850 1.150 1.150
assign (residue 14 and name HN) (residue 14 and name HD1#) 3.100 1.400 1.400
assign (residue 14 and name HN) (residue 14 and name HD2#) 3.100 1.400 1.400
assign (residue 14 and name HN) (residue 14 and name HG) 2.350 0.650 0.650
assign (residue 14 and name HA) (residue 13 and name HB#) 3.350 1.650 1.650
assign (residue 14 and name HA) (residue 64 and name HD1#) 3.350 1.650 1.650
assign (residue 14 and name HB1) (residue 11 and name HA) 2.850 1.150 1.150
assign (residue 14 and name HB1) (residue 14 and name HA) 3.350 1.650 1.650
assign (residue 14 and name HB1) (residue 14 and name HD1#) 3.100 1.400 1.400
assign (residue 14 and name HB2) (residue 11 and name HA) 2.850 1.150 1.150
assign (residue 14 and name HB2) (residue 14 and name HA) 3.350 1.650 1.650
assign (residue 14 and name HB2) (residue 14 and name HD1#) 3.350 1.650 1.650
assign (residue 14 and name HD1#) (residue 64 and name HD1#) 3.350 1.650 1.650
assign (residue 14 and name HD2#) (residue 10 and name HB#) 3.350 1.650 1.650
assign (residue 14 and name HD2#) (residue 10 and name HD#) 3.350 1.650 1.650
assign (residue 14 and name HD2#) (residue 10 and name HE#) 3.350 1.650 1.650
assign (residue 14 and name HD2#) (residue 10 and name HG#) 3.350 1.650 1.650
assign (residue 14 and name HD2#) (residue 13 and name HB#) 3.850 2.150 2.150
assign (residue 14 and name HD2#) (residue 14 and name HA) 3.100 1.400 1.400
assign (residue 14 and name HD2#) (residue 14 and name HB1) 3.100 1.400 1.400
assign (residue 14 and name HD2#) (residue 14 and name HB2) 3.100 1.400 1.400
assign (residue 14 and name HD2#) (residue 60 and name HB1) 3.600 1.900 1.900
assign (residue 14 and name HD2#) (residue 61 and name HG1) 3.350 1.650 1.650
assign (residue 14 and name HD2#) (residue 61 and name HG2) 3.100 1.400 1.400
assign (residue 14 and name HD2#) (residue 64 and name HB) 3.600 1.900 1.900
assign (residue 14 and name HD2#) (residue 64 and name HD1#) 3.850 2.150 2.150
assign (residue 14 and name HG) (residue 14 and name HD2#) 3.100 1.400 1.400

NOE interactions to residue E15
assign (residue 15 and name HN) (residue 11 and name HA) 2.850 1.150 1.150
assign (residue 15 and name HN) (residue 12 and name HA) 2.850 1.150 1.150
assign (residue 15 and name HN) (residue 14 and name HB1) 2.350 0.650 0.650
assign (residue 15 and name HN) (residue 14 and name HB2) 2.850 1.150 1.150
assign (residue 15 and name HN) (residue 15 and name HB#) 2.350 0.650 0.650
assign (residue 15 and name HN) (residue 15 and name HG1) 2.850 1.150 1.150
assign (residue 15 and name HN) (residue 15 and name HG2) 2.850 1.150 1.150
assign (residue 15 and name HA) (residue 15 and name HB#) 2.850 1.150 1.150
assign (residue 15 and name HA) (residue 15 and name HG1) 2.850 1.150 1.150
assign (residue 15 and name HA) (residue 18 and name HB) 2.850 1.150 1.150
assign (residue 15 and name HA) (residue 18 and name HG1#) 3.600 1.900 1.900
assign (residue 15 and name HA) (residue 18 and name HG2#) 3.600 1.900 1.900
assign (residue 15 and name HB#) (residue 15 and name HG1) 2.850 1.150 1.150
assign (residue 15 and name HG1) (residue 15 and name HB#) 2.850 1.150 1.150
assign (residue 15 and name HG1) (residue 15 and name HG2) 2.850 1.150 1.150
assign (residue 15 and name HG1) (residue 19 and name HD#) 3.350 1.650 1.650

NOE interactions to residue E16
assign (residue 16 and name HN) (residue 16 and name HB#) 2.350 0.650 0.650
assign (residue 16 and name HN) (residue 16 and name HG#) 2.850 1.150 1.150
assign (residue 16 and name HA) (residue 16 and name HB#) 2.850 1.150 1.150
assign (residue 16 and name HA) (residue 19 and name HB#) 2.850 1.150 1.150
assign (residue 16 and name HB#) (residue 13 and name HA) 2.850 1.150 1.150

NOE interactions to residue K17
assign (residue 17 and name HN) (residue 13 and name HA) 2.850 1.150 1.150
assign (residue 17 and name HN) (residue 16 and name HB#) 2.350 0.650 0.650
assign (residue 17 and name HA) (residue 20 and name HB#) 3.100 1.400 1.400

NOE interactions to residue V18
assign (residue 18 and name HN) (residue 15 and name HA) 2.850 1.150 1.150

assign (residue 18 and name HN) (residue 17 and name HB#) 2.850 1.150 1.150
assign (residue 18 and name HN) (residue 18 and name HB) 2.350 0.650 0.650
assign (residue 18 and name HN) (residue 18 and name HG1#) 3.600 1.900 1.900
assign (residue 18 and name HN) (residue 18 and name HG2#) 3.100 1.400 1.400
assign (residue 18 and name HA) (residue 18 and name HB) 2.850 1.150 1.150
assign (residue 18 and name HA) (residue 18 and name HG1#) 3.100 1.400 1.400
assign (residue 18 and name HA) (residue 18 and name HG2#) 3.100 1.400 1.400
assign (residue 18 and name HA) (residue 21 and name HB1) 2.850 1.150 1.150
assign (residue 18 and name HA) (residue 21 and name HB2) 2.850 1.150 1.150
assign (residue 18 and name HA) (residue 21 and name HG) 2.850 1.150 1.150
assign (residue 18 and name HA) (residue 64 and name HD1#) 3.600 1.900 1.900
assign (residue 18 and name HB) (residue 15 and name HA) 2.850 1.150 1.150
assign (residue 18 and name HB) (residue 18 and name HA) 2.850 1.150 1.150
assign (residue 18 and name HB) (residue 18 and name HG1#) 3.100 1.400 1.400
assign (residue 18 and name HB) (residue 18 and name HG2#) 3.100 1.400 1.400
assign (residue 18 and name HG1#) (residue 15 and name HA) 3.600 1.900 1.900
assign (residue 18 and name HG1#) (residue 18 and name HA) 3.100 1.400 1.400
assign (residue 18 and name HG1#) (residue 18 and name HB) 3.100 1.400 1.400
assign (residue 18 and name HG1#) (residue 30 and name HB1) 3.600 1.900 1.900
assign (residue 18 and name HG1#) (residue 31 and name HA) 3.100 1.400 1.400
assign (residue 18 and name HG1#) (residue 31 and name HD#) 3.350 1.650 1.650
assign (residue 18 and name HG2#) (residue 15 and name HA) 3.600 1.900 1.900
assign (residue 18 and name HG2#) (residue 18 and name HA) 3.100 1.400 1.400
assign (residue 18 and name HG2#) (residue 18 and name HB) 3.100 1.400 1.400
assign (residue 18 and name HG2#) (residue 31 and name HA) 3.600 1.900 1.900
assign (residue 18 and name HG2#) (residue 64 and name HD1#) 3.850 2.150 2.150
assign (residue 18 and name HG2#) (residue 64 and name HG2#) 3.850 2.150 2.150

NOE interactions to residue K19
assign (residue 19 and name HN) (residue 16 and name HA) 2.850 1.150 1.150
assign (residue 19 and name HN) (residue 16 and name HB#) 3.350 1.650 1.650
assign (residue 19 and name HN) (residue 18 and name HB) 2.350 0.650 0.650
assign (residue 19 and name HN) (residue 18 and name HG1#) 3.100 1.400 1.400
assign (residue 19 and name HN) (residue 18 and name HG2#) 3.600 1.900 1.900
assign (residue 19 and name HN) (residue 19 and name HB#) 2.350 0.650 0.650
assign (residue 19 and name HN) (residue 19 and name HD#) 2.850 1.150 1.150
assign (residue 19 and name HN) (residue 19 and name HE#) 3.350 1.650 1.650
assign (residue 19 and name HN) (residue 19 and name HG#) 2.850 1.150 1.150
assign (residue 19 and name HN) (residue 20 and name HB#) 3.100 1.400 1.400
assign (residue 19 and name HA) (residue 18 and name HG1#) 3.600 1.900 1.900
assign (residue 19 and name HA) (residue 18 and name HG2#) 3.600 1.900 1.900
assign (residue 19 and name HA) (residue 19 and name HG1) 3.350 1.650 1.650
assign (residue 19 and name HA) (residue 19 and name HG2) 2.850 1.150 1.150
assign (residue 19 and name HB#) (residue 16 and name HA) 2.850 1.150 1.150
assign (residue 19 and name HB#) (residue 19 and name HG1) 3.350 1.650 1.650
assign (residue 19 and name HB#) (residue 19 and name HG2) 2.850 1.150 1.150
assign (residue 19 and name HE1) (residue 19 and name HD#) 3.350 1.650 1.650

NOE interactions to residue A20
assign (residue 20 and name HN) (residue 16 and name HB#) 3.350 1.650 1.650
assign (residue 20 and name HN) (residue 18 and name HA) 2.850 1.150 1.150
assign (residue 20 and name HN) (residue 18 and name HG2#) 3.600 1.900 1.900
assign (residue 20 and name HN) (residue 19 and name HB#) 2.350 0.650 0.650
assign (residue 20 and name HN) (residue 20 and name HB#) 2.600 0.900 0.900
assign (residue 20 and name HN) (residue 21 and name HB1) 2.850 1.150 1.150
assign (residue 20 and name HN) (residue 21 and name HG) 3.350 1.650 1.650
assign (residue 20 and name HA) (residue 20 and name HB#) 3.100 1.400 1.400
assign (residue 20 and name HB#) (residue 17 and name HA) 3.100 1.400 1.400
assign (residue 20 and name HB#) (residue 20 and name HA) 3.100 1.400 1.400
assign (residue 20 and name HB#) (residue 21 and name HA) 3.600 1.900 1.900
assign (residue 20 and name HB#) (residue 21 and name HD2#) 3.850 2.150 2.150

NOE interactions to residue L21
assign (residue 21 and name HN) (residue 18 and name HA) 2.850 1.150 1.150
assign (residue 21 and name HN) (residue 20 and name HB#) 3.100 1.400 1.400
assign (residue 21 and name HN) (residue 21 and name HB1) 2.350 0.650 0.650
assign (residue 21 and name HN) (residue 21 and name HD1#) 3.100 1.400 1.400
assign (residue 21 and name HN) (residue 21 and name HD2#) 3.100 1.400 1.400
assign (residue 21 and name HN) (residue 21 and name HG) 2.350 0.650 0.650
assign (residue 21 and name HN) (residue 27 and name HG2#) 3.600 1.900 1.900
assign (residue 21 and name HA) (residue 20 and name HB#) 3.600 1.900 1.900
assign (residue 21 and name HA) (residue 21 and name HB1) 2.850 1.150 1.150
assign (residue 21 and name HA) (residue 21 and name HB2) 2.850 1.150 1.150
assign (residue 21 and name HA) (residue 21 and name HD1#) 3.100 1.400 1.400
assign (residue 21 and name HA) (residue 21 and name HD2#) 3.100 1.400 1.400
assign (residue 21 and name HA) (residue 21 and name HG) 2.850 1.150 1.150

assign (residue 21 and name HB1) (residue 18 and name HA) 2.850 1.150 1.150
assign (residue 21 and name HB1) (residue 21 and name HA) 2.850 1.150 1.150
assign (residue 21 and name HB1) (residue 21 and name HD1#) 3.350 1.650 1.650
assign (residue 21 and name HB1) (residue 21 and name HD2#) 3.350 1.650 1.650
assign (residue 21 and name HB1) (residue 21 and name HG) 3.350 1.650 1.650
assign (residue 21 and name HB1) (residue 27 and name HD1#) 3.600 1.900 1.900
assign (residue 21 and name HB1) (residue 27 and name HG2#) 3.600 1.900 1.900
assign (residue 21 and name HB2) (residue 21 and name HA) 2.850 1.150 1.150
assign (residue 21 and name HB2) (residue 21 and name HD1#) 3.350 1.650 1.650
assign (residue 21 and name HB2) (residue 21 and name HG) 3.350 1.650 1.650
assign (residue 21 and name HB2) (residue 27 and name HD1#) 3.600 1.900 1.900
assign (residue 21 and name HB2) (residue 27 and name HG2#) 3.600 1.900 1.900
assign (residue 21 and name HB2) (residue 67 and name HA) 3.350 1.650 1.650
assign (residue 21 and name HB2) (residue 67 and name HB1) 3.350 1.650 1.650
assign (residue 21 and name HD1#) (residue 21 and name HG) 3.350 1.650 1.650
assign (residue 21 and name HD2#) (residue 20 and name HB#) 3.850 2.150 2.150
assign (residue 21 and name HD2#) (residue 21 and name HA) 3.100 1.400 1.400
assign (residue 21 and name HD2#) (residue 21 and name HB1) 3.600 1.900 1.900
assign (residue 21 and name HD2#) (residue 21 and name HB2) 3.100 1.400 1.400
assign (residue 21 and name HD2#) (residue 21 and name HD1#) 3.350 1.650 1.650
assign (residue 21 and name HD2#) (residue 21 and name HG) 3.100 1.400 1.400

NOE interactions to residue G22
assign (residue 22 and name HN) (residue 19 and name HA) 3.350 1.650 1.650
assign (residue 22 and name HN) (residue 20 and name HB#) 3.600 1.900 1.900
assign (residue 22 and name HN) (residue 21 and name HA) 2.850 1.150 1.150
assign (residue 22 and name HN) (residue 21 and name HB1) 2.850 1.150 1.150
assign (residue 22 and name HN) (residue 21 and name HB2) 2.850 1.150 1.150
assign (residue 22 and name HN) (residue 21 and name HD2#) 3.600 1.900 1.900
assign (residue 22 and name HN) (residue 22 and name HA1) 2.850 1.150 1.150
assign (residue 22 and name HN) (residue 22 and name HA2) 2.850 1.150 1.150
assign (residue 22 and name HN) (residue 27 and name HD1#) 3.600 1.900 1.900
assign (residue 22 and name HN) (residue 27 and name HG2#) 3.600 1.900 1.900

NOE interactions to residue G23
assign (residue 23 and name HN) (residue 27 and name HD1#) 3.350 1.650 1.650
assign (residue 23 and name HN) (residue 27 and name HG2#) 3.600 1.900 1.900
assign (residue 23 and name HA1) (residue 27 and name HG2#) 3.600 1.900 1.900

NOE interactions to residue G24
assign (residue 24 and name HN) (residue 27 and name HB) 2.850 1.150 1.150
assign (residue 24 and name HN) (residue 27 and name HG2#) 3.600 1.900 1.900

NOE interactions to residue G25
assign (residue 25 and name HN) (residue 24 and name HA1) 2.850 1.150 1.150
assign (residue 25 and name HN) (residue 24 and name HA2) 2.850 1.150 1.150

NOE interactions to residue R26
assign (residue 26 and name HN) (residue 26 and name HB#) 2.850 1.150 1.150
assign (residue 26 and name HN) (residue 26 and name HG#) 2.850 1.150 1.150
assign (residue 26 and name HA) (residue 26 and name HB#) 2.850 1.150 1.150
assign (residue 26 and name HA) (residue 26 and name HG#) 2.850 1.150 1.150
assign (residue 26 and name HB#) (residue 26 and name HA) 2.850 1.150 1.150
assign (residue 26 and name HB#) (residue 26 and name HG#) 2.850 1.150 1.150
assign (residue 26 and name HB#) (residue 67 and name HD1#) 3.350 1.650 1.650
assign (residue 26 and name HD1) (residue 26 and name HB#) 3.350 1.650 1.650
assign (residue 26 and name HD1) (residue 26 and name HG#) 3.350 1.650 1.650
assign (residue 26 and name HD1) (residue 67 and name HD2#) 2.600 0.900 0.900
assign (residue 26 and name HD2) (residue 26 and name HB#) 3.350 1.650 1.650
assign (residue 26 and name HD2) (residue 26 and name HG#) 3.350 1.650 1.650
assign (residue 26 and name HD2) (residue 67 and name HD2#) 3.100 1.400 1.400
assign (residue 26 and name HG#) (residue 26 and name HA) 2.850 1.150 1.150
assign (residue 26 and name HG#) (residue 26 and name HB#) 2.850 1.150 1.150
assign (residue 26 and name HG#) (residue 67 and name HD2#) 3.350 1.650 1.650

NOE interactions to residue I27
assign (residue 27 and name HN) (residue 27 and name HB) 2.850 1.150 1.150
assign (residue 27 and name HN) (residue 27 and name HD1#) 3.100 1.400 1.400
assign (residue 27 and name HN) (residue 27 and name HG1#) 3.100 1.400 1.400
assign (residue 27 and name HN) (residue 27 and name HG2#) 3.100 1.400 1.400
assign (residue 27 and name HA) (residue 26 and name HB#) 3.350 1.650 1.650
assign (residue 27 and name HA) (residue 27 and name HB) 2.850 1.150 1.150
assign (residue 27 and name HA) (residue 27 and name HD1#) 3.100 1.400 1.400
assign (residue 27 and name HA) (residue 27 and name HG2#) 3.100 1.400 1.400
assign (residue 27 and name HA) (residue 30 and name HB1) 2.850 1.150 1.150
assign (residue 27 and name HA) (residue 30 and name HD1#) 3.100 1.400 1.400

assign (residue 27 and name HA) (residue 30 and name HG) 2.850 1.150 1.150
assign (residue 27 and name HB) (residue 27 and name HA) 2.850 1.150 1.150
assign (residue 27 and name HB) (residue 27 and name HD1#) 3.600 1.900 1.900
assign (residue 27 and name HB) (residue 27 and name HG1#) 3.100 1.400 1.400
assign (residue 27 and name HB) (residue 27 and name HG2#) 3.100 1.400 1.400
assign (residue 27 and name HD1#) (residue 21 and name HB1) 3.600 1.900 1.900
assign (residue 27 and name HD1#) (residue 21 and name HB2) 3.100 1.400 1.400
assign (residue 27 and name HD1#) (residue 27 and name HA) 3.100 1.400 1.400
assign (residue 27 and name HD1#) (residue 27 and name HB) 3.100 1.400 1.400
assign (residue 27 and name HD1#) (residue 27 and name HG1#) 3.350 1.650 1.650
assign (residue 27 and name HD1#) (residue 27 and name HG2#) 3.350 1.650 1.650
assign (residue 27 and name HD1#) (residue 30 and name HB1) 3.600 1.900 1.900
assign (residue 27 and name HG2#) (residue 18 and name HA) 3.600 1.900 1.900
assign (residue 27 and name HG2#) (residue 18 and name HG1#) 3.600 1.900 1.900
assign (residue 27 and name HG2#) (residue 21 and name HB1) 3.600 1.900 1.900
assign (residue 27 and name HG2#) (residue 21 and name HB2) 3.600 1.900 1.900
assign (residue 27 and name HG2#) (residue 26 and name HB#) 3.350 1.650 1.650
assign (residue 27 and name HG2#) (residue 27 and name HA) 3.100 1.400 1.400
assign (residue 27 and name HG2#) (residue 27 and name HB) 3.100 1.400 1.400
assign (residue 27 and name HG2#) (residue 27 and name HD1#) 3.850 2.150 2.150
assign (residue 27 and name HG2#) (residue 27 and name HG1#) 3.850 2.150 2.150
assign (residue 27 and name HG2#) (residue 30 and name HB1) 3.600 1.900 1.900

NOE interactions to residue E28
assign (residue 28 and name HN) (residue 27 and name HB) 2.850 1.150 1.150
assign (residue 28 and name HN) (residue 27 and name HD1#) 3.600 1.900 1.900
assign (residue 28 and name HN) (residue 27 and name HG1#) 3.350 1.650 1.650
assign (residue 28 and name HN) (residue 27 and name HG2#) 3.100 1.400 1.400

NOE interactions to residue E29
assign (residue 29 and name HN) (residue 29 and name HB#) 2.350 0.650 0.650
assign (residue 29 and name HN) (residue 29 and name HG#) 2.350 0.650 0.650

NOE interactions to residue L30
assign (residue 30 and name HN) (residue 27 and name HA) 2.850 1.150 1.150
assign (residue 30 and name HN) (residue 27 and name HD1#) 3.600 1.900 1.900
assign (residue 30 and name HN) (residue 27 and name HG2#) 3.600 1.900 1.900
assign (residue 30 and name HN) (residue 30 and name HB2) 2.350 0.650 0.650
assign (residue 30 and name HN) (residue 30 and name HD1#) 3.100 1.400 1.400
assign (residue 30 and name HN) (residue 30 and name HD2#) 3.100 1.400 1.400
assign (residue 30 and name HA) (residue 30 and name HB1) 3.350 1.650 1.650
assign (residue 30 and name HA) (residue 30 and name HB2) 2.850 1.150 1.150
assign (residue 30 and name HA) (residue 30 and name HD1#) 3.350 1.650 1.650
assign (residue 30 and name HA) (residue 30 and name HG) 2.850 1.150 1.150
assign (residue 30 and name HA) (residue 33 and name HB#) 2.850 1.150 1.150
assign (residue 30 and name HB1) (residue 27 and name HA) 2.850 1.150 1.150
assign (residue 30 and name HB1) (residue 30 and name HD2#) 3.100 1.400 1.400
assign (residue 30 and name HB1) (residue 30 and name HG) 3.350 1.650 1.650
assign (residue 30 and name HB2) (residue 30 and name HA) 2.850 1.150 1.150
assign (residue 30 and name HB2) (residue 30 and name HB1) 2.350 0.650 0.650
assign (residue 30 and name HB2) (residue 30 and name HD1#) 3.100 1.400 1.400
assign (residue 30 and name HB2) (residue 30 and name HD2#) 3.100 1.400 1.400
assign (residue 30 and name HB2) (residue 30 and name HG) 2.850 1.150 1.150
assign (residue 30 and name HD1#) (residue 26 and name HG#) 3.350 1.650 1.650
assign (residue 30 and name HD1#) (residue 27 and name HA) 3.600 1.900 1.900
assign (residue 30 and name HD1#) (residue 30 and name HB1) 3.100 1.400 1.400
assign (residue 30 and name HD1#) (residue 30 and name HB2) 3.100 1.400 1.400
assign (residue 30 and name HD1#) (residue 30 and name HG) 3.100 1.400 1.400
assign (residue 30 and name HD1#) (residue 33 and name HB#) 3.350 1.650 1.650
assign (residue 30 and name HD1#) (residue 33 and name HG#) 3.350 1.650 1.650
assign (residue 30 and name HD1#) (residue 60 and name HB1) 3.350 1.650 1.650
assign (residue 30 and name HD1#) (residue 60 and name HB2) 3.350 1.650 1.650
assign (residue 30 and name HD1#) (residue 60 and name HD1#) 3.350 1.650 1.650
assign (residue 30 and name HD1#) (residue 63 and name HB1) 3.350 1.650 1.650
assign (residue 30 and name HD1#) (residue 63 and name HB2) 3.350 1.650 1.650
assign (residue 30 and name HD1#) (residue 64 and name HA) 3.600 1.900 1.900
assign (residue 30 and name HD1#) (residue 64 and name HD1#) 3.850 2.150 2.150
assign (residue 30 and name HD1#) (residue 64 and name HG11) 3.350 1.650 1.650
assign (residue 30 and name HD1#) (residue 64 and name HG12) 3.350 1.650 1.650
assign (residue 30 and name HD2#) (residue 26 and name HG#) 3.350 1.650 1.650
assign (residue 30 and name HD2#) (residue 30 and name HA) 3.100 1.400 1.400
assign (residue 30 and name HD2#) (residue 30 and name HB1) 3.100 1.400 1.400
assign (residue 30 and name HD2#) (residue 30 and name HB2) 3.100 1.400 1.400
assign (residue 30 and name HD2#) (residue 30 and name HG) 3.100 1.400 1.400
assign (residue 30 and name HD2#) (residue 33 and name HB#) 3.350 1.650 1.650
assign (residue 30 and name HD2#) (residue 33 and name HG#) 3.350 1.650 1.650

assign (residue 30 and name HD2#) (residue 60 and name HD1#) 3.350 1.650 1.650
assign (residue 30 and name HD2#) (residue 63 and name HB1) 3.350 1.650 1.650
assign (residue 30 and name HD2#) (residue 63 and name HB2) 3.350 1.650 1.650
assign (residue 30 and name HD2#) (residue 63 and name HG#) 3.350 1.650 1.650
assign (residue 30 and name HD2#) (residue 64 and name HG11) 3.350 1.650 1.650
assign (residue 30 and name HD2#) (residue 64 and name HG12) 3.600 1.900 1.900

NOE interactions to residue K31
assign (residue 31 and name HN) (residue 27 and name HA) 2.850 1.150 1.150
assign (residue 31 and name HN) (residue 27 and name HG2#) 3.600 1.900 1.900
assign (residue 31 and name HN) (residue 30 and name HB1) 2.350 0.650 0.650
assign (residue 31 and name HN) (residue 30 and name HB2) 2.850 1.150 1.150
assign (residue 31 and name HN) (residue 31 and name HB#) 2.350 0.650 0.650
assign (residue 31 and name HN) (residue 31 and name HD#) 2.850 1.150 1.150
assign (residue 31 and name HN) (residue 31 and name HE#) 2.850 1.150 1.150
assign (residue 31 and name HN) (residue 31 and name HG#) 2.850 1.150 1.150
assign (residue 31 and name HA) (residue 18 and name HG1#) 3.100 1.400 1.400
assign (residue 31 and name HA) (residue 18 and name HG2#) 3.600 1.900 1.900
assign (residue 31 and name HA) (residue 27 and name HG2#) 3.600 1.900 1.900
assign (residue 31 and name HA) (residue 31 and name HB#) 2.850 1.150 1.150
assign (residue 31 and name HA) (residue 31 and name HD#) 3.350 1.650 1.650
assign (residue 31 and name HA) (residue 31 and name HG#) 2.850 1.150 1.150
assign (residue 31 and name HB1) (residue 31 and name HA) 2.850 1.150 1.150
assign (residue 31 and name HB1) (residue 31 and name HG#) 2.850 1.150 1.150
assign (residue 31 and name HB2) (residue 18 and name HG1#) 3.600 1.900 1.900
assign (residue 31 and name HB2) (residue 31 and name HA) 2.850 1.150 1.150
assign (residue 31 and name HB2) (residue 31 and name HG#) 2.850 1.150 1.150
assign (residue 31 and name HD1) (residue 27 and name HG2#) 3.600 1.900 1.900
assign (residue 31 and name HD1) (residue 31 and name HG#) 2.850 1.150 1.150
assign (residue 31 and name HD2) (residue 31 and name HG#) 2.850 1.150 1.150
assign (residue 31 and name HG1) (residue 31 and name HA) 2.850 1.150 1.150
assign (residue 31 and name HG1) (residue 31 and name HD#) 2.850 1.150 1.150
assign (residue 31 and name HG1) (residue 31 and name HE#) 3.350 1.650 1.650
assign (residue 31 and name HG2) (residue 31 and name HA) 2.850 1.150 1.150
assign (residue 31 and name HG2) (residue 31 and name HE#) 3.350 1.650 1.650

NOE interactions to residue K32
assign (residue 32 and name HN) (residue 31 and name HG#) 2.850 1.150 1.150
assign (residue 32 and name HN) (residue 32 and name HB#) 2.350 0.650 0.650
assign (residue 32 and name HN) (residue 32 and name HD#) 2.850 1.150 1.150
assign (residue 32 and name HN) (residue 32 and name HG#) 2.850 1.150 1.150

NOE interactions to residue K33
assign (residue 33 and name HN) (residue 31 and name HA) 2.850 1.150 1.150
assign (residue 33 and name HN) (residue 33 and name HB#) 2.350 0.650 0.650
assign (residue 33 and name HN) (residue 33 and name HG#) 2.350 0.650 0.650
assign (residue 33 and name HD#) (residue 33 and name HE#) 2.350 0.650 0.650
assign (residue 33 and name HE#) (residue 33 and name HD#) 2.350 0.650 0.650
assign (residue 33 and name HG#) (residue 33 and name HD#) 2.350 0.650 0.650

NOE interactions to residue C34
assign (residue 34 and name HN) (residue 31 and name HA) 2.850 1.150 1.150
assign (residue 34 and name HN) (residue 33 and name HB#) 2.850 1.150 1.150
assign (residue 34 and name HN) (residue 33 and name HG#) 2.850 1.150 1.150
assign (residue 34 and name HN) (residue 34 and name HB1) 2.350 0.650 0.650
assign (residue 34 and name HN) (residue 34 and name HB2) 2.350 0.650 0.650
assign (residue 34 and name HN) (residue 37 and name HB2) 3.350 1.650 1.650
assign (residue 34 and name HN) (residue 60 and name HD2#) 3.100 1.400 1.400
assign (residue 34 and name HA) (residue 34 and name HB1) 2.850 1.150 1.150
assign (residue 34 and name HA) (residue 34 and name HB2) 2.850 1.150 1.150
assign (residue 34 and name HA) (residue 37 and name HB1) 2.850 1.150 1.150
assign (residue 34 and name HA) (residue 60 and name HD2#) 3.100 1.400 1.400
assign (residue 34 and name HB1) (residue 31 and name HA) 2.850 1.150 1.150
assign (residue 34 and name HB1) (residue 34 and name HA) 2.850 1.150 1.150
assign (residue 34 and name HB1) (residue 34 and name HB1) 2.350 0.650 0.650
assign (residue 34 and name HB1) (residue 34 and name HB2) 2.350 0.650 0.650
assign (residue 34 and name HB1) (residue 60 and name HD2#) 3.600 1.900 1.900
assign (residue 34 and name HB2) (residue 31 and name HA) 2.850 1.150 1.150
assign (residue 34 and name HB2) (residue 34 and name HA) 2.850 1.150 1.150
assign (residue 34 and name HB2) (residue 34 and name HB1) 2.350 0.650 0.650
assign (residue 34 and name HB2) (residue 34 and name HB2) 2.350 0.650 0.650
assign (residue 34 and name HB2) (residue 60 and name HD2#) 3.100 1.400 1.400
assign (residue 18 and name HG1#) (residue 34 and name HB1) 3.600 1.900 1.900
assign (residue 18 and name HG1#) (residue 34 and name HB2) 3.600 1.900 1.900
assign (residue 18 and name HG2#) (residue 34 and name HB1) 3.600 1.900 1.900
assign (residue 18 and name HG2#) (residue 34 and name HB2) 3.600 1.900 1.900

assign (residue 35 and name HN) (residue 34 and name HB1) 2.350 0.650 0.650
assign (residue 35 and name HN) (residue 34 and name HB2) 2.850 1.150 1.150
assign (residue 37 and name HN) (residue 34 and name HA) 2.850 1.150 1.150
assign (residue 60 and name HD1#) (residue 34 and name HA) 3.600 1.900 1.900
assign (residue 60 and name HD1#) (residue 34 and name HB2) 3.600 1.900 1.900
assign (residue 60 and name HD2#) (residue 34 and name HA) 3.100 1.400 1.400
assign (residue 60 and name HD2#) (residue 34 and name HB1) 3.350 1.650 1.650
assign (residue 60 and name HD2#) (residue 34 and name HB2) 3.600 1.900 1.900

NOE interactions to MP ligand bound to residue C34
assign (residue 34 and name HH1) (residue 15 and name HA) 3.350 1.650 1.650
assign (residue 34 and name HH2) (residue 15 and name HA) 3.350 1.650 1.650
assign (residue 34 and name HH1) (residue 18 and name HB) 3.350 1.650 1.650
assign (residue 34 and name HH2) (residue 18 and name HB) 2.850 1.150 1.150
assign (residue 34 and name HH#) (residue 18 and name HG1#) 3.600 1.900 1.900
assign (residue 34 and name HH#) (residue 18 and name HG2#) 3.600 1.900 1.900
assign (residue 34 and name HH#) (residue 19 and name HA) 3.350 1.650 1.650
assign (residue 34 and name HH#) (residue 19 and name HG1) 3.350 1.650 1.650
assign (residue 34 and name HH#) (residue 19 and name HG2) 3.350 1.650 1.650
assign (residue 34 and name HH#) (residue 19 and name HE2) 3.350 1.650 1.650
assign (residue 34 and name HH#) (residue 31 and name HA) 3.350 1.650 1.650
assign (residue 34 and name HH#) (residue 31 and name HG1) 3.350 1.650 1.650
assign (residue 34 and name HH#) (residue 31 and name HG2) 3.350 1.650 1.650
assign (residue 34 and name HH#) (residue 31 and name HD1) 3.350 1.650 1.650
assign (residue 34 and name HH#) (residue 31 and name HD2) 3.350 1.650 1.650
assign (residue 34 and name HH#) (residue 31 and name HE#) 3.350 1.650 1.650
assign (residue 34 and name HZ1) (residue 15 and name HA) 2.850 1.150 1.150
assign (residue 34 and name HZ2) (residue 15 and name HA) 2.850 1.150 1.150
assign (residue 34 and name HZ#) (residue 15 and name HB#) 3.350 1.650 1.650
assign (residue 34 and name HZ1) (residue 18 and name HB) 2.850 1.150 1.150
assign (residue 34 and name HZ2) (residue 18 and name HB) 2.850 1.150 1.150
assign (residue 34 and name HZ#) (residue 18 and name HG1#) 3.600 1.900 1.900
assign (residue 34 and name HZ#) (residue 18 and name HG2#) 3.600 1.900 1.900
assign (residue 34 and name HZ#) (residue 31 and name HA) 3.350 1.650 1.650
assign (residue 34 and name HZ#) (residue 34 and name HB1) 3.350 1.650 1.650
assign (residue 34 and name HZ#) (residue 34 and name HB2) 3.350 1.650 1.650
assign (residue 34 and name HZ#) (residue 35 and name HA) 3.350 1.650 1.650
assign (residue 34 and name HZ#) (residue 35 and name HG1) 3.350 1.650 1.650
assign (residue 34 and name HZ#) (residue 35 and name HG2) 3.350 1.650 1.650
assign (residue 34 and name HZ#) (residue 38 and name HD1) 3.350 1.650 1.650
assign (residue 34 and name HZ#) (residue 38 and name HD2) 3.350 1.650 1.650
assign (residue 34 and name HZ#) (residue 38 and name HE#) 3.350 1.650 1.650

NOE interactions to residue E35
assign (residue 35 and name HN) (residue 31 and name HA) 2.850 1.150 1.150
assign (residue 35 and name HN) (residue 35 and name HG#) 3.350 1.650 1.650
assign (residue 35 and name HN) (residue 38 and name HB#) 3.350 1.650 1.650
assign (residue 35 and name HA) (residue 35 and name HB1) 2.350 0.650 0.650
assign (residue 35 and name HA) (residue 35 and name HB2) 2.850 1.150 1.150
assign (residue 35 and name HA) (residue 35 and name HG1) 3.350 1.650 1.650
assign (residue 35 and name HA) (residue 35 and name HG2) 3.350 1.650 1.650
assign (residue 35 and name HA) (residue 38 and name HB#) 3.350 1.650 1.650
assign (residue 35 and name HB2) (residue 35 and name HA) 2.850 1.150 1.150

NOE interactions to residue E36
assign (residue 36 and name HN) (residue 36 and name HB#) 3.350 1.650 1.650
assign (residue 36 and name HN) (residue 36 and name HG1) 2.350 0.650 0.650
assign (residue 36 and name HN) (residue 36 and name HG2) 2.350 0.650 0.650
assign (residue 36 and name HN) (residue 37 and name HB1) 3.350 1.650 1.650
assign (residue 36 and name HN) (residue 37 and name HB2) 3.350 1.650 1.650
assign (residue 36 and name HA) (residue 36 and name HB#) 3.350 1.650 1.650
assign (residue 36 and name HA) (residue 36 and name HG#) 3.350 1.650 1.650
assign (residue 36 and name HA) (residue 39 and name HB#) 2.350 0.650 0.650
assign (residue 36 and name HA) (residue 39 and name HD#) 2.350 0.650 0.650

NOE interactions to residue L37
assign (residue 37 and name HN) (residue 36 and name HB#) 3.350 1.650 1.650
assign (residue 37 and name HN) (residue 36 and name HG1) 3.350 1.650 1.650
assign (residue 37 and name HN) (residue 36 and name HG2) 2.850 1.150 1.150
assign (residue 37 and name HN) (residue 37 and name HB1) 2.350 0.650 0.650
assign (residue 37 and name HN) (residue 37 and name HD1#) 3.100 1.400 1.400
assign (residue 37 and name HN) (residue 37 and name HD2#) 3.100 1.400 1.400
assign (residue 37 and name HA) (residue 37 and name HB1) 2.350 0.650 0.650
assign (residue 37 and name HA) (residue 37 and name HB2) 3.350 1.650 1.650
assign (residue 37 and name HA) (residue 37 and name HD1#) 3.100 1.400 1.400
assign (residue 37 and name HB2) (residue 11 and name HG2#) 3.600 1.900 1.900

assign (residue 37 and name HB2) (residue 37 and name HB1) 2.350 0.650 0.650
assign (residue 37 and name HD1#) (residue 37 and name HA) 3.100 1.400 1.400
assign (residue 37 and name HD1#) (residue 41 and name HB) 3.600 1.900 1.900
assign (residue 37 and name HD1#) (residue 54 and name HA) 3.350 1.650 1.650
assign (residue 37 and name HD1#) (residue 57 and name HA) 3.100 1.400 1.400
assign (residue 37 and name HD1#) (residue 37 and name HA) 3.100 1.400 1.400
assign (residue 37 and name HD1#) (residue 60 and name HB1) 3.600 1.900 1.900
assign (residue 37 and name HD1#) (residue 60 and name HB2) 3.600 1.900 1.900
assign (residue 37 and name HD2#) (residue 57 and name HA) 3.100 1.400 1.400
assign (residue 37 and name HG) (residue 11 and name HG2#) 3.600 1.900 1.900
assign (residue 37 and name HG) (residue 37 and name HA) 2.850 1.150 1.150
assign (residue 37 and name HG) (residue 37 and name HD2#) 3.100 1.400 1.400

NOE interactions to residue K38
assign (residue 38 and name HN) (residue 11 and name HG1#) 3.600 1.900 1.900
assign (residue 38 and name HN) (residue 11 and name HG2#) 3.100 1.400 1.400
assign (residue 38 and name HN) (residue 37 and name HB1) 2.850 1.150 1.150
assign (residue 38 and name HN) (residue 37 and name HB2) 2.850 1.150 1.150
assign (residue 38 and name HN) (residue 37 and name HG) 3.350 1.650 1.650
assign (residue 38 and name HN) (residue 38 and name HB#) 2.350 0.650 0.650
assign (residue 38 and name HN) (residue 38 and name HD#) 2.850 1.150 1.150
assign (residue 38 and name HN) (residue 38 and name HE#) 2.850 1.150 1.150
assign (residue 38 and name HN) (residue 38 and name HG1) 2.850 1.150 1.150
assign (residue 38 and name HN) (residue 38 and name HG2) 3.350 1.650 1.650
assign (residue 38 and name HA) (residue 38 and name HG1) 2.850 1.150 1.150
assign (residue 38 and name HA) (residue 38 and name HG2) 2.850 1.150 1.150
assign (residue 38 and name HA) (residue 41 and name HB) 2.850 1.150 1.150
assign (residue 38 and name HA) (residue 41 and name HD1#) 3.100 1.400 1.400
assign (residue 38 and name HD1) (residue 38 and name HG1) 2.850 1.150 1.150
assign (residue 38 and name HD1) (residue 38 and name HG2) 2.850 1.150 1.150
assign (residue 38 and name HG1) (residue 38 and name HA) 2.850 1.150 1.150
assign (residue 38 and name HG1) (residue 11 and name HG1#) 3.600 1.900 1.900
assign (residue 38 and name HG2) (residue 11 and name HG1#) 3.600 1.900 1.900
assign (residue 38 and name HG2) (residue 38 and name HA) 2.850 1.150 1.150

NOE interactions to residue K39
assign (residue 39 and name HN) (residue 39 and name HD#) 2.850 1.150 1.150

NOE interactions to residue K40
assign (residue 40 and name HN) (residue 40 and name HG#) 2.850 1.150 1.150
assign (residue 40 and name HB1) (residue 37 and name HA) 2.850 0.650 0.650

NOE interactions to residue I41
assign (residue 41 and name HN) (residue 38 and name HA) 2.850 1.150 1.150
assign (residue 41 and name HN) (residue 40 and name HD#) 2.850 1.150 1.150
assign (residue 41 and name HN) (residue 40 and name HG#) 2.850 1.150 1.150
assign (residue 41 and name HN) (residue 41 and name HB) 2.350 0.650 0.650
assign (residue 41 and name HN) (residue 41 and name HD1#) 3.100 1.400 1.400
assign (residue 41 and name HN) (residue 41 and name HG11) 2.350 0.650 0.650
assign (residue 41 and name HN) (residue 41 and name HG12) 2.850 1.150 1.150
assign (residue 41 and name HN) (residue 41 and name HG2#) 3.100 1.400 1.400
assign (residue 41 and name HN) (residue 44 and name HG) 3.350 1.650 1.650
assign (residue 41 and name HA) (residue 11 and name HG2#) 3.600 1.900 1.900
assign (residue 41 and name HA) (residue 41 and name HB) 2.850 1.150 1.150
assign (residue 41 and name HA) (residue 41 and name HD1#) 3.100 1.400 1.400
assign (residue 41 and name HA) (residue 41 and name HG11) 2.850 1.150 1.150
assign (residue 41 and name HA) (residue 41 and name HG12) 2.850 1.150 1.150
assign (residue 41 and name HA) (residue 41 and name HG2#) 3.100 1.400 1.400
assign (residue 41 and name HA) (residue 44 and name HB1) 2.850 1.150 1.150
assign (residue 41 and name HA) (residue 44 and name HD1#) 3.100 1.400 1.400
assign (residue 41 and name HA) (residue 44 and name HD2#) 3.600 1.900 1.900
assign (residue 41 and name HA) (residue 44 and name HG) 2.850 1.150 1.150
assign (residue 41 and name HA) (residue 53 and name HG1#) 3.600 1.900 1.900
assign (residue 41 and name HB) (residue 38 and name HA) 2.850 1.150 1.150
assign (residue 41 and name HB) (residue 41 and name HA) 2.850 1.150 1.150
assign (residue 41 and name HB) (residue 41 and name HD1#) 3.100 1.400 1.400
assign (residue 41 and name HB) (residue 41 and name HG12) 2.850 1.150 1.150
assign (residue 41 and name HB) (residue 41 and name HG2#) 2.600 0.900 0.900
assign (residue 41 and name HD1#) (residue 7 and name HA) 3.600 1.900 1.900
assign (residue 41 and name HD1#) (residue 7 and name HB1) 3.600 1.900 1.900
assign (residue 41 and name HD1#) (residue 7 and name HB2) 3.100 1.400 1.400
assign (residue 41 and name HD1#) (residue 7 and name HG) 3.350 1.650 1.650
assign (residue 41 and name HD1#) (residue 11 and name HG1#) 3.850 2.150 2.150
assign (residue 41 and name HD1#) (residue 11 and name HG2#) 3.350 1.650 1.650
assign (residue 41 and name HD1#) (residue 38 and name HA) 3.350 1.650 1.650
assign (residue 41 and name HD1#) (residue 41 and name HA) 3.600 1.900 1.900

assign (residue 41 and name HD1#) (residue 41 and name HB) 3.100 1.400 1.400
assign (residue 41 and name HD1#) (residue 41 and name HG11) 3.100 1.400 1.400
assign (residue 41 and name HD1#) (residue 41 and name HG12) 3.100 1.400 1.400
assign (residue 41 and name HD1#) (residue 41 and name HG2#) 3.350 1.650 1.650
assign (residue 41 and name HD1#) (residue 53 and name HB) 3.350 1.650 1.650
assign (residue 41 and name HD1#) (residue 53 and name HG1#) 3.850 2.150 2.150
assign (residue 41 and name HG11) (residue 41 and name HA) 2.850 1.150 1.150
assign (residue 41 and name HG11) (residue 41 and name HD1#) 3.100 1.400 1.400
assign (residue 41 and name HG11) (residue 41 and name HG12) 2.350 0.650 0.650
assign (residue 41 and name HG11) (residue 53 and name HG1#) 3.600 1.900 1.900
assign (residue 41 and name HG12) (residue 41 and name HA) 2.850 1.150 1.150
assign (residue 41 and name HG12) (residue 41 and name HB) 2.850 1.150 1.150
assign (residue 41 and name HG12) (residue 41 and name HD1#) 3.100 1.400 1.400
assign (residue 41 and name HG12) (residue 41 and name HG2#) 3.600 1.900 1.900
assign (residue 41 and name HG12) (residue 41 and name HG11) 2.350 0.650 0.650
assign (residue 41 and name HG2#) (residue 7 and name HB1) 3.350 1.650 1.650
assign (residue 41 and name HG2#) (residue 7 and name HB2) 3.350 1.650 1.650
assign (residue 41 and name HG2#) (residue 8 and name HG1) 3.600 1.900 1.900
assign (residue 41 and name HG2#) (residue 8 and name HG2) 3.600 1.900 1.900
assign (residue 41 and name HG2#) (residue 41 and name HB) 3.100 1.400 1.400

NOE interactions to residue E42
assign (residue 42 and name HN) (residue 41 and name HB) 2.350 0.650 0.650
assign (residue 42 and name HN) (residue 41 and name HD1#) 3.600 1.900 1.900
assign (residue 42 and name HN) (residue 41 and name HG2#) 3.100 1.400 1.400
assign (residue 42 and name HN) (residue 42 and name HG1) 2.350 0.650 0.650
assign (residue 42 and name HN) (residue 42 and name HG2) 3.350 1.650 1.650

NOE interactions to residue E43
assign (residue 43 and name HN) (residue 41 and name HG2#) 3.600 1.900 1.900
assign (residue 43 and name HN) (residue 43 and name HB#) 2.350 0.650 0.650
assign (residue 43 and name HN) (residue 43 and name HG1) 2.350 0.650 0.650
assign (residue 43 and name HN) (residue 44 and name HG) 3.350 1.650 1.650
assign (residue 43 and name HA) (residue 43 and name HG1) 2.850 1.150 1.150
assign (residue 43 and name HA) (residue 43 and name HG2) 2.350 0.650 0.650
assign (residue 43 and name HB1) (residue 43 and name HA) 2.850 1.150 1.150

NOE interactions to residue L44
assign (residue 44 and name HN) (residue 41 and name HA) 2.850 1.150 1.150
assign (residue 44 and name HN) (residue 41 and name HG2#) 3.600 1.900 1.900
assign (residue 44 and name HN) (residue 43 and name HB#) 3.350 1.650 1.650
assign (residue 44 and name HN) (residue 44 and name HD1#) 3.100 1.400 1.400
assign (residue 44 and name HN) (residue 44 and name HD2#) 3.350 1.650 1.650
assign (residue 44 and name HA) (residue 44 and name HB1) 2.850 1.150 1.150
assign (residue 44 and name HA) (residue 44 and name HB2) 2.850 1.150 1.150
assign (residue 44 and name HA) (residue 44 and name HD1#) 3.600 1.900 1.900
assign (residue 44 and name HA) (residue 44 and name HD2#) 3.100 1.400 1.400
assign (residue 44 and name HB1) (residue 41 and name HA) 2.850 1.150 1.150
assign (residue 44 and name HB1) (residue 44 and name HB2) 2.350 0.650 0.650
assign (residue 44 and name HB1) (residue 44 and name HG) 2.850 1.150 1.150
assign (residue 44 and name HD2#) (residue 41 and name HA) 3.600 1.900 1.900
assign (residue 44 and name HD2#) (residue 44 and name HA) 3.100 1.400 1.400
assign (residue 44 and name HD2#) (residue 44 and name HB1) 3.600 1.900 1.900
assign (residue 44 and name HD2#) (residue 44 and name HB2) 3.100 1.400 1.400
assign (residue 44 and name HD2#) (residue 44 and name HG) 3.100 1.400 1.400
assign (residue 44 and name HD2#) (residue 50 and name HA) 3.100 1.400 1.400

NOE interactions to residue G45
assign (residue 45 and name HN) (residue 44 and name HB1) 3.350 1.650 1.650
assign (residue 45 and name HN) (residue 44 and name HB2) 3.350 1.650 1.650

NOE interactions to residue E49
assign (residue 49 and name HN) (residue 44 and name HD2#) 3.600 1.900 1.900
assign (residue 49 and name HN) (residue 48 and name HA#) 2.350 0.650 0.650
assign (residue 49 and name HN) (residue 49 and name HB#) 2.350 0.650 0.650
assign (residue 49 and name HN) (residue 49 and name HG#) 2.850 1.150 1.150
assign (residue 49 and name HA) (residue 52 and name HB#) 3.350 1.650 1.650
assign (residue 49 and name HB1) (residue 49 and name HA) 2.850 1.150 1.150
assign (residue 49 and name HG1) (residue 49 and name HA) 2.850 1.150 1.150
assign (residue 49 and name HB1) (residue 52 and name HB#) 3.350 1.650 1.650

NOE interactions to residue V50
assign (residue 50 and name HN) (residue 50 and name HB) 2.350 0.650 0.650
assign (residue 50 and name HN) (residue 50 and name HG2#) 3.100 1.400 1.400
assign (residue 50 and name HA) (residue 44 and name HD2#) 3.600 1.900 1.900
assign (residue 50 and name HB) (residue 50 and name HA) 2.850 1.150 1.150

assign (residue 50 and name HB) (residue 50 and name HG1#) 3.100 1.400 1.400
assign (residue 50 and name HB) (residue 50 and name HG2#) 3.100 1.400 1.400
assign (residue 50 and name HG1#) (residue 3 and name HB#) 3.350 1.650 1.650
assign (residue 50 and name HG1#) (residue 3 and name HD2) 3.600 1.900 1.900
assign (residue 50 and name HG1#) (residue 50 and name HA) 3.100 1.400 1.400
assign (residue 50 and name HG1#) (residue 50 and name HB) 3.100 1.400 1.400
assign (residue 50 and name HG1#) (residue 54 and name HG1) 3.600 1.900 1.900
assign (residue 50 and name HG2#) (residue 3 and name HB#) 3.350 1.650 1.650
assign (residue 50 and name HG2#) (residue 3 and name HD2) 3.600 1.900 1.900

NOE interactions to residue K51
assign (residue 51 and name HN) (residue 49 and name HA) 2.850 1.150 1.150
assign (residue 51 and name HN) (residue 49 and name HG1) 2.850 1.150 1.150
assign (residue 51 and name HN) (residue 50 and name HG1#) 3.600 1.900 1.900
assign (residue 51 and name HN) (residue 51 and name HB#) 2.350 0.650 0.650
assign (residue 51 and name HN) (residue 51 and name HD#) 2.850 1.150 1.150
assign (residue 51 and name HN) (residue 51 and name HG#) 2.850 1.150 1.150

NOE interactions to residue K52
assign (residue 52 and name HN) (residue 49 and name HG#) 2.850 1.150 1.150
assign (residue 52 and name HN) (residue 52 and name HB#) 2.350 0.650 0.650
assign (residue 52 and name HN) (residue 52 and name HD#) 2.850 1.150 1.150
assign (residue 52 and name HN) (residue 52 and name HG#) 2.850 1.150 1.150
assign (residue 52 and name HB#) (residue 52 and name HD#) 2.350 0.650 0.650
assign (residue 52 and name HB#) (residue 52 and name HG#) 2.350 0.650 0.650

NOE interactions to residue V53
assign (residue 53 and name HN) (residue 53 and name HB) 2.350 0.650 0.650
assign (residue 53 and name HN) (residue 53 and name HG2#) 3.100 1.400 1.400
assign (residue 53 and name HA) (residue 56 and name HB#) 2.850 1.150 1.150
assign (residue 53 and name HA) (residue 56 and name HG1) 2.850 1.150 1.150
assign (residue 53 and name HA) (residue 56 and name HG2) 2.850 1.150 1.150
assign (residue 53 and name HB) (residue 41 and name HD1#) 3.100 1.400 1.400
assign (residue 53 and name HB) (residue 41 and name HG2#) 3.600 1.900 1.900
assign (residue 53 and name HB) (residue 53 and name HA) 2.850 1.150 1.150
assign (residue 53 and name HG1#) (residue 40 and name HB1) 3.100 1.400 1.400
assign (residue 53 and name HG1#) (residue 40 and name HB2) 3.600 1.900 1.900
assign (residue 53 and name HG1#) (residue 41 and name HA) 3.600 1.900 1.900
assign (residue 53 and name HG1#) (residue 41 and name HB) 3.600 1.900 1.900
assign (residue 53 and name HG1#) (residue 41 and name HD1#) 3.850 2.150 2.150
assign (residue 53 and name HG1#) (residue 41 and name HG11) 3.100 1.400 1.400
assign (residue 53 and name HG1#) (residue 50 and name HA) 3.600 1.900 1.900
assign (residue 53 and name HG1#) (residue 53 and name HA) 3.100 1.400 1.400
assign (residue 53 and name HG1#) (residue 53 and name HB) 3.100 1.400 1.400
assign (residue 53 and name HG1#) (residue 54 and name HA) 3.600 1.900 1.900
assign (residue 53 and name HG2#) (residue 37 and name HA) 3.600 1.900 1.900
assign (residue 53 and name HG2#) (residue 40 and name HB1) 3.100 1.400 1.400
assign (residue 53 and name HG2#) (residue 40 and name HB2) 3.350 1.650 1.650
assign (residue 53 and name HG2#) (residue 40 and name HD#) 3.350 1.650 1.650
assign (residue 53 and name HG2#) (residue 44 and name HG) 3.600 1.900 1.900
assign (residue 53 and name HG2#) (residue 49 and name HG2) 3.600 1.900 1.900
assign (residue 53 and name HG2#) (residue 50 and name HA) 3.600 1.900 1.900
assign (residue 53 and name HG2#) (residue 53 and name HA) 3.100 1.400 1.400
assign (residue 53 and name HG2#) (residue 53 and name HB) 3.100 1.400 1.400
assign (residue 53 and name HG2#) (residue 54 and name HA) 3.600 1.900 1.900

NOE interactions to residue E54
assign (residue 54 and name HN) (residue 53 and name HB) 3.350 1.650 1.650
assign (residue 54 and name HN) (residue 54 and name HB2) 3.350 1.650 1.650
assign (residue 54 and name HN) (residue 54 and name HG1) 2.350 0.650 0.650
assign (residue 54 and name HN) (residue 54 and name HG2) 3.350 1.650 1.650
assign (residue 54 and name HA) (residue 7 and name HD1#) 3.100 1.400 1.400
assign (residue 54 and name HA) (residue 7 and name HD2#) 3.100 1.400 1.400
assign (residue 54 and name HA) (residue 54 and name HB1) 2.850 1.150 1.150
assign (residue 54 and name HA) (residue 54 and name HB2) 2.350 0.650 0.650
assign (residue 54 and name HA) (residue 54 and name HG1) 3.350 1.650 1.650
assign (residue 54 and name HA) (residue 54 and name HG2) 3.350 1.650 1.650
assign (residue 54 and name HA) (residue 57 and name HB) 2.850 1.150 1.150
assign (residue 54 and name HA) (residue 57 and name HG1#) 3.100 1.400 1.400
assign (residue 54 and name HB1) (residue 54 and name HG1) 2.850 1.150 1.150
assign (residue 54 and name HB1) (residue 54 and name HG2) 2.350 0.650 0.650
assign (residue 54 and name HG1) (residue 7 and name HD1#) 3.350 1.650 1.650
assign (residue 54 and name HG1) (residue 54 and name HG2) 2.350 0.650 0.650
assign (residue 54 and name HG2) (residue 7 and name HD1#) 3.600 1.900 1.900
assign (residue 54 and name HG2) (residue 7 and name HD2#) 3.100 1.400 1.400
assign (residue 54 and name HG2) (residue 54 and name HA) 2.850 1.150 1.150

assign (residue 54 and name HG2) (residue 54 and name HB1) 2.350 0.650 0.650
assign (residue 54 and name HG2) (residue 54 and name HB2) 2.350 0.650 0.650

NOE interactions to residue E55
assign (residue 55 and name HN) (residue 6 and name HB#) 3.600 1.900 1.900
assign (residue 55 and name HN) (residue 53 and name HA) 3.350 1.650 1.650

NOE interactions to residue E56
assign (residue 56 and name HN) (residue 53 and name HA) 2.850 1.150 1.150
assign (residue 56 and name HB1) (residue 53 and name HA) 2.850 1.150 1.150
assign (residue 56 and name HG1) (residue 53 and name HA) 2.850 1.150 1.150

NOE interactions to residue V57
assign (residue 57 and name HN) (residue 53 and name HA) 2.850 1.150 1.150
assign (residue 57 and name HN) (residue 54 and name HA) 2.850 1.150 1.150
assign (residue 57 and name HN) (residue 57 and name HB) 2.350 0.650 0.650
assign (residue 57 and name HN) (residue 57 and name HG1#) 3.100 1.400 1.400
assign (residue 57 and name HN) (residue 57 and name HG2#) 3.100 1.400 1.400
assign (residue 57 and name HA) (residue 57 and name HB) 2.850 1.150 1.150
assign (residue 57 and name HA) (residue 57 and name HG1#) 3.100 1.400 1.400
assign (residue 57 and name HA) (residue 57 and name HG2#) 3.100 1.400 1.400
assign (residue 57 and name HA) (residue 60 and name HB1) 2.850 1.150 1.150
assign (residue 57 and name HA) (residue 60 and name HB2) 2.850 1.150 1.150
assign (residue 57 and name HB) (residue 54 and name HA) 2.850 1.150 1.150
assign (residue 57 and name HB) (residue 57 and name HA) 2.850 1.150 1.150
assign (residue 57 and name HB) (residue 57 and name HG1#) 3.100 1.400 1.400
assign (residue 57 and name HB) (residue 57 and name HG2#) 3.100 1.400 1.400
assign (residue 57 and name HG1#) (residue 37 and name HD1#) 3.350 1.650 1.650
assign (residue 57 and name HG1#) (residue 54 and name HA) 3.600 1.900 1.900
assign (residue 57 and name HG1#) (residue 57 and name HA) 3.100 1.400 1.400
assign (residue 57 and name HG1#) (residue 57 and name HB) 3.100 1.400 1.400
assign (residue 57 and name HG1#) (residue 57 and name HG2#) 3.350 1.650 1.650
assign (residue 57 and name HG1#) (residue 58 and name HB1) 3.600 1.900 1.900
assign (residue 57 and name HG1#) (residue 61 and name HG1) 3.600 1.900 1.900
assign (residue 57 and name HG1#) (residue 61 and name HG2) 3.600 1.900 1.900
assign (residue 57 and name HG2#) (residue 37 and name HB1) 3.350 1.650 1.650
assign (residue 57 and name HG2#) (residue 37 and name HB2) 3.350 1.650 1.650
assign (residue 57 and name HG2#) (residue 37 and name HD1#) 3.350 1.650 1.650
assign (residue 57 and name HG2#) (residue 54 and name HA) 3.100 1.400 1.400
assign (residue 57 and name HG2#) (residue 57 and name HA) 3.100 1.400 1.400
assign (residue 57 and name HG2#) (residue 57 and name HB) 3.100 1.400 1.400
assign (residue 57 and name HG2#) (residue 57 and name HG1#) 3.350 1.650 1.650
assign (residue 57 and name HG2#) (residue 60 and name HB2) 3.600 1.900 1.900

NOE interactions to residue K58
assign (residue 58 and name HN) (residue 54 and name HA) 3.350 1.650 1.650
assign (residue 58 and name HN) (residue 57 and name HG1#) 3.350 1.650 1.650
assign (residue 58 and name HN) (residue 57 and name HG2#) 3.100 1.400 1.400
assign (residue 58 and name HN) (residue 58 and name HB#) 2.350 0.650 0.650
assign (residue 58 and name HN) (residue 58 and name HD#) 2.850 1.150 1.150
assign (residue 58 and name HN) (residue 58 and name HE#) 3.350 1.650 1.650
assign (residue 58 and name HN) (residue 58 and name HG#) 2.850 1.150 1.150

NOE interactions to residue K59
assign (residue 59 and name HN) (residue 57 and name HA) 3.350 1.650 1.650
assign (residue 59 and name HN) (residue 59 and name HB#) 2.350 0.650 0.650
assign (residue 59 and name HN) (residue 59 and name HD#) 2.850 1.150 1.150
assign (residue 59 and name HN) (residue 59 and name HG1) 2.350 0.650 0.650
assign (residue 59 and name HN) (residue 60 and name HB1) 3.350 1.650 1.650
assign (residue 59 and name HN) (residue 60 and name HB2) 3.350 1.650 1.650

NOE interactions to residue L60
assign (residue 60 and name HN) (residue 57 and name HA) 2.850 1.150 1.150
assign (residue 60 and name HN) (residue 57 and name HG1#) 3.600 1.900 1.900
assign (residue 60 and name HN) (residue 59 and name HB#) 2.350 0.650 0.650
assign (residue 60 and name HN) (residue 59 and name HD#) 3.350 1.650 1.650
assign (residue 60 and name HN) (residue 60 and name HB1) 2.350 0.650 0.650
assign (residue 60 and name HN) (residue 60 and name HB2) 2.350 0.650 0.650
assign (residue 60 and name HN) (residue 60 and name HD1#) 3.100 1.400 1.400
assign (residue 60 and name HN) (residue 60 and name HD2#) 3.100 1.400 1.400
assign (residue 60 and name HA) (residue 60 and name HB1) 2.850 1.150 1.150
assign (residue 60 and name HA) (residue 60 and name HB2) 2.850 1.150 1.150
assign (residue 60 and name HA) (residue 60 and name HD1#) 3.100 1.400 1.400
assign (residue 60 and name HA) (residue 60 and name HD2#) 3.100 1.400 1.400
assign (residue 60 and name HA) (residue 63 and name HB1) 2.850 1.150 1.150
assign (residue 60 and name HA) (residue 63 and name HG#) 2.850 1.150 1.150

assign (residue 60 and name HB1) (residue 57 and name HA) 2.850 1.150 1.150
assign (residue 60 and name HB1) (residue 60 and name HA) 2.850 1.150 1.150
assign (residue 60 and name HB1) (residue 60 and name HB2) 2.350 0.650 0.650
assign (residue 60 and name HB1) (residue 60 and name HD1#) 3.100 1.400 1.400
assign (residue 60 and name HB1) (residue 60 and name HD2#) 3.100 1.400 1.400
assign (residue 60 and name HB1) (residue 60 and name HG) 2.850 1.150 1.150
assign (residue 60 and name HB2) (residue 57 and name HA) 2.850 1.150 1.150
assign (residue 60 and name HB2) (residue 60 and name HA) 2.850 1.150 1.150
assign (residue 60 and name HB2) (residue 60 and name HB1) 2.350 0.650 0.650
assign (residue 60 and name HB2) (residue 60 and name HD1#) 3.100 1.400 1.400
assign (residue 60 and name HB2) (residue 60 and name HD2#) 3.100 1.400 1.400
assign (residue 60 and name HB2) (residue 60 and name HG) 2.850 1.150 1.150
assign (residue 60 and name HD1#) (residue 30 and name HA) 3.100 1.400 1.400
assign (residue 60 and name HD1#) (residue 30 and name HB1) 3.100 1.400 1.400
assign (residue 60 and name HD1#) (residue 30 and name HB2) 3.600 1.900 1.900
assign (residue 60 and name HD1#) (residue 30 and name HD2#) 3.850 2.150 2.150
assign (residue 60 and name HD1#) (residue 57 and name HA) 3.600 1.900 1.900
assign (residue 60 and name HD1#) (residue 60 and name HA) 3.100 1.400 1.400
assign (residue 60 and name HD1#) (residue 60 and name HB1) 3.100 1.400 1.400
assign (residue 60 and name HD1#) (residue 60 and name HB2) 3.100 1.400 1.400
assign (residue 60 and name HD1#) (residue 60 and name HD2#) 3.350 1.650 1.650
assign (residue 60 and name HD1#) (residue 60 and name HG) 3.100 1.400 1.400
assign (residue 60 and name HD1#) (residue 63 and name HB1) 3.350 1.650 1.650
assign (residue 60 and name HD1#) (residue 63 and name HB2) 3.350 1.650 1.650
assign (residue 60 and name HD1#) (residue 64 and name HG11) 3.600 1.900 1.900
assign (residue 60 and name HD2#) (residue 30 and name HB1) 3.350 1.650 1.650
assign (residue 60 and name HD2#) (residue 30 and name HB2) 3.350 1.650 1.650
assign (residue 60 and name HD2#) (residue 60 and name HA) 3.100 1.400 1.400
assign (residue 60 and name HD2#) (residue 60 and name HB1) 3.100 1.400 1.400
assign (residue 60 and name HD2#) (residue 60 and name HB2) 3.100 1.400 1.400
assign (residue 60 and name HD2#) (residue 60 and name HG) 3.100 1.400 1.400
assign (residue 60 and name HG) (residue 60 and name HB1) 2.850 1.150 1.150
assign (residue 60 and name HG) (residue 60 and name HB2) 2.850 1.150 1.150
assign (residue 60 and name HG) (residue 60 and name HD1#) 3.100 1.400 1.400
assign (residue 60 and name HG) (residue 60 and name HD2#) 3.100 1.400 1.400
assign (residue 60 and name HG) (residue 64 and name HD1#) 3.600 1.900 1.900

NOE interactions to residue E61
assign (residue 61 and name HN) (residue 14 and name HD2#) 3.350 1.650 1.650
assign (residue 61 and name HN) (residue 57 and name HA) 2.850 1.150 1.150
assign (residue 61 and name HN) (residue 57 and name HG1#) 3.600 1.900 1.900
assign (residue 61 and name HN) (residue 58 and name HA) 3.350 1.650 1.650
assign (residue 61 and name HN) (residue 60 and name HB1) 2.350 0.650 0.650
assign (residue 61 and name HN) (residue 60 and name HB2) 2.850 1.150 1.150
assign (residue 61 and name HN) (residue 61 and name HB#) 2.350 0.650 0.650
assign (residue 61 and name HN) (residue 61 and name HB2) 2.850 1.150 1.150
assign (residue 61 and name HN) (residue 61 and name HG1) 2.350 0.650 0.650
assign (residue 61 and name HA) (residue 14 and name HD2#) 3.100 1.400 1.400
assign (residue 61 and name HA) (residue 61 and name HB1) 2.850 1.150 1.150
assign (residue 61 and name HA) (residue 61 and name HB2) 2.850 1.150 1.150
assign (residue 61 and name HA) (residue 61 and name HG1) 2.850 1.150 1.150
assign (residue 61 and name HA) (residue 61 and name HG2) 2.850 1.150 1.150
assign (residue 61 and name HA) (residue 64 and name HB) 2.850 1.150 1.150
assign (residue 61 and name HA) (residue 64 and name HD1#) 3.100 1.400 1.400
assign (residue 61 and name HA) (residue 64 and name HG12) 2.850 1.150 1.150
assign (residue 61 and name HA) (residue 64 and name HG2#) 3.600 1.900 1.900
assign (residue 61 and name HG1) (residue 61 and name HA) 2.850 1.150 1.150
assign (residue 61 and name HG2) (residue 14 and name HD2#) 3.600 1.900 1.900
assign (residue 61 and name HG2) (residue 58 and name HA) 3.350 1.650 1.650
assign (residue 61 and name HG2) (residue 61 and name HA) 2.850 1.150 1.150

NOE interactions to residue E62
assign (residue 62 and name HN) (residue 60 and name HA) 3.350 1.650 1.650
assign (residue 62 and name HN) (residue 62 and name HB#) 2.350 0.650 0.650
assign (residue 62 and name HN) (residue 62 and name HG#) 2.350 0.650 0.650

NOE interactions to residue E63
assign (residue 63 and name HN) (residue 30 and name HD2#) 3.350 1.650 1.650
assign (residue 63 and name HN) (residue 60 and name HA) 2.850 1.150 1.150
assign (residue 63 and name HN) (residue 60 and name HD1#) 3.350 1.650 1.650
assign (residue 63 and name HN) (residue 63 and name HB#) 2.350 0.650 0.650
assign (residue 63 and name HN) (residue 63 and name HG#) 2.350 0.650 0.650
assign (residue 63 and name HN) (residue 64 and name HA) 3.350 1.650 1.650
assign (residue 63 and name HB2) (residue 30 and name HD2#) 3.350 1.650 1.650

NOE interactions to residue I64

assign (residue 64 and name HN) (residue 60 and name HD1#) 3.100 1.400 1.400
assign (residue 64 and name HN) (residue 64 and name HB) 2.350 0.650 0.650
assign (residue 64 and name HN) (residue 64 and name HD1#) 3.100 1.400 1.400
assign (residue 64 and name HN) (residue 64 and name HG11) 2.350 0.650 0.650
assign (residue 64 and name HN) (residue 64 and name HG12) 2.850 1.150 1.150
assign (residue 64 and name HN) (residue 64 and name HG2#) 3.100 1.400 1.400
assign (residue 64 and name HN) (residue 67 and name HD1#) 3.100 1.400 1.400
assign (residue 64 and name HN) (residue 67 and name HD2#) 3.600 1.900 1.900
assign (residue 64 and name HA) (residue 64 and name HB) 2.850 1.150 1.150
assign (residue 64 and name HA) (residue 64 and name HD1#) 3.100 1.400 1.400
assign (residue 64 and name HA) (residue 64 and name HG11) 2.850 1.150 1.150
assign (residue 64 and name HA) (residue 64 and name HG12) 2.850 1.150 1.150
assign (residue 64 and name HA) (residue 64 and name HG2#) 3.100 1.400 1.400
assign (residue 64 and name HA) (residue 67 and name HD1#) 3.100 1.400 1.400
assign (residue 64 and name HA) (residue 67 and name HG) 2.850 1.150 1.150
assign (residue 64 and name HB) (residue 61 and name HA) 2.850 1.150 1.150
assign (residue 64 and name HB) (residue 64 and name HA) 2.850 1.150 1.150
assign (residue 64 and name HB) (residue 64 and name HD1#) 3.100 1.400 1.400
assign (residue 64 and name HB) (residue 64 and name HG11) 2.850 1.150 1.150
assign (residue 64 and name HB) (residue 64 and name HG12) 2.850 1.150 1.150
assign (residue 64 and name HB) (residue 67 and name HD1#) 3.600 1.900 1.900
assign (residue 64 and name HD1#) (residue 64 and name HG12) 3.100 1.400 1.400
assign (residue 64 and name HD1#) (residue 14 and name HB1) 3.600 1.900 1.900
assign (residue 64 and name HD1#) (residue 14 and name HB2) 3.600 1.900 1.900
assign (residue 64 and name HD1#) (residue 14 and name HD2#) 3.850 2.150 2.150
assign (residue 64 and name HD1#) (residue 18 and name HG2#) 3.850 2.150 2.150
assign (residue 64 and name HD1#) (residue 30 and name HD1#) 3.850 2.150 2.150
assign (residue 64 and name HD1#) (residue 60 and name HA) 3.600 1.900 1.900
assign (residue 64 and name HD1#) (residue 60 and name HB1) 3.600 1.900 1.900
assign (residue 64 and name HD1#) (residue 60 and name HG) 3.100 1.400 1.400
assign (residue 64 and name HD1#) (residue 61 and name HA) 3.600 1.900 1.900
assign (residue 64 and name HD1#) (residue 64 and name HA) 3.600 1.900 1.900
assign (residue 64 and name HD1#) (residue 64 and name HB) 3.100 1.400 1.400
assign (residue 64 and name HD1#) (residue 64 and name HG11) 3.100 1.400 1.400
assign (residue 64 and name HD1#) (residue 64 and name HG2#) 3.350 1.650 1.650
assign (residue 64 and name HG11) (residue 30 and name HD1#) 3.100 1.400 1.400
assign (residue 64 and name HG11) (residue 30 and name HD2#) 3.600 1.900 1.900
assign (residue 64 and name HG11) (residue 64 and name HA) 2.850 1.150 1.150
assign (residue 64 and name HG11) (residue 64 and name HG12) 2.350 0.650 0.650
assign (residue 64 and name HG12) (residue 30 and name HD1#) 3.600 1.900 1.900
assign (residue 64 and name HG12) (residue 64 and name HA) 2.850 1.150 1.150
assign (residue 64 and name HG12) (residue 64 and name HB) 2.850 1.150 1.150
assign (residue 64 and name HG12) (residue 64 and name HD1#) 3.100 1.400 1.400
assign (residue 64 and name HG12) (residue 64 and name HG11) 2.350 0.650 0.650
assign (residue 64 and name HG12) (residue 64 and name HG2#) 3.100 1.400 1.400
assign (residue 64 and name HG2#) (residue 64 and name HG11) 3.350 1.650 1.650
assign (residue 64 and name HG2#) (residue 67 and name HD1#) 3.350 1.650 1.650

NOE interactions to residue K65

assign (residue 65 and name HN) (residue 64 and name HB) 2.350 0.650 0.650
assign (residue 65 and name HN) (residue 64 and name HD1#) 3.600 1.900 1.900
assign (residue 65 and name HN) (residue 64 and name HG2#) 3.100 1.400 1.400
assign (residue 65 and name HN) (residue 65 and name HB#) 2.350 0.650 0.650
assign (residue 65 and name HN) (residue 65 and name HD#) 2.850 1.150 1.150

NOE interactions to residue K66

assign (residue 66 and name HN) (residue 64 and name HA) 2.850 1.150 1.150
assign (residue 66 and name HN) (residue 64 and name HG2#) 3.600 1.900 1.900
assign (residue 66 and name HN) (residue 66 and name HB2) 2.350 0.650 0.650
assign (residue 66 and name HN) (residue 66 and name HD#) 2.850 1.150 1.150
assign (residue 66 and name HN) (residue 66 and name HE#) 2.850 1.150 1.150
assign (residue 66 and name HN) (residue 66 and name HG#) 2.350 0.650 0.650
assign (residue 66 and name HN) (residue 67 and name HD1#) 3.600 1.900 1.900
assign (residue 66 and name HN) (residue 67 and name HD2#) 3.600 1.900 1.900
assign (residue 66 and name HA) (residue 66 and name HB1) 2.850 1.150 1.150
assign (residue 66 and name HA) (residue 66 and name HB2) 2.850 1.150 1.150
assign (residue 66 and name HA) (residue 66 and name HD#) 2.850 1.150 1.150
assign (residue 66 and name HA) (residue 66 and name HE#) 3.350 1.650 1.650
assign (residue 66 and name HA) (residue 66 and name HG1) 2.850 1.150 1.150
assign (residue 66 and name HA) (residue 66 and name HG2) 2.850 1.150 1.150
assign (residue 66 and name HB1) (residue 66 and name HA) 2.850 1.150 1.150
assign (residue 66 and name HB2) (residue 66 and name HA) 2.850 1.150 1.150
assign (residue 66 and name HB2) (residue 66 and name HB1) 2.350 0.650 0.650
assign (residue 66 and name HG1) (residue 66 and name HA) 2.850 1.150 1.150
assign (residue 66 and name HG2) (residue 66 and name HA) 2.850 1.150 1.150

NOE interactions to residue L67

assign (residue 67 and name HN) (residue 64 and name HA)	2.850	1.150	1.150
assign (residue 67 and name HN) (residue 64 and name HG2#)	3.600	1.900	1.900
assign (residue 67 and name HN) (residue 66 and name HD#)	3.350	1.650	1.650
assign (residue 67 and name HN) (residue 67 and name HD1#)	3.100	1.400	1.400
assign (residue 67 and name HN) (residue 67 and name HD2#)	3.100	1.400	1.400
assign (residue 67 and name HN) (residue 67 and name HG)	2.350	0.650	0.650
assign (residue 67 and name HA) (residue 67 and name HB1)	2.850	1.150	1.150
assign (residue 67 and name HA) (residue 67 and name HB2)	2.850	1.150	1.150
assign (residue 67 and name HA) (residue 67 and name HD2#)	3.100	1.400	1.400
assign (residue 67 and name HB1) (residue 67 and name HA)	2.850	1.150	1.150
assign (residue 67 and name HB1) (residue 67 and name HB2)	2.350	0.650	0.650
assign (residue 67 and name HB1) (residue 67 and name HD1#)	3.100	1.400	1.400
assign (residue 67 and name HB1) (residue 67 and name HG)	2.850	1.150	1.150
assign (residue 67 and name HB2) (residue 67 and name HA)	2.850	1.150	1.150
assign (residue 67 and name HB2) (residue 67 and name HB1)	2.350	0.650	0.650
assign (residue 67 and name HB2) (residue 67 and name HD1#)	3.100	1.400	1.400
assign (residue 67 and name HD1#) (residue 67 and name HB1)	3.100	1.400	1.400
assign (residue 67 and name HG) (residue 64 and name HA)	2.850	1.150	1.150
assign (residue 67 and name HG) (residue 67 and name HB1)	2.850	1.150	1.150
assign (residue 67 and name HG) (residue 67 and name HB2)	2.850	1.150	1.150

APPENDIX E: Atom Nomenclature and SASA Analysis for 4MP-C32

Table E.1. Atom nomenclature for residue 4MP-C32 used in the structure-calculation CNS program, and in this study.

Atoms CNS[a]	Atoms (this study)[b]
N	backbone N
H	backbone H
C	backbone C
O	backbone O
CA	backbone CA
HA	backbone HA
CB	sidechain CB
HB1	sidechain HB1
HB2	sidechain HB2
SG	sidechain SG
SD	sidechain phenol S1
CE	sidechain phenol C4
CZ1	sidechain phenol C3
HZ1	sidechain phenol H3
CZ2	sidechain phenol C5
HZ2	sidechain phenol H5
CH1	sidechain phenol C2
HH1	sidechain phenol H2
CH2	sidechain phenol C6
HH2	sidechain phenol H6
CI	sidechain phenol C1
OI	sidechain phenol O1
HI	sidechain phenol HO1

[a]Using the program CNS, the 4MP molecule was treated as an extension to residue C32, hence the Greek lettering in that nomenclature. The NOE list follows this nomenclature. [b]For purposes of this study, the 4MP molecule was treated as a ligand with its own atom naming scheme.

Table E.2. Solvent accessible surface area (SASA) of atoms associated with the 4MP-C32 residue in 4MP-α_3C

Residue	Atoms	Average SASA (%)	SASA limits (%)
4MP-C32	backbone N	0 ± 0	0
4MP-C32	backbone H	0 ± 0	0
4MP-C32	backbone C	0 ± 0	0
4MP-C32	backbone O	0 ± 0	0.0 – 0.2
4MP-C32	backbone CA	0 ± 0	0
4MP-C32	backbone HA	0 ± 0	0
4MP-C32	sidechain CB	0 ± 0	0
4MP-C32	sidechain HB1	0 ± 0	0
4MP-C32	sidechain HB2	0 ± 0	0.0 – 0.1
4MP-C32	sidechain SG	0 ± 0.1	0.0 – 0.3
4MP-C32	sidechain phenol S	3.6 ± 4.9	0.0 – 15.7
4MP-C32	sidechain phenol C4	7.9 ± 10.3	0.0 – 38.7
4MP-C32	sidechain phenol C3	19.2 ± 18.6	0.0 – 52.1
4MP-C32	sidechain phenol H3	5.0 ± 6.6	0.0 – 18.0
4MP-C32	sidechain phenol C5	15.4 ± 17.0	0.0 – 51.8
4MP-C32	sidechain phenol H5	2.1 ± 4.3	0.0 – 16.7
4MP-C32	sidechain phenol C2	23.6 ± 16.5	0.0 – 52.2
4MP-C32	sidechain phenol H2	1.3 ± 2.7	0.0 – 9.8
4MP-C32	sidechain phenol C6	20.4 ± 16.8	0.0 – 56.4
4MP-C32	sidechain phenol H6	1.8 ± 4.5	0.0 – 16.1
4MP-C32	sidechain phenol C1	40.1 ± 15.5	7.6 – 65.2
4MP-C32	sidechain phenol O	29.7 ± 20.0	1.3 – 74
4MP-C32	sidechain phenol H	30.6 ± 30.3	0 – 88.4
4MP-C32	all atoms	7.9 ± 2.3	3.4 – 13.4

REFERENCES:

(1) Stubbe, J., van der Donk, W.A. *Chem. Rev.* **1998**, *98*, 705.

(2) Sjöberg, B.-M., Reichard, P., Gräslund, A., Ehrenberg, A. *J. Biol. Chem.* **1977**, *252*, 536.

(3) Larsson, A., Sjöberg, B.-M. *EMBO J.* **1986**, *5*, 2037.

(4) Kim, S.-T., Sancar, A., Essenmacher, C., Babcock, G.T. *Proc. Natl. Acad. Sci. U.S.A.* **1993**, *90*, 8023.

(5) Aubert, C., Vos, M.H., Mathis, P., Eker, A.P.M., Brettel, K. *Nature* **2000**, *405*, 586.

(6) Barry, B. A., Babcock, G.T. *Proc. Natl. Acad. Sci. U.S.A.* **1987**, *84*, 7099.

(7) Debus, R. J., Barry, B.A., Sithole, I., Babcock, G.T., McIntosh, L. *Biochemistry* **1988**, *27*, 9071.

(8) Metz, J. G., Nixon, P.J., Rönger, M., Brudvig, G.W., Diner, B.A. *Biochemistry* **1989**, *28*, 6960.

(9) Whittaker, J. M. *Chem. Rev.* **2003**, *103*, 2347.

(10) Whittaker, M. M., Whittaker, J.W. *J. Biol. Chem.* **1990**, *265*, 9610.

(11) Harriman, A. *J. Phys. Chem.* **1987**, *91*, 6102.

(12) DeFelippis, M. R., Murthy, C.P., Broitman, F., Weinraub, D., Faraggi, M., Klapper, M.H. *J. Phys. Chem.* **1991**, *95*, 3416.

(13) Tommos, C., Skalisky, J.J., Pilloud, D.L., Wand, A.J., Dutton, P.L. *Biochemistry* **1999**, *38*, 9495.

(14) DeFelippis, M. R., Murthy, C.P., Faraggi, M., Klapper, M.H. *Biochemistry* **1989**, *28*, 4847.

(15) Westerlund, K., Berry, B.W., Privett, H.K., Tommos, C. *Biochim. Biophys. Acta* **2005**, *1707*, 103.

(16) Knappe, J., Neugebauer, F.A., Blaschkowski, H.P., Gänzler, M. *Proc. Natl. Acad. Sci. U.S.A.* **1984**, *81*, 1332.

(17) Sun, X. Y., Ollagnier, S., Schmidt, P.P., Atta, M., Mulliez, E., Lepape, L., Eliasson, R., Gräslund, A., Fontecave, M., Reichard, P., Sjöberg, B.-M. *J. Biol. Chem.* **1996**, *271*, 6827.

(18) Sofia, H. J., Chen, G., Hetzler, B.G., Reyes-Spindola, J.F., Miller, N.E. *Nucleic Acids Res.* **2001**, *29*, 1097.

(19) Bertini, I., Gray, H.B., Stiefel, E.I., Valentine, J.S. *Biological Inorganic Chemistry: Structure and Reactivity*; University Science Books: Sausalito, 2007.

(20) Yonetani, T., Schleyer, H., Ehrenberg, A. *J. Biol. Chem.* **1966**, *241*, 3240.

(21) Sivaraja, M., Goodin, D.B., Smith, M., Hoffman, B.M. *Science* **1989**, *245*, 738.

(22) Shin, S., Tarboush, N.A., Davidson, V.L. *Biochemistry* **2010**, *49*, 5810.

(23) Choi, M., Shin, S., Davidson, V.L. *Biochemistry* **2012**, *51*, 6942.

(24) Proshlyakov, D. A., Pressler, M.A., DeMaso, C., Leykam, J.F., DeWitt, D.L., Babcock, G.T. *Science* **2000**, *290*, 1588.

(25) Tsai, A. L., Palmer, G., Kulmacz, R.J. *J. Biol. Chem.* **1992**, *267*, 17753.
(26) Tsai, A. L., Kulmacz, R.J., Palmer, G. *J. Biol. Chem.* **1995**, *270*, 10503.
(27) Hsi, L. C., Hoganson, C.W., Babcock, G.T., Smith, W.L. *Biochem. Biophys. Res. Commun.* **1994**, *202*, 1592.
(28) Ivancich, A., Jouve, H.M., Gaillard, J. *J. Am. Chem. Soc.* **1996**, *118*, 12852.
(29) Ivancich, A., Jouve, H.M., Sartor, B., Gaillard, J. *Biochemistry* **1997**, *36*, 9356.
(30) Dixon, W. T., Murphy, D. *J. Chem. Soc. Faraday Trans. 2* **1976**, *72*, 1221.
(31) Binstead, R. A., Moyer, B.A., Samuels, G.J., Meyer, T.J. *J. Am. Chem. Soc.* **1981**, *103*, 2897.
(32) Hawkins, C. L., Davies, M.J. *Biochim. Biophys. Acta* **2001**, *1504*, 196.
(33) Jin, F., Leitich, J., von Sonntag, C. *J. Chem. Soc. Perkin Trans.* **1993**, *2*, 1583.
(34) Hunter, E. P. L., Desrosiers, M.F., Simic, M.G. *Free Radical Biology & Medicine* **1989**, *6*, 581.
(35) Savéant, J.-M. *Elements of Molecular and Biomolecular Electrochemistry: An Electrochemical Approach to Electron Transfer Chemistry*; Wiley-Interscience: Hoboken, 2006.
(36) Osteryoung, J., O'Dea, J.J. In *Electroanalytical Chemistry*; Bard, A. J., Ed.; Marcel Dekker: New York, 1986; Vol. 5, p 209.
(37) Miles, A. B., Compton, R.G. *J. Phys. Chem.* **2000**, *104*, 5331.
(38) Garay, F., Lovric, M. *J. Electroanal. Chem.* **2002**, *518*, 91.
(39) Bard, A. J., Faulkner, L.R. *Electrochemical Methods. Fundamentals and Applications.*; 2 ed.; John Wiley & Sons, 2001.
(40) Ehrenberg, A., Reichard, P. *J. Biol. Chem.* **1972**, *247*, 3485.
(41) Stubbe, J., Nocera, D.G., Yee, C.S., Chang, M.C.Y. *Chem. Rev.* **2003**, *103*, 2167.
(42) Seyedsayamdost, M. R., Chan, C.T.Y., Mugnaini, V., Stubbe, J., Bennati, M. *J. Am. Chem. Soc.* **2007**, *129*, 15748.
(43) Uhlin, U., Eklund, H. *Nature* **1994**, *370*, 533.
(44) Bennati, M., Robblee, J.H., Mugnaini, V., Stubbe, J., Freed, J.H., Borbat, P. *J. Am. Chem. Soc.* **2005**, *127*, 15014.
(45) Page, C. C., Moser, C.C., Chen, X., Dutton, P.L. *Nature* **1999**, *402*, 47.
(46) Nordlund, P., Sjöberg, B.-M., Eklund, H. *Nature* **1990**, *345*, 593.
(47) Pizano, A. A., Lutterman, D.A., Holder, P.G., Teets, T.S., Stubbe, J., Nocera, D.G. *Proc. Natl. Acad. Sci. U.S.A.* **2012**, *109*, 39.
(48) Seyedsayamdost, M. R., Stubbe, J. *J. Am. Chem. Soc.* **2006**, *128*, 2522.
(49) Seyedsayamdost, M. R., Yee, C.S., Reece, S.Y., Nocera, D.G., Stubbe, J. *J. Am. Chem. Soc.* **2006**, *128*, 1562.
(50) Seyedsayamdost, M. R., Xie, J., Chan, C.T.Y., Schultz, P.G., Stubbe, J. *J. Am. Chem. Soc.* **2007**, *129*, 15060.
(51) Umena, Y., Kawakami, K., Shen, J-R., Kamiya, N *Nature* **2011**, *473*, 55.

(52) Grabolle, M., Dau, H. *Biochim. Biophys. Acta* **2005**, *1708*, 209.
(53) Rappaport, F., Diner, B.A. *Coord. Chem. Rev.* **2008**, *252*, 259.
(54) Boussac, A., Etienne, A.L. *Biochim. Biophys. Acta* **1984**, *766*, 576.
(55) Debus, R. J. *Biochim. Biophys. Acta* **2001**, *1503*, 164.
(56) Dai, Q.-H., Tommos, C., Fuentes, E.J., Blomberg, M.R.A., Dutton, P.L., Wand, A.J. *J. Am. Chem. Soc.* **2002**, *124*, 10952.
(57) Sjödin, M., Styring, S., Åkermark, B., Sun, L., Hammarström, L. *J. Am. Chem. Soc.* **2000**, *122*, 3932.
(58) Sun, L., Burkitt, M., Tamm, M., Raymond, M.K., Abrahamsson, M., LeGourriérec, D., Frapart, Y., Magnuson, A., Kenéz, P.H., Brandt, P., Tran, A., Hammarström, L., Styring, S., Åkermark, B. *J. Am. Chem. Soc.* **1999**, *121*, 6834.
(59) Burdinski, D., Wieghardt, K., Steenken, S. *J. Am. Chem. Soc.* **1999**, *121*, 10781.
(60) Magnuson, A., Berglund, H., Korall, P., Hammarström, L., Åkermark, B., Styring, S., Sun, L. *J. Am. Chem. Soc.* **1997**, *119*, 10720.
(61) Reece, S. Y., Nocera, D.G. *J. Am. Chem. Soc.* **2005**, *127*, 9448.
(62) Thomas, F., Jarjayes, O., Jamet, H., Hamman, S., Saint-Aman, E., Duboc, C., Pierre, J-L. *Angew. Chem. Int. Ed.* **2004**, *43*, 594.
(63) Maki, T., Araki, Y., Ishida, Y., Onomura, O., Matsumura, Y. *J. Am. Chem. Soc.* **2001**, *123*, 3371.
(64) Rhile, I. J., Markle, T.F., Nagao, H., DiPasquale, A.G., Lam, O.P., Lockwood, M.A., Rotter, K., Mayer, J.M. *J. Am. Chem. Soc.* **2006**, *128*, 6075.
(65) Markle, T. F., Rhile, I.J., DiPasquale, A.G., Mayer, J.M. *Proc. Natl. Acad. Sci. U.S.A.* **2008**, *105*, 8185.
(66) Costentin, C., Louault, C., Robert, M., Savéant, J-M. *J. Am. Chem. Soc.* **2008**, *130*, 15817.
(67) Bordwell, F. G., Cheng, J.-P. *J. Am. Chem. Soc.* **1991**, *113*, 1736.
(68) Rhile, I. J., Mayer, J.M. *Angew. Chem. Int. Ed.* **2005**, *44*, 1598.
(69) Markle, T. F., Mayer, J.M. *Angew. Chem. Int. Ed.* **2008**, *47*, 738.
(70) Benisvy, L., Bill, E., Blake, A.J., Collison, D., Davies, E.S., Garner, C.D., Guindy, C.I., McInnes, E.J.L., McArdle, G., McMaster, J., Wilson, C., Wolowska, J. *Dalton Trans.* **2004**, 3647.
(71) Moore, G. F., Hambourger, M., Kodis, G., Michl, W., Gust, D., Moore, T.A., Moore, A.L. *J. Phys. Chem. B* **2010**, *114*, 14450.
(72) Sibert, R., Josowicz, M., Porcelli, F., Veglia, G., Range, K., Barry, B.A. *J. Am. Chem. Soc.* **2007**, *129*, 4393.
(73) Sibert, R., Josowicz, M., Barry, B.A. *ACS Chem. Biol.* **2010**, *5*, 1157.
(74) Costentin, C., Robert, M., Savéant, J-M. *Acc. Chem. Res.* **2010**, *43*, 1019.
(75) Costentin, C., Louault, C., Robert, M., Savéant, J-M. *Proc. Natl. Acad. Sci.* **2009**, *106*, 18143.
(76) Koder, R. L., Dutton, P.L. *Dalton Trans.* **2006**, *25*, 3045.
(77) Bryson, J. W., Desjarlais, J.R., Handel, T.M., DeGrado, W.F. *Protein Science* **1998**, *7*, 1404.
(78) Regan, L., DeGrado, W.F. *Science* **1988**, *241*, 976.

(79) Kuhlman, B., Dantas, G., Ireton, G.C., Varani, G., Stoddard, B.L., Baker, D. *Science* **2003**, *302*, 1364.
(80) Koder, R. L., Anderson, J.L.R., Solomon, L.A., Reddy, K.S., Moser, C.C., Dutton, P.L. *Nature* **2009**, *458*, 305.
(81) Discher, B. M., Koder, R.L., Moser, C.C., Dutton, P.L. *Curr. Opin. Chem. Biol.* **2003**, *7*, 741.
(82) Gibney, B. R., Mulholland, S.E., Rabanal, F., Dutton, P.L. *Proc. Natl. Acad. Sci. U.S.A.* **1996**, *93*, 15041.
(83) Reedy, C. J., Gibney, B.R. *Chem. Rev.* **2004**, *104*, 617.
(84) Hay, S., Westerlund, K., Tommos, C. *Biochemistry* **2005**, *44*, 11891.
(85) Dempsey, J. L., Winkler, J.R., Gray, H.B. *Chem. Rev.* **2010**, *110*, 7024.
(86) Lee, J. K., Ross, R.T. *J. Phys. Chem. B* **1998**, *102*, 4612.
(87) Strickland, E. H., Wilchek, M., Horwitz, J., Billups, C. *J. Biol. Chem.* **1972**, *247*, 572.
(88) Noronha, M., Lima, J.C., Lamosa, P., Santos, H., Maycock, C., Ventura, R., Maçanita, A.L. *J. Phys. Chem. A.* **2004**, *108*, 2155.
(89) Lakowicz, J. R. *Principles of Fluorescence Spectroscopy*; 2nd ed.; Springer: New York, 1999.
(90) Macura, S., Ernst, R.R. *Mol. Phys.* **1980**, *41*, 95.
(91) van Holde, K. E., Johnson, W.C., Ho, P.S. *Principles of Physical Biochemistry*; 2 ed.; Prentice Hall: Upper Saddle River, 2006.
(92) Sönnichsen, F. D., Van Eyk, J.E., Hodges, R.S., Sykes, B.D. *Biochemistry* **1992**, *31*, 8790.
(93) Chen, Y.-H., Yang, J.T., Chau, K.H. *Biochemistry* **1974**, *13*, 3350.
(94) Santoro, M. M., Bolen, D.W. *Biochemistry* **1988**, *27*, 8063.
(95) Tommos, C., Valentine, K.G., Martínez-Rivera, M.C., Liang, L., Moorman, V.R. *Biochemistry*. **2013**, *52*, 1409.
(96) Rusling, J. F., Suib, S.L. *Adv. Mater.* **1994**, *6*, 922.
(97) Martínez-Rivera, M. C., Berry, B.W, Valentine, K.G., Westerlund, K., Hay, S. and Tommos, C. *Journal of the American Chemical Society* **2011**, *133*, 17786.
(98) Parry, E. P., Osteryoung, J. *Anal. Chem.* **1965**, *37*, 1634.
(99) Osteryoung, R. A., Osteryoung, J., Albery, W.J., Rogers, G.T. *Phil. Trans. Roy. Soc. London Ser. A.* **1981**, *302*, 315.
(100) Compton, R. G., Banks, C.E. *Understanding Voltammetry*; World Scientific: New jersey, 2007.
(101) Zoski, C. G. *Handbook of Electrochemistry*; Elsevier: Amsterdam, 2007.
(102) McCreery, R. L. In *Interfacial chemistry*; Wiechowski, A., Ed.; Dekker: New York, 1999.
(103) Chen, P., McCreery, R.L. *Anal. Chem.* **1996**, *68*, 3958.
(104) Louro, R. O., Catarino, T., Salgueiro, C.A., LeGall, J., Xavier, A.V. *JBIC* **1996**, *1*, 34.
(105) Bento, I., Matias, P.M., Baptista, A.M., da Costa, P.N., van Dongen, W.M.A.M., Saraiva, L.M., Schneider, T.R., Soares, C.M., Carrondo, M.A. *Proteins* **2004**, *54*, 135.

(106) Clark, W. M. *Oxidation-Reduction Potentials of Organic Systems*; The Williams & Wilkins Company: Baltimore, 1960.
(107) Wasielewski, M. R., Breslow, R. *J. Am. Chem. Soc.* **1976**, *98*, 4222.
(108) Mirčeski, V., Komorsky-Lovrić, Š., Lovrić, M. *Square-Wave Voltammetry. Theory and Application.*; Springer: Berlin, 2007.
(109) Skoog, D. A., West, D.M., Holler, F.J., Crouch, S.R. *Fundamentals of Analytical Chemistry*; 8th ed.; Brooks/Cole: London, 2004.
(110) Gasteiger, E., Hoogland, C., Gattiker, A., Duvaud, S., Wilkins, M.R., Appel, R.D., Bairoch, A. In *The Proteomics Protocols Handbook*; Walker, J. M., Ed.; Humana Press: 2005.
(111) Bhugun, I., Savéant, J.-M. *J. Electroanal. Chem.* **1995**, *395*, 127.
(112) O'Dea, J. J., Osteryoung, J., Osteryoung, R.A. *Anal. Chem.* **1981**, *53*, 695.
(113) Jeuken, L. J. C., McEvoy, J.P., Armstrong, F.A. *J. Phys. Chem. B* **2002**, *106*, 2304.
(114) Berry, B. W., Martínez-Rivera, M.C., Tommos, C. *Proc. Natl. Acad. Sci.* **2012**, *109*, 9739.
(115) Zheng, G., Prince, W.S. *J. Biomol. NMR* **2009**, *45*, 295.
(116) McDermott, C. A., Kneten, K.R., McCreery, R.L. *J. Electrochem. Soc.* **1993**, *140*, 2593.
(117) Silberberg, M. S. *Chemistry: The Molecular Nature of Matter and Change*; 4 ed.; Mc Graw Hill: Boston, 2006.
(118) Mahoney, L. R., DaRooge, M.A. *J. Am. Chem. Soc.* **1975**, *97*, 4722.
(119) ; 1.2r3pre ed.; Schrödinger, LLC.
(120) Ehrhardt, M. R., Erijman, L., Weber, G., Wand, A.J. *Biochemistry* **1996**, *35*, 1599.
(121) Lee, J. K., Ross, R.T., Thampi, S., Leurgans, S. *J. Phys. Chem.* **1992**, *96*, 9158.
(122) Willis, K. J., Szabo, A.G. *J. Phys. Chem.* **1991**, *95*, 1585.
(123) Bodenhausen, G., Ruben, D.J. *Chem. Phys. Lett.* **1980**, *69*, 185.
(124) Bax, A., Ikura, M., Kay, L.E., Torchia, D.A., Tschudin, R. *J. Magn. Reson.* **1990**, *86*, 304.
(125) Norwood, T. J., Boyd, J., Heritage, J.E., Soffe, N., Campbell, I.D. *J. Magn. Reson.* **1990**, *87*, 488.
(126) Palmer, A. G. I., Cavanagh, J., Wright, P.E., Rance, M. *J. Magn. Reson.* **1991**, *93*, 151.
(127) Kay, L. E., Keifer, P., Saarinen, T. *J. Am. Chem. Soc.* **1992**, *114*, 10663.
(128) Grzesiek, S., Bax, A. *J. Am. Chem. Soc.* **1993**, *115*, 12593.
(129) Schleucher, J., Schwendinger, M., Sattler, M., Schmidt, P., Schedletzky, O., Glaser, S.J., Sørensen, O.W., Griesinger, C. *J. Biomol. NMR* **1994**, *4*, 301.
(130) Cavanagh, J., Fairbrother, W.J., Palmer, A.G. III, Rance, M., Skelton, N.J. *Protein NMR Spectroscopy: Principles and Practice*; 2 ed.; Elsevier Academic Press: Amsterdam, 2007.
(131) Levitt, M. H. *Spin Dynamics: Basics of Nuclear Magnetic Resonance*; 2nd ed.; John Wiley & Sons, Ltd.: West Sussex, 2008.

(132) Seavey, B. R., Farr, E.A., Westler, W.M., Markley, J.L. *J. Biomol. NMR* **1991**, *1*, 217.
(133) Bax, A., Davis, D.G. *J. Magn. Reson.* **1985**, *63*, 207.
(134) Bothner-By, A. A., Stephens, R.L., Lee, J., Warren, C.D., Jeanloz, R.W. *J. Am. Chem. Soc.* **1984**, *106*, 811.
(135) Sattler, M., Schleucher, J., Griesinger, C. *Prog. Nucl. Magn. Reson. Spectrosc.* **1999**, *34*, 93.
(136) Kay, L. E., Ikura, M., Tschudin, R., Bax, A. *J. Magn. Reson.* **1990**, *89*, 496.
(137) Grzesiek, S., Bax, A. *J. Magn. Reson.* **1992**, *96*, 432.
(138) Schleucher, J., Sattler, M., Griesinger, C. *Angew. Chem. Int. Ed. Engl.* **1993**, *32*, 1489.
(139) Kay, L. E., Xu, G.Y., Yamazaki, T. *J. Magn. Reson. Ser. A* **1994**, *109*, 129.
(140) Clubb, R. T., Thanabal, V., Wagner, G. *J. Magn. Reson.* **1992**, *97*, 213.
(141) Grzesiek, S., Bax, A. *J. Am. Chem. Soc.* **1992**, *114*, 6291.
(142) Wittekind, M., Mueller, L. *J. Magn. Reson. Ser. B* **1993**, *101*, 201.
(143) Montelione, G. T., Lyons, B.A., Emerson, S.D., Tashiro, M. *J. Am. Chem. Soc.* **1992**, *114*, 10974.
(144) Logan, T. M., Olejniczak, E.T., Xu, R.X., Fesik, S.W. *J. Biomol. NMR* **1993**, *3*, 225.
(145) Grzesiek, S., Anglister, J., Bax, A. *J. magn. Reson. Ser. B* **1993**, *101*, 114.
(146) Lyons, B. A., Montelione, G.T. *J. Magn. Reson. Ser. B* **1993**, *101*, 206.
(147) Bax, A., Clore, G.M., Gronenborn, A.M. *J. Magn. Reson.* **1990**, *88*, 425.
(148) Kay, L. E., Xu, G.Y., Singer, A.U., Muhandiram, D.R., Forman-Kay, J.D. *J. Magn. Reson. Ser. B* **1993**, *101*, 333.
(149) Moseley, H. N. B., Sahota, G., Montelione, G.T. *J. Biomol. NMR* **2004**, *28*, 341.
(150) Kay, L. E., Clore, G.M., Bax, A., Gronenborn, A.M. *Science* **1990**, *249*, 411.
(151) Muhandiram, D. R., Xu, G.Y., Kay, L.E. *J. Biomol. NMR* **1993**, *3*, 463.
(152) Zuiderweg, E. R. P., Petros, A.M., Fesik, S.W., Olejniczak, E.T. *J. Am. Chem. Soc.* **1991**, *113*, 370.
(153) Clore, G. M., Kay, L.E., Bax, A., Gronenborn *Biochemistry* **1991**, *30*, 12.
(154) Vuister, G. W., Clore, G.M., Gronenborn, A.M., Powers, R., Garrett, D.S. Tschudin, R., Bax, A. *J. Magn. Reson. Ser. B* **1993**, *101*, 210.
(155) Marion, D., Kay, L.E., Sparks, S.W., Torchia, D.A., Bax, A. *J. Am. Chem. Soc.* **1989**, *111*, 1515.
(156) Marion, D., Driscoll, P.C., Kay, L.E., Wingfield, P.T., Bax, A., Gronenborn, A.M., Clore, G.M. *Biochemistry* **1989**, *28*, 6150.
(157) Goddard, T. D., Kneller, D.G.; University of California, San Francisco: San Francisco, CA.

(158) Wüthrich, K. *NMR of Proteins and Nucleic Acids*; John Wiley & Sons: New York, 1986.
(159) Branden, C., Tooze, J. *Introduction to Protein Structure*; 2nd ed.; Garland Publishing: New York, 1999.
(160) Brünger, A. T., Adams, P.D., Clore, G.M., DeLano, W.L., Gros, P., Grosse-Kunstleve, R.W., Jiang, J.S., Kuszewski, J., Nilges, M., Pannu, N.S., Read, R.J., Rice, L.M., Simonson, T., Warren, G.L. *Acta Crystallographica Section D - Biological Crystallography* **1998**, *54*, 905.
(161) Shen, Y., Delaglio, F., Corneliscu, G., Bax, A. *J. Biomol. NMR* **2009**, *44*, 213.
(162) Koradi, R., Billeter, M., Wüthrich, K. *J. Mol. Graph.* **1996**, *14*, 51.
(163) Ellman, G. L. *Arch. Biochem. Biophys.* **1959**, *82*, 70.
(164) Krezel, A., Bal, W. *J. Bioinorg. Chem.* **2004**, *98*, 161.
(165) ; 95.0 ed.; Molecular Simulations: San Diego, CA.
(166) Brünger, A. T. *X-PLOR Version 3.1. A System for X-ray Crystallography and NMR*; Yale University Press: New Haven, 1992.